Label-free detection of tuberculosis DNA with capacitive field-effect biosensors

Dissertation
zur
Erlangung des Doktorgrades
der Naturwissenschaften
(Dr. rer. nat.)

dem

Fachbereich Pharmazie der
Philipps-Universität Marburg
vorgelegt von

Thomas Stefan Bronder
aus
Mönchengladbach

Marburg/Lahn
2020

Gutachter:	**Prof. Dr. Michael Josef Schöning**
Gutachter:	**Prof. Dr. Michael Keusgen**

Eingereicht am:	**20.10.2020**
Tag der mündlichen Prüfung am:	**08.12.2020**

Hochschulkennziffer:	**1180**

E R K L Ä R U N G

Ich versichere, dass ich meine Dissertation

Label-free detection of tuberculosis DNA with capacitive field-effect biosensors

selbständig ohne unerlaubte Hilfe angefertigt und mich dabei keiner anderen als der von mir ausdrücklich bezeichneten Quellen bedient habe. Alle vollständig oder sinngemäß übernommenen Zitate sind als solche gekennzeichnet.

Die Dissertation wurde in der jetzigen oder einer ähnlichen Form noch bei keiner anderen Hochschule eingereicht und hat noch keinen sonstigen Prüfungszwecken gedient.

Marburg, den.....

.....
(Unterschrift mit Vor- und Zuname)

Everything is possible with the right DNA.

Abstract

A novel label-free DNA-detection method based on polyelectrolyte-modified electrolyte-insulator-semiconductor (EIS) sensor chips is developed in this thesis. This approach is motivated by the increasing demand on simple, easy to operate, cheap and reliable sensor platforms for the point-of-care detection of DNA from pathogens such as mycobacteria.

Field-effect EIS sensors are chosen because of their ability to detect surface-potential changes with high sensitivity; with EIS sensors, the binding of charged molecules such as single-stranded DNA (ssDNA) or double-stranded DNA (dsDNA) can be monitored without a complex setup. The SiO_2 surface-modification process of the EIS chips is carried out via adsorption of positively charged poly(allylamine hydrochloride) (PAH) on which the negatively charged DNA can bind by electrostatic attraction between the positive PAH charge and the negative DNA backbone resulting in a PAH/DNA bilayer. Compared to other binding methods, the adsorptive binding leads to a flat orientation of the DNA molecules, thus, the detectable intrinsic negative charge of the DNA is located closer to the sensor surface resulting in a higher contribution of signal generation. Results from electrochemical measurements of capacitance-voltage and constant-capacitance characteristics have been used as indicators for the respective surface-modification steps.

A modification protocol is first established for the binding of positively charged PAH as well as the subsequent binding of dsDNA molecules. Both binding events of the charged molecules lead to a surface-potential change, which could be successfully monitored by electrochemical measurements. The developed protocol is also used to detect dsDNA molecules with light-addressable potentiometric sensors (LAPS), which belong to the group of EIS sensors. The LAPS technology allows to measure surface-potential changes at defined locations on the oxide layer, but requires a light source to focus to these respective regions. The dsDNA adsorption could also be monitored with LAPS, here a lower detection limit of 0.1 nM was determined.

In order to monitor the hybridization reaction, a probe ssDNA is first immobilized onto the PAH-modified EIS-sensor surface. Then, the chip is exposed to solutions with target single-stranded complementary DNA (cDNA) and non-complementary DNA (ncDNA). In the case of cDNA, a hybridization reaction leads to a further change of the surface potential, which could be monitored by the EIS-sensor setup. Comparisons between incubation in solutions containing cDNA and ncDNA shows signal differences with a factor of 11. It was also investigated to reuse the sensor surface by simple repeating of the surface-modification steps without any kind of removing of the previous layers. It is possible to detect signal changes up to five PAH/DNA layers. The signal differences decrease by increasing the number of layers. This effect can be explained by the Debye charge-screening effect. To prove the assumption of the charge screening, additional experiments have been performed, in which the dependence of the ionic strength of the measurement solution on the resulting measured sensor signal is investigated. In addition, experiments are carried out, in which solutions containing polymerase-chain-reaction (PCR)-amplified cDNA have been analyzed with the developed sensing method. These cDNA-containing PCR solutions have

been used to mimic realistic point-of-care test conditions. A test series with different concentrations of the PCR samples was performed in order to determine the lower detection limit (0.3 nM) and the sensitivity (7.2 mV/decade). In final experiments, the electrochemical detection of extracted and amplified target DNA from tuberculosis-spiked (positive) and non-spiked (negative) human sputum samples has been carried out with the developed method. A clear difference between the signals of positive and negative samples proved the successful recognition and ability to distinguish both probes under realistic conditions.

All results of the electrochemical investigations have been validated by fluorescence-microscopy measurements.

Overall, the developed label-free method fulfills the requirements of a simple, easy to operate, cheap and reliable procedure for DNA sensing. The detection of amplified genomic DNA from real tuberculosis-spiked sputum samples underlines the potential for promising realizations of this technology as a basis for medical devices for identification of pathogens.

Keywords:
DNA sensing, label-free, field-effect biosensor, tuberculosis, hybridization detection

Content

Abbreviations

A	adenine
AC	alternating current
A_c	capacitor plate area
AFM	atomic force microscopy
AIDS	acquired immunodeficiency syndrome
AuNP	gold nanoparticle
bp	base pair
c	concentration (mol/L)
C	cytosine
CCD	charge-coupled device
C_{dl}	electrochemical double-layer capacitance
C_{EIS}	EIS-chip capacitance
C_{inv}	capacitance at inversion region
ConCap	constant-capacitance
C_{ox}	oxide capacitance
C_{sc}	semiconductor capacitance
C–V	capacitance-voltage
d	capacitor plate distance
Da	Dalton unit
DAPI	4′,6-diamidino-2-phenylindole
DC	direct current
DNA	deoxyribonucleic acid
dNTP	deoxynucleotide triphosphate
dsDNA	double-stranded DNA
e, q	elementary charge, no to be confused with Euler number
ε_0	vacuum permittivity
E_0	vacuum energy
E_c	conduction band energy
E_F	Fermi energy
EIS	electrolyte-insulator-semiconductor
E_v	valence band energy

ε_r	relative permittivity
ζ	Zeta potential
f	frequency
ϕ	quantum yield
Φm	work function (metal)
Φsc	work function (semiconductor)
FAM	6-carboxyfluorescein
FFT	fast Fourier transformation
FITC	fluorescein isothiocyanate
G	guanine
HIV	human immunodeficiency virus
I_{ph}	photocurrent
I_s	ionic strength
ISFET	ion-sensitive field-effect transistor
LAPS	light-addressable potentiometric sensor
LED	light-emitting diode
k_B	Boltzmann constant
λ_D	Debye-screening length
LED	light-emitting diode
M	molar concentration (mol/L), not to be confused with the molar mass [M]: g/mol
MOS	metal-oxide-semiconductor
MIS	metal-insulator-semiconductor
ncDNA	non-complementary DNA
N_A	number of adenine nucleotides in a DNA sequence
N_C	number of cytosine nucleotides in a DNA sequence
N_G	number of guanine nucleotides in a DNA sequence
N_P	number of immobilized probe ssDNA molecules
N_T	number of thymine nucleotides in a DNA sequence
PAH	poly(allylamine hydrochloride)
PE	polyelectrolyte
PEI	polyethylenimine
pH	pondus hydrogenii
PLL	poly-L-lysine

PSS	polystyrene sulfonate
PZC	point-of-zero charge
PCR	polymerase chain reaction
R	resistance
RE	reference electrode
R_{RE}	resistance of reference electrode
RNA	ribonucleic acid
RT	room temperature
scr	space-charge region
SiNW	silicon nanowire
ssDNA	single-stranded DNA
SG	Sybr-Green I
T	thymine
TB	tuberculosis
T_m	melting temperature
U_{fb}	flat-band voltage
U_g	gate voltage
V	voltage
φ	potential
$\varphi_{electrode}$	electrode potential
φ_{oHL}	potential at the outer Helmholtz-layer
$\varphi_{solution}$	potential of the solution
ω	angular frequency
z	ion valency
Z	complex impedance
Z_{setup}	setup impedance

Element symbols and SI units (base and derived units) are always expressed abbreviated in this work and not included in this list.

1 Introduction

1.1 DNA AS RECEPTOR MOLECULE FOR (BIO)SENSING

Deoxyribonucleic acid (DNA) is a vital biomolecule which can be found in every known lifeform on planet earth. It is composed of a chain-like arrangement of monomers (nucleotides) whose sequence coded the complete genome of an organism. The growth, development and spreading of all organisms is ensured by the cell-division process in which the DNA, as a carrier of the genetic information, is replicated and transferred to the new cell [1]. The genetic code of DNA expresses the "biological blueprint" for the "construction" of a complete lifeform. It plays an essential role in the production of proteins (the code specifies the structure of almost all proteins) and is therefore very important for the organization of the organism [2]. Every individual differs in size, function, appearance, structure, behavior etc., because of the differences in the protein and structural composition; this is a result of differences in the DNA sequence. Looking at the complete genome, all natural individuals (excluding clones and some other exceptions) have their own and unique DNA nucleotide sequence. As it is possible to determine the DNA sequence, it can be used in many ways for detection purposes.

The detection of DNA is nowadays used as an important feature in a popular analysis method that almost everyone is familiar with: The parental testing method. This method checks and proves that two individuals are parent and child [3, 4]. This test is based on a conformity-check between the two DNA samples taken from the child and the parent (father) by comparison according to specific traits and similarities [5].

Large parts of an individual's genome can be similar or equal not only between parents and their offspring but also within a species. In order to get a better understanding of the human genes, the "human genome project" was initiated to determine the nucleotide base-pair sequence of human DNA. From the results of this project, which was completed in April 2003, it turns out that 99.9% of all 3.2 billion bases of a human genome are identical with all other human beings [6]. This is because of the fact that only 1-3% of the complete genome are coded as genes [7]. More detailed information about the structure and properties of the DNA is presented in **Chapter 2.1**.

However, the genomic differences in DNA code between two species are very clear and distinct. Therefore, specific sequence sections can be very characteristically assigned to a certain species. This circumstance can also be used as basis for different detection purposes and gives us many opportunities for several sensorial applications: As an example, unknown tissue or cells can be clearly assigned to a certain organism by identification/comparison of the unknown DNA (sequence) with a genomic sequence. In particular from the medical point of view, this detection concept has a great benefit: It can be used for the detection of a pathogenic infection (e.g., bacterial, viral or fungal) of an (human) organism. To do this, the DNA of the target microorganism must be identified from a sample of the infected individual. The identification of pathogens by comparison between two DNA strands does not necessarily require a full sequence analysis; a simple

binding detection between two complementary DNA strands (a probe single-stranded DNA molecule (ssDNA) with known sequence and a complementary single-stranded target DNA molecule (cDNA) with an expected but unknown sequence) can be used as evidence for the conformity. This binding between two complementary DNA strands is also known as hybridization and results in forming a double-stranded DNA (dsDNA) molecule. More details about the binding of DNA are presented in **Chapter 2.1**.

The recognition of the hybridization event is (probably) the most important way of DNA detection, where an increasing number of DNA-sensing strategies and devices are based on. In comparison to other detection methods for microbiological/pathogen infections, DNA-based sensing procedures have a huge advantage in terms of precision and reliability (a more detailed perspective onto the advantages and disadvantages is given in **Chapter 1.2**). All in all, there is a variety of DNA-based detection concepts and ideas for sensing applications for a broad field of interests.

1.2 CHIP-BASED DNA-DETECTION TECHNIQUES – SHORT OVERVIEW AND STATE-OF-THE-ART

In this part, a closer look on different DNA-(hybridization) detection methods and their applications is given; also, their individual advantages and disadvantages are discussed. All explained and described sensing methods rely on the DNA detection from liquid media.

The history of hybridization detection generally started more than 40 years ago: One of the first techniques for detecting a DNA-hybridization event was the radioactive-labeling method introduced by Edwin Southern in 1975 [8]. Plenty other different ways of DNA-hybridization detection have been established in the last decades such as mass-sensitive, optical, (electro)chemical and thermal-based strategies [9–12]. Each technique has its individual advantages and drawbacks. However, it turns out that particularly chip-based methods offer benefits in terms of cheaper and simpler detection of the DNA molecules and DNA hybridization [10]. The possibility of miniaturization, also allows the detection of very low amounts of sample volumes. Especially from a medical point of view, DNA-sensing methods (for identification of pathogens) that fulfill the requirements for fast, reliable and cheap detection and demand on low sample volumes are advantageous and preferable. Therefore, chip-based platforms are well suited for such purposes.

(Chip-based) DNA detection can be generally classified into labeled and label-free methods. In the following section, both types of detection methods are presented and discussed on chosen examples. A detailed list of methods can be found in these reviews [13–15].

1.2.1 Labeled DNA-detection methods

As the name implies, labeled DNA-sensing methods rely on an indirect measurement of a certain labeling molecule, which is somehow involved in the reaction or interacts with the target molecule to be detected. Many different labeling methods were discovered and designed resulting now in a broad range of available marker molecules for DNA detection.

- Radioactive labeling of DNA

As already mentioned, the radioactive labeling was one of the first strategies of DNA detection. Here, DNA fragments (with known sequence) are radioactively marked, typically by incorporation of nucleotides (A, T, C or G), which have a radioactive phosphorus isotope. Unknown DNA molecules are immobilized onto a surface, which will afterwards be exposed to the radioactive DNA fragments. Upon hybridization, the molecules bind to the surface. A washing step removes all remaining DNA fragments. The radioactive signal can be measured by exposing the surface to an X-ray-sensitive film and indicates the successful hybridization. Anyhow, handling of radioactive material is unfavorable because of many safety aspects.

- DNA detection by using (magnetic) particles

Another approach for labeling can be performed by using magnetic particles. For instance, streptavidin-coated magnetic nanoparticles can be bounded to biotin-functionalized DNA. A change of the magnetic field upon hybridization can be very precisely measured afterwards [16]. Another on-chip method is based on DNA labeling with nanobeads, which can be optically detected by means of changes in the reflection and transmission of light [17]. However, both methods disadvantageously require complicated and time-consuming binding steps.

- Fluorescence-labeled optical DNA detection

The fluorescence-labeling process has been tremendously established as reliable and versatile tool for DNA detection. It is the by far most important and most frequently used method nowadays. The dye does not need to be bound to the target molecule in any case. Several other strategies for fluorescence-signal generation were developed. Some fluorophores are also able to intercalate with the DNA. These dyes usually bind (mostly unspecific towards the sequence) to double-stranded DNA, which is only formed after successful hybridization. A different way of labeled DNA sensing by means of fluorescence detection involves the use of quencher molecules. If a quencher (bound to ssDNA) and a fluorophore (bound to cDNA) are brought together in close proximity (e.g., by a hybridization reaction), then the fluorescence-signal generation can be strongly inhibited (quenched) by the quenching molecule. Upon DNA denaturation, both molecules are separated, which leads to an abort of the quenching effect and enables the fluorescence-signal generation of the fluorophore. A more detailed explanation about fluorescence-quenching methods is given in **Chapter 2.6**.

A major disadvantage of all fluorescence-based detection methods relies – besides the necessity of the optical equipment – in the stability of the fluorescence dyes. Effects such as unspecific quenching or bleaching caused by a variety of factors (unintended illumination, environment conditions (the liquid media itself can cause a quenching), temperature- and/or pH-variations, etc.) can negatively affect the desired properties and can finally lead to a complete failure of the measurement. Many of these effects appear slowly and with (mostly) low intensities so that fluctuations in measurement results might not clearly be assigned and correlated with these effects. More details are given in **Chapter 2.6**.

- Redox-mediated DNA detection

Another very popular technique become well established for labeled DNA detection: The electrochemical detection of redox-active species. Redox active agents, such as potassium ferrocyanide/ferricyanide or methylene blue [18–20], can be used for the indirect detection of DNA. These redox-active species can interact with the surface in different manner: In some applications, the mediator is reduced/oxidized on a free (metallized) surface, in other applications, the mediator interacts with the DNA and influences the surface [21].

If molecules react (become reduced/oxidized) at/with the surface, a redox current can be monitored as measurement signal. The amount of redox current is depending on the size of free area of the sensor surface. In the case of an immobilization, a larger area of the surface is occupied by DNA molecules, which hinders a free reaction of the redox molecule resulting in a reduced redox current [22]. When a hybridization occurs, the measured signal can increase or decrease depending on the grafting density of immobilized DNA molecules: For high immobilization densities, the hybridized cDNA molecules will additionally block the remaining free areas of the surface resulting in a further decrease of redox current; while, for a low immobilization density, the immobilized probe ssDNA molecules lay flat on the surface and tilt up upon hybridization [23]. Here, more surface becomes uncovered due to the hybridization event resulting in an increase of redox current.

This particular labeled DNA-detection technique requires a metallized or conductive sensing layer, which makes the procedure more complex and effortful. Some recent research studies critically question the reliability of this detection principle [24].

1.2.2 Label-free DNA-detection methods

Besides the labeled methods for detection of DNA molecules and DNA hybridization, plenty label-free techniques were established. Skipping the labeling process leads to a reduced effort, complexity, saves time and costs [25–28]. Within the label-free approaches, especially the electrochemical methods provide great benefits according to preparation time and costs due to the simple read-out possibilities, as well as the reduced effort and better compatibility of implementation in microfluidic and portable instrumentation [29]. The following parts give a brief overview of chosen and promising label-free DNA-detection strategies.

- Heat-transfer resistance

A very interesting approach of DNA detection is focused by P. Wagner's group from KU Leuven. They developed a real-time measurement method based on the monitoring of a thermal heat resistivity of the denaturation process of DNA [30]. Depending on the binding situation of immobilized DNA strands, a change in heat resistivity can be measured, e.g., upon hybridization. This method is very sensitive, since unspecific bindings can be almost completely excluded, see the explanation regarding stringency in **Chapter 2.1**. It allows the detection of target DNA concentrations down to the lower µM-range [31]. Despite of these benefits, a major drawback of this technique is the requirement of a complicated (silane-based, covalent) immobilization technique and the quite complicated setup and sensor-chip processing.

- Surface plasmon resonance

DNA detection can also be carried out using the physical effect of surface plasmon resonance [32]. Briefly, the surface of a dielectric (mostly clear and transparent) substrate (glass) must be metallized with a very thin (some nm) layer of metal (e.g., gold). Then, a totally reflected light beam is directed to the sensor surface under a changing angle. The light intensity of the reflected beam is continuously measured. At a certain (resonance) angle, the measured light intensity dramatically drops. In this resonance case, the light energy is transferred into energy for generating a surface plasmon. This method can be used to detect surface-loading processes: Immobilization of biomolecules such as DNA leads to a change in the resonance angle. Also, a hybridization with immobilized probe ssDNA molecules results in a change of the resonance conditions. The main advantage is the outstanding ultra-low sensitivity down to the lower aM range (which is equivalent to one single DNA molecule in a 10 µL sample). Anyhow, a very complex setup and complicated sensor preparation are unfavorable for a fast, cheap and simple detection method.

- Impedimetric-based detection methods

There are different ways of realizing an electrochemical measurement setup based on impedimetric signal-change detection. A convenient method is based on measuring the charge-transfer resistance of a sensor chip in liquid solution versus a counter- and a reference electrode [33–35]. A surface-binding reaction leads to a change in the measured resistance value. Depending on the amount of bounded molecules (and their dielectric constant), the respective resistance increases. A hybridization of cDNA molecules with the immobilized ssDNA further leads to a change in the sensor signal. This method also requires a metallized surface and a – more-or-less – complicated immobilization process. Impedance-change measurements were already performed in the past for the detection of DNA from *Mycobacterium tuberculosis* [36].

Another way to detect impedance changes induced by DNA binding or hybridization can be carried out utilizing silicon-nanowire (SiNW) transistors [37]. Usually, measurements of a threshold-voltage shift indicate a biomolecule-surface binding on an ion-sensitive transistor structure. A binding of molecules is also changing the SiNW-interface impedance, which can be monitored indirectly. The advantage here is a less dependency on the Debye-screening effect.

Impedance-based sensing strategies actually offer a good compromise between sensor performance such as sensitivity and reproducibility, as well as the required effort for sensor fabrication and -modification. However, an unspecific adsorption of species cannot be differentiated from a DNA binding and can be misinterpreted as hybridization reaction.

- Field-effect based approaches

A very favorable platform for the detection of DNA molecules and DNA hybridization is given by field-effect sensors, as their production (in established cleanroom facilities) as microchips is quite simple, cheap and can be realized in large quantities by the use of microfabrication processes [38]. Furthermore, the detection usually does not require labeling; many research groups have developed various types of field-effect-based sensors for the detection of DNA and DNA-hybridization reaction. Some of the most noteworthy field-effect sensors are the ion-sensitive field-effect transistor (ISFET), SiNW, the light-

addressable potentiometric sensor (LAPS) or the electrolyte-insulator-semiconductor (EIS) sensor [39–47]. The EIS sensor represents the field-effect device with the simplest structure and is the easiest to fabricate.

All field-effect structures consist of a semiconductor part with mobile charge carriers; the distribution of those charge carriers can be affected by an external electromagnetic field (such field can be very small, e.g., induced by a local potential change caused by charged molecules in close proximity to the semiconductor part). This redistribution can be recognized on very different ways. For instance, the most common technique for ISFETs is based on the measurement of a current change between two electrodes (source and drain) as a function of a voltage sweep between the source and the gate that is represented by a reference electrode, which is immersed in the electrolyte solution and provides a constant potential. In contrast to that, for EIS sensors, typically a change in the sensor's capacitance characteristic measured as function of the applied voltage (two-electrode arrangement between a reference electrode and the bulk semiconductor material) indicates a surface-potential change, e.g., induced by immobilized biomolecules (for a detailed explanation of the EIS functioning, see **Chapter 2.4.2**). The field effect itself (besides other factors) gives those sensors their ability and sensitivity for charge detection; the advantages are a fast readout, no necessity for labeling, possibility for cheap sensor fabrication, simple setup, and a low sample volume for detection. Disadvantages are due to the incompatible miniaturization of the reference electrode (because of the requirement of a certain geometrical size), it inheres drift and hysteresis, and it is difficult to integrate with other semiconductor circuit elements.

Anyhow, the advantages outweigh the disadvantages, thus EIS-sensor structures have been chosen as sensing platform for the DNA experiments in this thesis. In order to measure high sensor signals during the DNA-hybridization event with field-effect (EIS) sensors, the molecules must be located close to the sensor surface. Probe DNA molecules can be immobilized to the surfaces via different methods. Two commonly used ways are the covalent binding of a functionalized group (such as silane) to the surface [48], and the adsorptive binding by electrostatic attraction between the DNA and the (functionalized) surface [49]. Although the binding strength of covalently bounded molecules is very high (which makes the whole system generally more robust), complicated and time-consuming chemical reactions are usually involved for the covalent attachment method. Another disadvantage here is that the probe DNA is usually immobilized in a perpendicular manner (actually, the DNA is not fully 90° perpendicular-oriented but rather between 40° and 60° [50], see **Figure 1.1**): Therefore, the up-tilted DNA (and also their intrinsic charges) has a larger distance to the sensor surface. These charges contribute less to the charge redistribution in the semiconductor resulting in a reduced measurement signal: This consequences a charge-screening effect induced by oppositely charged counterions. Briefly, only charges within the so-called Debye-screening length λ_D have a significant impact on the charge redistribution in the semiconductor. More details are presented in the theory section, **Chapter 2**. In contrast to the covalent binding, adsorptive binding has the advantage that the DNA can be flat-oriented on the sensor surface (see **Figure 1.1**). Therefore, the intrinsic charges are located closer to the surface, leading to a higher signal generation. Adsorptive binding of DNA, however, requires a surface modification with a

positively charged layer if the sensor surface is negatively charged (for most oxides at neutral pH).

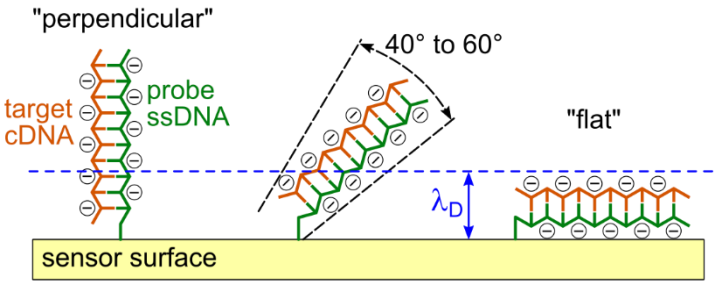

Figure 1.1: Different binding angles for covalently attached dsDNA (the "flat" condition also represents schematically an adsorptively immobilized DNA molecule).

In this thesis, poly(allylamine-hydrochloride) (PAH) was chosen as polyelectrolyte (PE) for sensor modification; it has no toxic or cancerogenic threat for human and its positive charge allows the binding of DNA in a flat-oriented manner, which leads to a high sensor signal. In a study of Manalis' group, a similar approach was carried out in which poly-L-lysine (PLL) was used for the sensor modification for EIS sensors to detect DNA [49]. Here, output signals of only about 2 mV were measured; even after repeated application of multiple sensor functionalization layers, always 2 mV was determined at every DNA-detection step: The measured signal amplitude was independent from the layer number, which is somehow difficult to explain considering the Debye-screening effect. They improved their setup by sensor implementation into a microfluidic system, which enables to perform an on-chip polymerase-chain-reaction (PCR) [51]. After that, a sensor signal of ~10 mV was measured before and after the thermocycle process with PLL-modified EIS sensors.

A signal generation in EIS sensors can also be achieved by illumination of the semiconductor with a light beam, resulting in a LAPS system. A more detailed explanation of this technology is given in **Chapter 2.5**. Briefly, a charge separation in the semiconductor material is achieved by introducing modulated light of a specific wavelength. When applying a voltage to the LAPS structure, a photocurrent is generated and can be read out by an electronic system. The amplitude of the generated photocurrent is dependent on the charge distribution in the semiconductor, which also depends on the surface potential of the sensor. In this way, DNA-detection experiments can also be carried out [52]. LAPS sensors have the advantage to detect surface-potential changes in a spatially resolved manner. This gives the possibility to realize a sensor array, which allows simultaneous measurements of multiple spots. In this thesis, PAH-modified LAPS was utilized as DNA sensors.

1.2.3 Commercially available DNA-detection devices

A short list of commercially available DNA-based detection devices gives an insight on which and how the DNA-detection technology is used and realized: The highest estimated demand on DNA-based detection devices lies in the medical and laboratory field [53, 54].

The most important requirement for many DNA-detection platforms is the ability to perform point-of-care tests. Selected commercially available DNA-detection devices are overviewed subsequently.

- *Unyvero A50 Analyzer*
  (Curetis GmbH, Holzgerlingen, Germany)

The *Unyvero A50 Analyzer* allows the detection of more than 100 different common pathogens (which covers over 90% of all cases of infectious diseases including clinically most relevant antibiotic resistant bacteria). The obtained sample is given onto a cartridge. Here, the process starts with a DNA-purification step, followed by a PCR-amplification step. The detection is carried out by means of a fluorescence-signal detection of fluorescence-labeled amplicons. Using a blood sample also enables to detect several types of *Mycobacteria* (but no *Mycobacteria tuberculosis*). The time for a complete detection is about 4-5 h. Since the weight of more than 68 kg and the geometric dimensions of more than 500 mm x 500 mm x 500 mm the intended place of use for this device is in clinics and hospitals and not suited for portable point-of-care or field-tests.

- *MultiFinder*
  (PathoFinder B.V., Maastricht, Netherlands) [55]

The *MultiFinder's* detection method is based on a melting-curve analysis. DNA from a wide scope of target pathogens such as different types of influenza, *Bordetella pertussis* or *Legionella pneumophila*, can be detected. First, the target DNA in solution is hybridized with two unique probe molecules (primers) with a short complementary sequence, which correlates to the respective pathogen's genome. The probe molecules are joined together with a ligation step [56]. Then, the new DNA strand is amplified and has a unique length (due to the chosen primers), which can be clearly identified by size diffraction. This technique offers the possibility to identify up to 22 different pathogenic RNA or DNA targets within 6 hours. This kit still requires additional equipment, like a reader or sensing device.

- *IonTorrent*
  (Thermo Fisher Scientific, Waltham, Massachusetts, USA)

The *IonTorrent* device is a DNA-sequence analyzer based on field-effect detection of generated H^+-ions during the DNA-amplification process. The device is equipped with an ISFET sensor and a microfluidic channel. A DNA with unknown sequence is identified indirectly by building up the complementary strand: Solved nucleotides (A, C, T, G) pass the sensor alternately and participate on the strand-elongation process. Each type of nucleotide that is incorporated into the elongating DNA strand releases one H^+-ion, resulting in a pH change of 0.02 for each nucleotide under the given circumstances (buffer capacity, temperature, etc.). Observing the pH value during exposition to the respective nucleotide gives the exact sequence [57–60]. Although this complete procedure requires a complicated preparation process, a complete genome sequencing can be performed for less than 1,000 US$. This device gives full answer on the sequence but is not recommended and suited as point-of-care tool for fast DNA detection.

- *Mobinostics Analyzer*
  (Boehringer Ingelheim, Ingelheim am Rhein, Germany) [61]

The *Mobinostics* platform is a battery-driven, portable measurement device with a functionality scope comparable to a complete diagnostic laboratory. The intend of use is to support a veterinarian in making and confirming a diagnose for infected animals in field. A taken sample (blood or saliva) is directly put into a cartridge, which is designed as disposable to prevent spreading of infected material. No delivery of the sample to a laboratory is required. The genetic material (DNA) is amplified by a PCR and detected electronically by means of a biochip. All necessary liquids and equipment are already prepared ready-to-use and deployed onto the cartridge. This mobile device is suited for field-testing but its detection scope does not cover human diseases.

- *PanPlex* [62], *Vivalytic Analyser* [63]
  (Fraunhofer Institute for Microengineering and Microsystems (IMM), Mainz, Germany),
  (Bosch Healthcare Solutions GmbH, Waiblingen, Germany)

The *PanPlex* device is a fully automated analyzing tool for *Influenza* infection. A sample is taken by a swab and put into a lysis buffer in which the pathogens transferred into liquid phase. After the lysis, a PCR reaction amplifies the genomic material. The detection is based on the TaqMan probe-fluorescence method during the amplification process. This fluorescence-quencher combined method is described in **Chapter 2.6**.

The *vivalytic analyser* is a commercialized all-in-one solution for the detection of respective pathogens. It is based on the same detection principle used in the *PanPlex* device, the TaqMan probe-fluorescence method. The lysis in this device is ultrasonically supported. Up to 14 different types of viruses and 8 types of bacteria can be detected by one of this RNA/DNA-based tests.

- *ID Now*
  (Abbott, North Chicago, Illinois, USA)

Abbotts *ID Now* device is a molecular diagnostic platform for the qualitative detection of infectious diseases [64]. Currently (mid 2020), three different test assays are available for the *ID Now*: “STREP A” for group A *Streptococcus* [65], “INFLUENZA A & B2” for *Influenza* infection [66] and “RSV” for the respiratory syncytial virus [67]. Because of the rare selection of assays, the fields of application are yet only covering the testing of respiratory diseases. The *ID Now* instrument utilizes an isothermal amplification. Only a single temperature level (around 60 °C) and no thermal cycling is required to perform the amplification. However, instead of using only two primers, like for PCR, the isothermal amplification requires typically four to six different primers. A swap with the sample material is inserted into a receiver and stirred for about 10 seconds. Afterwards, the prepared sample is manually transferred to a cartridge in which the amplification and detection is performed. Besides of the target nucleic acid, an internal control is also implemented in the cartridge. The detection is carried out by optical measurement of the fluorescence signal induced by a fluorescence-labeled molecular beacon that is designed to specifically identify the amplified targets. The complete test can be run in less than 15 min. The cycle threshold can be reached even faster for positive samples, which means that a

positive result can be detected within 2 minutes (for the *Influenza* assay) [66]. The available assays for the *ID Now* have a sensitivity of ~93% to ~98%, for *Influenza* B2 even 100%.

The presented products are in market or planned to launch soon; from this short overview, one can conclude three resumes: 1) there is in increasing demand and interest in DNA-based sensing devices, 2) a PCR or isothermal amplification (which is the main determined part in the complete detection chain) is usually performed before or during the DNA detection, 3) there is obviously still no favorable approach for detection established yet: fluorescence-based, melting-curve analyses, field-effect-based and other electronic methods are used.

1.3 MOTIVATION, AIMS AND OUTLINE

1.3.1 Motivation and aims of this thesis

A steadily increasing demand on solutions for development and realization of point-of-care platforms based on DNA detection for the identification of diseases exists (compare **Chapter 1.2.3**). A common and very critical disease for humans is the lung disease tuberculosis (TB). It is caused by the pathogenic bacteria *Mycobacterium tuberculosis*, which was discovered and described by Robert Koch in 1882 [68]. According to the World Tuberculosis Report 2018 [69], TB is within the top-ten causes of death and the leading cause of death from a single infectious agent (above HIV/AIDS). Approximately 1.3 million TB-death cases were registered among HIV-negative people in 2017, and additional 0.3 million TB deaths from TB among HIV-positive people. Another serious situation is given by the fact that approximately 1.7 billion people (which is 23% of the complete world's human population!) are estimated to have a latent TB infection. These people have a higher risk for developing an active TB disease. A major reason for these high numbers is an increased antimicrobial resistance which is caused, among others, by wrong medication. Around 0.5 million people developed a resistant TB, 82% of these even had a multi-resistant form of TB.

There is a tremendous global interest in curing this disease from all infected human beings, so that all states of the UN and WHO have declared and committed to achieve the ending of tuberculosis epidemic by 2030 [69]. In order to achieve this goal, a correct and direct medication must be applied to the infected people. Thus, a wide-scaled and precise identification and diagnosis – especially in developing countries – is necessary. This can be ideally achieved by utilizing point-of-care instruments, which are small, light, flexible and mobile and inhere a fast, simple and inexpensive but reliable diagnosis mechanism based on DNA detection.

Motivated by the current problems and challenges described above, the aim of this work was to develop a detection technique, which is capable for the specific sensing of solved target DNA from a bacterial origin and can be implemented and fulfill the requirements for a point-of-care device. For the detection, the label-free sensing method with field-effect EIS sensors for liquid analytes was chosen because of their particular attributes on fast, simple and cheap realization and measurement. In order to keep the fabrication of the EIS as simple as possible, SiO_2 was chosen as oxide, since it can be easily generated due to a

simple oxidation process and does not require additional coating or modification steps. The surface-potential-sensitive EIS chips are modified with a polyelectrolyte layer in order to ensure a flat-oriented DNA binding, resulting in a higher output signal induced by the negative intrinsic charge of DNA. Fragments of the tuberculosis genome were chosen as example sequence for the tested DNA.

1.3.2 Outline of this thesis

This work is highly interdisciplinary and combines aspects and influences from different scientific fields, like (surface-)chemistry, solid-state- and semiconductor physics, electronics, (micro)biotechnology and genomics.

In **Chapter 2** (Theory), the theoretical fundamentals are described, which includes the explanation of the physical and chemical properties of DNA and the surface modification that allows the surface binding of DNA. This binding is necessary to detect DNA molecules and the hybridization event. Furthermore, the electrochemical signal generation of the field-effect EIS sensors is explained in detail and compared with LAPS systems. At the end of the theory chapter, the functioning of the fluorescence-reference method is briefly described. A reference method is necessary to verify the electrochemical measurement results of the EIS sensors and ensure the reliability of the experiments.

The identification of target DNA by means of field-effect-based label-free EIS sensors relies on the "classical" identification of the hybridization event. There are two ways to recognize this event: Firstly, the DNA can be indirectly detected from the solution (by so-called in-solution hybridization); thereby an immobilization of complete (already hybridized) dsDNA molecules on the sensor surface is realized and detected. Alternatively, the hybridization can occur directly on the sensor surface (so-called in-situ- or on-chip hybridization), by combination with previously immobilization probe ssDNA.

For both types of recognition, a suitable protocol must be developed in which DNA can bind to the sensor surface. The first version of this protocol was investigated and described in **Chapter 3**, the protocol optimization was then described in the following publications. The chosen EIS-sensor structure has been investigated with regard to its capability of surface modification with a layer of positively charged PAH that allows a subsequent binding of 20 bp dsDNA. In contrast to the most common immobilization techniques, in which the DNA is orientated in a perpendicular manner, with the used adsorption method, the DNA lays flat on the sensor surface. This has a major effect on the signal amplitude, since EIS sensors are sensitive for detection of charge changes at the sensor surface. The intrinsic charges of the flat-oriented DNA contribute stronger to the sensor signal than for perpendicular-oriented molecules. Further details and explanation of the theoretical context can be found in **Chapter 2.3**. Special attention was focused during the development of the surface-modification step on the fact, that the protocol should be also quick, easy and inexpensive to perform; in addition, it would be also preferable if the protocol requires only non-hazard/non-toxic chemicals. First experiments, in which short (20 bp) dsDNA molecules were immobilized onto the PAH-coated sensor surface, were performed: The results are presented in **Chapter 3**. Both, the sensor modification as well as the DNA-immobilization protocol were proven electrochemically by means of C–V- and ConCap-measuring modes.

First attempts to implement the developed protocol of dsDNA detection, including the previous PAH modification of the surface, into a LAPS system, was studied in **Chapter 4**. This approach was examined because LAPS technology offers certain advantages – especially in terms of parallelization due to the possibility of spatially resolved measurements. This could be useful for further cost reduction. In addition, the short DNA sequence was extended from previously 20 bp to 52 bp. This extension was made to mimic more realistic conditions, since a real detectable sample is usually obtained after a PCR reaction, which requires a longer DNA strand than 20 bp (for specific binding of the primers). A comparison between the signal changes in LAPS- and EIS setups can be done, since both sensing devices are based on field-effect surface-potential charge detection. In this experiment, solutions containing different concentrations of dsDNA have been investigated. The sensitivity and the lower detection limit could also be determined.

After the development of the modification protocol for DNA detection (which allows a simple and fast sensing of PAH/DNA immobilization in low ionic-strength solution), in **Chapter 5** the protocol has been adapted for the detection of the on-chip hybridization event. For this purpose, the sensors were exposed to a solution containing target cDNA molecules after an immobilization step of ssDNA onto the PAH-modified surface. Prior to the addition of the target hybridization-solution, the surface was blocked to prevent non-specific attachment of the target cDNA. All processes were electrochemically measured and analyzed. In addition, to verify the specificity of the developed procedure, the sensor was exposed to a solution containing non-complementary DNA (ncDNA) prior to the hybridization step. A large sensor signal after incubation in cDNA solution is expected. In contrast to that, the measurement after incubated ncDNA solution should result in a small or even no signal change. The comparison of these test results can also serve as an indicator of selectivity.

In **Chapter 6**, the reusability of the biosensor chip was investigated. A reusability of a sensor device (e.g., by a surface regeneration step) allows to increase the number of measurements per chip and thus, increases the measured throughput, which can lead to a further reduction of material and costs. Up to five subsequent DNA measurements with one single chip were investigated. In detail: The binding of ssDNA, dsDNA as well as the hybridization of cDNA to previously attached probe ssDNA was carried out and tried to recorded for five times each. The electrochemical measurements can indicate the respective surface-potential changes. In addition, investigations were carried out with respect to the measured signal change as a function of the ionic strength of the solution, which can demonstrate the influence of the Debye-screening effect.

In **Chapter 7**, a “positive sample” (target cDNA solved in PCR-buffer solution containing all necessary substances to perform a PCR) was examined with the PAH-modified EIS sensors. Such solutions mimic more realistic conditions, implying real identification of pathogens from a sample material. For determination of the selectivity, experiments have been carried out in which the PAH-modified sensors were incubated in a “negative sample” solution (containing no target DNA, but all substances for a PCR reaction, including primers). Here, a significant difference between the positive (large signal) and negative (small signal) sample is expected. A significant difference can be used as indicator for a proper selectivity of the method. Furthermore, the signal response after incubation of a concentration range of target cDNA was also investigated to determine the

sensitivity and lower detection limit. Finally, experiments were performed in which the PAH-modified EIS sensor was exposed to real samples of tuberculosis DNA, which was extracted from a tuberculosis-spiked sputum sample and amplified by means of PCR. This final and most realistic experiment has been performed in order to prove the practical applicability of the developed procedure.

REFERENCES

[1] C. Szalai, V. Laszlo, E. Pap, A. Falus, F. Oberfrank: *Medical Genetics and Genomics*, Budapest University of Technology and Economics, Budapest, Hungary (2016).

[2] R. Renneberg, V. Berkling, V. Loroch: *Biotechnology for Beginners (2nd Edition)*, Academic Press, New York, USA (2016).

[3] R.C. Elston: *Probability and paternity testing*, Am. J. Hum. Genet. 39 (1986) 112–122.

[4] L. Kaiser, G. Sever: *Paternity testing: I. calculation of paternity indexes*, Am. J. Med. Genet. 15 (1983) 323–329.

[5] X.H. Liao, T.S. Lau, K.F.N. Ngan, J. Wang: *Deduction of paternity index from DNA mixture*, Forensic Sci. Int. 128 (2002) 105–107.

[6] E.D. Green, M.S. Guyer: *Charting a course for genomic medicine from base pairs to bedside*, Nature 470 (2011) 204–213.

[7] The ENCODE Project Consortium: *An integrated encyclopedia of DNA elements in the human genome*, Nature 489 (2012) 57–74.

[8] E.M. Southern: *Detection of specific sequences among DNA fragments separated by gel electrophoresis*, J. Mol. Biol. 98 (1975) 503–517.

[9] T.G. Drummond, M.G. Hill, J.K. Barton: *Electrochemical DNA sensors*, Nat. Biotechnol. 21 (2003) 1192–1199.

[10] J. Wang: *Electrochemical nucleic acid biosensors*, Anal. Chim. Acta. 469 (2002) 63–71.

[11] B. Van Grinsven, K. Eersels, M. Peeters, P. Losada-Pérez, T. Vandenryt, T.J. Cleij, P. Wagner: *The heat-transfer method: A versatile low-cost, label-free, fast, and user-friendly readout platform for biosensor applications*, ACS Appl. Mater. Interfaces. 6 (2014) 13309–13318.

[12] J.R. Epstein, I. Biran, D.R. Walt: *Fluorescence-based nucleic acid detection and microarrays*, Anal. Chim. Acta 469 (2002) 3–36.

[13] P. de-los-Santos-Alvarez, M.J. Lobo-Castanon, A.J. Miranda-Ordieres, P. Tunon-Blanco: *Current strategies for electrochemical detection of DNA with solid electrodes*, Anal. Bioanal. Chem. 378 (2004) 104–118.

[14] D. Grieshaber, R. MacKenzie, J. Vörös, E. Reimhult: *Electrochemical biosensors – sensor principles and architectures*, Sensors 8 (2008) 1400–1458.

[15] F.R.R. Teles, L.P. Fonseca: *Trends in DNA biosensors*, Talanta 77 (2008) 606–623.

[16] J. Pivetal, G. Ciuta, M. Frenea-Robin, N. Haddour, N.M. Dempsey, F. Dumas-Bouchiat, P. Simonet: *Magnetic nanoparticle DNA labeling for individual bacterial cell detection and recovery*, J. Microbiol. Methods 107 (2014) 84–91.

[17] J. Reichert, A. Csaki, J. Köhler, W. Fritzsche: *Chip-based optical detection of DNA hybridization by means of nanobead labeling*, Anal. Chem. 72 (2000) 6025–6029.

[18] J.I.A. Rashid, N.A. Yusof: *The strategies of DNA immobilization and hybridization detection mechanism in the construction of electrochemical DNA sensor: A review*, Sens. Biosensing. Res. 16 (2017) 19–31.

[19] S.O. Kelley, J.K. Barton: *Electrochemistry of methylene blue bound to a DNA-modified electrode*, Bioconjugate Chem. 8 (1997) 31–37.

[20] K.M. Millan, S.R. Mikkelsen: *Sequence-selective biosensor for DNA based on electroactive hybridization indicators*, Anal. Chem. 65 (1993) 2317–2323.

[21] A. Walter, J. Wu, G.U. Flechsig, D.A. Haake, J. Wang: *Redox cycling amplified electrochemical detection of DNA hybridization: Application to pathogen E. coli bacterial RNA*, Anal. Chim. Acta 689 (2011) 29–33.

[22] G.F. Miranda, L. Feng, S.C.-C. Shiu, R.M. Dirkzwager, Y.-W. Cheung, J.A. Tanner, M.J. Schöning, A. Offenhäusser, D. Mayer: *Aptamer-based electrochemical biosensor for highly sensitive and selective malaria detection with adjustable dynamic response range and reusability*, Sens. Actuators B 225 (2018) 235–243.

[23] A.B. Steel, R.L. Levicky, T.M. Herne, M.J. Tarlov: *Immobilization of nucleic acids at solid surfaces: Effect of oligonucleotide length on layer assembly*, Biophys. J. 79 (2000) 975–981.

[24] S. Vogt, Q. Su, C. Gutiérrez-Sánchez, G. Nöll: *Critical view on electrochemical impedance spectroscopy using the ferri/ferrocyanide redox couple at gold electrodes*, Anal. Chem. 88 (2016) 4383–4390.

[25] D. Goncalves, D.M. Prazeres, V. Chu, J.P. Conde: *Detection of DNA and proteins using amorphous silicon ion-sensitive thin-film field effect transistors*, Biosens. Bioelectron. 24 (2008) 545–551.

[26] S. Ingebrandt, A. Offenhäusser: *Label-free detection of DNA using field-effect transistors*, Phys. Status Solidi A 203 (2006) 3399–3411.

[27] M.J. Schöning, A. Poghossian: *Bio FEDs (field-effect devices): State-of-the-art and new directions*, Electroanal. 18 (2006) 1893–1900.

[28] A. Poghossian, M.J. Schöning: *Silicon-based chemical and biological field-effect sensors (edited by C.A. Grimes, E.C. Dickey, M.V. Pishko),* in Encyclopedia of sensors 10, American Scientific Publishers, Santa Clarita, California, USA (2006).

[29] A. Poghossian, A. Cherstvy, S. Ingebrandt, A. Offenhäusser, M.J. Schöning, *Possibilities and limitations of label-free detection of DNA hybridization with field-effect-based devices*, Sens. Actuators B 111–112 (2005) 470–480.

[30] M.S. Murib, W.S. Yeap, Y. Eurlings, B. van Grinsven, H.-G. Boyen, B. Conings, L. Michiels, M. Ameloot, R. Carleer, J. Warmer, P. Kaul, K. Haenen, M.J. Schöning, W. de Ceuninck, P. Wagner: *Heat-transfer based characterization of DNA on synthetic sapphire chips*, Sens. Actuators B 230 (2016) 260–271.

[31] P. Cornelis, T. Vandenryt, G. Wackers, E. Kellens, P. Losada-Pérez, R. Thoelen, W. De Ceuninck, K. Eersels, S. Drijkoningen, K. Haenen, M. Peeters, B. van Grinsven, P. Wagner: *Heat transfer resistance as a tool to quantify hybridization efficiency of DNA on a nanocrystalline diamond surface*, Diamond Relat. Mater. 48 (2014) 32–36.

[32] T.T. Goodrich, H.J. Lee, R.M. Corn: *Enzymatically amplified surface plasmon resonance imaging method using RNase H and RNA microarrays for the ultrasensitive detection of nucleic acids*, Anal. Chem. 76 (2004) 6173–6178.

[33] M. Riedel, J. Kartchemnik, M.J. Schöning, F. Lisdat: *Impedimetric DNA detection – steps forward to sensorial application*, Anal. Chem. 86 (2014) 7867–7874.

[34] J. Kafka, O. Pänke, B. Abendroth, F. Lisdat: *A label-free DNA sensor based on impedance spectroscopy*, Electrochim. Acta 53 (2008) 7467–7474.

[35] S. Pan, L. Rothberg: *Chemical control of electrode functionalization for detection of DNA hybridization by electrochemical impedance spectroscopy*, Langmuir 21 (2005) 1022–1027.

[36] M. Matsishin, A. Rachkov, A. Errachid, S. Dzyadevych, A. Soldatkin: *Development of impedimetric DNA biosensor for selective detection and discrimination of oligonucleotide sequences of the rpoB gene of Mycobacterium tuberculosis*, Sens. Actuators B 222 (2016) 1152–1158.

[37] M. Schwartz, T.C. Nguyen, X.T. Vu, P. Wagner, R. Thoelen, S. Ingebrandt: *Impedimetric sensing of DNA with silicon nanowire transistors as alternative transducer principle*, Phys. Status Solidi A 215 (2018) 1700740.

[38] S. Vigneshvar, C.C. Sudhakumari, B. Senthilkumaran, H. Prakash: *Recent advances in biosensor technology for potential applications – an overview*, Front. Bioeng. Biotechnol. 4 (2016) 1–9.

[39] B. Veigas, E. Fortunato, P. Baptista: *Field effect sensors for nucleic acid detection: Recent advances and future perspectives*, Sensors 15 (2015) 10380–10398.

[40] C.-S. Lee, S.K. Kim, M. Kim: *Ion-sensitive field-effect transistor for biological sensing*, Sensors 9 (2009) 7111–7131.

[41] R.M. Penner: *Chemical sensing with nanowires*, Annu. Rev. Anal. Chem. 5 (2012) 461–485.

[42] Z. Gao, A. Agarwal, A.D. Trigg, N. Singh, C. Fang, C.H. Tung, Y. Fan, K.D. Buddharaju, J. Kong: *Silicon nanowire arrays for label-free detection of DNA*, Anal. Chem. 79 (2007) 3291–3297.

[43] C. Wu, T. Bronder, A. Poghossian, C.F. Werner, M. Bäcker, M.J. Schöning: *Label-free electrical detection of DNA with a multi-spot LAPS: First step towards light-addressable DNA chips*, Phys. Status Solidi A 211 (2014) 1423–1428.

[44] C. Wu, T. Bronder, A. Poghossian, C.F. Werner, M.J. Schöning: *Label-free detection of DNA using a light-addressable potentiometric sensor modified with a positively charged polyelectrolyte layer*, Nanoscale 7 (2015) 6143–6150.

[45] J. Wang, L. Du, S. Krause, C. Wu, P. Wang: *Surface modification and construction of LAPS towards biosensing applications*, Sens. Actuators B 265 (2018) 161–173.

[46] J. Wang, Y. Zhou, M. Watkinson, J. Gautrot, S. Krause: *High-sensitivity light-addressable potentiometric sensors using silicon on sapphire functionalized with self-assembled organic monolayers*, Sens. Actuators B 209 (2015) 230–236.

[47] M.H. Abouzar, A. Poghossian, A.G. Cherstvy, A.M. Pedraza, S. Ingebrandt, M.J. Schöning: *Label-free electrical detection of DNA by means of field-effect nanoplate capacitors: Experiments and modeling*, Phys. Status Solidi A 209 (2012) 925–934.

[48] F. Luderer, U. Walschus: *Immobilization of oligonucleotides for biochemical sensing by self-assembled monolayers: Thiol-organic bonding on gold and silanization on silica surfaces,* in Immobilisation of DNA on Chips I, Springer-Verlag, Berlin, Germany (2005).

[49] J. Fritz, E.B. Cooper, S. Gaudet, P.K. Sorger, S.R. Manalis: *Electronic detection of DNA by its intrinsic molecular charge*, Proc. Natl. Acad. Sci. U.S.A. 99 (2002) 14142–14146.

[50] S. Wenmackers, V. Vermeeren, M. vandeVen, M. Ameloot, N. Bijnens, K. Haenen, L. Michiels, P. Wagner: *Diamond-based DNA sensors: Surface functionalization and read-out strategies*, Phys. Status Solidi A 206 (2009) 391–408.

[51] C.S.J. Hou, M. Godin, K. Payer, R. Chakrabarti, S.R. Manalis: *Integrated microelectronic device for label-free nucleic acid amplification and detection*, Lab Chip 7 (2007) 347–354.

[52] J. Wang, Y. Zhou, M. Watkinson, J. Gautrot, S. Krause: *High-sensitivity light-addressable potentiometric sensors using silicon on sapphire functionalised with self-assembled organic monolayers*, Sens. Actuators B 209 (2015) 230–236.

[53] J. Gray, L.J. Coupland: *The increasing application of multiplex nucleic acid detection tests to the diagnosis of syndromic infections*, Epidemiol. Infect. 142 (2014) 1–11.

[54] S. Cagnin, M. Caraballo, C. Guiducci, P. Martini, M. Ross, M. Santaana, D. Danley, T. West, G. Lanfranchi: *Overview of electrochemical DNA biosensors: New approaches to detect the expression of life*, Sensors 9 (2009) 3122–3148.

[55] http://www.pathofinder.com, information downloaded from internet: 07. March 2019.

[56] M. Reijans, G. Dingemans, C.H. Klaassen, J.F. Meis, J. Keijdener, B. Mulders, K. Eadie, W. van Leeuwen, A. van Belkum, A.M. Horrevorts, G. Simons: *RespiFinder: A new multiparameter test to differentially identify fifteen respiratory viruses*, J. Clin. Microbiol. 46 (2008) 1232–1240.

[57] J.M. Rothberg, W. Hinz, T.M. Rearick, J. Schultz, W. Mileski, M. Davey, J.H. Leamon, K. Johnson, M.J. Milgrew, M. Edwards, J. Hoon, J.F. Simons, D. Marran, J.W. Myers, J.F. Davidson, A. Branting, J.R. Nobile, B.P. Puc, D. Light, T.A. Clark, M. Huber, J.T. Branciforte, I.B. Stoner, S.E. Cawley, M. Lyons, Y. Fu, N. Homer, M. Sedova, X. Miao, B. Reed, J. Sabina, E. Feierstein, M. Schorn, M. Alanjary, E. Dimalanta, D. Dressman, R. Kasinskas, T. Sokolsky, J.A. Fidanza, E. Namsaraev, K.J. McKernan, A. Williams, G.T. Roth, J. Bustillo: *An integrated semiconductor device enabling non-optical genome sequencing*, Nature 475 (2011) 348–352.

[58] C. Toumazou, L.M. Shepherd, S.C. Reed, G.I. Chen, A. Patel, D.M. Garner, C.-J.A. Wang, C.-P. Ou, K. Amin-Desai, P. Athanasiou, H. Bai, I.M.Q. Brizido, B. Caldwell, D. Coomber-Alford, P. Georgiou, K.S. Jordan, J.C. Joyce, M. La Mura, D. Morley, S. Sathyavruthan, S. Temelso, R.E. Thomas, L. Zhang: *Simultaneous DNA amplification and detection using a pH-sensing semiconductor system*, Nat. Methods 10 (2013) 641–646.

[59] K. Melpomeni, C. Toumazou: *Semiconductor technology for early detection of DNA methylation for cancer: From concept to practice*, Sens. Actuators B 178 (2013) 572–580.
[60] M. Kalofonou, P. Georgiou, C.-P. Ou, C. Toumazou: *An ISFET based translinear sensor for DNA methylation detection*, Sens. Actuators B 161 (2012) 156–162.
[61] https://mobinostics.com, information downloaded from internet: 07. March 2019.
[62] https://www.imm.fraunhofer.de, information downloaded from internet: 08. March 2019.
[63] https://www.bosch-vivalytic.com, information downloaded from internet: 08. March 2019.
[64] ID NOW Instrument User Manual Non-US (English), Abbott (2019), https://ensur.invmed.com/ensur/broker/ensurbroker.aspx?code=INNAT000&cs=27237221, information downloaded from internet: 26. June 2020.
[65] ID NOW Strep A 2 Product Sheet EME (English), Abbott (2019), https://ensur.invmed.com/ensur/contentAction.aspx?key=ensur.485871.S2R4E4A3.20190920.9289.4226651, information downloaded from internet: 26. June 2020.
[66] ID NOW Influenza A & B 2 Product Sheet EME (English), Abbott (2019), https://ensur.invmed.com/ensur/contentAction.aspx?key=ensur.484086.S2R4E4A3.20190729.9289.4250367, information downloaded from internet: 26. June 2020.
[67] ID NOW RSV Product Sheet EME (English), Abbott (2019), https://ensur.invmed.com/ensur/contentAction.aspx?key=ensur.490502.S2R4E4A3.20190918.9289.4236210, information downloaded from internet: 26. June 2020.
[68] Robert Koch: *Die Aetiologie der Tuberculose*, Berliner Klinische Wochenschrift 19 (1882) 221–230.
[69] World Health Organization: *Global Tuberculosis Report* 2018; WHO: Geneva (2018).

2 Theory

In this chapter, the theoretical principles of the used methods and techniques are described. First, general information about DNA molecules and their binding characteristics are given. Then, the surface-modification procedure is presented, which is a fundamental part of this thesis and later DNA-detection process. Then, the functioning and sensing principle of EIS sensors and LAPS are introduced. Finally, different mechanisms of fluorescence detection as a reference method for DNA sensing are explained.

2.1 Structure and properties of the DNA molecule

DNA is a chain-like molecule composed of linked nucleotides (monomers). The DNA nucleotides consist of three sub-units: A nitrogenous base, a 5-carbon sugar (deoxyribose), and a phosphate group. In a ssDNA, two nucleotides are connected to each other by a covalent bond between the phosphate group of the first nucleotide and the sugar molecule of the second nucleotide; then, with the phosphate residue of the second nucleotide and the sugar of the third nucleotide etc., resulting in a continuing chain. This interlinked phosphate-sugar arrangement is the so-called DNA backbone. In solution, the backbone is negatively charged due to a dissociation of a proton from the phosphate residue [1, 2].

Native DNA has a double-helix structure of two antiparallel ssDNA molecules forming a double-stranded DNA (dsDNA). Impressive images of a real DNA double helix can be seen, e.g., in [3]. The binding between both single strands is called hybridization and relies on base pairing of the four different types of nucleotides (adenine (A), cytosine (C), guanine (G) and thymine (T)), which only differ in the nitrogenous base. Preferably, A with T and C with G are building hydrogen-bond base pairs resulting in a usually strict complementarity between both ssDNA molecules [4]. As a consequence, it enables only the binding of two ssDNA chains with correct (complementary) nucleotide sequence and prevents the binding with a non-complementary ssDNA. The hybridization-based recognition is a fundamental mechanism, which opens numerous opportunities in which the identification of certain species or individuals can be carried out [5] (see also **Chapter 1.1**). This hybridization-based technique of identification of species can be used in scientific analytics, especially in forensic DNA tests, for the diagnosis of diseases, medical diagnostics and many more [6]. The nucleotide base order codes the genomic information of an organism. As an interesting fact, due to the very low density of DNA, 1 g of DNA can store 215 petabytes (a PB is one million gigabyte) of data – this is by far the densest data storage capacity ever reached [7]. DNA double strands can exist in different structural forms such as: A-DNA, B-DNA and Z-DNA. B-DNA is the most relevant form. This DNA type has a diameter of ~2 nm, and has a right-handed coil with 10 bp per coil twist, where one twist has a length of 3.4 nm.

For DNA sensing, the most important mechanism is the hybridization event, which allows specific combination of complementary sequences to form a double-stranded DNA molecule. The successfulness of a hybridization reaction depends – besides on the

sequence – on other important factors, mainly the temperature and composition of the solution (especially, the salt concentration and presence of inhibitors [8, 9]). In general, the hybridization conditions are summarized under the term stringency: A high stringency (given by a low salt concentration and high temperature) leads to a hybridization of only highly complementary DNA, while low-stringency conditions (high salt concentration and low temperature) can cause a binding of even not fully complementary DNA (target DNA strand contains some mismatches) [10].

In this context, another very important parameter is the melting temperature (T_m); it indicates the temperature at which 50% of all DNA strands in solution are hybridized while 50% are denaturated. Melting temperature analysis can also be utilized to define the hybridization ratio of DNA molecules in single-stranded or double-stranded state for a certain temperature. T_m is often used for designing of primers for a PCR. Parameters such as the salt concentration or the complementarity of the DNA sequences have – same as for the stringency – an impact on T_m. The value for T_m can be precisely calculated according to the equations described in the following literature [11–15].

For a rough estimation, a very simplified calculation method according to Wallace's rule [16] can be carried out using **Eq. 2.1**:

$$T_m = 4(N_C + N_G) + 2(N_A + N_T), \qquad \textbf{Eq. 2.1}$$

N_A, N_G, N_C, and N_T describe the number of each nucleotide in the DNA sequence. Note that this equation was originally designed for DNA molecules with base lengths between 14 bp and 20 bp, which hybridize to immobilized DNA in buffer environment of 0.9 M NaCl.

Nowadays, melting analysis can be easily simulated using software models. The schematic in **Figure 2.1** shows a simulated melting curve for a 20 bp DNA molecule with identical sequence and conditions used in the publication of **Chapter 3**.

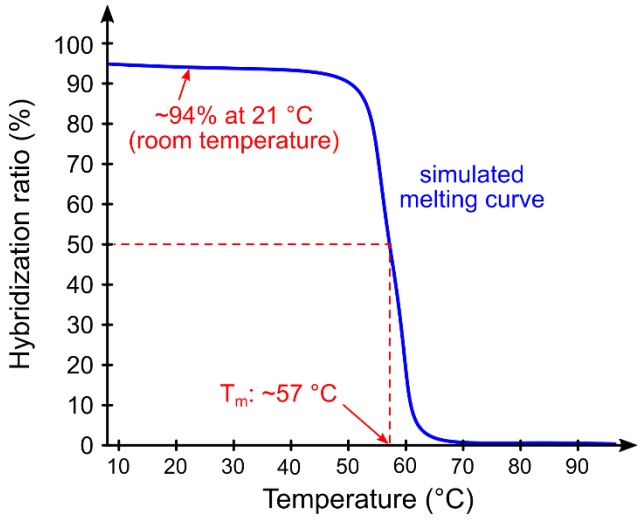

Figure 2.1: Example of a simulated melting temperature curve for a 20 bp DNA with indicated T_m. Above T_m, more DNA molecules are denaturated and in a single-stranded state, while below T_m, more DNA molecules become hybridized and forms double-stranded DNA.

The curve was simulated using the uMelt-simulation software developed by the Wittwer Lab for DNA analyses in Utah, USA [17]. One can see a very slight decrease of the curve with increasing temperature followed by a prompt drop at around 50 °C; here, the DNA double-strands start to denaturate. After a further temperature increase until around 63 °C, almost all DNA double-strands are denaturated. Using a simulated model, like the shown curve, can answer questions such as: Which hybridization ratio results for a given/chosen temperature? or is the DNA at room temperature already (and completely) denaturated? Please note that according to the simulation, a 20-mer ssDNA sequence with a complete ncDNA has a negative T_m even for salt concentrations of 1.5 M NaCl. Therefore, a hybridization between the designed ncDNA and ssDNA (in this work) at room temperature can be excluded.

In addition, divergences in hybridization-relevant parameters (in particular the temperature and salt concentration) can have a major influence on the hybridization event, which is desired to be detected in many DNA-sensing experiments [18, 19]. Therefore, it is highly important to know and elaborate the required parameters carefully and adequately.

2.2 THE ELECTROCHEMICAL DOUBLE-LAYER AT SOLID-LIQUID INTERFACES

To explain the molecular steady-state situation at solid-liquid interfaces, different models have been discussed in the past. Here, some fundamental and important events and chemical reactions are briefly presented.

If a metal electrode is immersed into a solution containing the respective metal ions, metal (cat)ions (from the solution) are getting reduced at the surface (electron decrease in the electrode) or metal atoms (of the electrode) oxidize to cations (electron increase in the electrode). Depending on the energetic favorability, the first or the second of these reactions will preferably happen. The electron increase/decrease results in a (local) potential change at the electrode. The potential of the electrode ($\varphi_{electrode}$) can also be influenced by applying an external voltage (therefore, a counter electrode is necessary) [20]. The electrode charge attracts ions from the solution; these ions located near to the surface, but keep their solvation shell. This results in a creation of a charge double-layer. It was first realized and published by Hermann Helmholtz in 1979 [21].

Two other effects also occur at the electrode/electrolyte interface: Polar water molecules attach the solid surface. Due to the differences in the electronegativity between the water-oxygen atoms and water-hydrogen atoms, electrons of the hydrogen atoms are located closer to the oxygen atoms resulting in an overall electrical polarity of the water molecules (dipole). Water molecules are oriented with respect on their own polarity and on the polarity of the electrode, as well as the electrode potential $\varphi_{electrode}$. Besides that, ions from the solution can directly attach the surface (by leaving their solvation shell, so-called "specifically adsorbed"). These three effects lead to a complex electrochemical double layer at the solid-liquid interface. According to Helmholtz, the potential of this double layer is linearly decreasing with increasing distance.

This model was supplemented and adjusted by consideration of the permanent thermal movement of ions based in the Debye-Hückel theory, resulting in the Gouy-Chapman

model, in which the full linear potential decrease is complemented with a part of exponential potential drop. Stern combines both models [22] to the Gouy-Chapman-Stern model. **Figure 2.2** illustrates the molecule arrangement at an electrode surface (here, negatively charged metal surface): The water-solvent molecules are arranged according to their partial charge. Cations are attracted to the surface and located in close proximity resulting in forming of the outer Helmholtz layer, at which a linear potential drop can be observed. The inner Helmholtz layer describes the distance between the electrode and the specifically adsorbed ions. In further distance, the potential decreases non-linearly due to diffusive transportation and other effects. These charge layers result in an electrochemical double-layer capacitance C_{dl}. The difference between the outer Helmholtz-layer potential φ_{oHL} and the electrolyte-solution potential $\varphi_{solution}$ is defined as Zeta potential ζ.

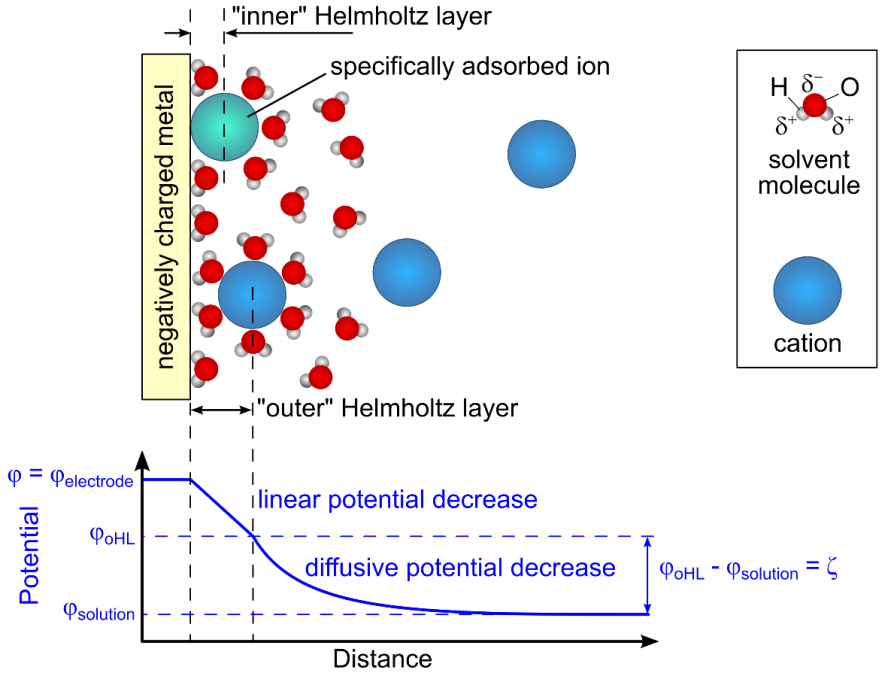

Figure 2.2: Schematic of the solvent molecule (water) and ion arrangement at a (negatively) charged surface. The respective potential over the distance is shown in the diagram below. Adapted from [20].

The Stern model of the electrochemical double layer was further complemented by scientists, e.g., David Grahame, who considered the non-linearity of permittivity and viscosity of the electrolyte solution [23]. However, a detailed explanation of all models would go beyond the scope of this chapter/thesis.

2.3 Surface Modification of a Silicon Dioxide-Layer with Polyelectrolytes

To ensure the detection of a surface-potential change, induced by the intrinsic molecular charge of DNA, first the DNA molecules must be immobilized onto the oxide surface of

the EIS-sensor chip. This is realized in this work by means of adsorptive binding of the DNA onto a layer of charged polyelectrolyte.

Polyelectrolytes diluted in solvents are chain-like molecules composed of monomers that carry ionizable chemical groups. The chemical groups can dissociate in polar solvents (such as water) and become charged [24]. Well-known polyelectrolytes are foremost the DNA molecule, but also poly(allylamine hydrochloride) (PAH), poly(sodium styrene sulfonate) (PSS), poly(ethylenimine) (PEI) and poly-L-lysine (PLL). They can be classified into strong and weak polyelectrolytes: PSS is a strong polyelectrolyte, since it is fully dissociated in solution; all monomers of the complete PSS chain are negatively charged [25, 26]. PAH is a weak polyelectrolyte; its charge ratio can vary and depend on different factors such as temperature and mainly the pH and the ionic strength of the solution [27]. A characteristic value for determination of the resulting charge is the isoelectric point (pH_{IEP}), the pH at which the net charge of the molecule is zero. Besides, the point-of-zero-charge (pH_{PZC}) defines the pH at which a surface has a zero net-charge [28]. A solution pH lower than the pH_{IEP}/pH_{PZC} leads to a protonation of the polyelectrolyte/surface, which makes it positively charged. By analogy, a resulting negative charge is given for pH values higher than the pH_{IEP}/pH_{PZC}. The pH_{PZC} is often used as synonym for the isoelectric point [28], however, this assumption is not correct. Both values are usually determined by different measurement methods: pH_{PZC} by titration, pH_{IEP} by electrokinetic measurements. Slight differences between both values for same materials were measured. A very comprehensive overview between the pH_{PZC} and pH_{IEP} is given in reference [29].

Another important parameter that can influence polyelectrolyte molecules is the ionic strength, which is determined by the salt concentration of the surrounding solvent. Without salt ions, the monomer charges repel each other so that the polyelectrolyte chain stretches apart. In surrounding of high ionic strength, counterions (with opposite charge than the monomer charge of the polyelectrolyte) screen the charges so that the repulsion forces are inhibited resulting in a coiling of the polyelectrolyte chain. One can conclude that the salt concentration mainly influences the structural form of the polyelectrolyte. The screening effect of charges by counterions is described in the Debye-Hückel theory by λ_D [30]. λ_D defines the distance at which the magnitude of an electric potential is decreased by $1/e \sim 36\%$.

The salt concentration and solution pH not only influence the charge of polyelectrolytes but also the charge situation of oxide surfaces: When an oxide gets in contact with an electrolyte solution, ions from the solution can attach to the electrolyte/insulator interface. Depending on the pH_{PZC} of the oxide, surface -OH groups (amphoteric hydroxyl groups for SiO_2 surfaces) become protonated or deprotonated for pH values $<pH_{PZC}$ or $>pH_{PZC}$, respectively. The distribution of charges at the insulator/electrolyte interface is described by the Helmholz-Gouy-Champman-Stern theory [31], while this theory does not include effects of chemical reaction with the surface.

In contrast to that, the site-binding model considers these effects and can express the correct net surface charge. **Figure 2.3** shows an illustration of the surface-charge situation at an exemplarily shown interface of electrolyte/SiO_2-insulator for three different pH values. The amphoteric hydroxyl groups are forming different amounts of $-OH_2^+$, -OH or $-O^-$ groups depending on the pH. The surface potential is changed by variation of the pH value: The more hydroxyl groups are expressed by the oxide, the more influence has the

pH on the surface potential. From that fact, the pH sensitivity of a material is depending on the number of available hydroxyl groups on its (oxide) surface.

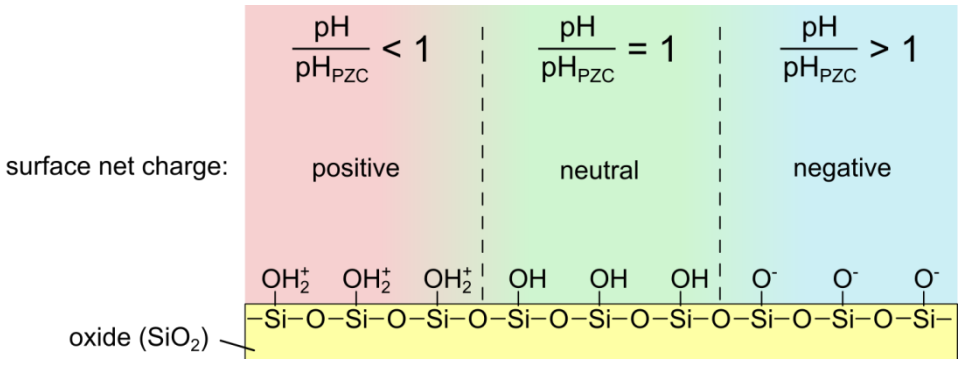

Figure 2.3: Illustration of the electrolyte/insulator SiO_2 interfaces with surface groups according to the site-binding model for pH values of the electrolyte higher (left), equal (middle) and lower (right) than the pH_{PZC}. The image was adapted from [32].

Since SiO_2 has a pH_{PZC} between pH 2–3 [33], the net charge is negative for neutral pH conditions. DNA molecules are also negatively charged in neutral pH solution. By bringing both into contact, the negative charges of DNA and the surface would repulse each other so that a binding is hindered. The pH_{PZC} of PAH is about 10.8 [34], which makes it positively charged under neutral pH conditions. In combination, solved (positively charged) PAH molecules are attracted by the (negatively charged) SiO_2 surface and adsorb as a thin film in the nm range. This surface modification allows the adsorptive immobilization of negatively charged DNA molecules.
The alternating surface modification of positively and negatively charged layers is known as layer-by-layer (LbL) technique [35]. Adsorptively immobilized ssDNA molecules lay on the sensor in a flat-oriented manner. This has a great advantage since the negative charges of the hybridized target cDNA molecules are located closer to the oxide surface compared to a binding of a perpendicular-oriented DNA strand. The flat-oriented binding results in a stronger effect of surface-potential change, which results in a high output signal for field-effect sensors.

2.4 Electrolyte-Insulator-Semiconductor (EIS) sensors and their ability to detect charged molecules without labeling

The following part describes the structure and briefly the fabrication process of EIS sensors. In addition, the mechanisms of EIS-signal generation for label-free DNA detection are presented. As indicated by the name, an EIS sensor consists of an electrolyte (solution), an insulator and a semiconductor part (**Figure 2.4**). EIS sensors are surface charge-sensitive and suited for the detection of substances, which are solved in aqueous media.

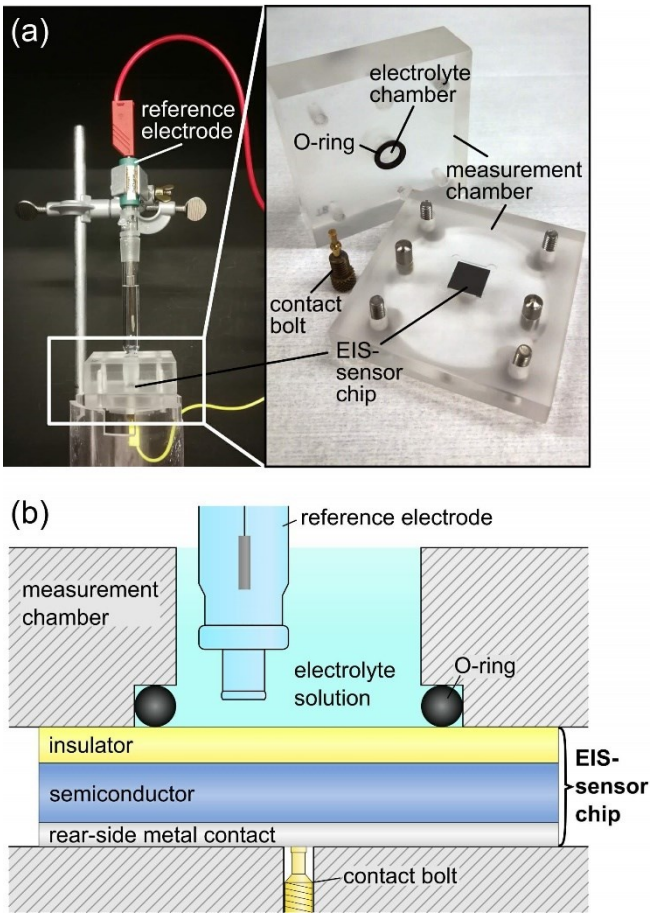

Figure 2.4: Photos of an exemplary measurement set-up (a, left) and chamber including the sensor chip (a, right). A schematic cross section of the measurement chamber with the EIS-sensor chip (b).

2.4.1 Fabrication of EIS-sensor chips and measurement setup for electrochemical detection

The EIS-sensor chips, used for the experiments in this work, were fabricated from boron-doped (p-type) silicon wafers. The wafers had a diameter of 3 inch or 4 inch and a thickness of approximately 400 µm. The crystallographic orientation was <100> and the resistivity was 1-10 Ωcm. The oxide separates the semiconductor material from the electrolyte solution and its quality is of high relevance. The oxidation can be carried out by either dry or wet oxidation (or combinations of both). Although the wet oxidation method provides high growth rates, a better oxide quality (e.g., by high homogeneity of SiO_2, low porosity, high dielectric constant etc.) can be achieved with the dry oxidation process [36, 37]. The insulator thickness is typically in the range of tens to few hundreds of nanometers (in this work, the SiO_2 layer was in the range of 15 nm to 70 nm) and can be generated in the case of oxides by oxidation growth – for silicon at temperatures between 800 °C and 1200 °C. In this study, the SiO_2 layers were always oxidized using the dry oxidation method. In order to modify or improve certain sensing properties (such as pH sensitivity), additional dielectric materials (e.g., Ta_2O_5, Al_2O_3, Si_3N_4) can be added on top of the initial

SiO_2 layer. Additional layers of Ta_2O_5 or Al_2O_3 can be also generated by oxidation after a previous metal deposition with Ta or Al, respectively.

For convenient handling of the sensors, the complete wafer can be divided into single, smaller EIS "chips" by cutting or cracking. To use the EIS chip for electrochemical purposes, there must be a reliable electrical connection to the semiconductor. This can be achieved by deposition of a thin metal layer, for instance, at the rear side of the semiconductor. Prior to the metal deposition, the eventually existing oxide at the rear side should be removed by, e.g., a chemical etching step. After this, the deposited metal can be comfortably connected to the measurement setup with any metal cable or suitable alternative. This described process for EIS-chip fabrication is only one of many. There is a broad spectrum of different procedures for metal- and insulator-layer generation, semiconductor doping, connection, etc. For electrochemical measurements with the EIS sensor, the chip is mounted into a proper measurement chamber: Such chamber must be made of a non-conductive material and should fulfill chemically inert properties. It should be designed to provide enough space for the electrolyte solution and for immersing a reference electrode.

To close the electrical circuit of the measurement setup and provide a constant potential, it is recommended to use a double-junction Ag/AgCl reference electrode (filled with, e.g., saturated (3 M) KCl solution), which is immersed into the electrolyte and ensures a constant potential. **Figure 2.4** shows photos of an exemplary EIS-measurement set-up and measurement chamber (a), as well as a cross-sectional illustration of an EIS sensor mounted into a measurement chamber (b).

2.4.2 Signal generation, capacitance/voltage- and constant-capacitance-operating modes of EIS devices[1]

If two semiconductor materials with different doping (n- and p-type) are brought into contact, diffusive- and drift-transportation of majority carriers from one into the other material leads to forming of a space-charge region at the contact interface (called p-n junction). The space-charge region does not spread over the complete semiconductor, but has a small thickness (width), which results from the equilibrium of both transportation processes (**Figure 2.5**). Details can be found in [38].

A space-charge region also exists inside the semiconductor of EIS- and metal-insulator-semiconductor- (MIS) or metal-oxide-semiconductor (MOS) structures. MOS structures have the same layout as EIS structures, but a metal contact as gate instead of the electrolyte solution (with a reference electrode). The fundamental effects for signal generation of MOS- and EIS structures are therefore comparable. For a more convenient explanation, the following section describes the signal generation and the corresponding processes and effects based on a MOS (sensor) structure. The explanation can be (later) adapted for EIS sensors.

[1] Parts of this chapter were adapted from the authors master thesis: “Entwicklung eines miniaturisierten Sensorchips für einen späteren Einsatz zum markierungsfreien Nachweis von Tuberkulose” (T.S. Bronder, University of Hannover, Germany, 2013).

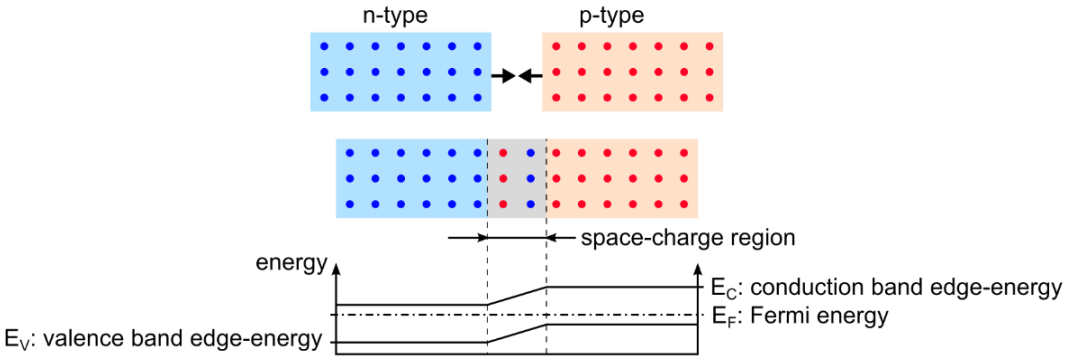

Figure 2.5: p-n junction before and after bringing into contact with energy levels in the band diagram. At the interface of both materials, a space-charge region is formed. Adapted from [39].

Figure 2.6 presents the band diagrams of a metal and a semiconductor material without contact (a) and of a MIS structure (b). The work functions Φ indicate the required energies to move an electron from the material (metal or semiconductor) into vacuum at a distance of no (electromagnetic) interaction (E_0). The Fermi energy E_F represents the energy at with the chance of electron occupation of states is 50%.

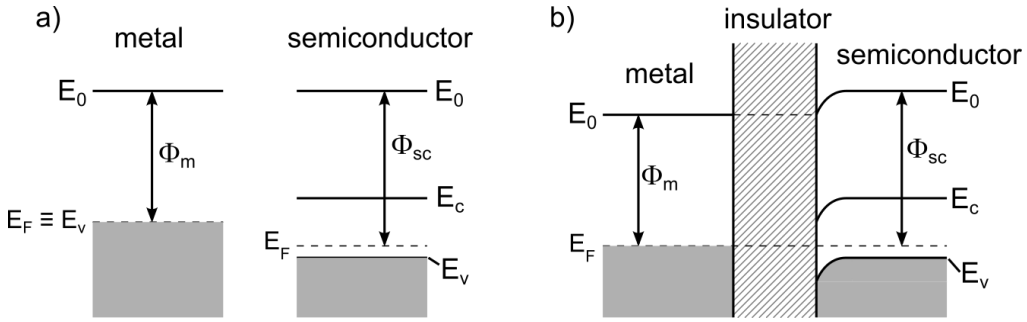

Figure 2.6: Band diagrams of (a) metal and semiconductor materials with indicated vacuum energy-level E_0, conduction band energy E_c, valence band energy E_v, work function Φ_m (for metal), Φ_{sc} (for semiconductor) and (b) MIS/MOS structure with band-bending effect in the semiconductor. Adapted from [40].

The combination of the metal and the insulator with the semiconductor material results in a band-bending process. This change of band energy occurs (almost) completely and locally at the semiconductor part, because the metal contains magnitudes of more free charge carriers than the semiconductor so that a potential balancing over the complete metal takes place (see **Figure 2.6b**). This band-bending process at the semiconductor leads to the formation of a local space-charge region. Depending on the applied (gate) voltage U_g to the system, the energy-band levels can be adjusted. Four different "cases" can be summarized to describe the possible scenarios for this system: accumulation, depletion, inversion and the flat-band condition. The following consideration assumes a p-type semiconductor as substrate.

Flat-band condition: In order to compensate the band-bending process shown in **Figure 2.6**, a certain voltage must be applied to the MOS system. In this state, the three energy bands E_v, E_c and E_0 normalize to a flat and horizontal line, respectively (see **Figure 2.7**). The required (gate) voltage for this situation is called flat-band voltage U_{fb}.

Accumulation: An applied voltage $U_g < U_{fb}$ results in an accumulation of mobile charge carriers (the majority charge carriers are represented by "holes" for a p-type semiconductor) at the insulator/semiconductor interface (see **Figure 2.7**). The holes only accumulate in the semiconductor material and not enter the (ideal) insulator.

Depletion: If the gate voltage U_g is increased ($U_g > U_{fb}$), the majority charge carriers (holes) from the insulator/semiconductor interface become more and more distracted from that interface deeper to the semiconductor material. One can say, that their number is depleted within this region.

Inversion: A further increase of U_g ($U_g >> U_{fb}$) results in a further depletion of majority charge carriers at the interface insulator/semiconductor. The amount of negative charges exceeds the holes of the p-type semiconductor at that region. The semiconductor type becomes locally inverted (from p-type to n-type) [38].

The applied voltage, described for the different conditions, has a direct influence on the thickness of the space-charge region, which will influence the overall sensor capacitance.

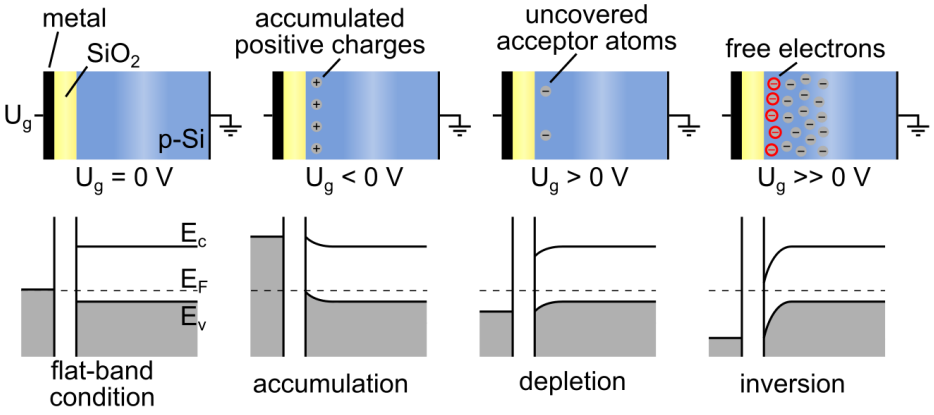

Figure 2.7: Illustration of an ideal MOS structure with different applied gate voltages (top) resulting in accumulation-, depletion- and inversion state as well as in the flat-band condition. The respective influence on the energy bands are shown in the band diagrams (bottom). Adapted from [41].

Replacing the metallic gate contact of the MOS structure by an electrolyte and a reference electrode results in an EIS structure with the corresponding states as described in **Figure 2.7**. However, the applied gate voltage in this case is adjusted at the reference electrode.

The oxide surface of the EIS sensor can change its charge in solution depending on different parameters (such as pH value). EIS sensors are usually fabricated with a very thin (nm range) oxide layer. Due to the small thickness, (external) electromagnetic fields induced by charges at or near the oxide/electrolyte interface can have an impact on the charge position and distribution inside the semiconductor at the oxide/semiconductor interface [41].

The combination of the "plane-oriented" charges located at both, the semiconductor/oxide and the oxide/electrolyte interface, defines the electronic behavior of the EIS structure, which can be described, at the end, by a simplified series arrangement of two plate capacitors (**Figure 2.8**): The "charge planes" over the oxide result in an oxide capacitor with the oxide capacitance C_{ox}. The plane inside the semiconductor forms a capacitor of the space-charge region of the Si with the capacitance C_{sc}. The electrochemical double-layer capacitance C_{dl} (**Chapter 2.2**), that is also present but in series to the total EIS chip capacitance (C_{EIS}), can be neglected, since the value for C_{dl} is usually much higher than C_{ox} and C_{sc} [42].

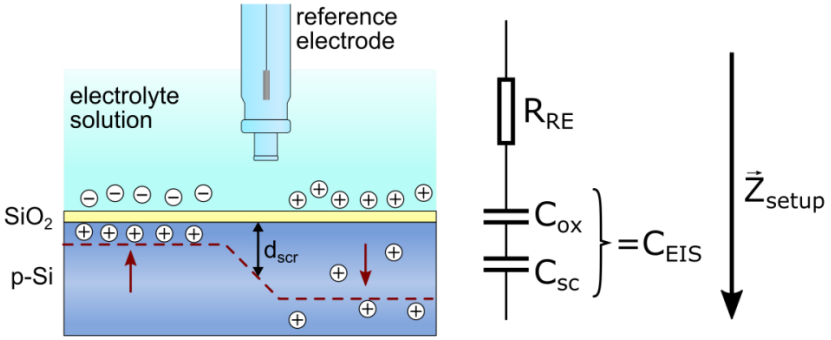

Figure 2.8: Schematic cross section of both interfaces (semiconductor/oxide and oxide/electrolyte) of an EIS sensor. Surface charges indicated by ⊕ and ⊖ symbols lead to attraction or repulsion of intrinsic mobile charge carriers in the semiconductor (⊕), resulting in a thickness change of the space-charge region (d_{scr}). The simplified equivalent circuit model for the EIS sensor is shown with the resistance of reference electrode (R_{RE}), the oxide capacitance (C_{ox}), the semiconductor capacitance (C_{SC}), the EIS-chip capacitance (C_{EIS}) and the complete setup impedance (Z_{setup}).

In general, the capacitance of a plate capacitor can be calculated according to **Eq. 2.2** [41]:

$$C = \varepsilon_0 \varepsilon_r \frac{A_c}{d} \qquad \textbf{Eq. 2.2}$$

with the vacuum permittivity ε_0, the relative permittivity ε_r, the plate area A_c and the plate distance d. By adaptation of this formula to the capacitances of the EIS sensor, the distance d is defined by the oxide thickness (for C_{ox}) together with the thickness of the space-charge region (d_{scr}). While the oxide thickness is constant, the thickness of the space-charge region can vary depending on the surface potential. This fact leads to a capacitance change of C_{sc}.

The value for C_{EIS} can be calculated from impedance measurements, where a small alternating current (AC) voltage must be applied in addition to the direct current (DC) signal in order to measure the capacitance. The measurement setup includes a reference electrode, which can be simplified in the electrical equivalent circuit by a resistor R_{RE}. The following equation can be used for the expression of Z_{setup} (**Eq. 2.3**):

$$Z_{setup} = R_{RE} + Z_{EIS} \qquad \textbf{Eq. 2.3}$$

with

$$Z_{EIS} = \frac{1}{j\omega C_{EIS}} \qquad \textbf{Eq. 2.4}$$

and

$$\omega = 2\pi f \qquad \textbf{Eq. 2.5}$$

with the frequency f of the superimposed AC voltage. Using an electrochemical setup allows to determine the capacitance of the sensor chip C_{EIS}; **Eq. 2.6** considers the series connection of C_{sc} and C_{ox} [43].

$$C_{EIS} = \frac{C_{ox}C_{sc}}{C_{ox} + C_{sc}}. \qquad \textbf{Eq. 2.6}$$

Measuring the capacitance signal (C_{EIS}) versus different applied DC-voltage steps results in a capacitance-voltage (C–V) curve [44]. A typical C–V curve has a sigmoidal-like shape and is exemplarily shown in **Figure 2.9** for a p-type EIS sensor (for a n-type EIS sensor, the C–V curve has an identical shape but with reversed polarity). The value for C_{EIS} is determined by the capacitances C_{sc} and C_{ox} as series arrangement of two plate capacitors. The curves can be subdivided into three parts: accumulation (black curve, green shaded), depletion (black curve, yellow shaded) and inversion (black curve, blue shaded). In the accumulation part, a negative (gate) voltage is applied via the reference electrode to the Si chip.

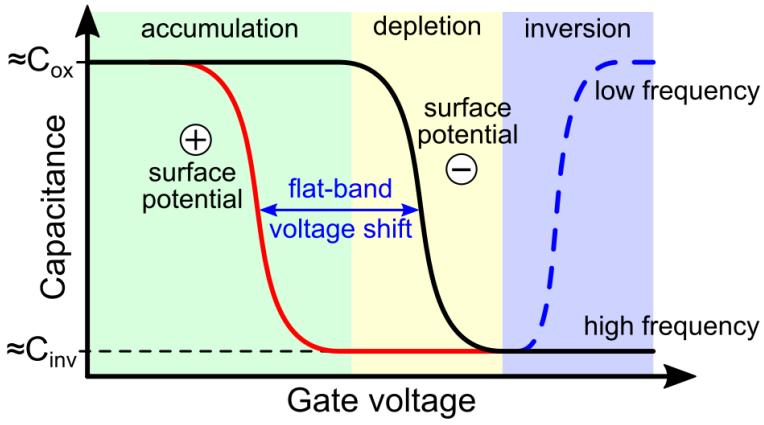

Figure 2.9: Schematic C–V curves for an EIS sensor with p-type Si with positive surface potential (red line) and negative surface potential (black line). The three shaded regions, accumulation, depletion and inversion, are indicated for the black curve.

The applied electric field leads to an accumulation of positively charged holes (majority carriers for the p-type EIS chip) at the semiconductor/oxide interface. Due to the attraction of holes at the interface, the value for C_{sc} increases and drastically exceeds the value of C_{ox}. Therefore, in the accumulation part, the sensor capacitance C_{EIS} is mainly determined by C_{ox}. If the applied (gate) voltage at the reference electrode is changed towards more positive potential, the concentration of holes at the semiconductor/oxide interface is decreasing and

a region of depleted mobile carriers is formed. In this depletion part, the width of the depletion region is increasing by increasing the applied voltage (changing towards more positive potential). The increase of the depletion-region width leads to a decrease of the total capacitance. If the applied (gate) voltage is further increased, the amount of negatively charged electrons can exceed the number of positively charged holes at the semiconductor/oxide interface. Here, a small area of n-type silicon is formed, called inversion layer. In the inversion state, for low AC frequencies, an exchange of charge carriers over the space-charge region is possible. Thus, the overall capacitance is defined mainly by C_{ox}. For high frequencies, however, the charge fluctuations are too fast, so that no (sorted) arrangement at the inversion layer takes place. Thus, the total capacitance does not increase again and remains at C_{inv} (inversion part) [41], (see **Figure 2.9**).

Monitoring a C–V curve can be used to detect surface-potential changes: Charges (from ions, charged molecules, etc.) at the EIS surface contribute directly to the surface potential. Depending on the additional surface charge, a higher or lower voltage is required to achieve the same setup capacitance as without additional charges, meaning that this surface potential is overlaid to the applied DC voltage. Therefore, a shift in the C–V curve is observable (red line and black line in **Figure 2.9**). The ideal monitoring condition is given by achieving the flat-band case. The voltage shift corresponds to the sign-inverted surface-potential change and serves as the (bio)sensor signal.

For measuring time-related processes, the capacitance C_{EIS} can be set to a fixed value, while the corresponding voltage is permanently adapted by a feedback control to hold this capacitance value constant. The chosen capacitance value must be set within the depletion region and should be about 60% of the maximal sensor capacitance [45] (ideally, fit the flat-band condition). The adapted voltage is recorded in real time during this procedure. This way of measurement is called constant-capacitance (ConCap) mode. A corresponding curve, exemplarily for two stationary surface-charge situations (more positive or negative charges) at subsequent time intervals, is schematically shown in **Figure 2.10**.

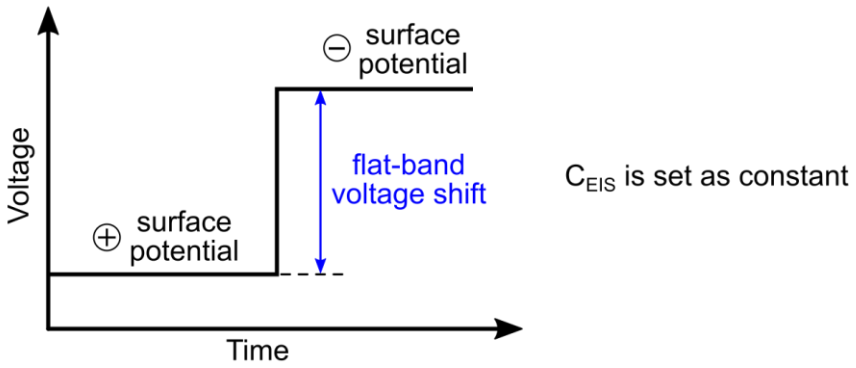

Figure 2.10: Schematic ConCap curve of an EIS sensor for positive and negative surface-potential situations. All other parameters remain constant.

One can conclude that the readout of the EIS-sensor capacitance by using an electrochemical setup allows to determine surface-potential changes, which can also be induced by binding of charged molecules. The EIS sensor – same as for all field-effect

devices – can be easily influenced by electromagnetic fields and light illumination. Therefore, measurements should be performed inside a dark Faradaic cage to prevent such disturbances.

2.4.3 Label-free detection of DNA using polyelectrolyte-modified EIS sensors

The basic strategy for the identification of a target DNA is based on the measurement of the surface-potential change during the hybridization process of target cDNA with immobilized probe ssDNA at the modified EIS-sensor surface due to the intrinsic negative charge of DNA molecules.

First, a probe ssDNA with known sequence that matches to the target DNA must be immobilized onto the sensor surface. Many different ways of attaching (immobilizing) ssDNA onto solid (sensor) surfaces have been developed in the past [46–48]. As already explained in **Chapter 1.2.2**, two of the most common methods are the covalent binding and the adsorptive binding. Although the covalent bond has the advantage of achieving a very high and adjustable DNA-immobilization density on the surface [49], in comparison to the adsorptive method, this process has major drawbacks regarding processing effort, time and costs. Since the DNA molecule as well as the SiO_2 EIS-surface are both negatively charged, no direct adsorption will occur. A surface modification with the cationic polyelectrolyte PAH is carried out to enable the adsorptive binding. Note, that the term *polyelectrolyte* is used in this work for PAH and not for DNA, although DNA is also a polyelectrolyte. Exposing the sensor surface to a solution with solved PAH molecules will result in a self-assembly of a thin polyelectrolyte layer onto the negatively charged SiO_2 surface. This self-assembly process is randomly and covers the complete surface within minutes [42]. After the adsorption, the surface becomes more positively charged and overcompensates the negative surface groups from the SiO_2 [50, 51]. Before adding the probe ssDNA, the surface must be washed in order to remove all unbound PAH molecules. In the next step, the PAH-modified sensor is exposed to probe ssDNA solution. The negative DNA backbone is attracted by the positively charged PAH and binds randomly onto the surface in a flat-oriented manner. The surface potential changes towards more negative direction upon immobilization. After the successful immobilization, the surface must be washed to remove unbound probe ssDNA molecules, then a solution containing target cDNA can be added to induce the hybridization. The target cDNA hybridizes with the immobilized ssDNA and leads to a further surface-charge change towards negative direction. In the case of addition of ncDNA instead of cDNA, no hybridization takes place and the surface potential remains constant. **Figure 2.11** illustrates the complete process schematically.

After each step, electrochemical C–V- and ConCap measurements can be applied to determine the surface-potential changes qualitatively and quantitatively. The results can be used as evidence for the respective reactions. **Figure 2.11** also shows exemplarily schematics of recorded ConCap curves after each described modification step. The entire process is referred as electrostatic layer-by-layer technique with the layers: PE / ssDNA / cDNA. The advantage of this technique is that neither the probe nor the target DNA has to be modified or labeled in any way for the detection event.

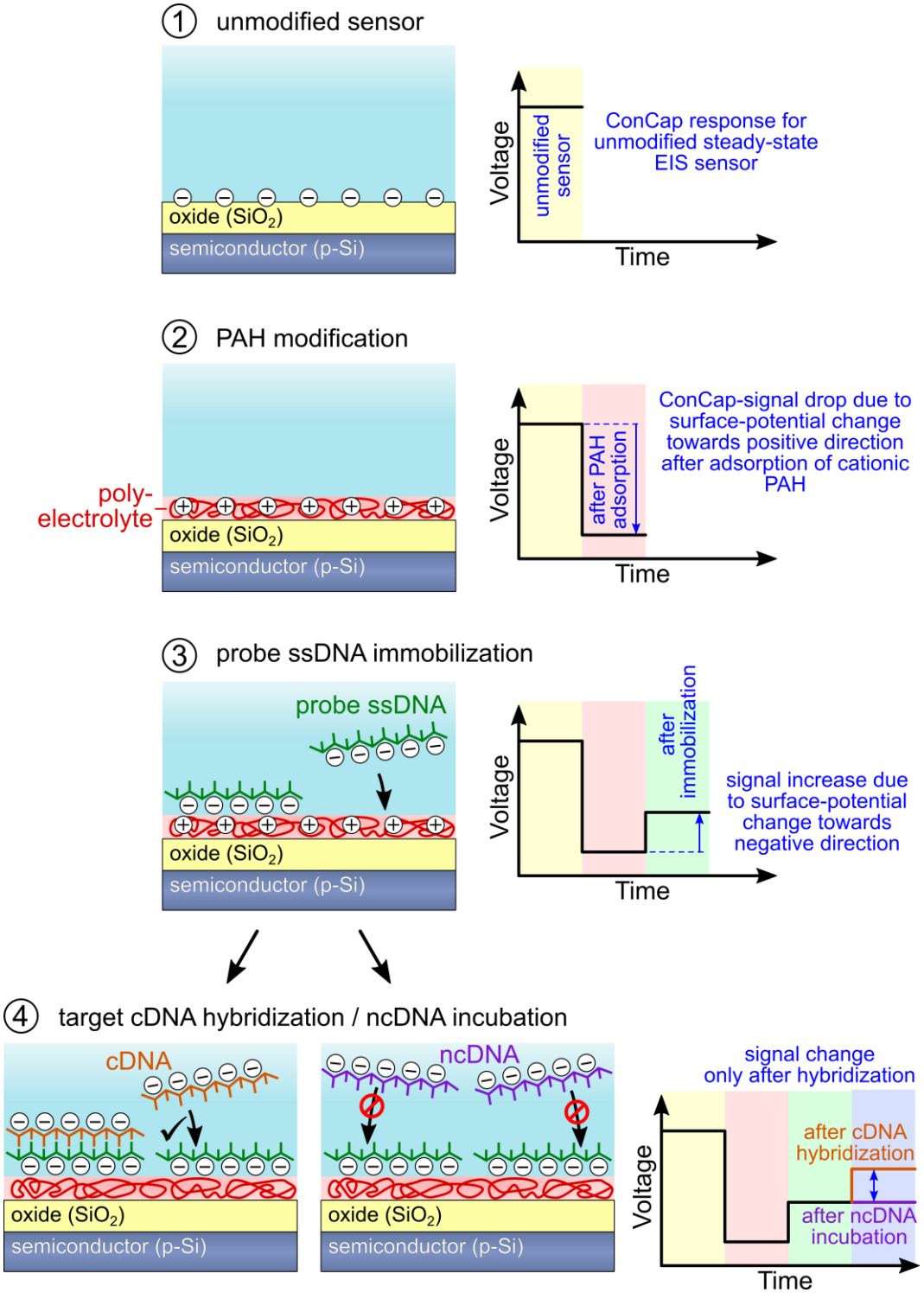

Figure 2.11: Illustration of the surface-modification steps for DNA detection with EIS sensors. Exemplary ConCap responses are shown after each step. Depending on the last signal change of step 4, the presence of target cDNA or target ncDNA can be distinguished.

2.5 DNA DETECTION WITH LAPS

LAPS sensors are a type of field-effect sensors with the same structural layout like EIS sensors and are also consisting of the three parts, electrolyte, isolator and semiconductor. The basic sensing principle of LAPS and EIS sensors is also identical. Both sensor types can detect a change of charge-carrier distribution inside the semiconductor caused by a change of the surface potential at the electrolyte-insulator interface [52, 53].

To briefly explain the LAPS setup and measurement principle: A LAPS chip is often fabricated from a silicon substrate (1-10 Ωcm resistivity) with a thermally oxidized SiO_2 layer with similar thicknesses as for EIS chips (approx. 10-100 nm). Equipped with a reference electrode (which is immersed into the electrolyte), a DC bias voltage (U_{bias}) is applied between the reference electrode and the semiconductor part. The connection to the semiconductor can be realized by an (aluminum) rear-side contact (see **Figure 2.12** (left)). By applying U_{bias}, a space-charge region at the interface semiconductor/insulator is formed [54].

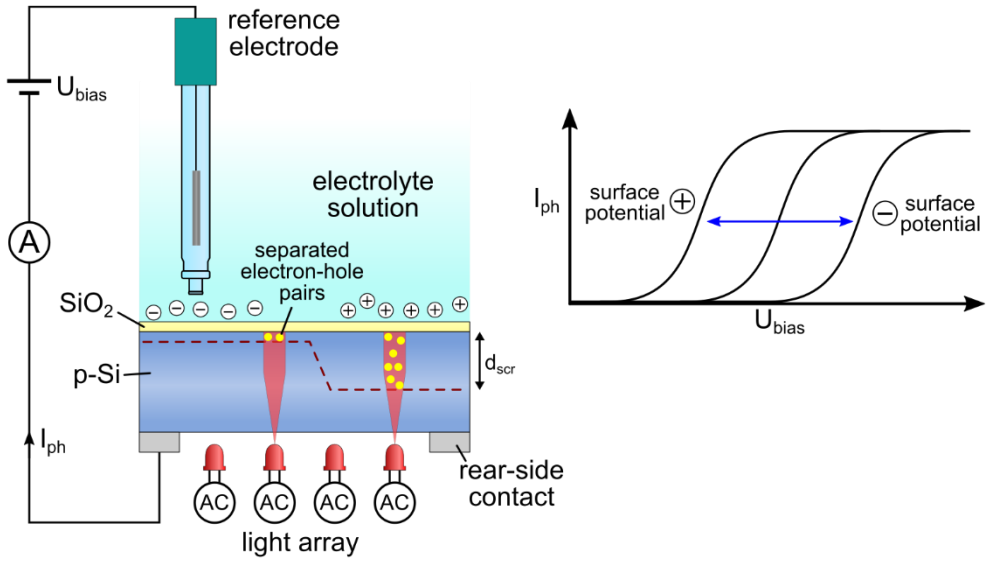

Figure 2.12: Schematic cross section of a LAPS setup (left) with two different surface-potential states (indicated by ⊕ and ⊖ symbols); the respective thickness of the space-charge region is shown as red-dotted line with separated electron-hole pairs. The photocurrent-voltage curve (right) shows the corresponding I_{ph}–V curves for a more positively or more negatively charged sensor surface.

A potential sweep of U_{bias} results in a change of the space-charge region thickness (same as for EIS sensors), which influences the sensor capacitance and leads to the three states of accumulation, depletion or inversion (explained in **Chapter 2.4.2**). The space-charge region thickness is not only influenced by U_{bias}, but also by surface-potential changes, e.g., by means of a change of the pH value or an adsorption of charged molecules at the electrolyte/insulator interface. These surface-potential changes are superimposed to U_{bias}. In order to read out the sensor signal, a modulated light beam is used to illuminate the LAPS chip. The modulation frequency is in the range of, e.g., 100 Hz to 100 kHz. Due to

the illumination, electron-hole pairs are generated by absorption of photons along the illuminated semiconductor material. The majority of electron-hole pairs recombine, however, electron-hole pairs within the space-charge region become separated because of the electric field [55]. The separation results in a photocurrent (I_{ph}), which can be measured. I_{ph} is usually characterized as a function of the applied voltage U_{bias}. The resulting I_{ph}–V (also I_{ph}–U_{bias}) curve has also a sigmoidal-like shape such as the equivalent C–V curve of EIS sensors. Depending on the surface potential of the LAPS chip, the recorded I_{ph}–V curve is shifted along the voltage axis (see **Figure 2.12** (right)). This horizontal shift in the transition part (around the inflection point) can be correlated to the surface-potential change. Such a curve shift induced by a surface-potential change can be caused, e.g., by an immobilization or hybridization reaction of (negatively charged) DNA at the surface of the LAPS. Besides the I_{ph}–V operating mode, the constant-photocurrent mode is frequently used: Here, I_{ph} is kept at a constant value by a feedback-controlled bias voltage. In case of a surface-potential change, the applied bias voltage is adjusted in order to compensate this change. The adjusted bias voltage is plotted against the time.

The advantage of LAPS is, that the light beam does not need to illuminate the whole sensor chip, it can be focused only to a certain area (spot) of the chip surface. The measured signal only corresponds to the surface potential at that illuminated spot [56]. This opens new measurement applications such as chemical imaging or multiwell analysis, where e.g., DNA arrays can be realized. With such DNA arrays, a multitude of different DNA strands can be analyzed simultaneously by using just one single LAPS chip. Instead of using one light spot, a LAPS can also be illuminated simultaneously by several light spots. In order to differentiate the signals from different spots, each light source must have a slightly different modulation frequency. A fast Fourier transformation can be used to recalculate the signals from time domain to frequency domain and identify the single spots individually [57]. The illumination of the LAPS chip can be technically performed from both sides (top and bottom). However, in order to prevent possible light interaction (e.g., scattering or adsorption) with the solution or with adsorbed particles on the electrolyte/insulator interface, LAPS chips are most commonly illuminated from the bottom side.

One can conclude that the use of LAPS chips is suitable for the detection of charged molecules and might be an appropriate method for DNA detection; in comparison to the EIS sensing-method, LAPS inhere the foremost advantage of spatial-resolved measurement possibility, which allows multi-spot recordings, but requires an illumination of the semiconductor with a modulated light source. It has a dependence of the signal generation on the modulation frequency and intensity of the light beam, and furthermore, possible cross-talk due to the internal reflections in the semiconductor can limit the fields of application of LAPS.

2.6 FLUORESCENCE-BASED DNA DETECTION AS REFERENCE FOR ELECTROCHEMICAL METHODS

The use of reference methods generally allows the verification of obtained measurement results (here from electrochemical investigations). Within this study, various sensor-surface modifications were performed. In order to verify these procedures, e.g., the

adsorption of polyelectrolytes or the binding of DNA molecules, fluorescence-staining methods were carried out and observed using a light microscope. The following part explains the basic fundamentals of fluorescence-signal generation and measurement as well as possible ways of staining. The fluorescence-based reference method described is only used to verify the binding on (non-transparent) sensor structures, so that the fluorescence detection is only considered and explained for reflected and not transmitted light (microscopy).

Fluorophores are chemical agents used for fluorescence-dye labeling of DNA molecules to allow an optical detection. Fluorophores can emit fluorescence light (with the emission wavelength λ_{em}) when they are illuminated by light (with the excitation wavelength λ_{ex}). Photons of the illumination light interact with the agent and loose a certain amount of energy. This energy difference results in light emission with a different color (wavelength) and is well-known as Stokes shift [58]. The ratio between emitted photons and absorbed (excited) photons is described as quantum yield ϕ [59]. Multiplication of ϕ with the extinction coefficient results in the output-fluorescence brightness. This brightness can be mainly influenced/decreased by two effects: photobleaching and quenching.

Photobleaching describes the steady and permanent loss of fluorescence ability due to prolonged exposure of the fluorophore to light [60, 61]. Photobleaching can cause high inaccuracies in quantitative measurements and should be reduced by avoiding unintended exposure as much as possible.

Quenching is the temporary decrease of fluorescence ability due to an energy transfer of the absorbed photons to a local acceptor. Quenching can be intentionally caused by specially designed quencher molecules (Q) or just by the surrounding solution. As example, the fluorescence dye SYBR Green I (SG) has a >1000-fold reduced fluorescence brightness when unbound in solution compared to bounded to dsDNA [62]. The strength of quenching is also different for binding to ssDNA or dsDNA [63]. Quenchers can be therefore utilized for detection purposes; the molecular beacon- and the TaqMan-probe fluorescence methods are very common examples of applications for intended fluorescence quenching. **Figure 2.13** shows two examples of fluorescence quenching. Due to the close proximity of the quencher and the fluorophore, the fluorescence signal is quenched (**Figure 2.13a)**. The molecular beacon strand opens upon hybridization with a target cDNA and separates quencher and fluorophore resulting in a measurable fluorescence signal. TaqMan probes (**Figure 2.13b**) can be used to verify a PCR. A TaqMan probe (short sequence with quenched fluorophore) is separated and cleaved during the DNA-elongation process by the DNA-polymerase enzyme. Due to the separation, the quenching is inhibited and a fluorescence signal is measurable. The TaqMan-probe method is implemented in commercially available DNA detection platforms (compare with **Chapter 1.2.3**).

In order to detect DNA by means of fluorescence microscopy without a quencher, the DNA must be labeled with the fluorescence dye. The cDNA itself can be functionalized with a fluorescence dye, e.g., by a chemical bond at the 5'- or 3'-end. For this type of labeling, the fluorescence dyes FITC [66] and FAM [67] were used in this study. After the labeling, the sensor surface is exposed to the cDNA for hybridization; then, the complete surface can be evaluated by means of fluorescence microscopy. The measured fluorescence intensity correlates with the amount of hybridized cDNA.

A different strategy is given by the use of intercalative or groove-binding fluorescence dyes. Here, the protocol changes slightly: The chip is first exposed to the DNA so that a hybridization occurs, afterwards the chip surface is stained. Intercalative or groove-binding fluorophores interact/bind to DNA in an autonomous way. Intercalators locate between the nucleobases of the DNA strand, while groove binder – as the name implies – bind to the minor or major groove of the DNA strand. Representatives are SG [68, 69] and 4′,6-Diamidin-2-phenylindol (DAPI) [70]. Not all dyes can be categorized to a certain binding type: DAPI reacts with DNA in an intercalative manner at GC-rich sequence parts, while for AT-rich regions, DAPI is forming a stable groove-complex binding. Whereas, the reaction with adenine-uracil-rich regions at RNA is intercalative again [71].

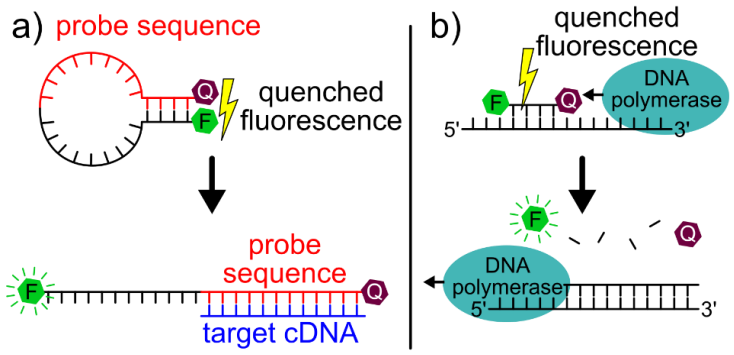

Figure 2.13: Two indirect DNA-hybridization detection methods based on fluorescence-quenching effects with quencher (Q) and fluorophore (F). Both molecules are separated upon hybridization of the molecular beacon (a) or during strand extension (b) caused by the DNA polymerase (it requires a previous hybridization of primer DNA). The images were adapted from Ref. [64] and Ref. [65].

Fluorescence images are often recorded by a charge-coupled device (CCD) chip and can be evaluated digitally to get a quantitative result. Quantitative fluorescence microscopy can be used to compare results of different experiments. To detect a fluorescence signal, special dichroic filters are used so that only light with λ_{ex} can pass the filter to the sensor. The returned light is filtered again so that only λ_{em} can pass the filter. This allows the specific detection of fluorescence signals from the sample. Basic handling procedures must be followed to achieve proper image and result quality: reducing of environmental light, increase of exposure time, decrease of gain, subtraction of the background signal and setting of high aperture. The following literature gives a very detailed insight about the proper procedures in quantitative fluorescence microscopy [72].

REFERENCES

[1] M.R. Green, J. Sambrook: *Precipitation of DNA with Ethanol*, Cold Spring Harb. Protoc. 2016 (2016) 1116–1120.

[2] D.L. Morris: *DNA-bound metal ions: Recent developments*, BioMol. Concepts 5 (2014) 397–407.

[3] F. Gentile, M. Moretti, T. Limongi, A. Falqui, G. Bertoni, A. Scarpellini, S. Santoriello, L. Maragliano, R.P. Zaccaria, E. di Fabrizio: *Direct imaging of DNA fibers: The visage of double helix*, Nano Lett. 12 (2012) 6453–6458.

[4] H. Lodish, A. Berk, P. Matsudaira, C.A. Kaiser, M. Krieger, M.P. Scott, L. Zipursky, J. Darnell: *Molecular Cell Biology*, WH Freeman, New York, USA (2004).

[5] P.D.N. Hebert, A. Cywinska, S.L. Ball, J.R. DeWaard: *Biological identifications through DNA barcodes*, Proc. Biol. Sci. 270 (2003) 313–321.

[6] P.A. Bryant, D. Venter, R. Robins-Browne, N. Curtis: *DNA microarrays in infectious diseases*, Lancet Infect. Dis. 4 (2004) 100–111.

[7] Y. Erlich, D. Zielinski: *DNA fountain enables a robust and efficient storage architecture*, Science 355 (2017) 950–954.

[8] I.G. Wilson: *Inhibition and facilitation of nucleic acid amplification*, Appl. Environ. Microbiol. 63 (1997) 3741–3751.

[9] J. Yang, J.Y. Lee, H.-P. Too, G.-M. Chow: *Inhibition of DNA hybridization by small metal nanoparticles*, Biophys. Chem. 120 (2006) 87–95.

[10] H. Berney, J. West, E. Haefele, J. Alderman, W. Lane, J.K. Collins: *A DNA diagnostic biosensor: Development, characterisation and performance*, Sens. Actuators B 68 (2000) 100–108.

[11] R. Owczarzy, B.G. Moreira, Y. You, M.A. Behlke, J.A. Walder: *Predicting stability of DNA duplexes in solutions containing magnesium and monovalent cations*, Biochemistry 47 (2008) 5336–5353.

[12] J. SantaLucia: *A unified view of polymer, dumbbell, and oligonucleotide DNA nearest-neighbor thermodynamics*, Proc. Natl. Acad. Sci. U.S.A. 95 (1998) 1460–1465.

[13] J. SantaLucia, D. Hicks: *The thermodynamics of DNA structural motifs*, Annu. Rev. Biophys. Biomol. Struct. 33 (2004) 415–440.

[14] N. Sugimoto, S. Nakano, M. Yoneyama, K. Honda: *Improved thermodynamic parameters and helix initiation factor to predict stability of DNA duplexes*, Nucleic Acids Res. 24 (1996) 4501–4505.

[15] G. Weber: *Optimization method for obtaining nearest-neighbour DNA entropies and enthalpies directly from melting temperatures*, Bioinformatics 31 (2015) 871–877.

[16] R.B. Wallace, J. Shaffer, R.F. Murphy, J. Bonner, T. Hirose, K. Itakura: *Hybridization of synthetic oligodeoxyribonucleotides to phi chi 174 DNA: The effect of single base pair mismatch*, Nucleic Acids Res. 6 (1979) 3543–3558.

[17] https://www.dna.utah.edu/umelt/um.php, downloaded from internet: 24. February 2019.

[18] D.H. Turner: *Thermodynamics of base pairing*, Curr. Opin. Struct. Biol. 6 (1996) 299–304.
[19] Z.J. Tan, S.-J. Chen: *Salt dependence of nucleic acid hairpin stability*, Biophys. J. 95 (2008) 738–752.
[20] C.H. Hamann, W. Vielstich: *Elektrochemie (3th edition)*, Wiley-VCH, Weinheim (1998).
[21] W.J. Moore: *Physikalische Chemie (4th edition)*, De Gruyter, Berlin, Germany (2010).
[22] O. Stern: *Zur Theorie der elektrolytischen Doppelschicht*, Historic Papers in Electrochemistry 30 (1924) 508–516.
[23] D.C. Grahame: *The electrical double layer and the theory of electrocapillarity*, Chem. Rev. 41 (1947) 441–501.
[24] J.-L. Barrat, J.-F. Joanny: *Theory of polyelectrolyte solutions*, Adv. Chem. Phys. 94 (1996) 1–66.
[25] J.A. Hiller, M.F. Rubner: *Reversible molecular memory and pH-switchable swelling transitions in polyelectrolyte multilayers*, Macromolecules 36 (2003) 4078–4083.
[26] K. Glinel, C. Dejugnat, M. Prevot. B. Schöler, M. Schönhoff, R. v. Klitzing: *Responsive polyelectrolyte multilayers*, Colloids Surf. A 303 (2007) 3–13.
[27] L. Shao, J.L. Lutkenhaus: *Thermochemical properties of free-standing electrostatic layer-by-layer assemblies containing poly(allylamine hydrochloride) and poly(acrylic acid)*, Soft Matter 6 (2010) 3363–3369.
[28] G. Parks: *The isoelectric points of solid oxides, solid hydroxides, and aqueous hydroxo complex systems*, Chem. Rev. 65 (1965) 177–198.
[29] M. Kosmulski: *Isoelectric points and points of zero charge of metal (hydr)oxides: 50 years after Parks' review*, Adv. Colloid Interface Sci. 238 (2016) 1–61.
[30] P. Debye, E. Hückel: *Zur Theorie der Elektrolyte. I. Gefrierpunktserniedrigung und verwandte Erscheinungen*, Physikalische Zeitschrift 24 (1923) 185–206.
[31] D.E. Yates, S. Levine, T.W. Healy: *Site-binding model of the electrical double layer at the oxide/water interface*, J. Chem. Soc. 70 (1974) 1807–1818.
[32] K.A. Yusof, R.A. Rahman, M.A. Zulkefle, S.H. Herman, W.F.H. Abdullah: *EGFET pH sensor performance dependence on sputtered TiO_2 sensing membrane deposition temperature*, J. Sens. 2016 (2016) 1–9.
[33] L.K. Meixner, S. Koch: *Simulation of ISFET operation based on the site-binding model*, Sens. Actuators B 6 (1992) 315–318.
[34] R.N. Smith, M. McCormick, C.J. Barrett, L. Reven, H.W. Spiess: *NMR studies of PAH/PSS polyelectrolyte multilayers adsorbed onto silica*, Macromolecules 37 (2004) 4830–4838.
[35] G.A. Evtugyn, T. Hianik: *Layer-by-layer polyelectrolyte assembles involving DNA as a platform for DNA sensors*, Curr. Anal. Chem. 7 (2011) 8–34.
[36] D. Rolka, A. Poghossian, M.J. Schöning: *Integration of a capacitive EIS sensor into a FIA system for pH and penicillin determination*, Sensors 4 (2004) 84–94.
[37] J. Wang, Y. Zhou, M. Watkinson, J. Gautrot, S. Krause: *High-sensitivity light-addressable potentiometric sensors using silicon on sapphire functionalized with self-assembled organic monolayers*, Sens. Actuators B 209 (2015) 230–236.

[38] S.M. Sze, K.K. Ng: *Physics of Semiconductor Devices (3rd edition)*, John Wiley & Sons, Inc., Hoboken, New Jersey, USA (2007).
[39] D. Meschede: *Gerthsen Physik*, Springer-Verlag, Heidelberg, Germany (2010).
[40] D. Schröder: *Elektrische Antriebe 3: Leistungselektronische Bauelemente*, Springer-Verlag, Berlin, Deutschland (1996).
[41] A. Poghossian, M.J. Schöning: *Silicon-based chemical and biological field-effect sensors (edited by C.A. Grimes, E.C. Dickey, M.V. Pishko),* in Encyclopedia of sensors 10, American Scientific Publishers, Santa Clarita, California, USA (2006).
[42] A. Poghossian, M. Weil, A.G. Cherstvy, M.J. Schöning: *Electrical monitoring of polyelectrolyte multilayer formation by means of capacitive field-effect devices*, Anal. Bioanal. Chem. 405 (2013) 6425–6436.
[43] A.P.F. Turner, I. Karube, G.S. Wilson: *Biosensors: Fundamentals and Applications*, Oxford University Press, Oxford, England (1987) 481–530.
[44] A. Poghossian, D.-T. Mai, Y. Mourzina, M.J. Schöning: *Impedance effect of an ion-sensitive membrane: Characterisation of an EMIS sensor by impedance spectroscopy, capacitance–voltage and constant–capacitance method*, Sens. Actuators B 103 (2004) 423–428.
[45] A. Poghossian, S. Ingebrandt, M.H. Abouzar, M.J. Schöning: *Label-free detection of charged macromolecules by using a field-effect-based sensor platform: Experiments and possible mechanisms of signal generation*, Appl. Phys. A 87 (2007) 517–524.
[46] S.B. Nimse, K. Song, M.D. Sonawane, D.R. Sayyed, T. Kim: *Immobilization techniques for microarray: Challenges and applications*, Sensors 14 (2014) 22208–22229.
[47] A. Sassolas, B.D. Leca-Bouvier, L.J. Blum: *DNA biosensors and microarrays*, Chem. Rev. 108 (2008) 109–139.
[48] J.I.A. Rashid, N.A. Yusof: *The strategies of DNA immobilization and hybridization detection mechanism in the construction of electrochemical DNA sensor: A review*, Sens. Biosensing. Res. 16 (2017) 19–31.
[49] A.B. Steel, R.L. Levicky, T.M. Herne, M.J. Tarlov: *Immobilization of nucleic acids at solid surfaces: Effect of oligonucleotide length on layer assembly*, Biophys. J. 79 (2000) 975–981.
[50] C. Geffroy, M.P. Labeau, K. Wong, B. Cabane, M.A. Cohen Stuart: *Kinetics of adsorption of polyvinylamine onto cellulose*, Colloids Surf. A 172 (2000) 47–56.
[51] R. Meszaros, L. Thompson, M. Bos, P. de Groot: *Adsorption and electrokinetic properties of polyethylenimine on silica surfaces*, Langmuir 18 (2002) 6164–6169.
[52] D.G. Hafeman, J.W. Parce, H.M. McConnell: *Light-addressable potentiometric sensor for biochemical systems*, Science 240 (1988) 1182–1185.
[53] Y. Mourzina, T. Yoshinobu, J. Schubert, H. Lüth, H. Iwasaki, M.J. Schöning: *Ion-selective light-addressable potentiometric sensor (LAPS) with chalcogenide thin film prepared by pulsed laser deposition*, Sens. Actuators B 80 (2001) 136–140.

[54] J.C. Owicki, L.J. Bousse, D.G. Hafeman, G.L. Kirk, J.D. Olson, H.G. Wada, J.W. Parce: *The light-addressable potentiometric sensor: Principles and biological applications*, Annu. Rev. Biophys. Biomol. Struct. 23 (1994) 87–113.

[55] T. Yoshinobu, K. Miyamoto, C.F. Werner, A. Poghossian, T. Wagner, M.J. Schöning: *Light-addressable potentiometric sensors for quantitative spatial imaging of chemical species*, Annu. Rev. Anal. Chem. 10 (2017) 19.1–19.22.

[56] K. Miyamoto, Y. Sugawara, S. Kanoh, T. Yoshinobu, T. Wagner, M.J. Schöning: *Image correction method for the chemical imaging sensor*, Sens. Actuators B 144 (2010) 334–348.

[57] Z. Qintao, W. Ping, W. J. Parak, M. George, G. Zhang: *A novel design of multi-light LAPS based on digital compensation of frequency domain*, Sens. Actuators B 73 (2001) 152–156.

[58] J.R. Lakowicz: *Principles of Fluorescence Spectroscopy (3th Edition)*, Plenum Press, New York, USA (1983).

[59] U. Resch-Genger, M. Grabolle, S. Cavaliere-Jaricot, R. Nitschke, T. Nann: *Quantum dots versus organic dyes as fluorescent labels*, Nat. Methods 5 (2008) 763–775.

[60] T. Bernas, J.P. Robinson, E.K. Asem, B. Rajwa: *Loss of image quality in photobleaching during microscopic imaging of fluorescent probes bound to chromatin*, J. Biomed. Opt. 10 (2005) 064015-1–9.

[61] L. Song, E.J. Hennink, T. Young, H.J. Tanke: *Photobleaching kinetics of fluorescein in quantitative fluorescence microscopy*, Biophys. J. 68 (1995) 2588–2600.

[62] A.I. Dragan, R. Pavlovic, J.B. McGivney, J.R. Casas-Finet, E. S. Bishop, R.J. Strouse, M.A. Schenerman, C.D. Geddes: *SYBR Green I: Fluorescence properties and interaction with DNA*, J. Fluoresc. 22 (2012) 1189–1199.

[63] G. Cosa, K.S. Focsaneanu, J.R.N. McLean, J.P. McNamee, J.C. Scaiano: *Photophysical properties of fluorescent DNA-dyes bound to single- and double-stranded DNA in aqueous buffered solution*, Photochem. Photobiol. 73 (2001) 585–599.

[64] S. Tyagi, F.R. Kramer: *Molecular beacons: Probes that fluoresce upon hybridization*, Nat. Biotechnol. 14 (1996) 303–308.

[65] I.V. Kutyavin, I.A. Afonina, A. Mills, V.V. Gorn, E.A. Lukhtanov, E.S. Belousov, M.J. Singer, D.K. Walburger, S.G. Lokhov, A.A. Gall, R. Dempcy, M.W. Reed, R.B. Meyer, J. Hedgpeth: *3'-Minor groove binder-DNA probes increase sequence specificity at PCR extension temperatures*, Nucleic Acids Res. 28 (2000) 655–661.

[66] O.I. Vinogradova, O.V. Lebedeva, K. Vasilev, H. Gong, J. Garcia-Turiel, B.-S. Kim: *Multilayer DNA/poly(allylamine hydrochloride) microcapsules: Assembly and mechanical properties*, Biomacromolecules 6 (2005) 1495–1502.

[67] D. Xiang, K. Zhai, W. Xiang, L. Wang: *Highly sensitive fluorescence quantitative detection of specific DNA sequences with molecular beacons and nucleic acid dye SYBR green I*, Talanta 129 (2014) 249–253.

[68] H. Zipper, C. Buta, K. Lämmle, H. Brunner, J. Bernhagen, F. Vitzthum: *Mechanisms underlying the impact of humic acids on DNA quantification by*

SYBR Green I and consequences for the analysis of soils and aquatic sediments, Nucleic Acids Res. 31 (2003) e39-1–16.

[69] H. Zipper, H. Brunner, J. Bernhagen, F. Vitzthum: *Investigations on DNA intercalation and surface binding by SYBR Green I, its structure determination and methodological implications*, Nucleic Acids Res. 32 (2004) e103-1–10.

[70] J. Kapuscinski, B. Skoczylas: *Simple and rapid fluorimetric DNA microassay method for DNA microassay*, Anal. Biochem. 83 (1977) 252–257.

[71] J. Kapuscinski: *DAPI: A DNA-specific fluorescent probe*, Biotech. Histochem. 70 (1995) 220–233.

[72] J.C. Waters: *Accuracy and precision in quantitative fluorescence microscopy*, J. Cell Biol. 185 (2009) 1135–1148.

3 Label-free detection of double-stranded DNA molecules with polyelectrolyte-modified capacitive field-effect sensors

tm – Technisches Messen 84 (2017)
628–634

Thomas S. Bronder, Arshak Poghossian, Michael Keusgen, Michael J. Schöning

Submitted: 03.02.2017
Accepted: 30.03.2017
Published: 26.04.2017

ABSTRACT

In this study, polyelectrolyte-modified field effect-based electrolyte-insulator semiconductor (EIS) devices have been used for the label-free electrical detection of double-stranded deoxyribonucleic acid (dsDNA) molecules. The sensor-chip functionalization with a positively charged polyelectrolyte layer provides the possibility of direct adsorptive binding of negatively charged target DNA oligonucleotides onto the SiO_2-chip surface. EIS sensors can be utilized as a tool to detect surface-charge changes; the electrostatic adsorption of oligonucleotides onto the polyelectrolyte layer leads to a measurable surface-potential change. Signals of 39 mV have been recorded after the incubation with the oligonucleotide solution. Besides the electrochemical experiments, the successful adsorption of dsDNA onto the polyelectrolyte layer has been verified via fluorescence microscopy. The presented results demonstrate that the signal recording of EIS chips, which are modified with a polyelectrolyte layer, can be used as a favorable approach for a fast, cheap and simple detection method for dsDNA.

ZUSAMMENFASSUNG

In dieser Studie wurden Polyelektrolyt-modifizierte Feldeffekt-basierte Elektrolyt-Isolator-Halbleiter (EIS)-Strukturen für die markierungsfreie elektrische Detektion von Doppelstrang-Desoxyribonukleinsäure (dsDNA)-Molekülen eingesetzt. Die Sensorchip-Funktionalisierung mit Hilfe einer positiv geladenen Polyelektrolyt-Schicht bietet die Möglichkeit der direkten adsorptiven Bindung von nachzuweisenden, negativ geladenen Ziel-DNA-Oligonukleotiden mit der SiO_2-Chipoberfläche an. EIS-Sensoren können zur Detektion von Ladungsänderungen an der Sensoroberfläche verwendet werden; dabei führt die elektrostatische Adsorption der (nachzuweisenden) Oligonukleotide auf der Polyelektrolyt-Schicht zu einer messbaren Veränderung des Oberflächenpotentials. Es wurden Sensorsignale von 39 mV nach der Inkubation des Chips mit Oligonukleotid-Lösungen gemessen. Neben den elektrochemischen Experimenten wurde die erfolgreiche Adsorption der dsDNA auf der Polyelektrolyt-Schicht mittels Fluoreszenzmikroskopie kontrolliert. Die vorgestellten Ergebnisse zeigen, dass die Signalerfassung mit EIS-Chips, die mit einer Polyelektrolyt-Schicht modifiziert wurden, zur schnellen, günstigen und einfachen Detektion von dsDNA erfolgen kann.

KEYWORDS

DNA biosensor, electrolyte-insulator-semiconductor sensor, field-effect, polyelectrolyte, label-free detection

3.1 INTRODUCTION

In the past, a broad spectrum of different techniques for the label-free detection of biomolecules based on field-effect devices has been developed [1–5]. Deoxyribonucleic acid (DNA) is a famous representative of such biomolecules and its detection is of great interest in many fields, including forensic DNA analysis, genomics, genosensing, medical diagnostics and biotechnology [2, 6–8]. In order to detect DNA with field-effect sensors, different transducer structures, like ion-sensitive field-effect transistors (ISFET) [9–11], silicon-nanowires (SiNW) [12, 13], light-addressable potentiometric sensors (LAPS) [14–16] and capacitive electrolyte-insulator-semiconductor (EIS) devices [17–19] have been developed during last decades.

A possible detection method for these devices is the recording of the DNA-binding process – either single-stranded DNA (ssDNA) or double-stranded DNA (dsDNA) molecules – on the field-effect sensor surface; owing to the binding event the charge distribution inside the space-charge region of the semiconductor is changed, which results in an output-signal change of the field-effect device. Compared to SiNW, ISFET or LAPS, the EIS structure is the simplest type of field-effect sensor, which offers the advantage of a fast and easy fabrication process. EIS-gate-insulator materials can be SiO_2 or Ta_2O_5, those oxides provide usually hydroxyl (-OH) surface groups, which are inappropriate (without any additional functionalization step) for the binding of many different target molecules. The range of target molecules can be highly increased by addition of a modification step using linker molecules or different surface-functionalization techniques, like silanization [20–22] or electrostatic adsorption of polyelectrolytes [6, 23–25]. Notably, the adsorption techniques provide advantages in terms of simplicity, fast preparation and costs [5]. Since in aqueous solution DNA molecules are negatively charged (due to the phosphate-sugar backbone), a direct immobilization onto an unmodified SiO_2 surface is hindered because of electrostatic repulsion forces between the phosphate groups of the DNA and the oxide layer, which are both negatively charged. In order to achieve the binding of DNA onto the sensitive area of an EIS sensor, a surface-modification step with a positively charged polyelectrolyte layer (e.g., poly(allylamine hydrochloride) (PAH) [26]) creates a surface that allows a direct adsorption of DNA molecules.

A field of application for dsDNA sensing might be the monitoring and verification of a polymerase chain reaction (PCR) DNA-amplification process. In this work, EIS sensors, functionalized with a positively charged, weak polyelectrolyte layer of PAH molecules, were used to detect the immobilization of unlabeled dsDNA molecules by recording of the surface-potential changes induced by their intrinsic molecular charge. In addition, the presence of dsDNA molecules has been controlled by means of fluorescence-microscopy investigations using the fluorescence dye SybrGreen (SG).

3.2 CHIP FABRICATION AND MEASUREMENT SETUP

The complete fabrication process for the polyelectrolyte-functionalized EIS sensors can be subdivided into four main steps, which are schematically shown in **Figure 3.1**: The fabrication started with a dry oxidation step (1) of a boron-doped (p-type) silicon wafer

(SiMat – Silicon Materials, Kaufering, Germany) with a resistivity of 1–10 Ωcm. During the oxidation process at 1050 °C for 25 min, a 50 nm thick SiO_2 layer is grown at the whole wafer surface. The next step was a chemical etching (2) of the rear-side oxide, which has been carried out with 40% hydrofluoric acid (Merck, Darmstadt, Germany) for 20–30 s. In order to create an Ohmic contact to the silicon substrate, a 300 nm thick layer of aluminum has been deposited via electron-beam evaporation (3) onto the SiO_2-free rear side, followed by a thermal annealing process at 400 °C for 10 min in N_2 atmosphere. After the annealing, the complete wafer has been separated into single 10 × 10 mm^2 chips by means of wafer dicing. The last step was the polyelectrolyte modification step of each SiO_2 chip (4) by means of drop-coating of 100 µL polyelectrolyte solution (50 µM PAH (abcr GmbH & Co. KG, Karlsruhe, Germany) in 100 mM NaCl, adjusted with NaOH to pH 5.5) onto the oxide surface of the EIS sensor with an incubation time of 10 min. The PAH-covered chip surfaces were rinsed thoroughly with deionized (DI) water to remove unbound PAH molecules and dried with nitrogen.

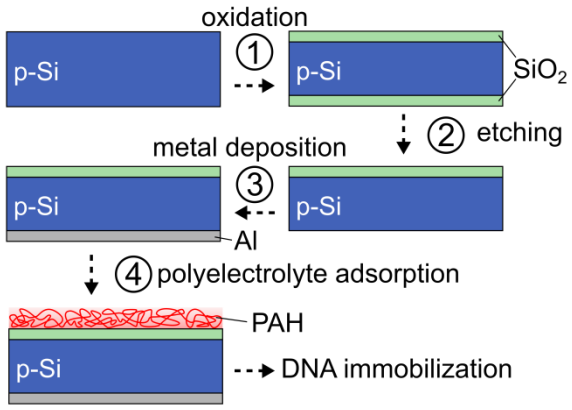

Figure 3.1: Schematic of the fabrication process steps of polyelectrolyte-modified EIS sensors.

After the fabrication- and modification steps, the sensors are ready to use for electrochemical characterization and DNA measurements. The sensors were mounted into a home-made measurement chamber (made of poly(methyl methacrylate)), which is schematically shown in **Figure 3.2**. The setup includes an O-ring sealing in order to prevent a leakage of the used solutions and to avoid an electrical shortcut between rear-side contact of the chip and reference electrode. Due to the geometric limitations of the O-ring, an active chip surface area of 0.5 cm^2 remains in contact to the solution. A liquid-junction Ag/AgCl reference electrode (Metrohm, Filderstadt, Germany) filled with 3 M KCl solution was used. The rear-side of the sensor chip and the reference electrode were connected in a two-electrode configuration to a Zennium electrochemical workstation (Zahner Elektrik, Kronach, Germany). Prior to the polyelectrolyte adsorption and the dsDNA immobilization, the sensors were electrochemically characterized in measurement buffer (0.33 mM phosphate-buffered saline (PBS), pH 7.0). 1 mL of 5 µM dsDNA solution have been prepared in a reaction tube (Eppendorf AG, Hamburg, Germany) by mixing of two solutions (each 500 µL of 1× TE buffer (10 mM Tris (tris(hydroxymethyl)-aminomethane)

and 1 mM EDTA (ethylenediaminetetraacetic acid) in DI water) pH 8.0) containing 10 µM complementary sequences of 20-mer ssDNA (5'-GTT-CTT-CTC-ATT-CTT-CCC-CT-3' and 5'-AGG-GGA-AGA-ATG-AGA-AGA-AC-3') (Biomers, Ulm, Germany) together. After mixing, the dsDNA solution has been heated up to ~95 °C in a water bath and slowly cooled down to room temperature by removing the tube out of the water bath. This procedure has been performed to achieve a high hybridization yield. In order to detect dsDNA molecules, the measurement buffer was removed and a solution containing the dsDNA molecules was pipetted onto the PAH-modified sensor surface. During an incubation time of 60 min, the negatively charged oligonucleotides immobilize via electrostatic adsorption forces onto the positively charged PAH layer (**Figure 3.2**, zoomed part). To remove unbound DNA molecules, the chip was rinsed at least three times with measurement buffer. After the last rinsing step, the chamber was filled again with measurement buffer and the electrochemical measurement was performed.

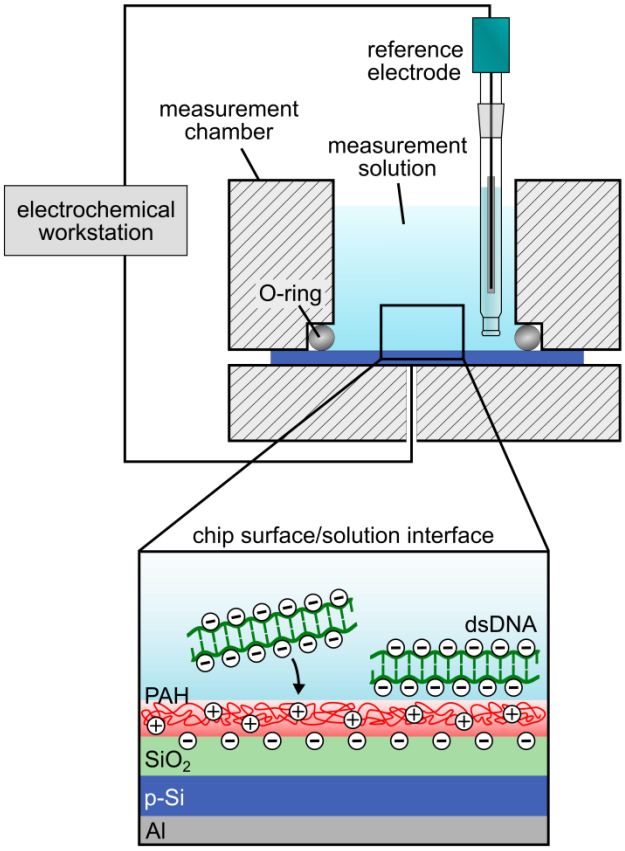

Figure 3.2: Illustration of the measurement setup including a mounted sensor chip and a zoomed cross section of the surface/solution interface.

3.3 SENSING PRINCIPLE

The EIS sensor consists basically of three parts: electrolyte (measurement buffer), insulating layer (SiO_2) and semiconductor substrate (p-doped silicon). An electrical

equivalent circuit of the EIS structure can be described as a serial arrangement of two capacitors. This arrangement consists of C_{OX} (the capacitance of the insulating SiO_2 layer) and C_{SCR} (the capacitance of the space-charge region inside the semiconductor). While C_{OX} is constant, the value of C_{SCR} depends on the space-charge region width, which can be affected – among others – by the bias voltage applied to the system. The total capacitance C of the system is approximated by **Eq. 3.1** [27]:

$$C = \frac{C_{OX}C_{SCR}}{C_{OX} + C_{SCR}} = \frac{C_{OX}}{\frac{C_{OX}}{C_{SCR}} + 1}. \qquad \textbf{Eq. 3.1}$$

By recording the total capacitance versus the applied bias voltage (C–V), a signal response with a sigmoidal-like shape can be measured (**Figure 3.3**, black solid line) with the three characteristic regions: accumulation, depletion and inversion.

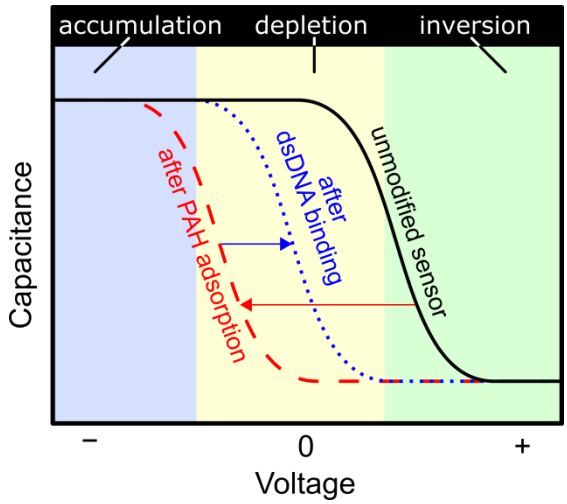

Figure 3.3: Theoretical shifts of C–V curve of the unmodified sensor after adsorption of PAH molecules onto the gate-oxide surface (red, dashed line) and after immobilization of dsDNA molecules onto the PAH layer (blue, dotted line). The three colored background regions indicate the accumulation, depletion and inversion part of the C–V curve after binding of dsDNA.

Besides the applied bias voltage, charge changes at or near the oxide surface can have also an influence on the width of the space-charge region and therefore, also on the total sensor capacitance C. Such surface-charge changes can occur during the electrostatic adsorption of charged polyelectrolytes, DNA or other (bio)molecules. As a result of a capacitance change, the C–V curve shifts to more negative or positive direction (dependent on the sign of the charge of the molecule) after a positive or negative surface-potential change, respectively. For example, after the adsorption of the positively charged PAH molecules onto a SiO_2-gate EIS sensor, the C–V curve is shifted along the voltage axis to more negative values (**Figure 3.3**, red dashed line). In contrast to that, after the immobilization of negatively charged dsDNA molecules, the C–V curve is shifted to a more positive (less negative) voltage (**Figure 3.3**, blue dotted curve). The signal amplitude of

the horizontal potential shift of the C–V curve reflects the respective surface-potential change.

Besides the static characterization of the EIS sensor by means of C–V measurements, the so-called constant-capacitance (ConCap) mode [28] allows a direct and real-time monitoring of the EIS-surface potential. In the Con-Cap mode, the total capacitance C of the EIS sensor is kept constant by using a feedback circuit, which applies an instantly sign-inverted voltage to the sensor device. ConCap measurements provide the possibility to record the sensor-potential change in a time-resolved manner, which gives the advantage to evaluate parameters, like response time and signal stability of the field-effect sensor.

3.4 RESULTS

3.4.1 Electrostatic detection of dsDNA

The electrochemical characterization of EIS chips starts with the validation of the oxide layer in terms of its quality by measurements of the leakage current prior to the PAH-adsorption step. The leakage current has been recorded by applying a DC voltage in a range between –2 V and +2 V with a sweeping rate of 100 mV/s. The recorded leakage current of all chips used in this work was less than 30 nA. An example of a measured C–V curve (recorded in the range of –2 V to +2 V with a superimposed alternating voltage of 20 mV and 120 Hz) is shown in **Figure 3.4a**. As expected, the C–V curves of the unmodified sensor, after the modification with PAH and after the dsDNA immobilization, show a sigmoidal-like shape with the three characteristic regions for EIS chips: Accumulation (for applied voltage of less than –1.5 V), depletion (between –1.5 V and 0 V) and inversion (more than 0 V). A distinct shift in the depletion region of the C–V curves after PAH adsorption and dsDNA immobilization is clearly noticeable. The potential shift recorded after the adsorption step of PAH was 122 mV at 20 nF. PAH molecules are positively charged in solution with neutral pH value. Due to the electrostatic binding of polyelectrolyte molecules onto the SiO_2-gate oxide, the surface potential of the EIS chip is changed resulting in a shift of the C–V curve. After incubation of the PAH-modified EIS sensor with a solution containing dsDNA molecules, a signal shift of 39 mV has been recorded at 20 nF. Since DNAs are negatively charged molecules in solutions with neutral pH, the binding of DNA molecules with the PAH layer yields a signal change to more positive voltage direction. DNA- and PAH molecules attract each other because of their opposite charge resulting in an electrostatic adsorption of the oligonucleotides onto the polyelectrolyte layer. The signal shifts of the C–V curve serve as an indicator for the adsorption of PAH and immobilization of the dsDNA molecules onto the PAH-modified EIS sensor device.

Besides measurement of the C–V characteristics, experiments in ConCap mode (working point: 20 nF) have also been performed. **Figure 3.4b** shows the ConCap curve of the same sensor chip, which has also been used for the performed C–V measurements presented in **Figure 3.4a**. After the sensor functionalization with PAH- and dsDNA immobilization, signal changes of 97 mV and 41 mV have been observed, respectively. The obtained signals during ConCap measurements were stable with a very small drift. The measured signal amplitudes after polyelectrolyte adsorption and dsDNA immobilization

recorded in ConCap mode were comparable with the potential shifts of the C–V curves; moreover, the direction of potential shifts of C–V- and ConCap-measurement results matches with the theoretical considerations described in **Section 3.3**. From the obtained electrochemical signals high signal stability and a short response time of the modified EIS sensors is noticeable. Similar to the recorded C–V curves, the signal changes measured via ConCap mode are also an indicator for a surface-potential change induced by modification steps with PAH and dsDNA.

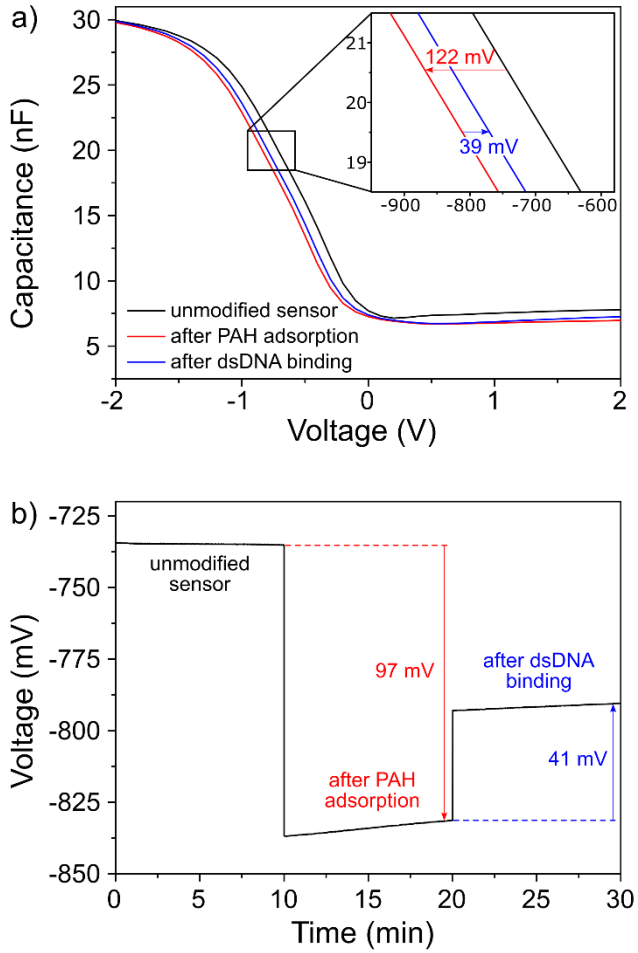

Figure 3.4: Recorded C–V curve (a) and ConCap response (b) of the unmodified sensor, after PAH adsorption and after dsDNA immobilization.

3.4.2 Fluorescence measurements

Fluorescence investigations have been established as a trustful reference method for the detection of DNA [29–32]. In this study, experiments with a fluorescence microscope have been performed in order to verify the results obtained from electrochemical characterization and prove the successful binding of target dsDNA molecules onto the PAH-modified SiO_2 surface. Three PAH-modified sensor chips were incubated with 5 µM

dsDNA solution for 60 min according to the protocol described in **Section 3.4.1**. To remove unbound dsDNA molecules, the chips were washed with measurement buffer for at least three times and dried with N_2. For the chip staining, a 50 µL drop of freshly prepared SG (Sigma-Aldrich, Taufkirchen, Germany) solution (dilution of 1:1000, stock solution:DI water) was pipetted onto the dsDNA-modified surface and incubated for 60 min at room temperature. SG is a fluorescence dye that can bind to dsDNA molecules [33–38]. The fluorescence intensity of SG enhances strongly (Dragan et al. reported an increase by a factor of >1000 [34]) upon binding to dsDNA molecules. Then, the surface was washed with DI water and dried with N_2. The fluorescence measurements were performed directly after the staining procedure in order to avoid photobleaching effects. The fluorescence observations have been performed using an Axio Imager A1m (Zeiss, Jena, Germany).

Figure 3.5a show an example of a recorded image for the SG-stained PAH/dsDNA-modified SiO_2-EIS surface. A strong and homogenous fluorescence signal has been detected. For comparison, **Figure 3.5b** depicts a recorded image of a PAH-modified EIS sensor without dsDNA molecules.

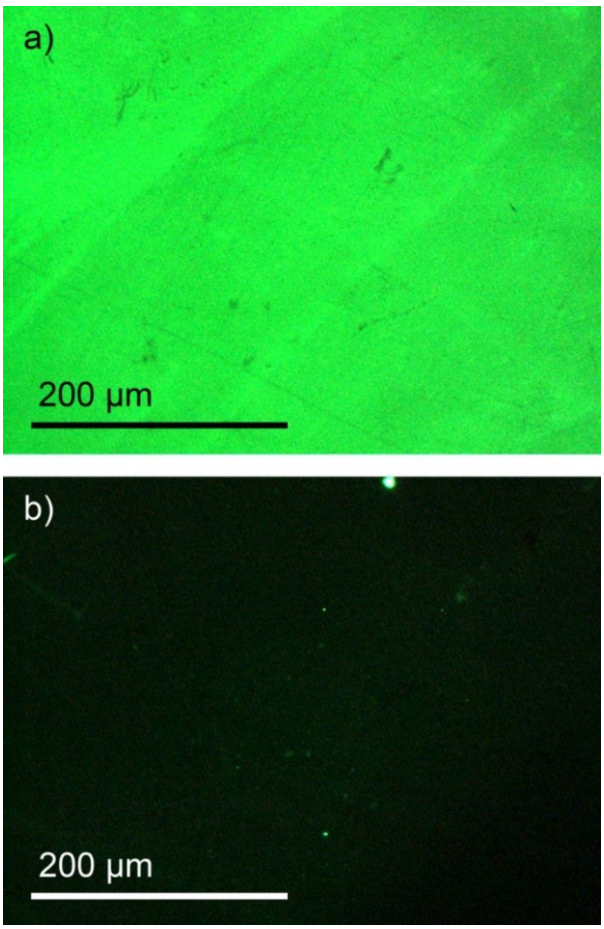

Figure 3.5: Exemplary fluorescence images of differently modified SiO_2 surfaces of two EIS chips stained with SG: (a) shows a PAH/dsDNA-modified surface; a strong fluorescence signal can be observed because of the presence of dsDNA-specific-bound fluorescence dye molecules. Almost no fluorescence signal can be identified for a PAH-modified surface without dsDNA (b).

The chip surfaces in **Figure 3.5b** were stained with SG solution using the same protocol as the sensors containing dsDNA molecules. As can be seen, almost no fluorescence signal has been observed for the sensor without dsDNA. The strong fluorescence intensity presented in **Figure 3.5a** evidences the presence of double-stranded oligonucleotides on the sensor surface. Even after one week of dark storage at room temperature, a strong and clear fluorescence signal was observed. The results obtained by fluorescence analysis are in good agreement with the results of field-effect measurements in **Section 3.4.1**.

3.5 CONCLUSION

We reported on the electrical detection of PAH- and dsDNA binding onto the SiO_2 gate-oxide layer of EIS sensors by means of C–V- and ConCap measurements. The results obtained in this study underline that the measurement of ConCap response before and after dsDNA adsorption onto PAH-modified charge-sensitive EIS sensors serves as an adequate and proper method for the label-free detection of DNA with field-effect-based sensors. The presence of dsDNA molecules on the EIS-sensor surface was verified by means of fluorescence-microscopic investigations using the fluorescence dye SG. The presented detection technique might have distinct potential for indication or verification of a PCR-amplification product. Further investigation is devoted to the detection of DNA in PCR samples as well as the influence of certain PCR components on the sensor signal.

ACKNOWLEDGEMENTS

The authors kindly acknowledge the financial support of the German Federal Ministry of Education and Research (Bundesministerium für Bildung und Forschung, BMBF; DiaCharge project 031A192D). Special thanks to H. Iken for sensor fabrication in the clean room, S. Scheja and M.P. Jessing for their assistance with sensor preparation and measurements.

REFERENCES

[1] C. Kataoka-Hamai, Y. Miyahara: *Label-free detection of DNA by field-effect devices*, IEEE Sens. J. 11 (2011) 3153–3160.

[2] A. Poghossian, M.J. Schöning: *Label-free sensing of biomolecules with field-effect devices for clinical applications*, Electroanal. 26 (2014) 1197–1213.

[3] W. Sant, M.L. Pourciel, J. Launay, T. Do Conto, A. Martinez, P. Temple-Boyer: *Development of chemical field effect transistors for the detection of urea*, Sens. Actuators B 95 (2003) 309–314.

[4] J.R. Siqueira, M.H. Abouzar, M. Bäcker, V. Zucolotto, A. Poghossian, O.N. Oliveira, M.J. Schöning: *Carbon nanotubes in nanostructured applications and materials science films: Potential application as amperometric and potentiometric field-effect (bio-)chemical sensors*, Phys. Status Solidi A 206 (2009) 462–467.

[5] A. Poghossian, M. Weil, A.G. Cherstvy, M.J. Schöning: *Electrical monitoring of polyelectrolyte multilayer formation by means of capacitive field-effect devices*, Anal. Bioanal. Chem. 405 (2013) 6425–6436.

[6] A. Sassolas, B.D. Leca-Bouvier, L.J. Blum: *DNA biosensors and microarrays*, Chem. Rev. 108 (2008) 109–139.

[7] P. de-los-Santos-Alvarez, M.J. Lobo-Castañón, A.J. Miranda-Ordieres, P. Tuñón-Blanco: *Current strategies for electrochemical detection of DNA with solid electrodes*, Anal. Bioanal. Chem. 378 (2004) 104–118.

[8] C.P. Chen, A. Ganguly, C.Y. Lu, T.Y. Chen, C.C. Kuo, R.S. Chen, W.H. Tu, W.B. Fischer, K.H. Chen, L.C. Chen: *Ultrasensitive in situ label-free DNA detection using a GaN nanowire-based extended-gate field-effect-transistor sensor*, Anal. Chem. 83 (2011) 1938–1943.

[9] D. Gonçalves, D.M.F. Prazeres, V. Chu, J.P. Conde: *Detection of DNA and proteins using amorphous silicon ion-sensitive thin-film field effect transistors*, Biosens. Bioelectron. 24 (2008) 545–551.

[10] C.S. Lee, S.K. Kim, M. Kim: *Ion-sensitive field-effect transistor for biological sensing*, Sensors 9 (2009) 7111–7131.

[11] S. Purushothaman, C.P. Ou, C. Toumazou: *Protons and single nucleotide polymorphism detection: A simple use for the ion sensitive field effect transistor*, Sens. Actuat. B. 114 (2006) 964–968.

[12] S. Ingebrandt, X.T. Vu, J.F. Eschermann, R. Stockmann, A. Offenhäusser: *Top-down processed SOI nanowire devices for biomedical applications*, ECS Trans. 35 (2011) 3–15.

[13] X.T. Vu, R. Stockmann, B. Wolfrum, A. Offenhäuser, S. Ingebrandt: *Fabrication and application of a microfluidic-embedded silicon nanowire biosensor chip*, Phys. Status Solidi A 207 (2010) 850–857.

[14] C. Wu, A. Poghossian, T.S. Bronder, M.J. Schöning: *Sensing of double-stranded DNA molecules by their intrinsic molecular charge using the light-addressable potentiometric sensor*, Sens. Actuators B 229 (2016) 506–512.

[15] C. Wu, T. Bronder, A. Poghossian, C.F. Werner, M. Bäcker, M.J. Schöning: *Label-free electrical detection of DNA with a multi-spot LAPS: First step towards light-addressable DNA chips*, Phys. Status Solidi A 211 (2014) 1423–1428.

[16] C. Wu, T. Bronder, A. Poghossian, C.F. Werner, M.J. Schöning: *Label-free detection of DNA using a light-addressable potentiometric sensor modified with a positively charged polyelectrolyte layer*, Nanoscale 7 (2015) 6143–6150.

[17] J. Fritz, E.B. Cooper, S. Gaudet, P.K. Sorger, S.R. Manalis: *Electronic detection of DNA by its intrinsic molecular charge*, Proc. Natl. Acad. Sci. U.S.A. 99 (2002) 14142–14126.

[18] T.S. Bronder, A. Poghossian, S. Scheja, C. Wu, M. Keusgen, D. Mewes, M.J. Schöning: *DNA immobilization and hybridization detection by the intrinsic molecular charge using capacitive field-effect sensors modified with a charged weak polyelectrolyte layer*, ACS Appl. Mater. Interfaces 7 (2015) 20068–20075.

[19] T.S. Bronder, A. Poghossian, S. Scheja, C.S. Wu, M. Keusgen, M.J. Schöning: *Electrostatic detection of unlabelled single- and double-stranded DNA using capacitive field-effect devices functionalized with a positively charged polyelectrolyte layer*, Procedia Eng. 120 (2015) 544–547.

[20] R. GhoshMoulick, X.T. Vu, S. Gilles, D. Mayer, A. Offenhäusser, S. Ingebrandt: *Impedimetric detection of covalently attached biomolecules on field-effect transistors*, Phys. Status Solidi A 206 (2009) 417–425.

[21] Y. Han, A. Offenhäusser, S. Ingebrandt: *Detection of DNA hybridization by a field-effect transistor with covalently attached catcher molecules*, Surf. Interface Anal. 38 (2006) 176–181.

[22] Y. Han, D. Mayer, A. Offenhäusser, S. Ingebrandt: *Surface activation of thin silicon oxides by wet cleaning and silanization*, Thin Solid Films 510 (2006) 175–180.

[23] Y. Omura, K.H. Kyung, S. Shiratori, S.H. Kim: *Effects of applied voltage and solution pH in fabricating multilayers of weakly charged polyelectrolytes and nanoparticles*, Ind. Eng. Chem. Res. 53 (2014) 11727–11733.

[24] M.H. Abouzar, A. Poghossian, J.R. Siqueira, O.N. Oliveira, W. Moritz, M.J. Schöning: *Capacitive electrolyte–insulator–semiconductor structures functionalised with a polyelectrolyte/enzyme multilayer: New strategy for enhanced field-effect biosensing*, Phys. Status Solidi A 207 (2010) 884–890.

[25] M.H. Abouzar, A. Poghossian, A.M. Pedraza, D. Gandhi, S. Ingebrandt, W. Moritz, M.J. Schöning: *An array of field-effect nanoplate SOI capacitors for (bio-)chemical sensing*, Biosens. Bioelectron. 26 (2011) 3023–3028.

[26] P. Mocchiutti, M.V. Galván, M.C. Inalbon, M.A. Zanuttini: *Improvement of paper properties of recycled unbleached softwood kraft pulps by poly(allylamine hydrochloride)*, BioResources 6 (2011) 570–583.

[27] A. Poghossian, M. Bäcker, D. Mayer, M.J. Schöning: *Gating capacitive field-effect sensors by the charge of nanoparticle/molecule hybrids*, Nanoscale 7 (2015) 1023–1031.

[28] D. Rolka, A. Poghossian, M.J. Schöning: *Integration of a capacitive EIS sensor into a FIA system for pH and penicillin determination*, Sensors 4 (2004) 84–94.

[29] J. Wang, Y. Zhou, M. Watkinson, J. Gautrot, S. Krause: *High-sensitivity light-addressable potentiometric sensors using silicon on sapphire functionalized with self-assembled organic monolayers*, Sens. Actuators B 209 (2015) 230–236.

[30] A. Macanovic, C. Marquette, C. Polychronakos, M.F. Lawrence: *Impedance-based detection of DNA sequences using a silicon transducer with PNA as the probe layer*, Nucleic Acids Res. 32 (2004) e20-1–7.

[31] P. Estrela, P. Migliorato, H. Takiguchi, H. Fukushima, S. Nebashi: *Electrical detection of biomolecular interactions with metal–insulator–semiconductor diodes*, Biosens. Bioelectron. 20 (2005) 1580–1586.

[32] G.J. Zhang, G. Zhang, J.H. Chua, R.E. Chee, E.H. Wong, A. Agarwal, K.D. Buddharaju, N. Singh, Z. Gao, N. Balasubramanian: *DNA sensing by silicon nanowire: Charge layer distance dependence*, Nano Lett. 8 (2008) 1066–1070.

[33] D. Marie, F. Partensky, S. Jacquet, D. Vaulot: *Enumeration and cell cycle analysis of natural populations of marine picoplankton by flow cytometry using the nucleic acid stain SYBR Green I*, Appl. Environ. Microbiol. 63 (1997) 186–193.

[34] A.I. Dragan, R. Pavlovic, J.B. McGivney, J.R. Casas-Finet, E. S. Bishop, R.J. Strouse, M.A. Schenerman, C.D. Geddes: *SYBR Green I: Fluorescence properties and interaction with DNA*, J. Fluoresc. 22 (2012) 1189–1199.

[35] S. Giglio, P.T. Monis, C.P. Saint: *Demonstration of preferential binding of SYBR Green I to specific DNA fragments in real-time multiplex PCR*, Nucleic Acids Res. 31 (2003) e136-1–5.

[36] R. Rasmussen, T. Morrison, M. Herrmann, C. Wittwer: *Quantitative PCR by continuous fluorescence monitoring of a double strand DNA specific binding dye*, Biochemica 2 (1998) 8–11.

[37] H. Zipper, H. Brunner, J. Bernhagen, F. Vitzthum: *Investigations on DNA intercalation and surface binding by SYBR Green I, its structure determination and methodological implications*, Nucleic Acids Res. 32 (2004) e103-1–10.

[38] J. Skeidsvoll, P.M. Ueland: *Analysis of double-stranded DNA by capillary electrophoresis with laser-induced fluorescence detection using the monomeric dye SYBR Green I*, Anal. Biochem. 231 (1995) 359–365.

4 Sensing of double-stranded DNA molecules by their intrinsic molecular charge using the light-addressable potentiometric sensor

Sensors and Actuators B: Chemical 229 (2016) 506–512

Chunsheng Wu*, Arshak Poghossian, **Thomas S. Bronder***, Michael J. Schöning
*Both authors contributed equally to this work.

Submitted: 12.12.2015
Accepted: 02.02.2016
Published: 04.02.2016

ABSTRACT

A multi-spot light-addressable potentiometric sensor (LAPS), which belongs to the family of semiconductor field-effect devices, was applied for label-free detection of double-stranded deoxyribonucleic acid (dsDNA) molecules by their intrinsic molecular charge. To reduce the distance between the DNA charge and sensor surface and thus, to enhance the electrostatic coupling between the dsDNA molecules and the LAPS, the negatively charged dsDNA molecules were electrostatically adsorbed onto the gate surface of the LAPS covered with a positively charged weak polyelectrolyte layer of PAH (poly(allylamine hydrochloride)). The surface-potential changes in each spot of the LAPS, induced by the layer-by-layer adsorption of a PAH/dsDNA bilayer, were recorded by means of photocurrent-voltage- and constant-photocurrent measurements. In addition, the surface morphology of the gate surface before and after consecutive electrostatic adsorption of PAH- and dsDNA layers was studied by atomic force-microscopy measurements. Moreover, fluorescence microscopy was used to verify the successful adsorption of dsDNA molecules onto the PAH-modified LAPS surface. A high sensor signal of 25 mV was registered after adsorption of 10 nM dsDNA molecules. The lower detection limit is down to 0.1 nM dsDNA. The obtained results demonstrate that the PAH-modified LAPS device provides a convenient and rapid platform for the direct label-free electrical detection of in-solution-hybridized dsDNA molecules.

KEYWORDS

LAPS, field-effect, DNA biosensor, label-free detection, poly(allylamine hydrochloride), layer-by-layer adsorption

4.1 INTRODUCTION

DNA (deoxyribonucleic acid) biosensors and microarrays are considered as powerful tools for a wide variety of applications, including, for instance, DNA sequencing, gene-expression analysis, clinical diagnostics, pathogen identification, drug and food industry, forensic and parental testing or detection of biowarfare and bioterrorism agents [1–4]. The most technologies for the development of DNA microarrays are currently based on labelling strategies and therefore, they utilize various labels (e.g., fluorescence, redox, enzymatic) for a signal readout and sensitivity enhancement [5]. Although the labeling procedure provides a high sensitivity, however, it requires additional sample preparation steps and has been proven to be complicated, time-consuming and might be not suited for portable point-of-care- or mobile diagnostic systems [6]. Therefore, various label-free strategies (e.g., quartz-crystal microbalance, surface-plasmon resonance, heat transfer, faradaic and non-faradaic impedimetry) have been developed and applied in DNA analytics [7, 8]. Especially, electrical detection of DNA molecules by their intrinsic molecular charge using semiconductor field-effect devices (FED) based on an electrolyte-insulator-semiconductor (EIS) system represents a promising label-free platform. It has been attracted much attention owing to the well-established semiconductor technologies available for the fabrication of miniaturized FED-based genosensors and DNA chips. In these devices, the adsorption and binding of charged molecules (e.g., DNA, proteins, polyelectrolytes) or charged nanoparticles on the gate surface of the FED changes the space-charge distribution in the semiconductor, resulting in a change in the output signal of the FED [9–11]. In previous studies, various kinds of FEDs, like capacitive EIS sensors, ion-sensitive field-effect transistors, Si-nanowire transistors and light-addressable potentiometric sensors (LAPS), have been applied for the detection of DNA-binding events; this includes adsorption, hybridization, single-nucleotide polymorphisms, DNA extension or amplification by polymerase chain reaction (PCR) as well as DNA sequencing [11–19]. In addition, owing to their surface charge-sensitive properties, FEDs are widely implemented for the detection of pH, ions and analyte concentrations in liquids [20–28].

For the detection of specific sequences from an unknown DNA sample, the highly selective base-pairing reaction known as hybridization reaction is mainly used, by which a single-stranded probe DNA (ssDNA) molecule binds specifically to its complementary single-stranded target DNA (cDNA), forming a double-stranded DNA (dsDNA). The vast majority of DNA-FEDs reported in literature detect the so-called on-chip hybridization event: Typically, probe ssDNA molecules of known sequences are immobilized onto the FED surface by adsorption or covalent attachment and the subsequent hybridization event is either detected *ex situ* by measuring the sensor signal before and after hybridization or *in situ* by monitoring the sensor signal during the hybridization process. At the same time, very little is known about the application of FEDs for direct label-free electrical detection of dsDNA formed after hybridization reaction occurred in the solution (further referred as in-solution hybridization). In some cases, this could offer several advantages over detection by on-chip hybridization, especially when FEDs are used for the detection of DNA amplification by PCR [29–31]. Since PCR generates dsDNA, no extra sample preparation steps such as the heating of the PCR product to generate cDNA for the on-chip hybridization followed by the rapid cooling to prevent re-hybridization, are required.

Moreover, by direct dsDNA detection, the surface-modification procedure can significantly be simplified, because no probe ssDNA has to be immobilized onto the sensor surface. Thus, direct dsDNA detection could reduce the detection time and costs and might even increase the reproducibility of DNA analysis.

In this work, a multi-spot (16 spots) LAPS modified with a positively charged weak polyelectrolyte layer of PAH (poly(allylamine hydrochloride)) was applied for the direct label-free electrical detection of in-solution-hybridized dsDNA molecules by their intrinsic molecular charge for the first time. It can be expected that in the presence of a positively charged polyelectrolyte layer, the electrostatically adsorbed dsDNA molecules will be preferentially flat-oriented on the LAPS surface. This results in molecular charges positioned near the gate surface within the Debye length (the Debye length defines the distance at which the electrostatic potential drops 1/e), yielding a reduced charge-screening effect and a higher detection signal. During experiments, a consecutive layer-by-layer (LbL) adsorption of PAH- and dsDNA molecules was monitored by means of photocurrent-voltage (I_{ph}–V_g) and constant-photocurrent measurements. For comparison, the adsorption of dsDNA directly on a bare LAPS surface (without PAH layer) has been studied, too. In addition, the surface morphology of the adsorbed PAH- and PAH/dsDNA layers was investigated by atomic-force microscopy (AFM), while fluorescence measurements were used to verify the successful dsDNA adsorption onto the PAH-modified LAPS surface.

4.2 MATERIALS AND METHODS

4.2.1 LAPS-chip fabrication

LAPS chips consisting of an Al–Si–SiO_2 structure with sizes of 2 cm × 2 cm were fabricated using a ~400 µm thick p-doped Si wafer (resistivity 1–10 Ωcm). A 60 nm high-quality SiO_2 layer was prepared by thermal dry oxidation of the Si. To create an Ohmic contact to Si, the SiO_2 layer on the rear side of the silicon wafer was etched and then, a 300 nm thick Al layer was deposited on the rear side of the silicon wafer and patterned to open a window for the backside illumination of the Si. After fabrication, each chip was cleaned in ultrasonic bath with acetone, isopropyl alcohol, ethanol, deionized (DI) water and conditioned in 0.66 mM phosphate buffer solution (PBS), pH 7.5, 10 mM NaCl (further referred as measurement solution) for at least 12 h, in order to reduce the drift of the SiO_2-gate LAPS devices.

4.2.2 Multi-spot LAPS setup

Figure 4.1 shows a schematic of the multi-spot LAPS consisting of an Al–Si–SiO_2 structure and measurement setup. Functioning of the multi-spot LAPS has been described in detail in Ref. [12]. Briefly, since the LAPS represents a potential (charge)-sensitive device, the adsorption or binding of charged molecules on the gate surface of the LAPS will modulate the flat-band voltage (the voltage at which the energy bands in the semiconductor continue horizontally up to the surface) and the space-charge capacitance in the semiconductor. In order to detect the changes in the space-charge- or depletion

capacitance induced by the molecular adsorption, the LAPS is illuminated with a modulated light, which generates an alternating photocurrent as the sensor signal. In the multi-spot LAPS setup, multiple regions (16 spots) on the back-side of the Si have been illuminated in parallel by using an array of 4 × 4 infrared light-emitting diodes (LED) with a wavelength of 950 nm, where each LED is modulated at a different frequency ranging from 1 to 1.75 kHz [12]. The diameter of the spot illuminated by a single LED was about 2 mm, which defines the measured area (active spot size) on the sensing surface.

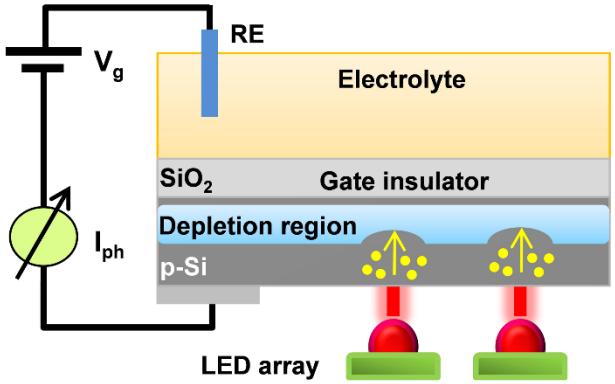

Figure 4.1: Schematic of the multi-spot LAPS consisting of an Al–Si–SiO_2 structure and measurement setup. RE: Reference electrode; I_{ph}: Photocurrent; V_g: Gate voltage.

For electrochemical characterization, the LAPS chip was mounted into a home-made measurement cell and a DC (direct current) voltage was applied onto the LAPS structure via a reference electrode (liquid-junction Ag/AgCl electrode filled with 3 M KCl, Metrohm, Germany). The effective contact area of the LAPS chip with the solution was about 2.25 cm^2. The surface-potential changes in each measurement spot induced due to the surface modification steps (i.e., consecutive adsorption of PAH and dsDNA molecules) were evaluated from the shifts of photocurrent-voltage (I_{ph}–V_g) curves along the voltage axis in the depletion region, or directly recorded by means of constant-photocurrent mode measurements. To reduce the influence of the charge-screening effect, the LAPS signal was readout in the same low ionic-strength measurement solution (0.66 mM PBS, pH 7.5, 10 mM NaCl). The measurements were carried out at room temperature (RT) in a dark Faraday box (to reduce the possible influence of ambient light and electromagnetic fields). The whole measurement setup was controlled by using a home-written LabVIEW software. All potential values are referred to the reference electrode.

4.2.3 Adsorption of PAH- and dsDNA molecules

The simple, fast and low-cost LbL method [32, 33] was utilized for both the preparation of the positively charged PAH layer on the negatively charged SiO_2 layer and the adsorption of the negatively charged dsDNA molecules on the PAH layer. For the preparation of the PAH layer, the cleaned SiO_2 surface of the LAPS chip was exposed to PAH solution (10 µM PAH (70 kDa, Sigma, Germany) adjusted with 10 mM NaCl,

pH 5.4) for 10 min at RT. At the pH value of 5.4, both the SiO_2 surface and PAH molecules can be considered to be enough charged (the point of zero charge of SiO_2 is between pH 2-3 and the isoelectric point for PAH amounts ~10.8 [34, 35]) to provide a successful electrostatic adsorption of positively charged PAH molecules on the negatively charged SiO_2 surface. The details of the PAH-adsorption procedure can be found in Refs. [10, 12]. After the PAH adsorption, the chip was washed with measurement solution to remove non-attached molecules from the sensor surface, followed by an electrochemical characterization of the PAH-covered LAPS device.

For dsDNA adsorption, the PAH-modified SiO_2 surface was exposed to a solution containing in-solution-hybridized dsDNA molecules for 1 h at RT, followed by rinsing to remove non-attached dsDNA molecules. Then, the LAPS modified with the PAH/dsDNA bilayer was electrochemically characterized in the measurement solution again. The in-solution hybridization was achieved by mixing the solutions containing 5 µM probe ssDNA (52-mer, with the sequence 5'-TGGAT CGCTG TGTAA GGACA CGTCG GCGTG GTCGT CTGCT GGGTT GATCT GG-3') and 5 µM complementary target cDNA (72-mer, with the sequence 5'-ACCTC CGTAA CCGTC ATTGT CCAGATCAAC CCAGC AGACG ACCAC GCCGA CGTGT CCTTA CACAG CGATCCA-3') for 1 h at RT. The ssDNA- and cDNA sequences were designed to mimic the PCR products. For this, the target cDNA contains not only the sequence complementary to the probe ssDNA but also the sequences for primer binding. All DNA sequences were custom-synthesized by Biomers (Ulm, Germany). The dsDNA solutions with different concentrations ranging from 0.1 nM to 1 µM were prepared by dilution of 5 µM dsDNA solution with the measurement solution.

4.3 RESULTS AND DISCUSSION

4.3.1 Electrochemical characterization of bare LAPS chips

The leakage current (which characterizes the quality of the gate-oxide layer) and potential sensitivity of the LAPS chips are crucial factors for a correct functioning and therefore, they should be checked before starting the PAH- and dsDNA adsorption processes. The leakage current has been measured between the reference electrode and rear-side contact of the LAPS chip. **Figure 4.2a** depicts an example of leakage-current measurement for the fabricated SiO_2-gate LAPS recorded in measurement solution by varying the applied gate voltage in the range from –1.25 to +1.25 V with a scan rate of 100 mV/s. For a correct functioning of the LAPS device, the leakage current should be very small. Therefore, in this study, only chips having a leakage current less than 10 nA were selected for further dsDNA detection experiments.

The potential sensitivity of the LAPS chips has been tested via I_{ph}–V_g measurements. **Figure 4.2b** shows a typical I_{ph}–V_g curve (averaged over all 16 measurement spots) of the bare LAPS recorded at the applied gate voltage ranging from –0.8 V to +0.8 V. The I_{ph}–V_g curve of the bare LAPS has a usual p-type behavior with typical accumulation (V_g < –0.4 V), depletion (–0.4 V < V_g < 0.2 V) and inversion (V_g > 0.4 V) regions. These results demonstrate the suitability of the developed LAPS as potential-sensitive device for further

experiments on the label-free detection of dsDNA molecules by their intrinsic molecular charge.

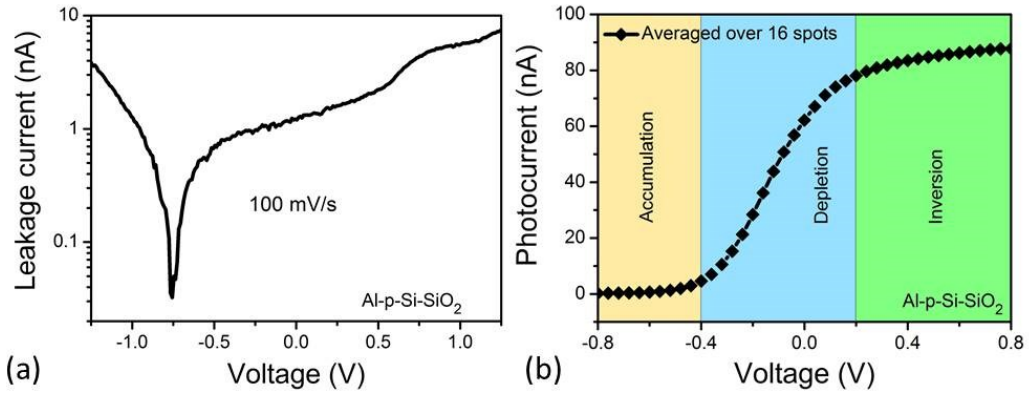

Figure 4.2: Leakage current (a) and I_{ph}–V_g curve (b) of the bare LAPS chip.

4.3.2 AFM characterization

In separate experiments, the LAPS chips were characterized by AFM measurements to gain a picture of how the morphology and roughness of the SiO_2-gate surface changes after the consecutive adsorption of PAH- and dsDNA layers. Tapping-mode AFM images were taken in air using a BioMAT Workstation (JPK Instruments, Germany) and silicon cantilevers (Nanoworld, Switzerland). The surface roughness was quantified from the AFM-height images by using the root-mean-square value (R_{rms}) and the surface-area difference. The scan size was 2 µm × 2 µm. **Figure 4.3** presents examples of AFM images of a bare SiO_2 surface (a) and a SiO_2 surface after PAH- (b) and dsDNA adsorption (c). For better comparison between the samples, the z-axis displaying the height was scaled to 5 nm for all images.

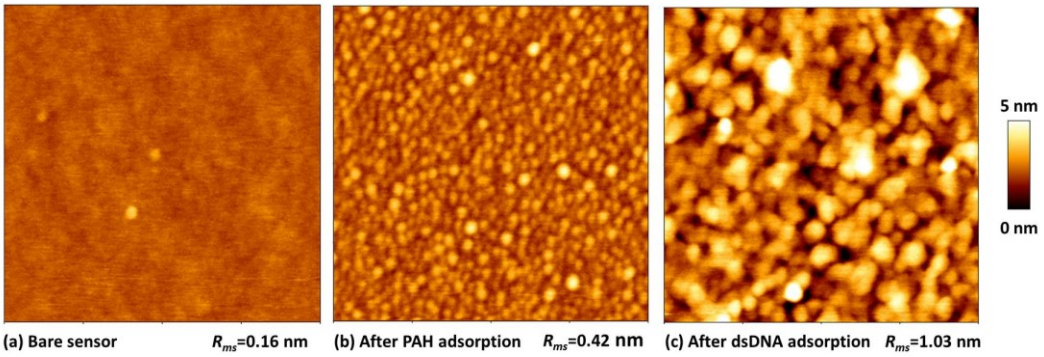

Figure 4.3: AFM-height images of a bare SiO_2 surface (a), a SiO_2 surface after PAH- (b) and dsDNA adsorption (c). Scan size is 2 µm × 2 µm.

The cleaned SiO_2 surface appears to be perfectly smooth with an average R_{rms} value of 0.16 nm. Apparent changes in surface morphology of the SiO_2 layer can be recognized

from AFM images after the adsorption of PAH- and dsDNA molecules. The surface roughness increases after the adsorption of PAH molecules (R_{rms} = 0.42 nm).

AFM images of the PAH layer taken from different areas of the sensor surface reveal that the PAH is homogeneously distributed over the surface assumedly with a flat orientation of the PAH molecules. The average height of the polyelectrolyte layer was ~2-3 nm, which is in agreement with results reported for a PAH layer prepared from 50 µM PAH solution adjusted with 100 mM NaCl [10]. However, some pin holes and worm-like structures can be observed on the AFM image of the PAH surface in **Figure 4.3b**, which is a general phenomenon for LbL-prepared polyelectrolyte films. In addition, small dots or globules appear on the AFM image, similar to that recently reported for a PAH layer adsorbed on a Si surface functionalized with a self-assembled monolayer [33]. Due to the sizes of the AFM tip used, one cannot finally conclude whether the dot-shaped structures lie on the thin PAH layer that covers the SiO_2 surface or directly on the SiO_2 surface. After dsDNA adsorption on the PAH-modified SiO_2 surface, the morphology of the surface changed significantly as shown in **Figure 4.3c**. On the one hand, the surface of the PAH/dsDNA bilayer appears to be dominated by large clusters. On the other hand, the surface roughness increases to the value of R_{rms} = 1.03 nm. These observations are consistent with results reported in Ref. [36]. Thus, the results of AFM characterization verify the successful formation of a PAH/dsDNA bilayer on the LAPS surface.

4.3.3 Label-free electrical detection of dsDNA molecules

Figure 4.4 shows the schematic structure of the LAPS modified with PAH- and PAH/dsDNA layers (left column) and I_{ph}–V_g curves (right column) exemplarily recorded from a single spot 11 of the LAPS before and after consecutive adsorption of PAH- (from 10 µM PAH solution) (a) and dsDNA (from 10 nM dsDNA solution) (b) molecules. In this experiment, the overall photocurrent was recorded at the applied bias-voltage range from –0.5 V to +0.3 V. To extract the photocurrent amplitudes for each measurement spot from the measured overall photocurrent, a fast Fourier transformation algorithm was used [37]. As expected, the consecutive adsorption of oppositely charged PAH- and dsDNA layers leads to alternating shifts of the I_{ph}–V_g curves along the voltage axis of about 45 mV and 25 mV, respectively. The direction of these shifts depends on the sign of the charge of the terminating layer that is consistent with the results reported previously for polyelectrolyte multilayers or PAH/ssDNA bilayers [10, 12]. On the other hand, the minimum photocurrent in the accumulation range of the I_{ph}–V_g curve remains nearly unchanged, indicating that the sensor is primarily sensitive to changes in the surface charge (or potential) rather than to the thickness or dielectric properties of the adsorbed layers. This implies that the potential at the top layer (i.e., the dsDNA charge) effectively propagates to the gate surface, resulting in a modulation of the surface potential and the flat-band voltage of the LAPS structure.

The potential changes induced by the electrostatic adsorption of PAH- and dsDNA layers as well as the drift of the LAPS signal have been directly monitored using dynamic constant-photocurrent mode measurements. **Figure 4.5a** exemplarily shows constant-photocurrent responses of the LAPS recorded in four spots (spots 3, 9, 11, and 13) before and after the LbL adsorption of PAH and after incubation of the PAH-modified SiO_2

surface with solution containing 10 nM in-solution-hybridized dsDNA molecules. In this experiment, the photocurrent has been set constant (in the depletion region nearly the inflection point of the I_{ph}–V_g curve) and the sensor response has been recorded during a time period of about 40 min.

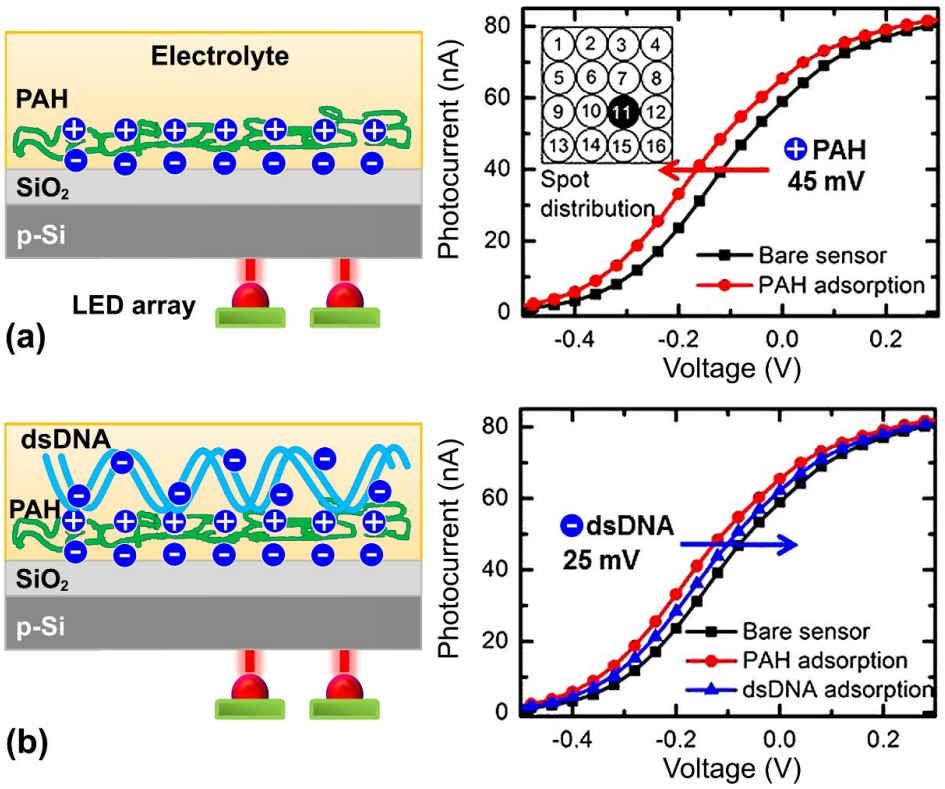

Figure 4.4: Schematic structure of the LAPS modified with PAH- and PAH/dsDNA layers (left column) and I_{ph}–V_g curves (right column) exemplarily recorded from single spot 11 of the LAPS before and after consecutive adsorption of PAH- (from 10 µM PAH solution) (a) and dsDNA (from 10 nM dsDNA solution) (b) molecules. The inset picture in graph (a) corresponds to the spot distribution.

As can be seen, the constant-photocurrent responses recorded in different spots possess a nearly similar shape, revealing a quasi-homogeneous surface coverage of the adsorbed PAH- and dsDNA layers. The potential shifts averaged over all 16 spots were 46.3 mV and 25.1 mV after the consecutive adsorption of PAH and dsDNA molecules, respectively. These results are in good agreement with signal values reported previously for on-chip hybridization experiments [12]. At the same time, the LAPS signal detected after the adsorption of dsDNA molecules onto the PAH layer was around two times higher than that of reported for the adsorption of dsDNA molecules onto a poly-L-lysine layer detected by means of a capacitive EIS sensor (~13 mV) [29].

To study the dependence of the LAPS signal on the concentration of dsDNA solution, the shift of the I_{ph}–V_g curve (averaged over 16 spots) was recorded after consecutive incubation (20 min) of the PAH-modified LAPS surface in solutions with different dsDNA concentrations of 0.1 nM, 1 nM, 10 nM, 100 nM, 1 µM and 5 µM, starting with a dsDNA concentration of 0.1 nM. After each change of dsDNA solution in the measurement cell,

the LAPS surface was rinsed with measurement solution. The results of these experiments are given in **Figure 4.5b**. With increasing dsDNA concentration from 0.1 nM to 5 µM, the LAPS signal is increased from ~8 mV to ~58 mV. A nearly linear dependence of the LAPS signal on the logarithm of dsDNA concentration was observed at least until 5 µM dsDNA. The lower detection limit is as low as 0.1 nM dsDNA that is in good agreement with results reported previously for DNA sensors based on silicon nanowires [38].

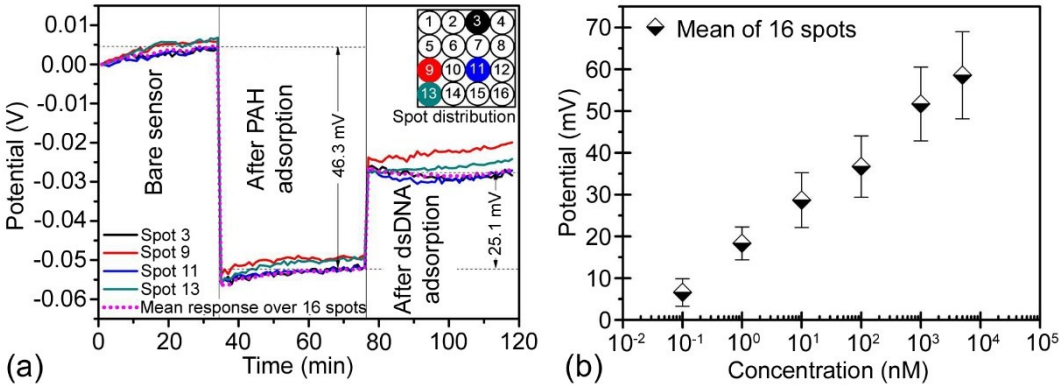

Figure 4.5: (a) Constant-photocurrent responses of the LAPS recorded in four spots (spots 3, 9, 11, and 13) before and after consecutive adsorption of 10 µM PAH and 10 nM dsDNA molecules, respectively. The LAPS response averaged over 16 spots (mean response) is added, too. The inset picture in the graph shows the spot distribution. (b) Dependence of the LAPS signal (averaged over 16 spots) on dsDNA concentration ranging from 0.1 nM to 5 µM.

If adsorbed PAH molecules do not form a closely packed dense layer on the LAPS surface, a possible unspecific adsorption of dsDNA molecules onto SiO_2 surface areas not covered with PAH could induce an undesired potential shift. To find out the impact of this unspecific dsDNA adsorption on the LAPS signal, in separate experiments, bare SiO_2-gate LAPS chips were exposed to 5 µM dsDNA solution for 1 h, followed by a rinsing step. Here, the unspecific adsorption of dsDNA molecules induces only a small potential shift of approximately 4 mV (see **Figure 4.6a**), which is about 15 times smaller than the signal (58 mV) induced due to the adsorption of dsDNA molecules on a PAH-covered LAPS surface.

4.3.4 Fluorescence-microscopy measurements

In addition to field-effect detection of dsDNA with the LAPS device, fluorescence measurements were performed as a reference method to verify the dsDNA attachment onto the PAH-covered LAPS surface. The fluorescence images were taken using an Axio Imager A1m (Carl Zeiss, Germany) fluorescence microscope with respective filter set. To visualize the successful electrostatic adsorption of the negatively charged dsDNA molecules onto the positively charged PAH layer, dsDNA molecules were modified (labeled) with a blue-fluorescent dye DAPI (4', 6-diamidino-2-phenylindole). For this, the PAH-coated LAPS surface was incubated with the solution containing 5 µM dsDNA and 300 nM DAPI molecules for 5 min. The DAPI molecules preferentially bind to the minor groove of

dsDNA, where their fluorescence is approximately 20-fold greater than in the non-bound state. For comparison, the fluorescence signal from the bare LAPS surface (without PAH layer) after exposing to the same dsDNA/DAPI solution was studied, too.

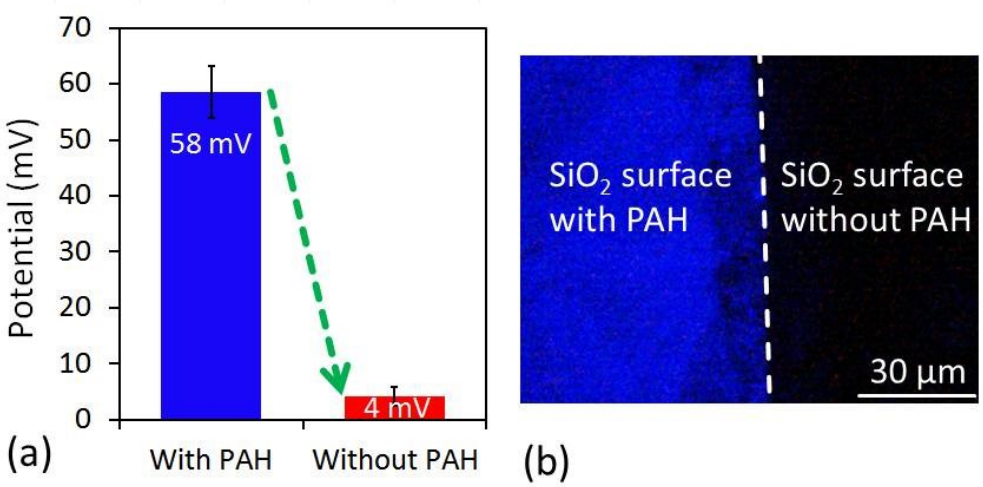

Figure 4.6: Mean signal values (n = 3) of PAH-modified and bare LAPS devices after exposing to 5 µM dsDNA solution (a) and fluorescence images (b) taken from the surface of the PAH-modified and bare LAPS devices after exposing to DAPI-labeled dsDNA solution. DAPI: Fluorescent dye 4', 6-diamidino-2-phenylindole.

Figure 4.6b shows the results of fluorescence measurements. A bright and homogeneous fluorescence signal was observed after incubation of the PAH-modified LAPS surface to the DAPI-labeled dsDNA solution, verifying a successful adsorption of dsDNA molecules onto the positively charged PAH layer. In contrast, as expected, almost no fluorescence signal has been detected after incubation of the bare LAPS surface with the DAPI-labeled dsDNA solution that is also in good correlation with the field-effect measurements presented in **Figure 4.6a**. The electrostatic repulsion between the dsDNA and SiO_2 surface (both are negatively charged) prevents the dsDNA adsorption. As a consequence, no DAPI-labeled dsDNA molecules remain on the bare LAPS surface after the washing step.

4.4 Conclusion

In summary, experiments performed in this study demonstrate for the first time the successful realization of a multi-light LAPS device for the direct label-free electrical detection of in-solution-hybridized dsDNA molecules. To achieve a high sensor signal, the negatively charged dsDNA molecules were electrostatically adsorbed onto the LAPS surface modified with a positively charged PAH layer, resulting in a dsDNA layer of preferentially flat-oriented molecules with the molecular charge positioned near the gate surface within the Debye length. High potential shifts of about 45 mVand 58 mV (averaged over 16 spots) were registered after consecutive adsorption of oppositely charged PAH

(10 μM) and dsDNA(5 μM) molecules, respectively. The lower detection limit is down to be about 0.1 nM dsDNA. The results of field-effect detection of dsDNA molecules were supported by fluorescence measurements using the fluorescent dye DAPI. The obtained results underline the potential of the LAPS in combination with the simple and rapid LbL-adsorption technique as a very promising approach for the future development of light-addressable label-free DNA chips. Further work will be focussing on the detection of dsDNA molecules directly in real PCR solutions.

ACKNOWLEDGEMENTS

This work was partially supported by the grant from BMBF (project DiaCharge 031A192D). C.S. Wu gratefully thanks the National Natural Science Foundation of China (Grant 31470956) and the Zhejiang Provincial Natural Science Foundation of China (Grant LY13H180002) for financial support. The authors thank H. Iken and J. Arreola for technical support.

REFERENCES

[1] W.W. Zhao, J.J. Xu, H.Y. Chen: *Photoelectrochemical DNA biosensors*, Chem. Rev. 114 (2014) 7421–7441.

[2] A. Sassolas, B.D. Leca-Bouvier, L.J. Blum: *DNA biosensors and microarrays*, Chem. Rev. 108 (2008) 109–139.

[3] F. Wei, P.B. Lillehoj, C.M. Ho: *DNA diagnostics: Nanotechnology-enhanced electrochemical detection of nucleic acids*, Pediatr. Res. 67 (2010) 458–468.

[4] A. Poghossian, M.J. Schöning: *Label-free sensing of biomolecules with field-effect devices for clinical applications*, Electroanal. 26 (2014) 1197–1213.

[5] C. Batchelor-McAuley, G.G. Wildgoose, R.G. Compton: *The physicochemical aspects of DNA sensing using electrochemical methods*, Biosens. Bioelectron. 24 (2009) 3183–3190.

[6] S. Mehrabani, A.J. Maker, A.M. Armani: *Hybrid integrated label-free chemical and biological sensors,* Sensors 14 (2014) 5890–5928.

[7] S. Cosnier, P. Mailley: *Recent advances in DNA sensors*, Analyst 133 (2008) 984–991.

[8] B. van Grinsven, N. Vanden Bon, H. Strauven, L. Grieten, M. Murib, K.L. Jiménez Monroy, S.D. Janssens, K. Haenen, M.J. Schöning, V. Vermeeren, M. Ameloot, L. Michiels, R. Thoelen, W. De Ceuninck, P. Wagner: *Heat-transfer resistance at solid–liquid interfaces: A tool for the detection of single-nucleotide polymorphisms in DNA*, ACS Nano 6 (2012) 2712–2721.

[9] A. Poghossian, M. Bäcker, D. Mayer, M.J. Schöning: *Gating capacitive field-effect sensors by the charge of nanoparticle/molecule hybrids*, Nanoscale 7 (2015) 1023–1031.

[10] A. Poghossian, M. Weil, A.G. Cherstvy, M.J. Schöning: *Electrical monitoring of polyelectrolyte multilayer formation by means of capacitive field-effect devices*, Anal. Bioanal. Chem. 405 (2013) 6425–6436.

[11] C. Kataoka-Hamai, Y. Miyahara: *Label-free detection of DNA by field-effect devices*, IEEE Sens. J. 11 (2011) 3153–3160.

[12] C.S. Wu, T. Bronder, A. Poghossian, C.F. Werner, M.J. Schöning: *Label-free detection of DNA using a light-addressable potentiometric sensor modified with a positively charged polyelectrolyte layer*, Nanoscale 7 (2015) 6143–6150.

[13] B. Veigas, E. Fortunato, P.V. Baptista: *Field effect sensors for nucleic acid detection: Recent advances and future perspectives*, Sensors 15 (2015) 10380–10398.

[14] M.H. Abouzar, A. Poghossian, A.G. Cherstvy, A.M. Pedraza, S. Ingebrandt, M.J. Schöning: *Label-free electrical detection of DNA by means of field-effect nanoplate capacitors: Experiments and modeling*, Phys. Status Solidi A 209 (2012) 925–934.

[15] N. Lu, A. Gao, P. Dai, T. Li, Y. Wang, X. Gao, S. Song, C. Fan, Y. Wang: *Ultra-sensitive nucleic acids detection with electrical nanosensors based on CMOS-compatible silicon nanowire field-effect transistors*, Methods 63 (2013) 212–218.

[16] A. Kulkarni, Y. Xu, C. Ahn, R. Amin, S.H. Park, S.T. Kim, M. Lee: *The label free DNA sensor using a silicon nanowire array*, J. Biotechnol. 160 (2012) 91–96.

[17] S. Purushothaman, C. Toumazou, C. Ou: *Protons and single nucleotide polymorphism detection: A simple use for the ion sensitive field effect transistor*, Sens. Actuators B 114 (2006) 964–968.

[18] T. Goda, M. Tabat, Y. Miyahara: *Electrical and electrochemical monitoring of nucleic acid amplification*, Front. Bioeng. Biotechnol. 3 (2015) 1–7.

[19] J. Fritz, E.B. Cooper, S. Gaudet, P.K. Sorger, S.R. Manalis: *Electronic detection of DNA by its intrinsic molecular charge*, Proc. Natl. Acad. Sci. U.S.A. 99 (2002) 14142–14146.

[20] A. Poghossian, A. Baade, H. Emons, M.J. Schöning: *Application of ISFETs for pH measurement in rain droplets*, Sens. Actuators B 76 (2001) 634–638.

[21] A. Poghossian: *The super-Nernstian pH sensitivity of Ta_2O_5-gate ISFETs*, Sens. Actuators B 7 (1992) 367–370.

[22] C. Jimenez-Jorquera, J. Orozco, A. Baldi: *ISFET based microsensors for environmental monitoring*, Sensors 10 (2010) 61–83.

[23] K. Nakazato: *An integrated ISFET sensor array*, Sensors 9 (2009) 8831–8851.

[24] J. Gun, M.J. Schöning, M.H. Abouzar, A. Poghossian, E. Katz: *Field-effect nanoparticle-based glucose sensor on a chip: Amplification effect of coimmobilized redox species*, Electroanal. 20 (2008) 1748–1753.

[25] A. Poghossian, M. Thust, M.J. Schöning, M. Müller-Veggian, P. Kordos, H. Lüth: *Cross-sensitivity of a capacitive penicillin sensor combined with a diffusion barrier*, Sens. Actuators B 68 (2000) 260–265.

[26] J.R. Siqueira, D. Molinnus, S. Beging, M.J. Schöning: *Incorporating a hybrid urease-carbon nanotubes sensitive nanofilm on capacitive field-effect sensors for urea detection*, Anal. Chem. 86 (2014) 5370–5375.

[27] C.S. Lee, S.K. Kim, M. Kim: *Ion-sensitive field-effect transistor for biological sensing*, Sensors 9 (2009) 7111–7131.

[28] J.R. Siqueira, M.H. Abouzar, M. Bäcker, V. Zucolotto, A. Poghossian, O.N. Oliveira, M.J. Schöning: *Carbon nanotubes in nanostructured films: Potential application as amperometric and potentiometric field-effect (bio-)chemical sensors*, Phys. Status Solidi A 206 (2009) 462–467.

[29] C.S.J. Hou, N. Milovic, M. Godin, P.R. Russo, R. Chakrabarti, S.R. Manalis: *Label-free microelectronic PCR quantification*, Anal. Chem. 78 (2006) 2526–2531.

[30] B. Veigas, R. Branquinho, J.V. Pinto, P.J. Wojcik, R. Martins, E. Fortunato, P.V. Baptista: *Ion sensing (EIS) real-time quantitative monitorization of isothermal DNA amplification*, Biosens. Bioelectron. 52 (2014) 50–55.

[31] J. Wang, Y.L. Zhou, M. Watkinson, J. Gautrot, S. Krause: *High-sensitivity light-addressable potentiometric sensors using silicon on sapphire functionalized with self-assembled organic monolayers*, Sens. Actuators B 209 (2015) 230–236.

[32] G.A. Evtugyn, T. Hianik: *Layer-by-layer polyelectrolyte assembles involving DNA as a platform for DNA sensors*, Curr. Anal. Chem. 7 (2011) 8–34.

[33] M. Schönhoff, V. Ball, A.R. Bausch, C. Dejugnat, N. Delorme, K. Glinel, R. Klitzing, R. Steitz: *Hydration and internal properties of polyelectrolyte multilayers*, Colloids Surf. A 303 (2007) 14–27.

[34] L.K. Meixner, S. Koch: *Simulation of ISFET operation based on the site-binding model*, Sens. Actuators B 6 (1992) 315–318.

[35] R.N. Smith, M. McCormick, C.J. Barrett, L. Reven, H.W. Spiess: *NMR studies of PAH/PSS polyelectrolyte multilayers adsorbed onto silica*, Macromolecules 37 (2004) 4830–4838.

[36] J. Beucken, M. Vos, P. Thuene, T. Hayakawa, T. Fukushima, Y. Okahata, F. Walboomers, N. Sommerdijk, R. Nolte, J. Jansen: *Fabrication, characterization, and biological assessment of multilayered DNA-coatings for biomaterial purposes*, Biomaterials 27 (2006) 691–701.

[37] Q. Zhang, P. Wang, W.J. Parak, M. George, G. Zhang: *A novel design of multi-light LAPS based on digital compensation of frequency domain*, Sens. Actuators B 73 (2001) 152–156.

[38] T. Adam, U. Hashim: *Highly sensitive silicon nanowire biosensor with novel liquid gate control for detection of specific single-stranded DNA molecules*, Biosens. Bioelectron. 67 (2015) 656–661.

5 DNA immobilization and hybridization detection by the intrinsic molecular charge using capacitive field-effect sensors modified with a charged weak polyelectrolyte layer

ACS Applied Materials & Interfaces 7 (2015) 20068–20075

Thomas S. Bronder, Arshak Poghossian, Sabrina Scheja, Chunsheng Wu, Michael Keusgen, Dieter Mewes, Michael J. Schöning

Submitted: 10.06.2015
Accepted: 26.08.2015
Published: 26.08.2015

ABSTRACT

Miniaturized setup, compatibility with advanced micro- and nanotechnologies, and ability to detect biomolecules by their intrinsic molecular charge favor the semiconductor field-effect platform as one of the most attractive approaches for the development of label-free DNA chips. In this work, a capacitive field-effect EIS (electrolyte-insulator-semiconductor) sensor covered with a layer-by-layer-prepared, positively charged weak polyelectrolyte layer of PAH (poly(allylamine hydrochloride)) was used for the label-free electrical detection of DNA (deoxyribonucleic acid) immobilization and hybridization. The negatively charged probe single-stranded DNA (ssDNA) molecules were electrostatically adsorbed onto the positively charged PAH layer, resulting in a preferentially flat orientation of the ssDNA molecules within the Debye length, thus yielding a reduced charge-screening effect and a higher sensor signal. Each sensor-surface modification step (PAH adsorption, probe ssDNA immobilization, hybridization with complementary target DNA (cDNA), reducing an unspecific adsorption by a blocking agent, incubation with noncomplementary DNA (ncDNA) solution) was monitored by means of capacitance-voltage- and constant-capacitance measurements. In addition, the surface morphology of the PAH layer was studied by atomic-force microscopy and contact-angle measurements. High hybridization signals of 34 mV and 43 mV were recorded in low-ionic strength solutions of 10 mM and 1 mM, respectively. In contrast, a small signal of 4 mV was recorded in the case of unspecific adsorption of fully mismatched ncDNA. The density of probe ssDNA- and dsDNA molecules as well as the hybridization efficiency was estimated using the experimentally measured DNA immobilization and hybridization signals and a simplified double-layer capacitor model. The results of field-effect experiments were supported by fluorescence measurements, verifying the DNA immobilization and hybridization event.

KEYWORDS

DNA, field-effect capacitive sensor, hybridization, intrinsic molecular charge, label-free detection, layer-by-layer technique, polyelectrolyte

5.1 INTRODUCTION

DNA (deoxyribonucleic acid) biosensors are considered as a very promising tool in many fields of applications ranging from diagnosis of genetic diseases, pathogen identification, and parental testing to drug screening and food industry [1–4]. The developed DNA-detection principles are very different: optical, electrochemical, impedimetric, spectrometric, and gravimetric methods are just a few of them [5–11]. The fundamental mechanism of many DNA-detection methods relies on the detection of the hybridization event in which a single-stranded probe DNA (ssDNA) binds specifically to a complementary single-stranded target DNA (cDNA), forming a double-stranded DNA (dsDNA) with a well-known helix structure.

Generally, DNA-detection principles can be divided into labeled, where either probe- or target DNA molecules are labeled with different markers, and label-free methods. Label-free methods have obvious advantages in terms of simplicity, rapidity and cost-efficiency [12, 13]. One favorable possibility to detect unlabeled DNA molecules is the detection of their intrinsic molecular charge by means of semiconductor field-effect devices (FED) [4, 13], because DNA molecules are negatively charged in a wide pH range. FEDs based on an electrolyte-insulator-semiconductor (EIS) structure, like capacitive EIS sensors, ion-sensitive field-effect transistors, Si-nanowire transistors and light-addressable potentiometric sensors (LAPS), are charge-sensitive devices and have been widely applied for the detection of pH [14, 15], ion- and analyte concentration in liquids [16–21] as well as charged molecules [4, 22] or charged nanoparticles [23, 24]. The ability of different kinds of FEDs for label-free detection of the DNA-hybridization event has been demonstrated in refs [25–35]. In these devices, the adsorption or binding of DNA molecules on the gate surface of the FED changes the space-charge distribution in the semiconductor, resulting in a change of the output signal of the FED. However, due to the screening of the DNA charge by counterions in the solution, the DNA-hybridization signal strongly depends on the ionic strength of the solution and the distance between the charge of the DNA molecules and the gate surface [4, 30, 36–38]. In addition, because the DNA charge is distributed along the molecule length, the DNA-immobilization method and orientation of molecules will have a strong impact on the DNA-hybridization signal [39–41]. These problems can be overcome by the immobilization of ssDNA molecules preferentially flat to the FED surface as well as by readout of the hybridization signal in a low-ionic strength solution.

Direct electrostatic immobilization of DNA molecules onto the FED surface is, in general, impossible due to electrostatic repulsion forces between the DNA and the FED surface with typically negatively charged gate insulators (e.g., SiO_2, Ta_2O_5, Si_3N_4). Therefore, a modification of the sensor surface by means of layer-by-layer (LbL) electrostatic adsorption of a cationic polyelectrolyte/ssDNA bilayer and subsequent hybridization with cDNA molecules becomes more popular in FED-based DNA biosensors design [25, 32, 42–45]. In contrast to often applied covalent immobilization methods that require time-consuming, cost-intensive procedures and complicated chemistry for functionalization of the gate surface and/or probe ssDNA, the LbL electrostatic adsorption technique is easy, fast, and applicable for substrates with any shapes and form [42, 46, 47].

The suitability of FEDs for the detection of adsorptively immobilized DNA has been demonstrated by modifying the gate surface of an EIS sensor [25] and a floating-gate field-effect transistor [44] by the positively charged poly-L-lysine. However, the recorded DNA-immobilization and hybridization signals were small (several mVs). On the other hand, recently, a high sensor signal has been reported by electrostatic adsorption of ssDNA (83 mV) [32] and dsDNA (20 mV) [45] on a LAPS surface modified with the positively charged weak polyelectrolyte of PAH (poly(allylamine hydrochloride)). Although LAPS devices are capable for addressable and multispot measurements, some disadvantages, such as necessity of illumination of the semiconductor with a modulated light source, dependence of the LAPS signal on the modulation frequency and intensity of the light, cross-talk due to the possible internal reflections in the semiconductor, and complicated readout circuit, might limit their application fields.

In the present work, the simplest FED – the capacitive EIS sensor – modified with a LbL-prepared PAH layer is applied for a label-free detection of electrostatic adsorption of probe ssDNA molecules onto the gate surface and subsequent hybridization with cDNA molecules. The EIS sensor represents a (bio)chemically sensitive capacitor, which can be easily fabricated at low cost (usually, no photolithographic process steps or complicated encapsulation procedures are needed).

Moreover, those sensors can be integrated with microfluidic cells on wafer level. In contrast to LAPS, a small AC (alternating current) voltage is applied to readout the EIS capacitance (no illumination with a modulated light is necessary). It can be expected that adsorptively immobilized probe ssDNA molecules will be preferentially flat-oriented on the EIS surface with negatively charged phosphate groups directed to the positively charged PAH molecules; the DNA nucleobases exposed to the surrounding solution allow to hybridize with their target cDNA molecules. As it has been discussed in refs [25, 32, 42–44], in the presence of a positively charged polyelectrolyte layer, both the Debye-screening effect and the electrostatic repulsion between target- and probe DNA molecules will be less effective, and therefore, a higher hybridization signal can be expected.

During experiments, each surface-modification step was monitored electrochemically in terms of signal direction and amplitude by using capacitance-voltage- (C–V) and constant-capacitance (ConCap) measurements. In addition, the surface morphology of the PAH layer was studied by atomic-force microscopy (AFM) and contact-angle measurements, while fluorescence measurements served as a reference method to verify the results of electrochemical detection of the DNA immobilization and hybridization event.

5.2 EXPERIMENTAL SECTION

5.2.1 Chip fabrication

EIS-sensor chips consisting of an Al/p-Si/SiO_2 structure were fabricated from a p-Si wafer (boron doped) with crystallographic orientation ⟨100⟩ and a resistivity of 1-10 Ωcm. First, a SiO_2-gate oxide was thermally grown by dry oxidation process at 1000 °C for 30 min to form a 30 nm thick oxide layer. Then, the rear-side oxide layer was etched by

HF (hydrofluoric acid) and subsequently, a 300 nm Al layer was deposited to create an Ohmic contact to the silicon substrate. The last step of the fabrication process was the separation of the wafer into single 10 mm × 10 mm chips. After fabrication, each chip was cleaned in ultrasonic bath with acetone, isopropyl alcohol, ethanol, and deionized (DI) water.

5.2.2 Measurement setup and electrochemical characterization

For electrochemical characterization, the EIS chips were mounted into a homemade measurement cell and connected to the electrochemical workstation. The rear-side and nonactive area of the chip were isolated from the electrolyte solution by means of an O-ring. The effective contact area of the EIS chip with the solution was about 0.7 cm^2. **Figure 5.1** shows a schematic cross section of the EIS structure and measurement setup including the electrochemical workstation (Zennium, Zahner Elektrik, Germany) and the reference electrode (liquid-junction Ag/AgCl electrode filled with 3 M KCl, Metrohm, Germany).

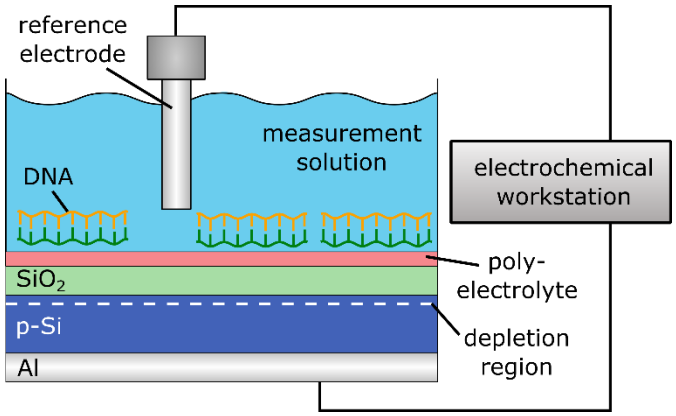

Figure 5.1: Cross-sectional illustration of the EIS sensor structure and measurement setup.

To reduce the influence of the charge-screening effect, the measurements were performed in low-ionic strength solution (1 mM and 10 mM NaCl, pH 5.45 adjusted by HCl, further referred as measurement solution). The pH value of all solutions was controlled with a MPC227 pH/Conductivity Meter (Mettler-Toledo, Germany). The surface-potential changes induced due to the surface-modification steps (PAH adsorption, probe ssDNA immobilization and target cDNA hybridization) were evaluated from the shifts of C–V curves along the voltage axis in depletion region or directly recorded by means of ConCap-mode measurements.

For the C–V measurements, a DC (direct current) gate voltage ranging from –1.5 V to +0.5 V (steps of 100 mV) and a small superimposed AC voltage with an amplitude of 20 mV and a frequency of 60 Hz was applied between the reference electrode and the rear-side Al contact. The ConCap mode allows the real-time dynamic monitoring of the sensor signal, whereas the capacitance of the sensor is kept constant at a certain working point by varying the gate voltage using a feedback-control circuit. This working point (constant

capacitance value) was chosen from the previously recorded C–V curve, typically within the depletion region at approximately 60% of the maximum capacitance. The measurements were performed at room temperature in a dark Faraday box (to reduce the possible influence of ambient light and electromagnetic fields). All potential values are referred to the reference electrode.

5.2.3 LbL adsorption of PAH/DNA bilayer and target cDNA hybridization

The LbL technique provides a simple, fast, low-cost and efficient technique for the electrostatic assembling of polyions with alternating charge [42, 46, 47]. In this study, the LbL technique has been utilized for the adsorption of positively charged PAH macromolecules on the negatively charged SiO_2-gate insulator and the immobilization of negatively charged probe ssDNA molecules onto the positively charged PAH layer. The LbL-immobilized ssDNA molecules usually form flat-elongated structures [42]. As a result, in low-ionic strength solutions used in this study, the full DNA charge could probably be positioned near the gate surface within the Debye length (approximately 3 and 10 nm in 10 and 1 mM solutions, respectively), yielding a higher sensor signal.

The schematic of the surface-modification steps is presented in **Figure 5.2**. Before polyelectrolyte adsorption, the surface of the SiO_2 layer was first activated with piranha solution (mixture of 60 µL H_2SO_4 (98%) and 30 µL H_2O_2 (35%)) by pipetting the freshly prepared mixture on the chip surface and incubating for at least 10 min at room temperature, followed by rinsing with DI water. This acid-treatment procedure was repeated three times.

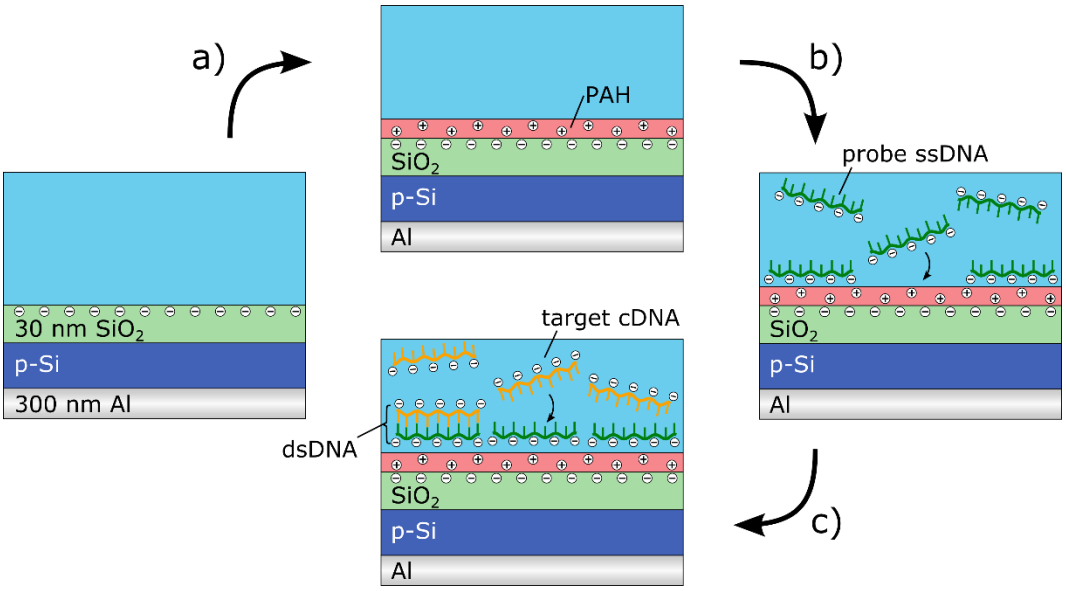

Figure 5.2: Schematic of the surface-modification steps: (a) PAH adsorption, (b) ssDNA immobilization, and (c) hybridization of complementary target cDNA with immobilized probe ssDNA molecules.

Then, 100 µL PAH solution (3 g/L PAH) was applied to the chip for 10 min to form the polyelectrolyte layer in accordance with the procedure described in ref [46]. The PAH solution was prepared by dissolving of PAH (70 kDa, purchased from Sigma) in 100 mM NaCl, pH 5.45. At pH 5.45, the surface of SiO_2 can be considered to be enough negatively charged (the pH_{pzc} at point of zero charge of SiO_2 is between 2 and 3 [48]) to provide electrostatic adsorption of almost fully charged PAH molecules [49]. The ionic strength of the PAH solution was chosen sufficiently high (100 mM NaCl) in order to achieve a higher amount of adsorbed polyelectrolyte molecules. After the PAH adsorption, the chip was washed again three times with measurement solution to remove nonattached molecules from the sensor surface, followed by an electrochemical characterization as described in **Section 5.2.2**.

The density and homogeneity of the immobilized probe ssDNA layer will be mainly defined by the quality of the underlying PAH layer. Therefore, in separate experiments, the chip-surface morphology and roughness were characterized by AFM measurements before and after the PAH adsorption. Tapping-mode AFM images were taken using a BioMAT Workstation (JPK Instruments, Germany) and commercial NCH Pointprobe silicon cantilevers (Nanoworld, Switzerland). The surface roughness was quantified by using the root-mean-square value (rms) and the surface-area difference.

For immobilization of 20-mer probe ssDNA, 60 µL of 5 µM ssDNA solution was applied onto the PAH-modified chip surface. The DNA solution has been prepared by dilution of ssDNA molecules in 1 × TE buffer (mixture of 10 mM Tris (tris(hydroxymethyl)aminomethane) and 1 mM EDTA (ethylenediaminetetraacetic acid) in DI water, adjusted to pH 8). After 60 min of incubation, the chip was washed three times with measurement solution to remove unattached probe ssDNA molecules.

For hybridization, the chip surface covered with the PAH/ssDNA bilayer was incubated with fully matched target cDNA solution (5 µM 20-mer cDNA dissolved in 1 × TE buffer, pH 8) for 40 min at RT, followed by rinsing with DI water to remove the nonhybridized target cDNA molecules.

The sequences of 20-mer probe ssDNA (5′-GTT-CTT-CTC-ATT-CTT-CCC-CT-3′), complementary target cDNA (5′-AG-GGG-AAG-AAT-GAG-AAG-AAC-3′) and fully mismatched ncDNA (5′-TC-CCC-TTC-TTA-CTC-TTC-TTG-3′) used in this study were purchased from Eurofins (Eurofins MWG Operon, Germany).

5.3 RESULTS AND DISCUSSION

5.3.1 Leakage-current measurements and surface-charge sensitivity of EIS chips

The quality of the oxide layer, drift of the output signal and the surface-charge sensitivity of the fabricated SiO_2-gate EIS chips are crucial factors, which should be checked before starting DNA-detection experiments. The quality of the gate-oxide layer has been tested by measuring the leakage current between the reference electrode and rear-side contact of the EIS chip by varying the applied gate voltage in the range from –2 to +2 V. For a correct functioning of the EIS sensors, the leakage current should be very small. Therefore, only chips having leakage current less than 10 nA were chosen for further DNA-detection experiments.

In separate experiments, the drift behavior of the bare SiO_2-gate EIS sensor has been studied. For this, the ConCap signal of the EIS sensor was recorded directly after applying the PBS buffer (pH 7) onto the bare sensor surface and after incubation in the same solution over 7 days. The drift of the EIS sensor was evaluated from the shift of the ConCap curve and amounted to be approximately 8 mV/day. In further experiments on DNA detection, before the surface modification processes, the sensors were conditioned in PBS buffer (or in measurement solution) for at least 12 h, in order to reduce the drift of SiO_2-gate EIS sensors.

Because the surface charge of the SiO_2 is known to be pH-dependent [50], the charge sensitivity of the EIS chips has been tested via the measurement of shifts of C–V curves along the voltage axis in various pH buffer solutions from pH 5 to pH 9. The pH sensitivity evaluated from these shifts of C–V curves in the depletion region was 42 mV/pH, which is comparable to values previously reported for thermally grown SiO_2 layers (e.g., refs [30, 51]). These results demonstrate the suitability of the developed EIS devices as charge-sensitive transducers for further experiments on the label-free detection of DNA immobilization and hybridization by their intrinsic molecular charge.

5.3.2 Surface characterization of PAH layer

Figure 5.3 shows an example of AFM image of the EIS-sensor surface after the PAH adsorption. The PAH layer was homogeneous as evidenced by the AFM images taken from different areas of the EIS surface. The cleaned and PAH-covered SiO_2 surfaces were smooth with average rms values of 0.12 and 0.55 nm, respectively. The PAH molecules form a densely packed layer assumedly with a flat conformation of the PAH molecules. However, some pin holes and worm-like structures can be observed on the AFM image of the PAH surface in **Figure 5.3**, which is a general phenomenon for LbL-prepared polyelectrolyte films. The average height of the polyelectrolyte layer was ~2–3 nm, which is in agreement with results reported for a PAH layer prepared from 50 µM PAH solution adjusted with 100 mM NaCl [46].

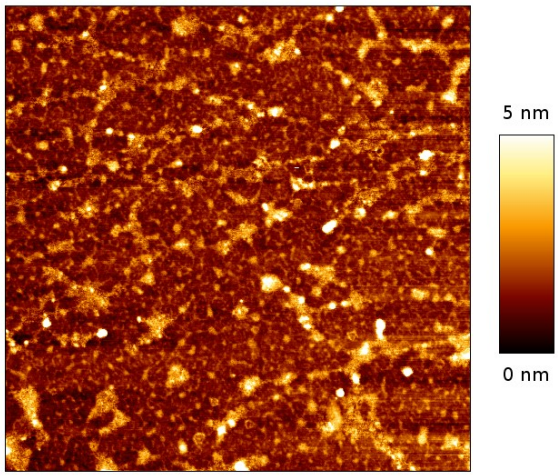

Figure 5.3: AFM image of the SiO_2 surface covered with PAH layer. Scan size is 2 µm × 2 µm.

In addition to AFM investigations, the wettability of the sensor surface before and after the cleaning step with piranha solution and after deposition of the PAH layer has been studied by water contact-angle measurements (see Supporting Information). After treatment in piranha solution, the SiO_2 surface becomes highly hydrophilic, which results in a decrease of the contact angle from 89° to less than 10°. The contact angle increases to 34° after the PAH adsorption that is in good agreement with the results reported for the PAH adsorption on a hydrophilic glass substrate [52].

5.3.3 Label-free detection of PAH adsorption, probe ssDNA immobilization and target cDNA hybridization

The capacitive EIS sensors were characterized before and after each surface-modification step by means of C–V- and ConCap method. **Figure 5.4** shows an example of label-free electrostatic detection of PAH adsorption, probe ssDNA immobilization and target cDNA hybridization with the EIS sensor. In this experiment, the C–V curves (a) and the ConCap response (b) of the EIS sensor were recorded in 10 mM NaCl solution (pH 5.45) before and after PAH adsorption, after ssDNA immobilization and after subsequent hybridization with target cDNA molecules. The recorded C–V curves exhibit a typical high-frequency shape. Dependent on the magnitude and polarity of the applied gate voltage, V_G, three regions in the C–V curves of the bare and modified EIS sensor can be distinguished: accumulation ($V_G < -1.25$ V), depletion (-1 V $< V_G <$ 0.1 V) and inversion ($V_G >$ 0.25 V).

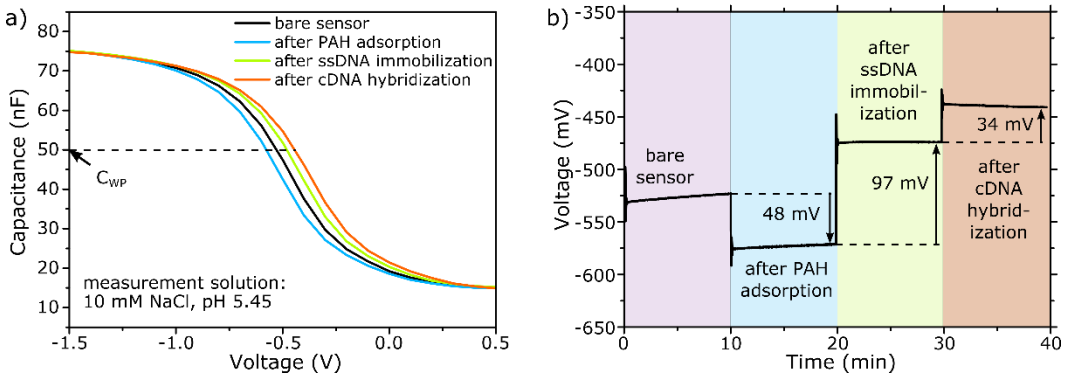

Figure 5.4: C–V curves (a) and ConCap response (b) of the capacitive p-Si-SiO_2 EIS sensor measured in 10 mM NaCl (pH 5.45) before and after PAH adsorption, after probe ssDNA immobilization and after hybridization with complementary cDNA molecules. Working point (constant capacitance) in depletion region was set to 50 nF.

The total capacitance of the EIS structure (C_{EIS}) can be represented as a series connection of the geometrical capacitance of the gate insulator (C_i) and the variable space-charge capacitance of the semiconductor (C_{sc}) that depends, among others, on the voltage applied to the gate and the charge (potential) at the gate-insulator/electrolyte interface (the electrochemical double-layer capacitance and capacitance of the adsorbed monolayer are usually much greater than C_i and C_{sc} and can thus, be neglected (e.g., ref [46]). As it can

be seen, after surface-modification steps, the maximum capacitance in the accumulation range of the C–V curve remains nearly unchanged ($C_{EIS} \approx C_i$), which is consistent with our previous results on the detection of charged macromolecules or nanoparticles with the capacitive EIS sensor [24, 46]. On the other hand, large shifts of C–V curves along the voltage axis have been observed in the depletion range, whereat the direction and magnitude of the shifts depend on the sign and amount of the adsorbed charge. This indicates that the adsorption and binding of charged macromolecules induces an interfacial potential change, resulting in a modulation of the flat-band voltage and capacitance of the EIS structure. The binding of positively charged PAH molecules to the negatively charged SiO_2 surface will increase the width of the depletion layer and decrease the space-charge capacitance in the Si, C_{sc}. This will result in a decrease of the total capacitance of the sensor and in a shift of the C–V curve in the direction of more negative gate voltages. In contrast, the electrostatic binding of negatively charged probe ssDNA molecules to the positively charged PAH and subsequent hybridization with complementary target cDNAs will lead to a decrease of the width of the depletion layer and an increase of the C_{sc}. As a result, the C–V curve will shift in the direction of more positive (or less negative) gate voltages.

Both the direction and the magnitude of potential shifts can directly be determined from the dynamic ConCap-mode measurements (**Figure 5.4b**). In addition, the real-time ConCap response makes the drift behavior of the bare and modified EIS sensor visible. As can be seen, immediately after exposing to the measurement solution, large signal changes induced due to the SiO_2-surface modification by the charged macromolecules have been registered. Then, small signal drift over time has been observed. In most cases, it takes several minutes to achieve equilibrium conditions and a relatively stable signal. Typically, the signal changes induced by the PAH adsorption, DNA immobilization or hybridization processes were much higher than that of caused due to the drift effect. A ConCap signal of approximately 48 mV was recorded after the adsorption of PAH molecules. The probe ssDNA-immobilization signal was 97 mV. After the hybridization process, the negative charge of the dsDNA molecules is increased, resulting in an additional potential shift (hybridization signal) of 34 mV in the direction of less negative voltages.

Let us estimate the density of probe ssDNA molecules (N_p) adsorbed on the PAH layer using the experimentally measured ssDNA-immobilization signal (ΔV_G). Adopting a simplified double-layer capacitor model described in ref. [53] and by assuming that (1) the double-layer capacitance, C_d, remains nearly unchanged after the adsorption of ssDNA molecules, (2) the probe ssDNA molecules are preferentially flat-oriented on the EIS surface with negatively charged phosphate groups directed to the positively charged PAH molecules, and (3) the charges inside the semiconductor and insulator as well as the screening of the DNA charge by counterions in the solution can be neglected, the following simplified relation between the surface-potential change ($\Delta\varphi$) and the excess-surface charge (ΔQ) can be obtained [23, 24]:

$$\Delta V_G \approx \Delta\varphi = \frac{\Delta Q}{C_d} = en\frac{N_p}{C_d} \qquad \textbf{Eq. 5.1}$$

where e is the elementary charge ($e = 1.6 \times 10^{-19}$ C), and n is the number of charged phosphate groups. The density of the adsorbed probe ssDNA molecules calculated from

expression (**Eq. 5.1**) amounts to be approximately $N_p = 6 \times 10^{11}$ ssDNA/cm^2, which is in good agreement with results ($N_p = 4 \times 10^{11}$ ssDNA/cm^2) reported for 20-mer DNA molecules covalently attached to the silanized SiO_2-gate surface of an ion-sensitive field-effect transistor [54]. The simulation parameters are $\Delta V_G = 97$ mV (evaluated from the ConCap curve in **Figure 5.4b**), n = 20; the double-layer capacitance C_d was taken to be 20 μF/cm^2 [55]. The density of hybridized dsDNA molecules calculated using **Eq. 5.1** and the measured hybridization signal of 34 mV (see **Figure 5.4b**) was 2.1×10^{11} dsDNA/cm^2. Thus, the hybridization efficiency amounts to be approximately 35%.

In general, the observed hybridization signal was smaller than the immobilization signal that is in agreement with results reported previously (e.g., refs [37, 56]). This effect could be explained by assuming that (1) not all adsorbed probe ssDNA molecules form a flat-oriented elongated structure with DNA nucleobases exposed to the surrounding solution and are ready to hybridize with target cDNA molecules, (2) the charge of dsDNA molecules is partially screened by small counterions in the solution, (3) some hybridized dsDNA molecules detach from the surface, or some combination thereof.

Usually, immobilized probe ssDNA molecules do not form a closely packed, dense layer. Therefore, negatively charged target cDNA or noncomplementary DNA (ncDNA) molecules can electrostatically adsorb onto those positively charged areas of PAH not covered with probe ssDNA, resulting in a false signal. To prevent or reduce an unspecific adsorption of cDNA or ncDNA, the surface areas of PAH not covered with the probe ssDNA have to be blocked by a chemical agent (e.g., bovine serum albumin (BSA)), which inhibits unspecific adsorption. Therefore, after probe ssDNA immobilization, 1% BSA (diluted in DI water, adjusted to pH 5.45) was applied to the chip surface for 60 min at RT, followed by rinsing with measurement solution. At pH 5.45, the BSA molecules are weakly negatively charged, because the isoelectric point of BSA is around pH 4.7 [57].

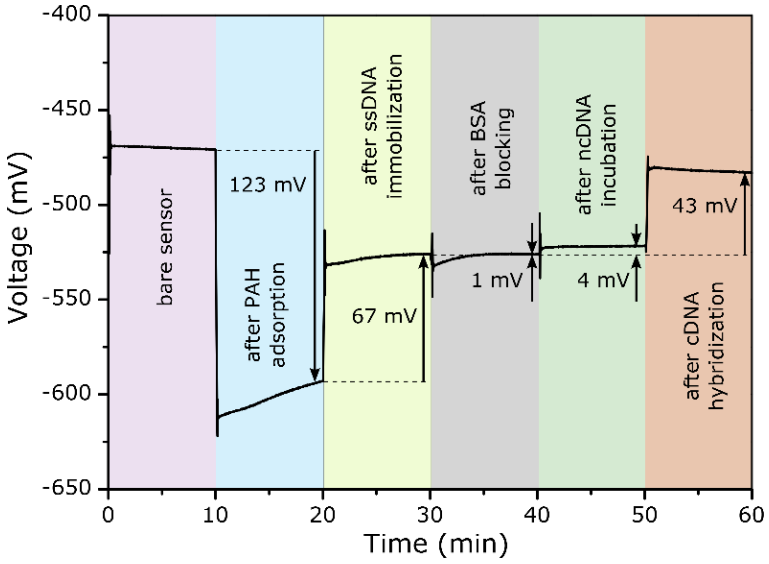

Figure 5.5: ConCap response of EIS sensor recorded in 1 mM NaCl solution (pH 5.45) before and after PAH adsorption, after probe ssDNA immobilization, after blocking with BSA, after incubation in a solution containing fully mismatched ncDNA molecules (5 μM) and after hybridization of probe ssDNA with target cDNA molecules (5 μM).

To find out the impact of unspecific adsorption of ncDNA molecules on the EIS signal, after blocking procedure, the sensor surface was exposed to fully mismatched ncDNA solution (5 μM 20-mer ncDNA dissolved in 1 × TE buffer, pH 8) for 40 min at RT, followed by rinsing with DI water.

Figure 5.5 depicts the ConCap response of an EIS sensor recorded in 1 mM NaCl solution (pH 5.45) before and after PAH adsorption, after probe ssDNA immobilization, after blocking with BSA, after incubation in a solution containing fully mismatched ncDNA molecules (5 μM) and after hybridization of probe ssDNA with target cDNA molecules (5 μM).

The DNA immobilization- and hybridization signals evaluated from the ConCap response in **Figure 5.5** were 67 and 43 mV, respectively. At the same time, unspecific adsorption of fully mismatched ncDNA molecules induces only a small potential shift of 4 mV. Thus, the DNA-hybridization signal was more than 10 times higher than the signal generated due to the unspecific adsorption of ncDNA molecules. This experiment demonstrates the specificity of the developed EIS sensor capable of distinguishing the complementary cDNA from fully mismatched ncDNA. As expected, due to the less-effective Debye-screening effect in a low-ionic strength solution, the hybridization signal measured in a 1 mM solution (Debye length $\lambda_D \approx 10$ nm) was higher (43 mV) than that of recorded in a 10 mM solution ($\lambda_D \approx 3$ nm; 34 mV; **Figure 5.4b**).

5.3.4 Fluorescence measurements

In addition to field-effect characterization of EIS-based DNA sensors by means of C–V- and ConCap methods, fluorescence measurements were performed as a reference method to verify the DNA immobilization and hybridization event using an Axio Imager A1m (Carl Zeiss AG, Germany) fluorescence microscope with respective filter set. To visualize the successful DNA immobilization onto the PAH layer, probe ssDNA (20-mer) was modified with the fluorescence dye 6-carboxyfluorescein (FAM). For verification of the hybridization reaction, first unmodified 20-mer probe ssDNA molecules were immobilized onto the surface of the PAH-modified EIS sensor, then the sensor was exposed to the solution containing FAM-modified target cDNA or ncDNA (also 20-mer), respectively. All surface modification- and washing steps were performed according to the protocols described above for electrochemical experiments.

Figure 5.6 shows the results of fluorescence measurements after exposing the bare and PAH-modified EIS-sensor surface to FAM-labeled probe ssDNA solution (5 μM) as well as after incubation of the EIS sensor modified with a PAH/probe-ssDNA bilayer with the 5 μM solution of FAM-labeled cDNA or ncDNA molecules. No fluorescence signal has been detected after exposing the bare EIS sensor to FAM-labeled probe ssDNA solution (**Figure 5.6a**). The electrostatic repulsion between the probe ssDNA and SiO_2 surface (both are negatively charged) prevents the immobilization process. As a consequence, no FAM-labeled ssDNA molecules remain on the sensor surface after the washing step. In contrast, a bright and homogeneous fluorescence signal was observed after incubation of the PAH-modified EIS sensor surface to FAM-labeled probe ssDNA solution (**Figure 5.6b**), verifying a successful immobilization of probe ssDNA molecules onto the positively

charged PAH layer. The fluorescence signal has also been observed even after six washing steps, without any loss of fluorescence intensity. In comparison to **Figure 5.6b**, a less bright fluorescence signal has been detected after hybridization of probe ssDNA with FAM-labeled cDNA (**Figure 5.6c**). This experiment verifies, on one hand, the successful hybridization process; on the other hand, it indicates that not all immobilized probe ssDNA molecules were hybridized with the target cDNA molecules (i.e., the hybridization efficiency was <100%), supporting the results of electrochemical measurements (see **Section 5.3.3**). As expected, practically no fluorescence signal has been detected after incubation of the EIS sensor modified with PAH/probe-ssDNA bilayer with the FAM-labeled ncDNA solution (**Figure 5.6d**) that is also in good correlation with the electrochemical measurements presented in **Figure 5.5**.

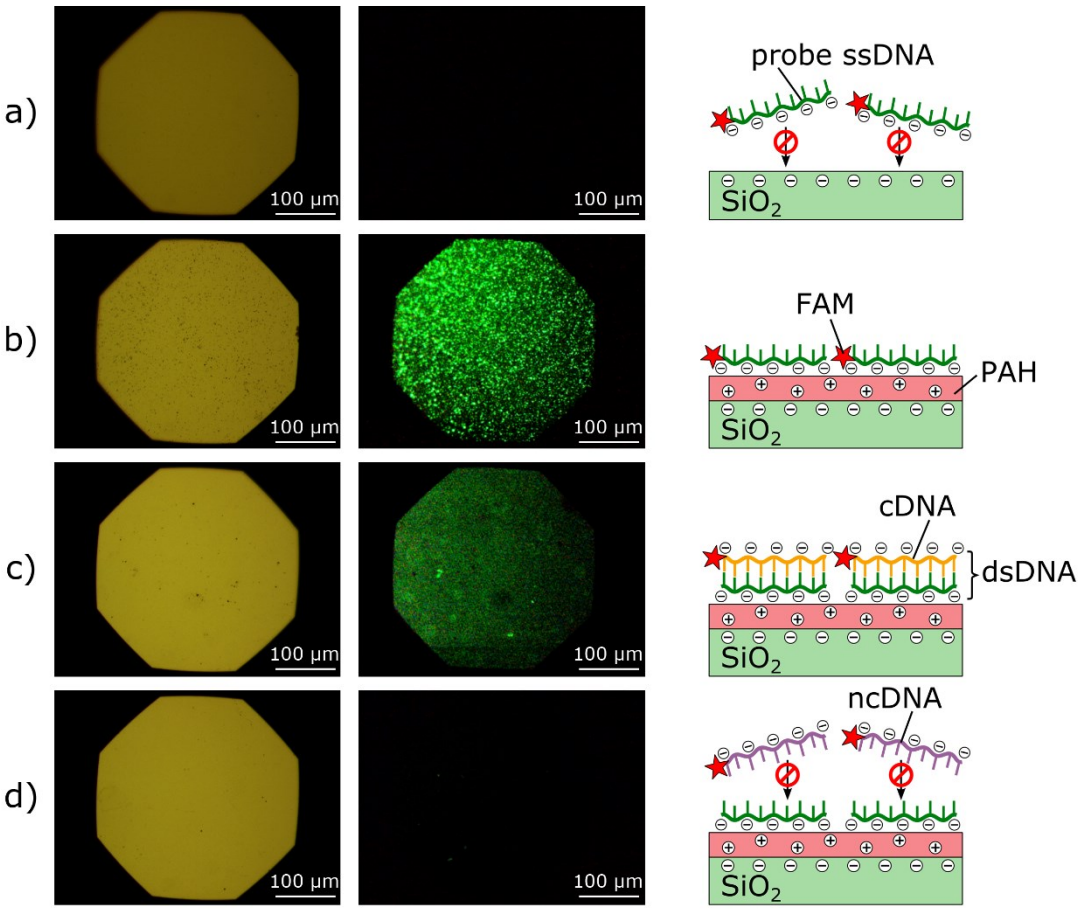

Figure 5.6: (Left column) Light-field- and (middle column) fluorescence-mode images after exposing the (a) bare and (b) PAH-modified EIS sensor to FAM-labeled probe ssDNA solution as well as after incubation of the EIS sensor modified with PAH/probe-ssDNA bilayer with the solution of FAM-labeled (c) cDNA- or (d) ncDNA molecules. The schematics in the right column visualize the corresponding binding tendency. For each fluorescence experiment, a separate EIS chip was used.

5.4 CONCLUSIONS

Among various concepts proposed for the label-free detection of DNA immobilization and hybridization, the semiconductor field-effect device platform, which is based on the electrostatic detection of DNA molecules by their intrinsic negative charge, is one of the most attractive approaches. In this work, a capacitive EIS sensor consisting of an Al–p-Si–SiO_2 structure modified with a weak polyelectrolyte layer of PAH has successfully been applied for label-free electrical detection of DNA immobilization and hybridization. The LbL technique was used for the electrostatic adsorption of positively charged PAH macromolecules on the negatively charged SiO_2 layer as well as for an easy and fast immobilization of negatively charged probe ssDNA molecules onto the positively charged PAH layer. The surface morphology of the PAH layer was studied by AFM- and contact-angle measurements; the EIS sensors were electrochemically characterized in the same measurement solution (1 mM or 10 mM NaCl, pH 5.45) after each surface-modification process (PAH adsorption, probe ssDNA immobilization, hybridization with cDNA, BSA blocking, unspecific adsorption of ncDNA) by means of C–V- and ConCap method. Large potential shifts of 97 and 34 mV have been observed after LbL immobilization of probe ssDNA onto the positively charged PAH layer and subsequent hybridization with cDNA, respectively. The density of probe ssDNA- and dsDNA molecules, estimated using the experimentally determined DNA immobilization- and hybridization signals together with a simplified double-layer capacitor model, were 6×10^{11} cDNA/cm^2 and 2.1×10^{11} dsDNA/cm^2, respectively. The hybridization efficiency estimated using the measured immobilization and hybridization signals is 35%. The advantage of the adsorptive immobilization technique is that both the probe ssDNA- as well as dsDNA (after hybridization) molecules preferentially lie flat near to the EIS surface with molecular charges positioned within the Debye length from the gate surface, resulting in a higher sensor signal. The hybridization signal increases from 34 to 43 mV with decreasing the ionic strength of the solution from 10 to 1 mM NaCl. At the same time, a small potential shift of 4 mV was recorded in the case of unspecific adsorption of fully mismatched ncDNA. This demonstrates the ability of capacitive EIS sensors to distinguish between complementary and mismatched DNA sequences. The results of field-effect experiments were supported by fluorescence measurements serving as a reference method to verify the DNA immobilization- and hybridization event.

The obtained results underline the potential of the capacitive EIS as a promising transducer platform for label-free electrical detection of DNA molecules by their intrinsic molecular charge. Future work will be directed to study the lower detection limit as well as to realize an array of capacitive EIS sensors in a differential-mode setup for the accurate detection of single-nucleotide polymorphisms.

ACKNOWLEDGMENTS

This work was funded by the Bundesministerium für Bildung und Forschung (DiaCharge project 031A192D). C. Wu thanks the National Natural Science Foundation of China (Grant 31470956), and the Zhejiang Provincial Natural Science Foundation of China

(Grant LY13H180002) for financial support. The authors gratefully thank the Institute of Applied Polymer Chemistry (FH Aachen) for technical support by contact-angle experiments, H. Iken for fabrication of EIS sensors and M. Bäcker for AFM measurements.

REFERENCES

[1] A. Sassolas, B.D. Leca-Bouvier, L.J. Blum: *DNA biosensors and microarrays*, Chem. Rev. 108 (2008) 109–139.

[2] F. Wei, P.B. Lillehoj, C.M. Ho: *DNA diagnostics: Nanotechnology-enhanced electrochemical detection of nucleic acids*, Pediatr. Res. 67 (2010) 458–468.

[3] S. Choi, M. Goryll, L.Y.M. Sin, P.K. Wong, J. Chae: *Microfluidic-based biosensors toward point-of-care detection of nucleic acids and proteins*, Microfluid. Nanofluid. 10 (2011) 231–247.

[4] A. Poghossian, M.J. Schöning: *Label-free sensing of biomolecules with field-effect devices for clinical applications*, Electroanal. 26 (2014) 1197–1213.

[5] L. Song, S. Ahn, D.R. Walt: *Fiber-optic microsphere-based arrays for multiplexed biological warfare agent detection*, Anal. Chem. 78 (2006) 1023–1033.

[6] X. Mao, L. Yang, X. Su, Y. Li: *A nanoparticle amplification based quartz crystal microbalance DNA sensor for detection of Escherichia coli O157:H7*, Biosens. Bioelectron. 21 (2006) 1178–1185.

[7] S. Cagnin, M. Caraballo, C. Guiducci, P. Martini, M. Ross, M. Santaana, D. Danley, T. West, G. Lanfranchi: *Overview of electrochemical DNA biosensors: New approaches to detect the expression of life*, Sensors 9 (2009) 3122–3148.

[8] B.P. Nelson, T.E. Grimsrud, M.R. Liles, R.M. Goodman, R.M. Corn: *Surface plasmon resonance imaging measurements of DNA and RNA hybridization adsorption onto DNA microarrays*, Anal. Chem. 73 (2001) 1–7.

[9] M. Lazerges, F. Bedioui: *Analysis of the evolution of the detection limits of electrochemical DNA biosensors*, Anal. Bioanal. Chem. 405 (2013) 3705–3714.

[10] J. Park, S. Park: *DNA hybridization sensors based on electrochemical impedance spectroscopy as a detection tool*, Sensors 9 (2009) 9513–9532.

[11] M. Riedel, J. Kartchemnik, M.J. Schöning, F. Lisdat: *Impedimetric DNA detection – steps forward to sensorial application*, Anal. Chem. 86 (2014) 7867–7874.

[12] S. Mehrabani, A.J. Maker, A.M. Armani: *Hybrid integrated label-free chemical and biological sensors*, Sensors 14 (2014) 5890–5928.

[13] C. Wu, F. Ko, Y. Yang, D. Hsia, B. Lee, T. Su: *Label-free biosensing of a gene mutation using a silicon nanowire field-effect transistor*, Biosens. Bioelectron. 25 (2009) 820–825.

[14] A. Poghossian: *The super-Nernstian pH sensitivity of Ta_2O_5-gate ISFETs*, Sens. Actuators B 7 (1992) 367–370.

[15] A. Poghossian, A. Baade, H. Emons, M.J. Schoning: *Application of ISFETs for pH measurement in rain droplets,* Sens. Actuators B 76 (2001) 634–638.

[16] A. Poghossian, D. Mai, Y. Mourzina, M.J. Schöning: *Impedance effect of an ion-sensitive membrane: Characterisation of an EMIS sensor by impedance spectroscopy, capacitance-voltage and constant-capacitance method*, Sens. Actuators B 103 (2004) 423–428.

[17] C. Jimenez-Jorquera, J. Orozco, A. Baldi: *ISFET based microsensors for environmental monitoring*, Sensors 10 (2010) 61–83.

[18] J. Gun, M.J. Schöning, M.H. Abouzar, A. Poghossian, E. Katz: *Field-effect nanoparticle-based glucose sensor on a chip: Amplification effect of coimmobilized redox species*, Electroanal. 20 (2008) 1748–1753.
[19] C. Lee, S. K. Kim, M. Kim: *Ion-sensitive field-effect transistor for biological sensing*, Sensors 9 (2009) 7111–7131.
[20] J.R. Siqueira, M.H. Abouzar, M. Bäcker, V. Zucolotto, A. Poghossian, O.N. Oliveira, M.J. Schöning: *Carbon nanotubes in nanostructured films: Potential application as amperometric and potentiometric field-effect (bio-)chemical sensors*, Phys. Status Solidi A 206 (2009) 462–467.
[21] K. Nakazato: *An integrated ISFET sensor array*, Sensors 9 (2009) 8831–8851.
[22] E. Stern, A. Vacic, M.A. Reed: *Semiconducting nanowire field-effect transistor biomolecular sensors*, IEEE Trans. Electron Devices 55 (2008) 3119–3130.
[23] J. Gun, V. Gutkin, O. Lev, H. Boyen, M. Saitner, P. Wagner, M. D'Olieslaeger, M.H. Abouzar, A. Poghossian, M.J. Schöning: *Tracing gold nanoparticle charge by electrolyte-insulator-semiconductor devices*, J. Phys. Chem. C 115 (2011) 4439–4445.
[24] A. Poghossian, M. Bäcker, D. Mayer, M.J. Schöning: *Gating capacitive field-effect sensors by the charge of nanoparticle/molecule hybrids*, Nanoscale 7 (2015) 1023–1031.
[25] J. Fritz, E.B. Cooper, S. Gaudet, P.K. Sorger, S.R. Manalis: *Electronic detection of DNA by its intrinsic molecular charge*, Proc. Natl. Acad. Sci. U.S.A. 99 (2002) 14142–14146.
[26] S. Ingebrandt, Y. Han, F. Nakamura, A. Poghossian, M.J. Schöning, A. Offenhäusser: *Label-free detection of single nucleotide polymorphisms utilizing the differential transfer function of field-effect transistors*, Biosens. Bioelectron. 22 (2007) 2834–2840.
[27] J. Hahm, C.M. Lieber: *Direct ultrasensitive electrical detection of DNA and DNA sequence variations using nanowire nanosensors*, Nano Lett. 4 (2004) 51–54.
[28] C. Kataoka-Hamai, Y. Miyahara: *Label-free detection of DNA by field-effect devices*, IEEE Sens. J. 11 (2011) 3153–3160.
[29] N. Lu, A. Gao, P. Dai, T. Li, Y. Wang, X. Gao, S. Song, C. Fan, Y. Wang: *Ultra-sensitive nucleic acids detection with electrical nanosensors based on CMOS-compatible silicon nanowire field-effect transistors*, Methods 63 (2013) 212–218.
[30] M.H. Abouzar, A. Poghossian, A.G. Cherstvy, A.M. Pedraza, S. Ingebrandt, M.J. Schöning: *Label-free electrical detection of DNA by means of field-effect nanoplate capacitors: Experiments and modeling*, Phys. Status Solidi A 209 (2012) 925–934.
[31] A. Kulkarni, Y. Xu, C. Ahn, R. Amin, S.H. Park, T. Kim, M. Lee: *The label free DNA sensor using a silicon nanowire array*, J. Biotechnol. 160 (2012) 91–96.
[32] C. Wu, T. Bronder, A. Poghossian, C.F. Werner, M.J. Schöning: *Label-free detection of DNA using a light-addressable potentiometric sensor modified with a positively charged polyelectrolyte layer*, Nanoscale 7 (2015) 6143–6150.
[33] M. Barbaro, A. Caboni, D. Loi, S. Lai, A. Homsy, P.D. van der Wal, N.F. de Rooij: *Label-free, direct DNA detection by means of a standard CMOS electronic chip*, Sens. Actuators B 171–172 (2012) 148–154.

[34] T. Adam, U. Hashim: *Highly sensitive silicon nanowire biosensor with novel liquid gate control for detection of specific single-stranded DNA molecules*. Biosens. Bioelectron. 67 (2015) 656–661.

[35] B. Veigas, E. Fortunato, P.V. Baptista: *Field effect sensors for nucleic acid detection: Recent advances and future perspectives*, Sensors 15 (2015) 10380–10398.

[36] S. Kuga, J. Yang, H. Takahashi, K. Hirama, T. Iwasaki, H. Kawarada: *Detection of mismatched DNA on partially negatively charged diamond surfaces by optical and potentiometric methods*, J. Am. Chem. Soc. 130 (2008) 13251–13263.

[37] Y. Liu, R.W. Dutton: *Effects of charge screening and surface properties on signal transduction in field effect nanowire biosensors*, J. Appl. Phys. 106 (2009) 014701-1–8.

[38] G.J. Zhang, G. Zhang, J.H. Chua, R.E Chee, E.H. Wong, A. Agarwal, K.D. Buddharaju, N. Singh, Z. Gao, N. Balasubramanian: *DNA sensing by silicon nanowire: Charge layer distance dependence*, Nano Lett. 8 (2008) 1066–1070.

[39] U. Rant, K. Arinaga, S. Fujita, N. Yokoyama, G. Abstreiter, M. Tornow: *Electrical manipulation of oligonucleotides grafted to charged surfaces*, Org. Biomol. Chem. 4 (2006) 3448–3455.

[40] S. Uno, M. Iio, H. Ozawa, K. Nakazato: *Full three-dimensional simulation of ion-sensitive field-effect transistor flatband voltage shifts due to DNA immobilization and hybridization*, Jpn. J. Appl. Phys. 49 (2010) 01AG07-1–8.

[41] Y. Nishio, S. Uno, K. Nakazato: *Three-dimensional simulation of DNA sensing by ion-sensitive field-effect transistor: Optimization of DNA position and orientation*, Jpn. J. Appl. Phys. 52 (2013) 04CL01-1–8.

[42] G.A. Evtugyn, T. Hianik: *Layer-by-layer polyelectrolyte assembles involving DNA as a platform for DNA sensors*, Curr. Anal. Chem. 7 (2011) 8–34.

[43] Y.L. Bunimovich, Y.S. Shin, W.S. Yeo, M. Amori, G. Kwong, J.R. Heath: *Quantitative real-time measurements of DNA hybridization with alkylated nonoxidized silicon nanowires in electrolyte solution*, J. Am. Chem. Soc. 128 (2006) 16323–16331.

[44] D. Braeken, G. Reekmans, C. Zhou, B. van Meerbergen, G. Callewaert, G. Borghs, C. Bartic: *Electronic DNA hybridisation detection in low-ionic strength solutions*, J. Exp. Nanosci. 3 (2008) 157–169.

[45] J. Wang, Y. Zhou, M. Watkinson, J. Gautrot, S. Krause: *High-sensitivity light-addressable potentiometric sensors using silicon on sapphire functionalized with self-assembled organic monolayers*, Sens. Actuators B 209 (2015) 230–236.

[46] A. Poghossian, M. Weil, A.G. Cherstvy, M.J. Schöning: *Electrical monitoring of polyelectrolyte multilayer formation by means of capacitive field-effect devices*, Anal. Bioanal. Chem. 405 (2013) 6425–6436.

[47] M. Schönhoff, V. Ball, A.R. Bausch, C. Dejugnat, N. Delorme, K. Glinel, R.V. Klitzing, R. Steitz: *Hydration and internal properties of polyelectrolyte multilayers*, Colloids Surf. A 303 (2007) 14–29.

[48] L.K. Meixner, S. Koch: *Simulation of ISFET operation based on the site-binding model*. Sens. Actuators B 6 (1992) 315–318.

[49] R.N. Smith, M. McCormick, C.J. Barrett, L. Reven, H.W. Spiess: *NMR studies of PAH/PSS polyelectrolyte multilayers adsorbed onto silica*, Macromolecules 37 (2004) 4830–4838.

[50] P. Bergveld: *Thirty years of ISFETOLOGY: What happened in the past 30 years and what may happen in the next 30 years*, Sens. Actuators B 88 (2003) 1–20.

[51] C. Cane, I. Gracia, A. Merlos: *Microtechnologies for pH ISFET chemical sensors*, Microelectron. J. 28 (1997) 389–405.

[52] D. Yoo, S.S. Shiratori, M.F. Rubner: *Controlling bilayer composition and surface wettability of sequentially adsorbed multilayers of weak polyelectrolytes*, Macromolecules 31 (1998) 4309–4318.

[53] R. E. G. van Hal, J. C. T. Eijkel, P. Bergveld: *A general model to describe the electrostatic potential at electrolyte oxide interfaces*, Adv. Colloid Interface Sci. 69 (1996) 31–62.

[54] F. Uslu, S. Ingebrandt, D. Mayer, S. Böcker-Meffert, M. Odenthal, A. Offenhäusser: *Labelfree fully electronic nucleic acid detection system based on a field-effect transistor device*, Biosens. Bioelectron. 19 (2004) 1723–1731.

[55] H. Einati, A. Mottel, A. Inberg, Y. Shacham-Diamand: *Electrochemical studies of self-assembled monolayers using impedance spectroscopy*, Electrochim. Acta 54 (2009) 6063–6069.

[56] S. Ingebrandt, X. Vu, J.F. Eschermann, R. Stockmann, A. Offenhäusser: *Top-down processed SOI nanowire devices for biomedical applications*, ECS Trans. 35 (2011) 3–15.

[57] S. Ge, K. Kojio, A. Takahara, T. Kajiyama: *Bovine serum albumin adsorption onto immobilized organotrichlorosilane surface: Influence of the phase separation on protein adsorption patterns*, J. Biomater. Sci., Polym. Ed. 9 (1998) 131–150.

5.5 SUPPORTING INFORMATION

5.5.1 Contact-angle measurements

The wettability of the sensor surface before and after the cleaning step with piranha solution and after deposition of the PAH layer has been studied by water contact-angle measurements. The determination of the contact angle was done by the sessile drop technique using a contact-angle goniometer OCA 15 (Data Physics Instruments, Germany) and deionized water as probe liquid. **Figure 5.7** depicts results of water droplet (5 µL) contact-angle measurements. Piranha solution is well known as strong oxidation agent and is used to hydroxylate SiO_2 surfaces. Due to the hydroxylation process, most of organic contamination can be removed and the surface becomes highly hydrophilic, which results in a decrease of the contact angle from 89° to less than 10°. The contact angle increases to 34° after the PAH adsorption that can be explained by assuming that the OH-groups of the SiO_2 surface are covered by PAH molecules, which exhibit cationic amino groups.

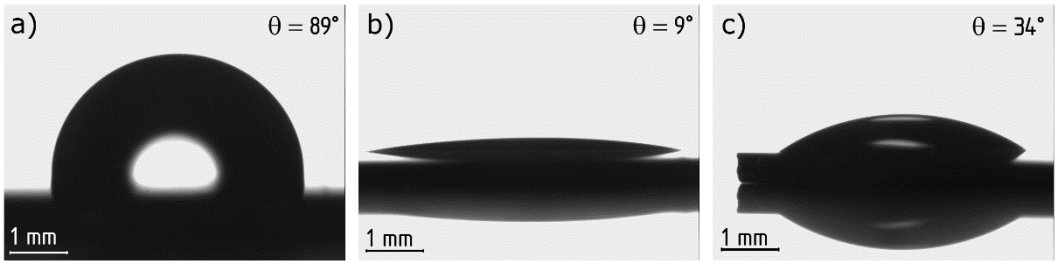

Figure 5.7: Results of water contact-angle measurements before (a) and after the cleaning step with piranha solution (b) and after PAH adsorption (c).

5.5.2 Sensor drift[1]

We reported that the drift was evaluated over a time period of seven days (**Chapter 5.3.1**) and – in order to reduce drift influence onto the sensor signal – the EIS sensors were conditioned in the measurement solution for 12 h.

The drift has also been evaluated before the conditioning phase. Here, fluctuations between 1-2 mV/h up to 20 mV/h were registered. Only chips with a maximum drift of approximately 2 mV/h were used for electrochemical experiments with DNA. Sensors with a higher drift after the conditioning phase were not further used for measurements. Reasons for sensor drift have been mainly and more investigated for ISFET than for EIS sensors, but they are valid for both types of field-effect devices:

Important factors for drift are reference-electrode potential-changes, leakage-current-induced polarization, temperature- or insulator changes and changes at the insulator-electrolyte-interface [1–3]. Moreover, obvious factors, like changes in the pH value and ion concentration of the electrolyte solution as well as the drain current have also an impact on the signal drift [4]. Other groups report effects of electric-field-enhanced ion migration within the gate insulator [5] or electron-induced creation of charges inside the insulator

[1] Content of **Chapter 5.5.2** is not part of the previously presented publication.

films [6], and other surface effects [7, 8]. One explanation for the signal drift affected by surface effects is given by the dispersive transport theory presented by Jamasb et al. [9]: Hydration at the electrolyte-insulator interface leads to a change of chemical composition of the oxide. By this, the dielectric constant continuously varies, resulting in a change of insulator capacitance.

5.5.3 Declaration of scientific novelty

Parts of this publication are already presented in the authors master thesis "Entwicklung eines miniaturisierten Sensorchips für einen späteren Einsatz zum markierungsfreien Nachweis von Tuberkulose" (T.S. Bronder, University of Hannover, Germany, 2013). This part declares the scientific novelty of the presented publication and explains the results and content beyond the range of the master thesis:

- The main goal of the master thesis was to develop and compare different surface-modification protocols that allow the electrochemical detection of target DNA with EIS sensors. Later on, based on the comparison of the different developed protocols, one procedure should be chosen, which fulfills the desired requirements for field-effect-based electrochemical DNA detection (described in introduction chapter) at the best and should be optimized. In this context, during the master thesis, the basic protocol of DNA immobilization onto PAH-modified EIS sensors was chosen and firstly developed.
- By further research after the master thesis, the protocols have been optimized and the signal height for cDNA-hybridization detection could be improved. Furthermore, the differentiation between cDNA- and ncDNA incubation by means of the observed signal height could be realized by using a blocking step with BSA. The discrimination between cDNA and ncDNA is the essential key-feature of a DNA-sensing device, which gives the ability of selectivity. All of these results have been presented in the shown publication, but not in the master thesis. Graphs with identical content in the master thesis and in the publication are only **Figure 5.4** – the general detection of DNA, and **Figure 5.6** – the fluorescence-reference experiment.
- In addition, besides the fluorescence experiments, contact-angle measurements were performed as a second reference method for the surface functionalization.

All new findings are very essential for the development of a DNA-detection protocol, which can be used later for the identification of bacteria. The importance of these new contents reasons the presentation in a scientific publication.

REFERENCES

[1] C.G. Jakobson, M. Feinsod, Y. Nemirovsky: *Low frequency noise and drift in ion sensitive field effect transistors*, Sens. Actuators B 68 (2000) 134–139.

[2] J. Chiang, S. Jan, J. Chou, Y. Chen: *Study on the temperature effect, hysteresis and drift of pH-ISFET devices based on amorphous tungsten oxide*, Sens. Actuators B 76 (2001) 624–628.

[3] J. Chou, C. Hsiao: *Drift behavior of ISFETs with a-Si : H-SiO_2 gate insulator*, Mater Chem Phys 63 (2000) 270–273.

[4] P. Hein, P. Egger: *Drift behaviour of ISFETs with Si_3N_4-SiO_2 gate insulator*, Sens. Actuators B 13-14 (1993) 655–656.

[5] M. Esashi, T. Matsuo: *Integrated micro multi ion sensor using field effect of semiconductor*, IEEE Trans. Biomed. Eng. 25 (1978) 184–192.

[6] L. Bousse, P. Bergveld: *The role of buried OH sites in the response mechanism of inorganic-gate pH-sensitive ISFETs*, Sens. Actuators 6 (1984) 65–78.

[7] K.M. Chang, K.Y. Chao, H.Y. Hsu, M.C. Huang: *Ultra-low drift voltage by using gate voltage control in oxide-based gate ISFET*, ECS Trans 6 (2008) 11–29.

[8] D. Kwon, B. Cho, C. Kim, B. Sohn: *Effects of heat treatment on Ta_2O_5 sensing membrane for low drift and high sensitivity pH-ISFET*, Sens. Actuators B 34 (1996) 441–445.

[9] S. Jamasb, S. Collins, R.L. Smith: *A physically-based model for drift in Al_2O_3-gate pH ISFET's*, 9th Int. Conf. Solid-State Sensors and Actuators (Transducers '97), Chicago, IL, USA, 15-19 June, (1997) 1379–1382.

6 Surface regeneration and reusability of label-free DNA biosensors based on weak polyelectrolyte-modified capacitive field-effect structures

Biosensors and Bioelectronics 126 (2019)
510–517

Thomas S. Bronder, Arshak Poghossian, Max P. Jessing, Michael Keusgen, Michael J. Schöning

Submitted: 20.09.2018
Accepted: 13.11.2018
Published: 01.02.2019

ABSTRACT

The reusability of capacitive field-effect electrolyte-insulator-semiconductor (EIS) sensors modified with a cationic weak polyelectrolyte (poly(allylamine hydrochloride) (PAH)) for the label-free electrical detection of single-stranded DNA (ssDNA), in-solution- and on-chip-hybridized double-stranded DNA (dsDNA) has been studied. It has been demonstrated that via simply regeneration of the gate surface of the EIS sensor by means of an electrostatic adsorption of a new PAH layer, the same biosensor can be reused for at least five DNA-detection measurements. Because of the reversal of the charge sign of the outermost layer after each surface modification with the cationic PAH or negatively charged DNA molecules, the EIS-biosensor signal exhibits a zigzag-like behavior. The amplitude of the signal changes has a tendency to decrease with increasing number of macromolecular layers. The direction of the EIS-signal shifts can serve as an indicator for a successful DNA-immobilization, or -hybridization process. In addition, we observed that the EIS-signal changes induced by each surface-modification step (PAH adsorption, immobilization of ssDNA or dsDNA molecules and on-chip hybridization of complementary target cDNA) is decreased with increasing the ionic strength of the measurement solution, due to the more efficient macromolecular charge-screening by counterions. The results of field-effect experiments were supported by fluorescence-intensity measurements of the PAH- or DNA-modified EIS surface using various fluorescence dyes.

KEYWORDS

DNA biosensor, label-free, field-effect sensor, reusability, weak polyelectrolyte, charge screening

6.1 INTRODUCTION

Deoxyribonucleic acid (DNA) sensors have been widely recognized as a powerful tool in many fields of application such as molecular diagnostics, forensics, parental testing, drug industry, food safety, identification of pathogens, environmental monitoring of biological warfare and bioterrorism agents, etc. [1–3]. Among different transducers suggested for label-free DNA detection, an electrolyte-gated field-effect device (FED) based on an electrolyte-insulator-semiconductor (EIS) system is one of the most popular and attractive platforms [4–7]. FEDs offer a lot of advantages, like small sizes, the possibility of real-time measurements, fast response and large-scale production at low cost by using of advanced nano- and microfabrication technologies, thus providing new opportunities for a next generation of label-free DNA chips with direct electronic readout.

FEDs are surface charge-sensitive devices and have been widely applied for the detection of various analytes in liquids, including charged macromolecules such as DNA or polyelectrolytes (see e.g., [8–15]). Most of FED-based DNA biosensors reported in literature rely on DNA-hybridization detection (see e.g., [16–19]), although detection of other DNA-recognition events, like single-nucleotide polymorphisms [20, 21], DNA extension [22] and sequencing [23], DNA amplification by polymerase chain reaction (PCR) [24–26], by-products (protons, pyrophosphates) of the nucleotide base incorporation reaction [27, 28], have also been proposed. In DNA-hybridization reaction, the probe single-stranded DNA (ssDNA) molecules of known sequence bind specifically to their complementary single-stranded target DNA (cDNA) and forming a double-stranded DNA (dsDNA). Typically, capture-probe ssDNA molecules are immobilized onto the gate surface of the FED chip and the target cDNA molecules are either detected by real-time monitoring the FED response directly during the hybridization process or by comparing the biosensor signal before and after hybridization. FEDs detect DNA molecules electrostatically by their intrinsic negative molecular charge that arises from the phosphate backbones. The adsorption/ binding of charged DNA to the gate surface of the FED modulates the space-charge distribution in the semiconductor, resulting in a change of the output signal of the FED [4–6]. Generally, due to the screening of the DNA molecular charge by counterions in the solution, the effectivity of an electrostatic coupling between the charged DNA and the FED and therefore, the magnitude of the DNA-hybridization signal is significantly affected by the Debye length or ionic strength of the electrolyte solution, by the distance between the gate surface and molecular charge and by the orientation of DNA macromolecules to the gate surface [29–33]. Thus, among others the gate surface-modification/functionalization and DNA-immobilization technique have a significant impact on the FED signal generated by the DNA hybridization. As a consequence, in addition to recording the DNA-hybridization signal in a low ionic-strength solution, the immobilization of DNA molecules flat to the FED surface with molecular charge lying within the Debye length from the gate surface represents a crucial factor to enhance the sensitivity of the FED to the DNA charge [34]. One approach to achieve flat orientation of DNA molecules on the surfaces is the layer-by-layer (LbL) electrostatic adsorption of a cationic polyelectrolyte/DNA bilayer [35], which has also been used for designing FED-based DNA biosensors. For example, poly-L-lysine-modified ion-sensitive field-effect transistors and EIS sensors were utilized for the detection of ssDNA- and

dsDNA-immobilization, DNA-hybridization process [34, 36, 37] as well as for monitoring PCR-amplified dsDNA [38, 39].

Recently, in our group, the feasibility for the label-free electrical detection of DNA with two kinds of FEDs, the capacitive EIS sensor and multi-spot light-addressable potentiometric sensor (LAPS), which were modified with a positively charged weak polyelectrolyte of poly(allylamine hydrochloride) (PAH), has been demonstrated [40–43]. The capacitive EIS- and LAPS devices modified with a PAH layer demonstrate high DNA-hybridization signals (several tens of mVs) and low detection limits (about 0.1–0.3 nM cDNA). Moreover, PAH-modified EIS sensors were applied for the detection of PCR-amplified tuberculosis DNA fragments and could be applied for a quick verification of the DNA amplification and successful PCR process [44, 45].

DNA biosensors are often designed as disposables for a single-use measurement. To make DNA biosensors reusable, the complex surface/interface architecture should be regenerated after it has been used. This is often realized by removing DNA molecules together with underlying linkers or molecular layers from the sensor's surface and modification of the surface for DNA coupling again, which is a complicated and time-consuming process in many cases (see e.g., a review on common techniques of biosensor regeneration [46]). In the present work, the possibility of a multiple surface regeneration and reusability of PAH-modified EIS sensors for the label-free electrostatic detection of i) ssDNA, ii) in-solution hybridized dsDNA, and iii) on-chip hybridization of complementary target cDNA with immobilized probe ssDNA is investigated. In addition, the impact of the ionic strength and charge screening on the EIS sensor signal has been examined. Fluorescence-microscopy measurements by using fluorescence dyes of FITC (fluorescein isothiocyanate), FAM (carboxyfluorescein) and SG (SybrGreen I) have been performed to validate the results of field-effect experiments.

6.2 MATERIALS AND METHODS

6.2.1 Materials and solutions

Polyelectrolyte solutions were prepared by solving PAH (Mw: 100.000–170.000 g/mol, from ABCR, Germany) or FITC-labeled PAH (PAH-FITC, monomer ratio 50:1 (PAH:FITC), Sigma Aldrich, Germany) in 100 mM NaCl to a concentration of 50 µM, followed by adjusting the pH value to pH 5.4 with NaOH. At this pH value, the weak polyelectrolyte PAH is positively charged, since the isoelectric point of PAH is at pH ~10 [47].

All synthetic DNA oligonucleotides used in this study were purchased from Biomers (Ulm, Germany): Probe ssDNA and FAM-labeled ssDNA (ssDNA-FAM) (52-mer, 5′-TGGAT-CGCTG-TGTAA-GGACA-CGTCG-GCGTG-GTCGT-CTGCT-GGGTT-GATCT-GG-3′); complementary target cDNA and FAM-labeled cDNA (cDNA-FAM) (72-mer, 5′-ACCTC-CGTAA-CCGTC-ATTGT-CCAGA-TCAAC-CCAGC-AGACG-ACCAC-GCCGA-CGTGT-CCTTA-CACAG-CGATC-CA-3′, the complementary part is underlined). Probe DNA-solutions were prepared by dilution of ssDNA or ssDNA-FAM in deionized (DI) water to a final concentration of 5 µM. For the preparation of target cDNA solutions (also 5 µM), cDNA or cDNA-FAM were diluted in 1x PBS (phosphate buffered

saline, pH 7.0) adjusted to 0.66 M NaCl. The dsDNA solution was prepared via mixing equal volumes of 5 µM probe ssDNA and 5 µM target cDNA solutions. Before using for surface modification, the dsDNA solution was heated up to 95 °C in a water bath and slowly cooled down to room temperature.

The SG solution has been prepared by 1:1000 dilution of SG stock solution (Sigma Aldrich, Germany) in DI water. The 450 µm thick 3″ boron-doped Si substrates with a crystallographic orientation of ⟨100⟩ and a specific electrical resistivity of 1–10 Ωcm were obtained from SiMat (Silicon Materials, Germany).

6.2.2 EIS-chip fabrication and sensor-surface modification

The capacitive EIS sensor is the simplest electrolyte-gated FED. In contrast to other types of FEDs, like ion-sensitive field-effect transistors or Si-nanowire transistors, capacitive EIS sensors have a simple structure and can be easily fabricated without any photolithographic process steps. The fabrication of the EIS-sensor chips used in this work is described in previous literature [40, 41, 45]. The square-shaped sensor chips (with sizes of 1 cm x 1 cm) consist of an Al/p-Si/SiO_2 structure. The high-quality thermally grown SiO_2 film (thickness: 30 nm – 50 nm) served as gate insulator. After preparation, the chips were cleaned ultrasonically in a solvent cascade of acetone, isopropyl alcohol, ethanol and DI water, each 3 min. After drying the chips with N_2, they were mounted into a custom-made measurement chamber and sealed with an O-ring (inner diameter: 8 mm) so that a remaining area of approximately 50 mm^2 of SiO_2 surface can get in contact with the solution.

For the surface modification, the biosensor chips were successively exposed to the PAH- or particular DNA solution for a time required for the PAH adsorption, ssDNA- and dsDNA immobilization or on-chip hybridization of target cDNA, respectively. The SiO_2-gate surface of the EIS chip, which is negatively charged in solutions with pH > pH_{pzc} of ~ 2–2.5 (pzc: Point of zero charge) [48, 49], was modified with positively charged PAH macromolecules by using the well-known layer-by-layer technique [50]. For this, 100 µL of 50 µM PAH solution was pipetted onto the chip surface and incubated for about 10 min according to the experimental protocol described in [41]. The PAH-modified EIS chips were used for the label-free electrostatic detection of ssDNA and in-solution-hybridized dsDNA molecules as well as on-chip hybridization of cDNA with immobilized probe ssDNA (**Figure 6.1**).

For the electrostatic immobilization of negatively charged ssDNA or in-solution-hybridized dsDNA molecules, 100 µL of probe ssDNA- or dsDNA solution was applied onto the EIS-sensor surface modified with the positively charged PAH molecules and incubated for 15 min. For the on-chip DNA hybridization, the PAH/ssDNA-modified sensor surface was exposed to 100 µL of 5 µM complementary target cDNA-solution for 40 min. To study the possibility of a multiple surface regeneration and the reusability of the EIS sensors for the DNA detection, the above described procedures were repeated until the desired number of multilayers was achieved (in this work, five layers of PAH/ssDNA, PAH/dsDNA or PAH/ssDNA-cDNA; note that the term ssDNA-cDNA is specified in this work to on-chip-hybridized dsDNA in order to distinguish from in-solution-hybridized

dsDNA). After each surface modification-, immobilization- and hybridization step, the chip surface was washed with 0.33 mM PBS solution (pH 7.0, ionic strength: 5 mM).

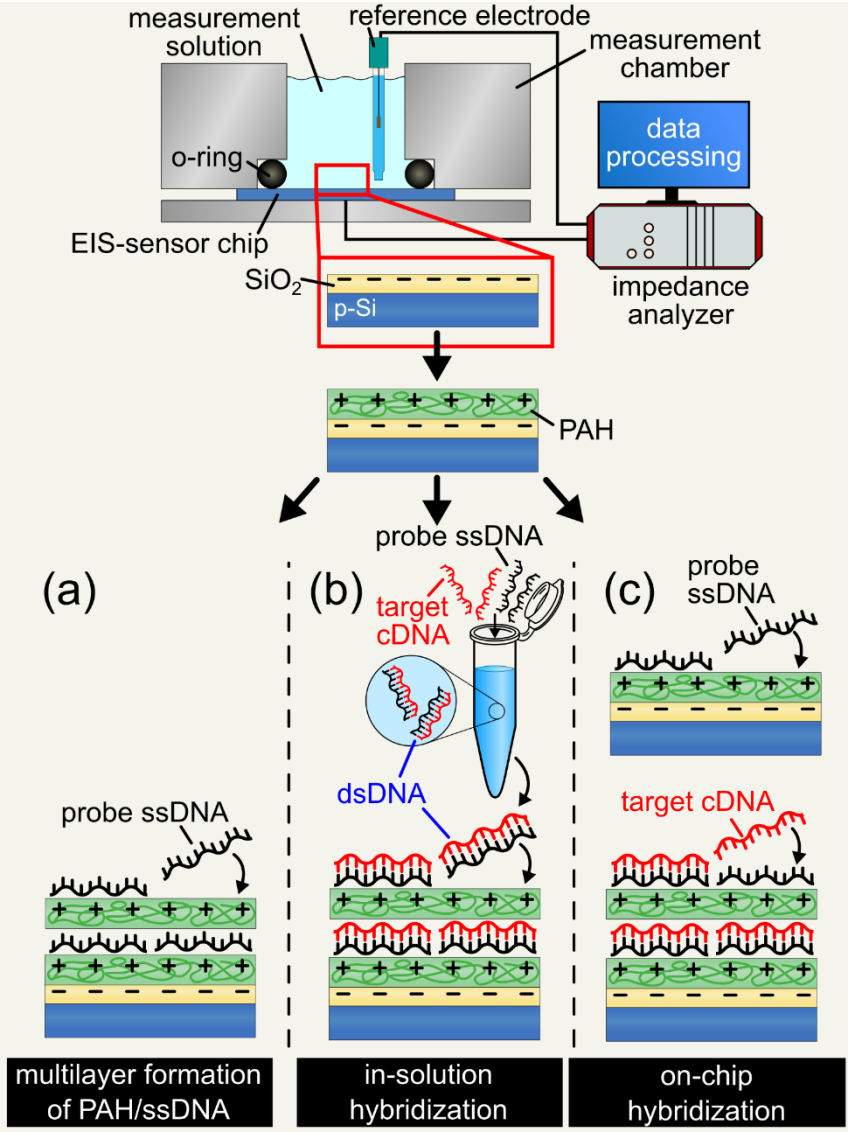

Figure 6.1: Cross section of the measurement chamber with an EIS-sensor chip and reference electrode connected to the impedance analyzer for electrochemical characterization. The PAH-modified EIS chips were used for the label-free electrostatic detection of ssDNA (a), in-solution hybridized dsDNA molecules (b) and on-chip hybridization of cDNA with immobilized probe ssDNA (c), respectively.

6.2.3 Electrochemical measurements

The EIS-sensor chips have been characterized electrochemically with constant-capacitance (ConCap) method in a two-electrode arrangement using a Zennium impedance analyzer (Zahner Elektrik, Germany). An Ag/AgCl reference electrode (Metrohm, Germany) filled with 3 M KCl was placed into the measurement buffer and connected to

the impedance analyzer. The aluminum rear-side contact of the EIS chip was also connected to the impedance analyzer to close the electrical circuit. For measurements of the sensor response in a dynamic ConCap mode before and after chip-surface modification steps, the capacitance value at/near the inflection point in the depletion region of the capacitance-voltage curve was set constant [51], while the resulting DC (direct current) voltage, which is required to keep the defined capacitance, was recorded. All ConCap measurements were performed by applying a small superimposed AC voltage (20 mV) with a frequency of 120 Hz. The measurement chamber with the installed sensor chip and reference electrode was filled with the respective solution and placed in a dark Faraday cage to prevent signal-interfering influences from the environment. The pH value of all solutions used in this study was checked before and after each measurement using a pH meter (Mettler Toledo, Germany) with a double-pore pH-glass electrode (Hamilton, Switzerland).

6.2.4 Optical measurements with fluorescence microscopy

Fluorescence images of the modified biosensor surfaces were taken using an Axio Imager A1m microscope, equipped with a fluorescence-filter set (both from Carl Zeiss AG, Germany). The filter set consists of an excitation band-pass filter (455-495 nm), a dichroic beam splitter (500 nm) and an emission band-pass filter (505-555 nm). Fluorescence experiments with three kinds of fluorescence dyes (SG, FITC and FAM) were carried out. These dyes were chosen because their maximum excitation (λ_{ex}) and emission (λ_{em}) wavelengths (SG: λ_{ex} = 498 nm, λ_{em} = 524 nm; FITC: λ_{ex} = 495 nm, λ_{em} = 525 nm and FAM: λ_{ex} = 497 nm, λ_{em} = 525 nm [52, 53]) fit well to the fluorescence-filter set of the microscope used in this experiment. The similarity of the excitation- and emission efficiency of the three dyes is beneficial for the data processing and normalization.

For taking fluorescence images from the surface of EIS sensors modified with the in-solution- or on-chip hybridized-dsDNA molecules, they were stained with SG dye. For this, chips were exposed to SG solution for 20 min, washed with 0.33 mM PBS buffer (pH 7.0) and dried with N_2 gas. In case of fluorescence measurements of the chip surfaces modified with PAH-FITC and ssDNA-FAM no additional treatment (fluorescence staining) was needed because these molecules were already labeled with the particular fluorescence dye.

For fluorescence quantification, the respective fluorescence intensity has been determined by the weighted summation of the brightness values from the histogram of the image [54, 55]. The histogram data were achieved using ImageJ analysis software.

6.3 RESULTS AND DISCUSSION

6.3.1 Surface regeneration and reusability of PAH-modified EIS sensors for DNA detection

In previous experiments, we demonstrated the feasibility of PAH-modified EIS sensors for the detection of on-chip- and in-solution DNA hybridization as well as PCR-amplified DNA fragments [40, 41, 45]. These were disposable sensors for single measurements. In

this work, we studied the possibility of a repeated surface regeneration and the reusability of the PAH-modified EIS sensors for multiple DNA-detection measurements.

At first, the capacitance-voltage curves of bare (unmodified) EIS sensors were recorded in order to check the correct functioning of the chips. Only chips with a (expected) sigmoidal-like shaped curve have been used for further experiments. From the obtained capacitance-voltage signals the working point (i.e., a constant-capacitance value) for subsequent ConCap measurements were chosen.

The ConCap results of reusability experiments are shown in **Figure 6.2**, where three PAH-modified EIS sensors (in total nine EIS sensors were tested) were used for multiple (five times) detection of ssDNA (**Figure 6.2a**), in-solution hybridized dsDNA (**Figure 6.2b**) and on-chip hybridization of complementary target cDNA with an immobilized probe ssDNA (**Figure 6.2c**). The ConCap signals in **Figure 6.2a-c** were recorded in a low ionic-strength buffer solution (0.33 mM PBS, pH 7.0, ionic strength: 5 mM) before and after each surface-modification step. After the first successful detection of DNA immobilization or hybridization by the PAH-modified EIS sensors, the surface of all sensors was regenerated by means of simple layer-by-layer adsorption of a second PAH layer on the immobilized ssDNA-, dsDNA- or on-chip-hybridized ssDNA-cDNA layer. Now, the EIS sensors with a positively charged outermost PAH layer are ready for the next electrical DNA-detection measurement. These procedures were repeated five times, demonstrating that via the simple surface regeneration with PAH, the same sensor could be reused for at least five DNA-detection measurements without removal of the underlying layers, which benefits in terms of saving time, effort and costs. The total number of deposited macromolecular layers in experiments shown in **Figure 6.2a**, **Figure 6.2b** and **Figure 6.2c** was 10, 10 and 15 layers, respectively.

From **Figure 6.2a-c**, it can be clearly recognized that the successive adsorption/immobilization of oppositely charged PAH/ssDNA-, PAH/dsDNA- and PAH/ssDNA-cDNA layers results in alternate shifting of the ConCap signal. The directions of these signal changes are dependent on the charge sign of the terminating molecular layer. The adsorption of cationic PAH macromolecules shifts the ConCap signal in the direction of more negative voltages. This is due to the feedback control in the ConCap mode, which requires the application of a more negative voltage on the gate for compensation of the positive charge of the PAH molecules and for keeping the EIS capacitance at a constant value. On the contrary, the immobilization of the negatively charged ssDNA, dsDNA and hybridization of cDNA with a probe ssDNA results in a shift of the ConCap response to the direction of less negative gate voltages. Thus, the direction of ConCap-signal shift can serve as an indicator for the verification of successful immobilization or hybridization of DNA molecules. **Figure 6.2d** exemplarily depicts the ConCap-signal changes as a function of the macromolecular layer number evaluated from **Figure 6.2c** for the EIS sensor modified with five $(PAH/ssDNA\text{-}cDNA)_5$ layers. The positively charged PAH layer may attract negatively charged target cDNA molecules and increase their local concentration near the EIS surface as well as may reduce the electrostatic repulsion between probe ssDNA and target cDNA and thus, accelerate the hybridization process even in low ionic-strength solutions. Because of the reversal of the charge sign of the outermost layer after each surface modification with the positively charged PAH layer and subsequent immobilization/hybridization of negatively charged DNA molecules, the signal changes

exhibit a zigzag-like behavior. Moreover, the amplitude of the signal changes tends to reduce with an increase of the number of macromolecular layers. For example, signal shifts of 117 mV, 36 mV and 22 mV recorded after the first modification with PAH-1, ssDNA-1 and cDNA-1, respectively, decrease to 14 mV, 10 mV and 3 mV after the fifth modification with PAH-5, ssDNA-5 and cDNA-5 layers. Similar behavior was observed in the case of reusability experiments with EIS sensors for multiple detections of ssDNA and dsDNA shown in **Figure 6.2a** and **Figure 6.2b**, respectively. These results are consistent with previous experiments on monitoring of layer-by-layer formation of oppositely charged polyelectrolyte multilayers of PAH/PSS (poly(sodium 4-styrene sulfonate)) using silicon thin-film resistors [56, 57] and capacitive field-effect sensors [51]. On the other hand, no signal reducing with increasing the layer number was observed for an EIS sensor modified with poly-L-lysine/DNA multilayer in other studies [36, 38] that could be probably due to, for instance, a highly porous multilayer structure.

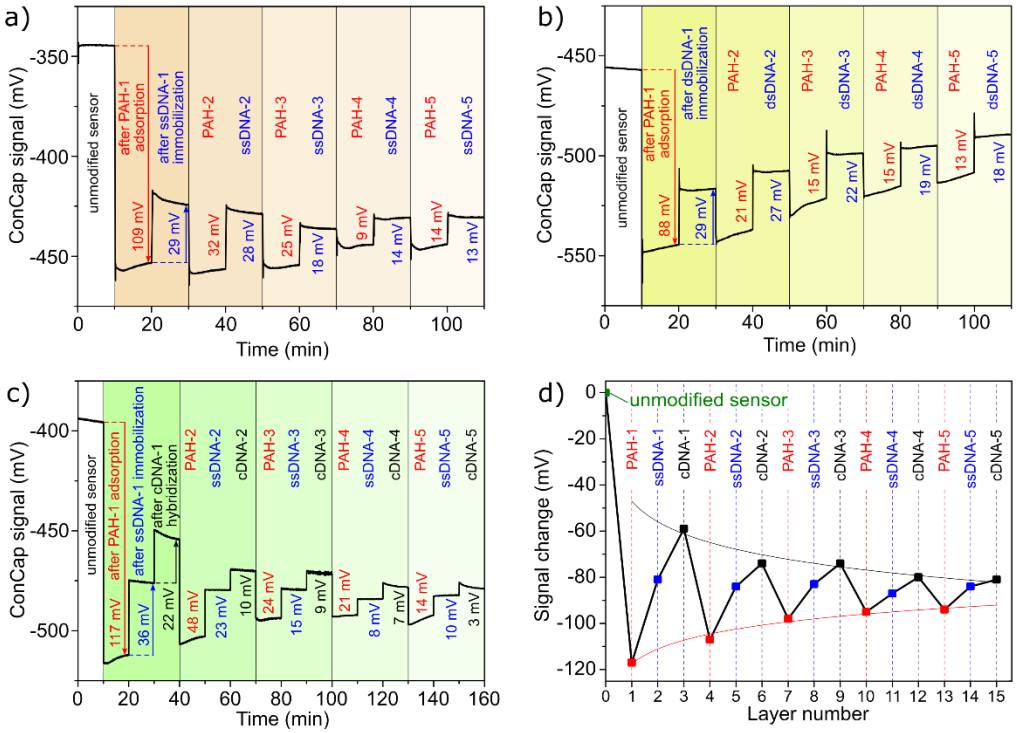

Figure 6.2: ConCap curves of EIS sensors modified with PAH/ssDNA (a), PAH/dsDNA (b), PAH/ssDNA-cDNA (c) multilayers and signal changes as a function of layer number (d), evaluated from (c).

To explain gate-surface potential changes of capacitive EIS sensors induced via layer-by-layer adsorption of polyelectrolytes, a theoretical electrostatic model has been developed in [51]. This model takes into account the ionic strength of the solution and the screening of macromolecular charge by the counterions as well as the distance between the charge of the terminating polyelectrolyte layer and the sensor surface. Although this model was developed for EIS sensors modified with a multilayer of oppositely charged PAH/PSS, it can also be applied to qualitatively explain the signal behavior of the EIS sensor modified

with the multilayer of the PAH/DNA system. The model predicts the decreasing of signal changes upon subsequent adsorption of oppositely charged polyelectrolytes as the ionic strength of the solution increased, because of a more efficient screening of the polyelectrolyte charge (the experimental results related to this issue are presented in **Subsection 6.3.2**: Influence of ionic strength on the sensor signal). The model also predicts reducing of the electrostatic interaction between the charged polyelectrolyte and the EIS-gate surface with increasing the distance between the terminating molecular layer and the gate surface. Thus, the signal changes generated due to the PAH adsorption or DNA immobilization/hybridization will reduce with the rise of the layer number and thickness of PAH/DNA multilayer that in fact, has been monitored in our experiments.

6.3.2 Influence of ionic strength on the sensor signal

The charge distribution in the immediate vicinity of the gate surface plays a critical role in transferring the molecular charge-induced signal to the EIS device. EIS sensors are known as charge-sensitive devices [58, 59]; they are able to detect charge changes that happen directly at the gate surface or within the order of the Debye length (λ_D) from the surface. Therefore, the Debye-screening length is obviously one of the important factors, which may significantly affect the working characteristics (output-signal change, sensitivity, detection limit, etc.) of FEDs for the detection of adsorption/binding of charged macromolecules onto the gate surface [30, 60, 61]. The charge of the macromolecules is screened by the dissolved small counterions in the solution: Positively charged macromolecules such as PAH will be surrounded by anions due to electrostatic interactions, while negatively charged species such as DNA will be surrounded by cations. As a result of the charge-screening effect, the electrostatic potential arising from the intrinsic charges of molecules decays exponentially with distance to nearly zero in the bulk-electrolyte solution. The Debye length is the distance over which the electrostatic potential decreases by a factor of e (~2.7). It is inversely proportional to the ionic strength of the electrolyte solution and for aqueous solutions is given by **Eq. 6.1** [29, 62]:

$$\lambda_D = \sqrt{\frac{\varepsilon_0 \varepsilon_r k_B T}{2 z^2 q^2 I_s}} \qquad \textbf{Eq. 6.1}$$

where ε_r is the dielectric constant of the electrolyte solution, ε_0 is the vacuum permittivity, k_B is the Boltzmann constant, T is the temperature, z is the valency of the ions in the electrolyte, q is the elementary charge, and I_s is the ionic strength of the electrolyte, which for a 1:1 monovalent salt can be replaced by the ion concentration. For a monovalent electrolyte at 25 °C, the Debye length can be simply determined from **Eq. 6.2**:

$$\lambda_D\ (in\ nm) \approx \frac{0.304}{\sqrt{I_s}}\ (in\ M) \qquad \textbf{Eq. 6.2}$$

To find out an influence of the ionic strength, the ConCap-signal changes induced by each surface-modification step (i.e., after PAH adsorption, immobilization of ssDNA- and

dsDNA molecules and after on-chip hybridization of cDNA) were recorded in PBS solutions (pH 7.0) with different ionic strength of 1 mM, 5 mM, 10 mM and 20 mM (the corresponding Debye lengths amount approximately 9.6 nm, 4.3 nm, 3 nm and 2.2 nm, respectively). The results of these experiments are depicted in **Figure 6.3**.

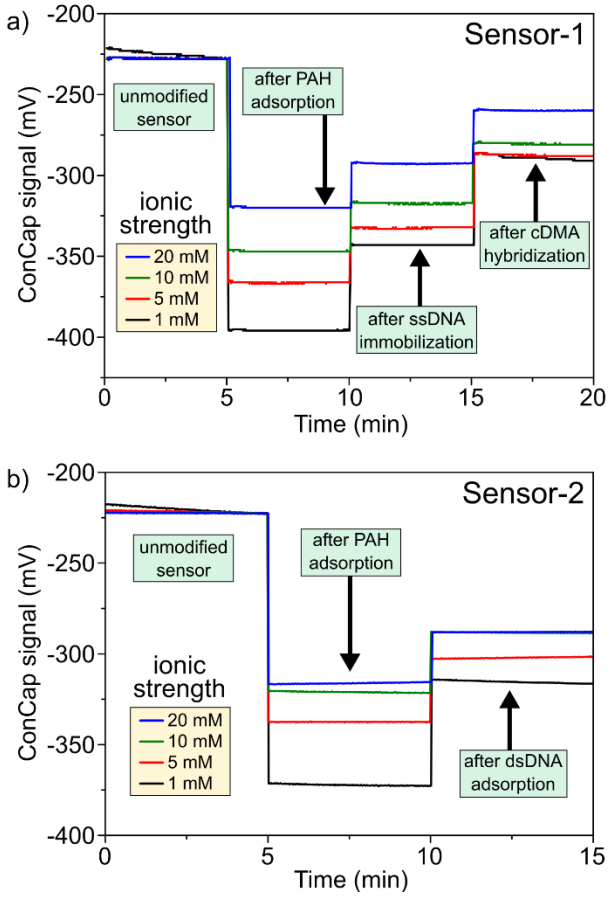

Figure 6.3: ConCap signal of two EIS biosensors recorded in 0.066 mM, 0.33 mM, 0.66 mM and 1.32 mM PBS solutions (pH 7.0) with different ionic strength of 1 mM, 5 mM, 10 mM and 20 mM, respectively. a) Sensor-1: before and after PAH adsorption, immobilization of probe ssDNA and on-chip hybridization of target cDNA molecules; b) Sensor-2: before and after PAH adsorption and dsDNA immobilization.

The ConCap-signal changes after each modification step evaluated from **Figure 6.3** are summarized in **Table 6.1**. As expected, with increasing the ionic strength of the solution, the amplitude of signal shifts after each modification step is decreased. This is due to the more efficient screening of the molecular charge of PAH or DNA by counterions in the solution. For example, the on-chip cDNA-hybridization signal is reduced from 52 mV recorded in PBS with ionic strength of 1 mM to 33 mV measured in PBS with ionic strength of 20 mM.

Table 6.1: ConCap-signal changes after each surface-modification step recorded in PBS solutions with different ionic strength.

		Sensor signal change / mV				
		Sensor-1 on-chip hybridization			Sensor-2 in-solution hybridization	
Ionic strength / mM	Debye length / nm	After PAH	After ssDNA	After cDNA	After PAH	After dsDNA
1	9.6	167	53	52	151	56
5	4.3	138	34	44	115	36
10	3.0	119	30	36	98	33
20	2.2	92	27	33	92	27

6.3.3 Fluorescence-intensity measurements of modified sensor surfaces

To verify the results of field-effect experiments, fluorimetric investigations were performed by using the fluorescence dyes FITC, FAM and SG. **Figure 6.4** shows a colored bar chart representing the normalized average fluorescence intensities of fluorescence images taken from the gate surfaces of the EIS sensors after various modification steps (in total 24 sensor chips were studied). The two orange-colored bars (1–2) represent the fluorescence signals for a SiO_2-gate surface modified with PAH or PAH-FITC, respectively. PAH molecules bind to the sensor surface in both cases, but a strong fluorescence only occurs for the PAH-FITC-modified chip because of the presence of the fluorescence dye.

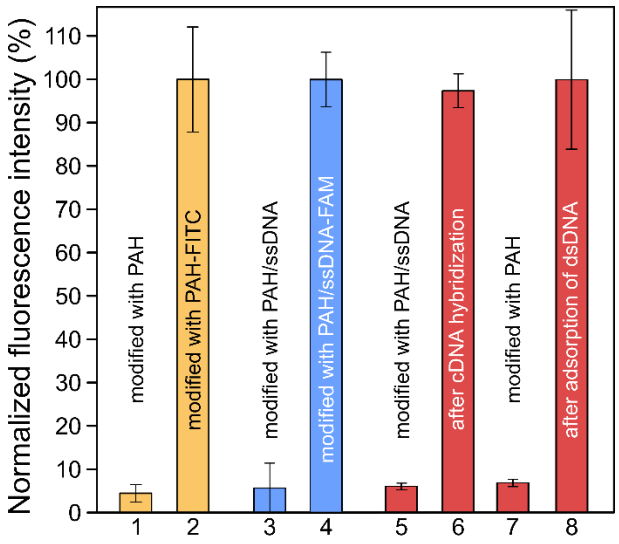

Figure 6.4: Bar chart of the normalized average fluorescence intensities of fluorescence images taken from the gate surfaces of EIS sensors after various modification steps by using fluorescence dyes of FITC (bar 1, 2), FAM (bar 3, 4) and SG (bar 5–8), respectively. The fluorescence signals were normalized for each fluorescence dye individually by setting the highest recorded value to 100%.

In order to prove an immobilization of ssDNA onto the PAH layer, additional reference experiments were carried out utilizing FAM-labeled ssDNA molecules. The fluorescence signals of two chip surfaces, which were modified with PAH/ssDNA and PAH/ssDNA-FAM (blue bars 3–4), were compared. As expected, a significant increase in fluorescence intensity has been detected from the chip surface modified with PAH/ssDNA-FAM. This experiment confirms the successful electrostatic immobilization of the negatively charged probe ssDNA-molecules onto the PAH-modified SiO_2 surface.

Finally, the red bars (5–8) in **Figure 6.4** represent the results of fluorescent experiments in which SG was used as fluorescence dye. For this purpose, two EIS sensors modified with the in-solution- (bar 8) or on-chip-hybridized dsDNA molecules (bar 6) were incubated in SG solution. For comparison, two other EIS sensors modified with PAH- or PAH/ssDNA layers (i.e., without in-solution- or on-chip-hybridized dsDNA) were also exposed to SG solution. SG dye is known for the strong brightness increase upon binding to dsDNA [52]. As can be seen, fluorescence intensities of less than 8% (bars 5 and 7) were detected for EIS sensors modified with PAH- or PAH/ssDNA layers, because no dsDNA is present on the sensor surface. In contrast, fluorescence intensity of approximately 100% was observed for the EIS sensor modified with PAH/ssDNA layers and exposed to target cDNA solution (bar 6). This result indicates the successful hybridization of the target cDNA molecules with the immobilized probe ssDNA and formation of dsDNA. A high fluorescence intensity of ~100% was also observed when in-solution-hybridized dsDNA molecules were directly immobilized onto the PAH-modified surface (bar 8). In both cases, SG binds to dsDNA molecules, resulting in a strong increase of brightness. Thus, the results of fluorescence-intensity measurements correlate well with the results obtained by field-effect experiments and validate successfully all surface-modification steps.

6.4 CONCLUSIONS

In this work, the reusability of PAH-modified capacitive field-effect EIS sensors for the label-free electrical detection of ssDNA, in-solution- and on-chip-hybridized dsDNA has been investigated. For this, the formation of five bilayers of PAH/ssDNA or PAH/dsDNA as well as five triple layers of PAH/ssDNA-cDNA onto the EIS-gate surface was monitored by means of dynamic ConCap measurements. It has been demonstrated that via simple regeneration of the EIS-sensor surface by means of adsorption of a new PAH layer, the same biosensor could be reused for at least five DNA-detection measurements. The consecutive adsorption of oppositely charged PAH/ssDNA-, PAH/dsDNA- and PAH/ssDNA-cDNA layers leads to alternating shifts of the ConCap signal. The direction of the EIS-signal shifts depends on the charge sign of the outermost molecular layer and therefore, can be used as an indicator for the verification of successful DNA immobilization or hybridization processes.

In addition, an influence of the Debye-screening effect (which is considered as one of the important factors affecting the sensitivity of FEDs to the macromolecular charge) on the EIS signal has been studied by recording ConCap responses after surface-modification steps in buffer solutions with different ionic strength. The ConCap-signal changes induced by each modification step (i.e., PAH adsorption, immobilization of ssDNA or dsDNA

molecules and on-chip hybridization of cDNA) is increased with decreasing the ionic strength of the solution, due to the less efficient screening of the molecular charge of the PAH or DNA by counterions. The results of field-effect measurements were supported by fluorescence-microscopy experiments using PAH- and ssDNA molecules labeled with fluorescence dyes of FITC and FAM, respectively, as well as via staining of the in-solution- and on-chip-hybridized dsDNA with SG dye.

It is worth to note, although in this work, a multilayer PAH/DNA system has been studied, the capacitive EIS platform can be extended for the label-free electrical monitoring of formation of multilayers composed of other oppositely charged cationic/anionic macromolecular systems as well as charged nanoparticle/molecule inorganic/organic nanohybrids.

ACKNOWLEDGEMENTS

The authors thank S. Scheja for technical support, H. Iken for wafer processing and C. Metzger-Boddien, H. Busch for valuable discussions. The authors wish to acknowledge the German Federal Ministry of Education and Research for the financial support (project “DiaCharge”, grant no.: 031A192D), Germany.

REFERENCES

[1] F. Wei, P.B. Lillehoj, C.M. Ho: *DNA diagnostics: Nanotechnology-enhanced electrochemical detection of nucleic acids*, Pediatr. Res. 67 (2010) 458–468.

[2] A. Sassolas, B.D. Leca-Bouvier, L.J. Blum: *DNA biosensors and microarrays*, Chem. Rev. 108 (2008) 109–139.

[3] W.W. Zhao, J.J. Xu, H.Y. Chen: *Photoelectrochemical DNA biosensors*, Chem. Rev. 114 (2014) 7421–7441.

[4] A. Poghossian, M.J. Schöning: *Label-free sensing of biomolecules with field-effect devices for clinical applications*, Electroanal. 26 (2014) 1197–1213.

[5] C. Kataoka-Hamai, Y. Miyahara: *Label-free detection of DNA by field-effect devices*, IEEE Sens. J. 11 (2011) 3153–3160.

[6] B. Veigas, E. Fortunato, P.V. Baptista: *Field effect sensors for nucleic acid detection: Recent advances and future perspectives*, Sensors 15 (2015) 10380–10398.

[7] C. Toumazou, T.S.L.K. Thay, P. Georgiou: *A new era of semiconductor genetics using ion-sensitive field-effect transistors: The gene-sensitive integrated cell*, Philos. Trans. R. Soc. A 372 (2014) 20130112-1–12.

[8] A. Poghossian, A. Baade, H. Emons, M.J. Schöning: *Application of ISFETs for pH measurement in rain droplets*, Sens. Actuators B 76 (2001) 634–638.

[9] J. Gun, M.J. Schöning, M.H. Abouzar, A. Poghossian, E. Katz: *Field-effect nanoparticle-based glucose sensor on a chip: Amplification effect of coimmobilized redox species*, Electroanal. 20 (2008) 1748–1753.

[10] C. Jimenez-Jorquera, J. Orozco, A. Baldi: *ISFET based microsensors for environmental monitoring*, Sensors 10 (2010) 61–83.

[11] A. Poghossian, M. Thust, M.J. Schöning, M. Müller-Veggian, P. Kordos, H. Lüth: *Cross-sensitivity of a capacitive penicillin sensor combined with a diffusion barrier*, Sens. Actuators B 68 (2000) 260–265.

[12] J.R. Siqueira, M.H. Abouzar, M. Bäcker, V. Zucolotto, A. Poghossian, O.N. Oliveira, M.J. Schöning: *Carbon nanotubes in nanostructured films: Potential application as amperometric and potentiometric field-effect (bio-)chemical sensors*, Phys. Status Solidi A 206 (2009) 462–467.

[13] K. Nakazato: *An integrated ISFET sensor array*, Sensors 9 (2009) 8831–8851.

[14] C.S. Lee, S.K. Kim, M. Kim: *Ion-sensitive field-effect transistor for biological sensing*, Sensors 9 (2009) 7111–7131.

[15] A. Poghossian, M. Bäcker, D. Mayer, M.J. Schöning: *Gating capacitive field-effect sensors by the charge of nanoparticle/molecule hybrids*, Nanoscale 7 (2015) 1023–1031.

[16] N. Lu, A. Gao, P. Dai, T. Li, A. Wang, X. Gao, S. Song, C. Fan, Y. Wang: *Ultra-sensitive nucleic acids detection with electrical nanosensors based on CMOS-compatible silicon nanowire field-effect transistors*, Methods 63 (2013) 212–218.

[17] C. Wu, T. Bronder, A. Poghossian, C.F. Werner, M. Bäcker, M.J. Schöning: *Label-free electrical detection of DNA with a multi-spot LAPS: First step towards light-addressable DNA chips*, Phys. Status Solidi A 211 (2014) 1423–1428.

[18] L. Bandiera, G. Cellere, S. Cagnin, A. De Toni, E. Zanoni, G. Lanfranchi, L. Lorenzelli: *A fully electronic sensor for the measurement of cDNA hybridization kinetics*, Biosens. Bioelectron. 22 (2007) 2108–2114.

[19] S. Ingebrandt, A. Offenhäusser: *Label-free detection of DNA using field-effect transistors*, Phys. Status Solidi A 203 (2006) 3399–3411.

[20] S. Purushothaman, C. Toumazou, C.P. Ou: *Protons and single nucleotide polymorphism detection: A simple use for the ion sensitive field effect transistor*, Sens. Actuators B 114 (2006) 964–968.

[21] S. Ingebrandt, Y. Han, F. Nakamura, A. Poghossian, M.J. Schöning, A. Offenhäusser: *Label-free detection of single nucleotide polymorphisms utilizing the differential transfer function of field-effect transistors*, Biosens. Bioelectron. 22 (2007) 2834–2840.

[22] M. Kamahori, Y. Ishige, M. Shimoda: *Detection of DNA hybridization and extension reactions by an extended-gate field-effect transistor: Characterizations of immobilized DNA-probes and role of applying a superimposed high-frequency voltage onto a reference electrode*, Biosens. Bioelectron. 23 (2008) 1046–1054.

[23] J.M. Rothberg, W. Hinz, T.M. Rearick, J. Schultz, W. Mileski, M. Davey, J.H. Leamon, K. Johnson, M.J. Milgrew, M. Edwards, J. Hoon, J.F. Simons, D. Marran, J.W. Myers, J.F. Davidson, A. Branting, J.R. Nobile, B.P. Puc, D. Light, T.A. Clark, M. Huber, J.T. Branciforte, I.B. Stoner, S.E. Cawley, M. Lyons, Y. Fu, N. Homer, M. Sedova, X. Miao, B. Reed, J. Sabina, E. Feierstein, M. Schorn, M. Alanjary, E. Dimalanta, D. Dressman, R. Kasinskas, T. Sokolsky, J.A. Fidanza, E. Namsaraev, K.J. McKernan, A. Williams, G.T. Roth, J. Bustillo: *An integrated semiconductor device enabling non-optical genome sequencing*, Nature 475 (2011) 348–352.

[24] T. Goda, M. Tabata, Y. Miyahara: *Electrical and electrochemical monitoring of nucleic acid amplification*, Bioeng. Biotechnol. 3 (2015) 1–7.

[25] C. Toumazou, L.M. Shepherd, S.C. Reed, G.I. Chen, A. Patel, D.M. Garner, C.J.A. Wang, C.P. Ou, K. Amin-Desai, P. Athanasiou, H. Bai, I.M.Q. Brizido, B. Caldwell, D. Coomber-Alford, P. Georgiou, K.S. Jordan, J.C. Joyce, M. La Mura, D. Morley, S. Sathyavruthan, S. Temelso, R.E. Thomas, L. Zhang: *Simultaneous DNA amplification and detection using a pH-sensing semiconductor system*, Nat. Methods 10 (2013) 641–646.

[26] E. Salm, Y. Zhong, B. Reddy, C. Duarte-Guevara, V. Swaminathan, Y.S. Liu, R. Bashir: *Electrical detection of nucleic acid amplification using an on-chip quasi-reference electrode and a PVC REFET*, Anal. Chem. 86 (2014) 6968–6975.

[27] B. Veigas, R. Branquinho, J.V. Pinto, P.J. Wojcik, R. Martins, E. Fortunato, P.V. Baptista: *Ion sensing (EIS) real-time quantitative monitorization of isothermal DNA amplification*, Biosens. Bioelectron. 52 (2014) 50–55.

[28] G.M. Credo, X. Su, K. Wu, O.H. Elibol, D.J. Liu, B. Reddy, T.W. Tsai, B.R. Dorvel, J.S. Daniels, R. Bashir, M. Varma: *Label-free electrical detection of pyrophosphate generated from DNA polymerase reactions on field-effect devices*, Analyst 137 (2012) 1351–1362.

[29] A. Poghossian, A. Cherstvy, S. Ingebrandt, A. Offenhäusser, M.J. Schöning: *Possibilities and limitations of label-free detection of DNA hybridization with field-effect-based devices*, Sens. Actuators B 111–112 (2005) 470–480.

[30] Y. Liu, R.W. Dutton: *Effects of charge screening and surface properties on signal transduction in field effect nanowire biosensors*, J. Appl. Phys. 106 (2009) 014701-1–8.

[31] G.J. Zhang, G. Zhang, J.H. Chua, R.E. Chee, E.H. Wong, A. Agarwal, K.D. Buddharaju, N. Singh, Z. Gao, N. Balasubramanian: *DNA sensing by silicon nanowire: Charge layer distance dependence*, Nano Lett. 8 (2008) 1066–1070.

[32] Y. Nishio, S. Uno, K. Nakazato: *Three-dimensional simulation of DNA sensing by ion-sensitive field-effect transistor: Optimization of DNA position and orientation*, Jpn. J. Appl. Phys. 52 (2013) 04CL01-1–8.

[33] S. Lai, M. Barbaro, A. Bonfiglio: *The role of polarization-induced reorientation of DNA strands on organic field-effect transistor-based biosensors sensitivity at high ionic strength*, Appl. Phys. Lett. 107 (2015) 103301-1–5.

[34] D. Braeken, G. Reekmans, C. Zhou, B. Van Meerbergen, G. Callewaert, G. Borghs, C. Bartic: *Electronic DNA hybridisation detection in low-ionic strength solutions*, J. Exp. Nanosci. 3 (2008) 157–169.

[35] G.A. Evtugyn, T. Hianik: *Layer-by-layer polyelectrolyte assembles involving DNA as a platform for DNA sensors*, Curr. Anal. Chem. 7 (2011) 8–34.

[36] J. Fritz, E.B. Cooper, S. Gaudet, P.K. Sorger, S.R. Manalis: *Electronic detection of DNA by its intrinsic molecular charge*, Proc. Natl. Acad. Sci. U.S.A. 99 (2002) 14142–14146.

[37] T.W. Lin, D. Kekuda, C.W. Chu: *Label-free detection of DNA using novel organic-based electrolyte-insulator-semiconductor*, Biosens. Bioelectron. 25 (2010) 2706–2710.

[38] C.S.J. Hou, N. Milovic, M. Godin, P.R. Russo, R. Chakrabarti, S.R. Manalis: *Label-free microelectronic PCR quantification*, Anal. Chem. 78 (2006) 2526–2531.

[39] C.S.J. Hou, M. Godin, K. Payer, R. Chakrabarti, S.R. Manalis: *Integrated microelectronic device for label-free nucleic acid amplification and detection*, Lab Chip 7 (2007) 347–354.

[40] T.S. Bronder, A. Poghossian, S. Scheja, C. Wu, M. Keusgen, D. Mewes, M.J. Schöning: *DNA immobilization and hybridization detection by the intrinsic molecular charge using capacitive field-effect sensors modified with a charged weak polyelectrolyte layer*, ACS Appl. Mater. Interfaces 7 (2015) 20068–20075.

[41] T.S. Bronder, A. Poghossian, M. Keusgen, M.J. Schöning: *Label-free detection of double-stranded DNA molecules with polyelectrolyte-modified capacitive field-effect sensors*, Tech. Mess. 84 (2017) 628–634.

[42] C.S. Wu, T. Bronder, A. Poghossian, C.F. Werner, M.J. Schöning: *Label-free detection of DNA using a light-addressable potentiometric sensor modified with a positively charged polyelectrolyte layer*, Nanoscale 7 (2015) 6143–6150.

[43] C. Wu, A. Poghossian, T.S. Bronder, M.J. Schöning: *Sensing of double-stranded DNA molecules by their intrinsic molecular charge using the light-addressable potentiometric sensor*, Sens. Actuators B 229 (2016) 506–512.

[44] A. Poghossian, T.S. Bronder, S. Scheja, C. Wu, T. Weinand, C. Metzger-Boddien, M. Keusgen, M.J. Schöning: *Label-free electrostatic detection of DNA amplification by PCR using capacitive field-effect devices*, Procedia Eng. 168 (2016) 514–517.

[45] T.S. Bronder, M.P. Jessing, A. Poghossian, M. Keusgen, M.J. Schöning: *Detection of PCR-amplified tuberculosis DNA fragments with polyelectrolyte-modified field-effect sensors*, Anal. Chem. 90 (2018) 7747–7753.

[46] J.A. Goode, J.V.H. Rushworth, P.A. Millner: *Biosensor regeneration: A review of common techniques and outcomes*, Langmuir 31 (2015) 6267–6276.

[47] M. Morga, Z. Adamczyk: *Monolayers of cationic polyelectrolytes on mica – electrokinetic studies*, J. Colloid Interface Sci. 407 (2013) 196–204.

[48] A. Poghossian: *Determination of the pH_{pzc} of insulators surface from capacitance–voltage characteristics of MIS and EIS structures*, Sens. Actuators B 44 (1997) 551–553.

[49] R.E.G. van Hal, J.C.T. Eijkel, P. Bergveld: *A general model to describe the electrostatic potential at electrolyte oxide interfaces*, Adv. Colloid Interface Sci. 69 (1996) 31–62.

[50] G. Decher, M. Eckle, J. Schmitt, B. Struth: *Layer-by-layer assembled multicomposite films*, Curr. Opin. Colloid Interface Sci. 3 (1998) 32–39.

[51] A. Poghossian, M. Weil, A.G. Cherstvy, M.J. Schöning: *Electrical monitoring of polyelectrolyte multilayer formation by means of capacitive field-effect devices*, Anal. Bioanal. Chem. 405 (2013) 6425–6436.

[52] D. Xiang, K. Zhai, W. Xiang, L. Wang: *Highly sensitive fluorescence quantitative detection of specific DNA sequences with molecular beacons and nucleic acid dye SYBR Green I*, Talanta 129 (2014) 249–253.

[53] F.J. Green: *The Sigma-Aldrich Handbook of Stains, Dyes, and Indicators*, Aldrich Chemical Co., Milwaukee (1990).

[54] N. Otsu: *A threshold selection method from gray-level histograms*, IEEE T. Syst. Man. Cybern. 9 (1979) 62–66.

[55] O. Holub, S.T. Ferreira: *Quantitative histogram analysis of images*, Comput. Phys. Commun. 175 (2006) 620–623.

[56] P.A. Neff, A. Naji, C. Ecker, B. Nickel, R. Klitzing, A.R. Bausch: *Electrical detection of self-assembled polyelectrolyte multilayers by a thin film resistor*, Macromolecules 39 (2006) 463–466.

[57] P.A. Neff, B.K. Wunderlich, R. Klitzing, A.R. Bausch: *Formation and dielectric properties of polyelectrolyte multilayers studied by a silicon-on-insulator based thin film resistor*, Langmuir 23 (2007) 4048–4052.

[58] P. Bergveld: *A critical evaluation of direct electrical protein detection methods*, Biosens. Bioelectron. 6 (1991) 55–72.

[59] A. Poghossian, S. Ingebrandt, M.H. Abouzar, M.J. Schöning: *Label-free detection of charged macromolecules by using a field-effect-based sensor platform: Experiments and possible mechanisms of signal generation*, Appl. Phys. A 87 (2007) 517–524.

[60] K.I. Chen, B.R. Li, Y.T. Chen: *Silicon nanowire field-effect transistor-based biosensors for biomedical diagnosis and cellular recording investigation*, Nano Today 6 (2011) 131–154.

[61] E. Stern, R. Wagner, F.J. Sigworth, R. Breaker, T.M. Fahmy, M.A. Reed: *Importance of the Debye screening length on nanowire field effect transistor sensors*, Nano Lett. 7 (2007) 3405–3409.

[62] T. Goda, A.B. Singi, Y. Maeda, A. Matsumoto, M. Torimura, H. Aoki, Y. Miyahara: *Label-free potentiometry for detecting DNA hybridization using peptide nucleic acid and DNA probes*, Sensors 13 (2013) 2267–2278.

6.5 SUPPORTING INFORMATION[1]

6.5.1 Reaction kinetics

One objective was to find out whether the surface-reaction kinetics can be monitored. Information about the reaction kinetics can be useful for determination of the required time for reaching a surface-saturation status, which means that no more molecules can bind to the sensor surface. This time period gives a good indication on how long the sensor surface must be incubated with the respective solution to acquire a stable sensor signal. With the information about the required time period, the modification protocols can be shortened, and thus an optimization of the entire procedure for fast and simple DNA detection with EIS sensors is possible. The propagation of the measured signal can also give an insight on factors, like the binding type or the influence of solution mixing, but these issues have not been further investigated in this thesis.

First experiments for studying the reaction kinetics were performed in which the ConCap signal was monitored in real time during the four surface-modification steps: Adsorption of PAH, immobilization of ssDNA, immobilization of (in-solution-hybridized) dsDNA and (on-chip) hybridization of cDNA. **Figure 6.5** shows the results of the four measurements. Each curve is divided into a pre-adding (yellow-shaded) and a post-adding (blue-shaded) part.

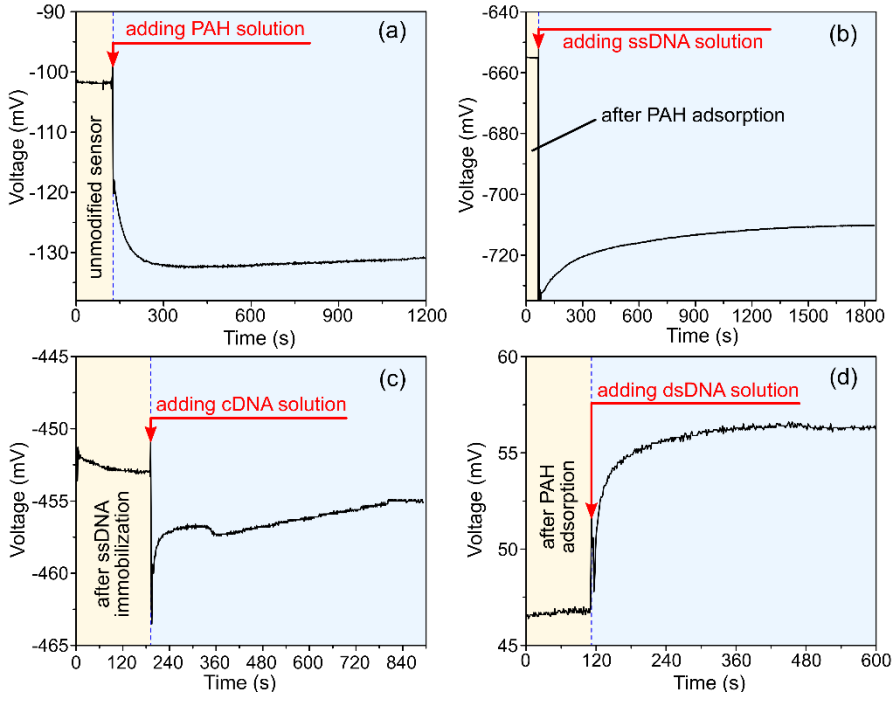

Figure 6.5: Real-time signal propagation during the four surface-modification steps monitored in ConCap mode: (a) PAH adsorption, (b) ssDNA immobilization, (c) cDNA hybridization and (d) dsDNA immobilization. The yellow- and blue-shaded parts indicate the period before and after adding the respective modification solution.

[1]The content of **Chapter 6.5** is not part of the previously presented publication.

The red arrows indicate the moment when the modification solution was added to the starting solution. All solutions are different for each reaction-kinetic experiment. In order to avoid misunderstandings, **Table 6.2** overviews the compositions and concentrations of the pre-adding-, the (added) modification- as well as the resulting post-adding solution, which is a mixture of both previous solutions.

Table 6.2: Volumes, compositions and concentrations of the pre-adding (starting) solution, modification solution and the post-adding solution (after mixing).

Figure	Pre-adding solution (500 µL)	(Added) modification solution (add 500 µL)	Post-adding solution (1000 µL)
Figure 6.5a	100 mM NaCl	100 µM PAH 100 mM NaCl	50 µM PAH 100 mM NaCl
Figure 6.5b	DI water	10 µM ssDNA DI water	5 µM ssDNA in DI water
Figure 6.5c	0.66 M NaCl 1x PBS	10 µM cDNA 0.66 M NaCl 1x PBS	5 µM cDNA 0.66 M NaCl 1x PBS
Figure 6.5d	0.33 M NaCl 0.5x PBS	5 µM dsDNA 0.33 M NaCl 0.5x PBS	2.5 µM dsDNA 0.33 M NaCl 0.5x PBS

The added modification solution was chosen so that the post-adding mixture has the same composition and concentration as the used solutions described in **Chapter 6.2**. The starting solution differs from the added modification solution only in the component which is necessary for the individual modification process (PAH-, ssDNA-, dsDNA- or cDNA-molecules).

Each curve shows a significant signal change after addition of modification solution. Noteworthy are the signal shifts before adding the respective analyte compared to the settled signal at the end of the measurement. A shift of 29 mV (**Figure 6.5a**) was measured during adsorption of PAH, while a larger signal shift of 55 mV during the immobilization of ssDNA (**Figure 6.5b**) was noticeable. The differences in signal-amplitude change can be explained by the strength of the charge screening, which is mainly influenced by the ionic strength of the solution. While the ssDNA immobilization is carried out in DI water environment that leads to a high signal change because of the absence of counterions, the adsorption of PAH is performed in 100 mM NaCl, thus more ions screen the adsorbed molecules and a smaller signal amplitude was recorded during the adsorption itself. A similar result was observed during the cDNA hybridization (**Figure 6.5c**) as well as the immobilization of dsDNA (**Figure 6.5d**), with signal changes of ~2 mV and ~9 mV, respectively. Both reactions occur in high ionic-strength solutions of 0.66 M NaCl and 0.33 M NaCl, respectively.

From each curve (a-d) shown in **Figure 6.5**, the t_{90} time was determined at which the signal reaches 90% of the value in steady-state condition. The values are $t_{90,PAH}$ = 58 s, $t_{90,ssDNA}$ = 568 s, $t_{90,cDNA}$ = 548 s and $t_{90,dsDNA}$ = 96 s. An interesting observation is the difference in t_{90} time for ssDNA and dsDNA: Both surface interactions are based on the electrostatic attachment of the charged phosphate backbone of the DNA and the positively charged PE-modified surface, but show larger differences in t_{90} time. A possible explanation for this relies in the very low-ionic strength of the ssDNA solution: Several factors (among others, the change of the pH, driven by the CO_2 diffusion) can influence the signal propagation and lead to a longer time for settling the signal, which is clearly observable in **Figure 6.5**. Due to that, the time for reaching the steady-state condition is prolonged for ssDNA.

In comparison to the chosen time periods for surface modification, which are 600 s for PAH adsorption, 900 s for ssDNA immobilization, 2400 s for cDNA hybridization and 900 s for dsDNA immobilization, possibilities for decreasing the modification time are only recommended for the PAH adsorption and the dsDNA immobilization step, because here, the differences in the time periods are significantly higher. Nonetheless, further experiments must be performed in order to verify that protocol changes have no negative influence on the overall signal response or the developed biosensor.

6.5.2 Reference experiments with fluorescence microscopy

Figure 6.6 shows a bar chart with four additional measurement results (bar 5, 6, 7 and 11) to the data shown in the presented paper. This supplemented fluorescence intensities serve as additional references.

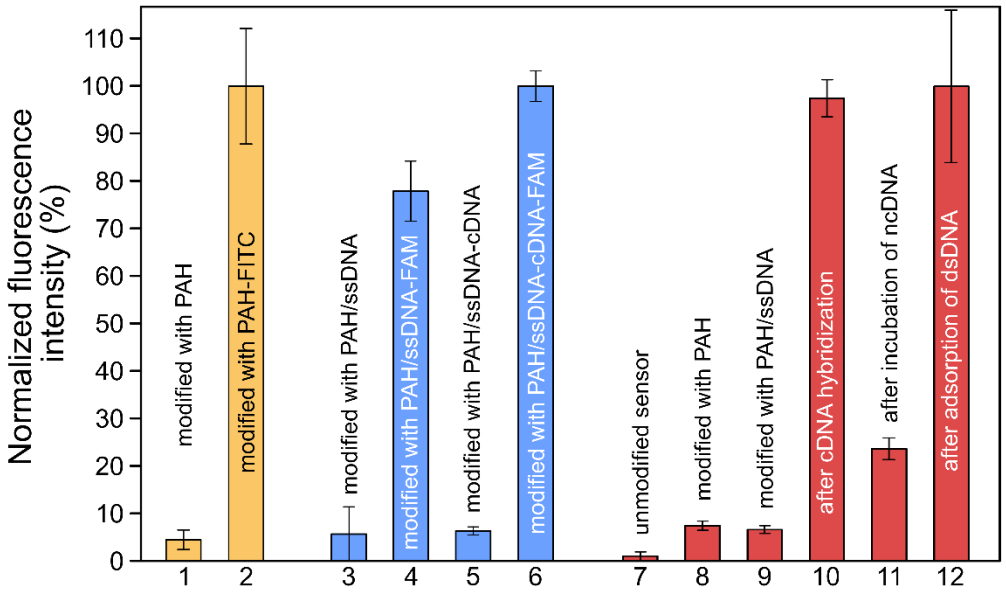

Figure 6.6: Bar chart of the normalized average fluorescence intensities of fluorescence images (each n = 3) of EIS-sensor surface after different modification steps and different fluorescence dyes. The normalization was for each dye individual by setting the highest recorded value to 100%.

To avoid repetitions, only the added results are discussed in this chapter. The experimental data has been achieved using FITC (bar 1, 2), FAM (bar 3–6) and SG (bar 7–12) fluorescence dye.

In order to verify the successful hybridization reaction with FAM fluorescence dye, an experiment has been carried out in which PAH/ssDNA-modified EIS sensors were incubated in cDNA- and cDNA-FAM solution, respectively. The measured fluorescence values have been shown in bar 5 and 6, respectively. The high fluorescence signal of the sensor surface incubated in cDNA-FAM solution indicates that the target molecules have successfully hybridized with the immobilized probe ssDNA (bar 6). As expected, weak intensity has been observed for the sample with cDNA (bar 5) but without dye, because of the absence of the fluorescence agent.

The fluorescence intensity of an unmodified sensor, presented in bar 7, is about 1%. The measurement of such low intensity demonstrates proper measurement conditions in which the influence of background light has been reduced to a minimum. A subtraction of the background signal would have no substantial influence on the obtained results.

In order to analyze the selectivity, experiments, in which the PAH/ssDNA-modified surface of an EIS sensor was incubated with ncDNA, has been performed. An unexpected high fluorescence intensity of approximately 23% was measured (bar 11). Even by subtracting a value of 5–10% (from bar 9; representing the offset-value for PAH/ssDNA-modified surfaces without any contact to target DNA), the remaining intensity indicates that the ncDNA molecules had some interaction with the modified surfaces. Possibilities for that could be, among others, some minor non-specific adsorption of ncDNA to the sensor surface, so called pi-stack events (a non-covalent integration between the nucleobases of a DNA [1–3] between ncDNA and immobilized ssDNA or partial hybridization of lower amounts of ncDNA). Nonetheless, a four-times higher fluorescence signal has been measured for surfaces, incubated with cDNA compared to those with ncDNA. These experimental results shown that a selectivity between complementary and non-complementary target DNA is given by the used sensors. Further investigations are planned to analyze the exact reasons for the signal occurred during ncDNA experiments with the aim of improving the selectivity.

It might be confusing that the fluorescence intensities of bar 1 or 3 and 5 are significantly higher than bar 7, although in all of these four measurements, no fluorescence dye should be present at the sensor surface. The reason for that relies in the non-compliance of comparison between measurements with different fluorescence dyes, because of different absolute fluorescence intensities.

REFERENCES

[1] C.R. Treadway, M.G. Hill, J.K. Barton: *Charge transport through a molecular π-stack: Double helical DNA*, Chem. Phys. 281 (2002) 409–428.

[2] S.O. Kelley, J.K. Barton: *DNA-mediated electron transfer from a modified base to ethidium: Π-stacking as a modulator of reactivity*, Chem. Biol. 5 (1998) 413–425.

[3] E.T. Kool: *Hydrogen bonding, base stacking, and steric effects in DNA replication*, Annu. Rev. Biophys. Biomol. Struct. 30 (2001) 1–22.

7 Detection of PCR-amplified tuberculosis DNA-fragments with polyelectrolyte-modified field-effect sensors

Analytical Chemistry 90 (2018)
7747–7753

Thomas S. Bronder, Max P. Jessing, Arshak Poghossian, Michael Keusgen, Michael J. Schöning

Submitted: 23.04.2018
Accepted: 17.05.2018
Published: 17.05.2018

ABSTRACT

Field-effect-based electrolyte-insulator-semiconductor (EIS) sensors were modified with a bilayer of positively charged weak polyelectrolyte (poly(allylamine hydrochloride) (PAH)) and probe single-stranded DNA (ssDNA) and are used for the detection of complementary single-stranded target DNA (cDNA) in different test solutions. The sensing mechanism is based on the detection of the intrinsic molecular charge of target cDNA molecules after the hybridization event between cDNA and immobilized probe ssDNA. The test solutions contain synthetic cDNA oligonucleotides (with a sequence of tuberculosis mycobacteria genome) or PCR-amplified DNA (which origins from a template DNA strand that has been extracted from *Mycobacterium avium paratuberculosis*-spiked human sputum samples), respectively. Sensor responses up to 41 mV have been measured for the test solutions with DNA, while only small signals of ∼5 mV were detected for solutions without DNA. The lower detection limit of the EIS sensors was ∼0.3 nM, and the sensitivity was ∼7.2 mV/decade. Fluorescence experiments using SybrGreen I fluorescence dye support the electrochemical results

KEYWORDS

DNA detection, label-free, tuberculosis, biosensor, field-effect, polyelectrolyte

7.1 INTRODUCTION

Field-effect sensor chips have been well established as promising tools for detection of biological/chemical agents or reactions. Besides the probably most well-known representative of a field-effect-based sensor, the ion-sensitive field-effect transistor (ISFET), which was introduced 1970 by Piet Bergveld [1], many other types of field-effect-based sensing devices were developed. Examples are light-addressable potentiometric sensors (LAPS) [2–7], silicon-nanowire sensors (SiNW) [8–12], or capacitive electrolyte-insulator-semiconductor (EIS) [13–18] structures. Field-effect-based sensing has the advantage that in many cases a labeling of either the analyte or the reaction partner is not required, which offers benefits in terms of effort, costs, and preparation time.

Field-effect-based chips rely on a sensing mechanism in which charge changes at the surface of the sensor alter the distribution of charge carriers in the space-charge region, which can affect certain sensor characteristics. Hence, different reactions, e.g., pH changes of solutions [19–22] (particularly induced by enzymatic reactions [23–26]), the binding of (charged) biomolecules, or the interaction of substances [27–29] with the sensor surface influence the surface-charge situation and therefore can be measured.

The detection of deoxyribonucleic acid (DNA) is of great interest in many application fields such as medical diagnostics [30–32], genomics [33], biological warfare-issues [34], etc.; DNA can be detected label-free by its intrinsic molecular charge induced by the negatively charged phosphate backbone [35, 36]. The sensing mechanism for DNA is often based on detecting the hybridization event between a probe single-stranded DNA (probe ssDNA) and a complementary single-stranded target DNA (cDNA) molecule, in which a DNA double-strand (dsDNA) is formed. Target template DNA, whose detection is of interest, is usually required to be amplified by means of polymerase chain reaction (PCR) before its (electrochemical) detection.

Recently, we demonstrated the ability of polyelectrolyte-modified capacitive EIS sensors for the label-free detection of DNA hybridization as well as dsDNA sensing in buffer solutions [18, 37] by their intrinsic negative molecular charge. Such EIS sensor belongs to the simplest field-effect device and can be fabricated without lithography or complex encapsulation, which makes it to a preferable choice as a field-effect sensing platform. In these experiments, positively charged weak polyelectrolyte poly(allylamine hydrochloride) (PAH) was used for sensor modification. Another group has investigated the possibility of detecting PCR-amplified DNA by means of poly-L-lysine (PLL)-functionalized field-effect sensors [38, 39]. Here, the target DNA was amplified by an integrated on-chip microfluidic thermocycler. This approach might, however, face difficulties because of the additional thermal influence on the sensor signal. Moreover, the expected sensor signal might be reduced due to the relatively high ionic strength of the measurement solution.

In this study, EIS sensors modified with PAH and probe ssDNA using the layer-by-layer technique [18, 40–42] were used to detect target oligonucleotide fragments in different PCR-test solutions: The first test solution (hereafter referred to as *artificial PCR solution*) contains all components required for a PCR reaction including synthetic cDNA. The second test solution (hereafter referred to as *real PCR solution*) contains PCR-amplified template DNA, which has been extracted from pathogenic tuberculosis-spiked

human sputum samples. As a control, a third test solution without DNA (hereafter referred to as *PCR-components solution*) has been used to investigate the influence of PCR components onto the sensor signal. The PAH/ssDNA-modified EIS sensors were exposed to the test solutions while electrochemical investigations including capacitance-voltage- (C–V) and constant-capacitance (ConCap) measurements have been carried out in measurement buffer with low-ionic strength. Furthermore, measurements with fluorescence microscopy by using the fluorescence dye SybrGreen I (SG) were performed to verify the electrochemical results.

7.2 EXPERIMENTAL SECTION

7.2.1 Chip fabrication

The used capacitive EIS-sensor chips have been fabricated from a 3 in. p-type silicon wafer (SiMat, Silicon Materials, Kaufering, Germany) with a crystal orientation of ⟨100⟩, resistivity of 1-10 Ωcm, and ∼400 µm thickness. During a dry oxidation process at 1050 °C for 40 min, a 45 nm thick SiO_2 layer has been grown on the complete wafer surface. Then, the rear side of the wafer has been chemically etched with 40% HF (Merck, Darmstadt, Germany) and subsequently coated with a 300 nm thick layer of Al in order to create an Ohmic contact to the semiconductor material, which allows an electrical connection for electrochemical measurements. Afterward, the complete wafer was subdivided into single 10 mm × 10 mm chips resulting in an Al–p-Si–SiO_2 structure. The separated chips were cleaned in a four-solvent cascade of acetone, isopropyl alcohol (both from Technic France, La Plaine Saint Denis, France), ethanol (Merck, Darmstadt, Germany), and deionized (DI) water, provided by a Millipore Super Q water system (Merck, Darmstadt, Germany). The chips were cleaned for 3 min in each solvent in an ultrasonic bath (Bandelin, Berlin, Germany).

7.2.2 Chip modification with PAH and immobilization of probe ssDNA

The modification steps of the sensor chip are shown schematically in **Figure 7.1** (left and right column). The cleaned chips were mounted and fixed into a measurement chamber made from poly(methyl methacrylate). The chips were sealed by a rubber O-ring with an inner diameter of 8 mm. The remaining (active) surface area was therefore ∼0.5 cm^2. In order to modify the SiO_2 surface with PAH, 100 µL of 50 µM PAH (abcr GmbH & Co. KG, Karlsruhe, Germany) solution (diluted in 100 mM NaCl, adjusted with NaOH to pH 5.4) was pipetted onto the oxide surface of the mounted EIS chip. After a 10 min incubation time, the sensor surface was rinsed three times with 0.33 mM phosphate-buffered saline (PBS) solution (pH 7.0, ionic strength of 5 mM), hereafter referred to as measurement solution.

For DNA immobilization, the PAH-modified surface was exposed to probe ssDNA-immobilization solution, which has been prepared by dilution of lyophilized probe ssDNA (with a sequence fragment complementary to DNA of *Mycobacterium avium paratuberculosis*) in DI water to a final concentration of 600 nM. The length and sequences

of all synthetic DNA oligonucleotides (Eurofins Genomics, Ebersberg, Germany) used in this work are presented in **Table 7.1**. 100 µL of the ssDNA immobilization solution was pipetted onto the PAH-modified sensor surface. After an incubation time of 15 min at room temperature, the surface was been rinsed with measurement solution for three times to remove unbound ssDNA molecules.

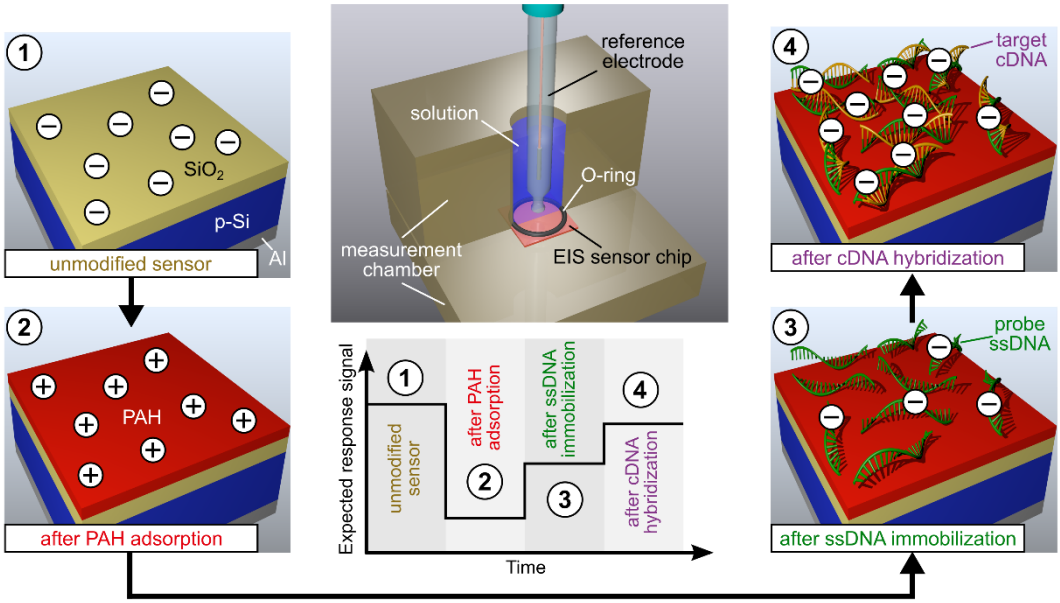

Figure 7.1: Rendered image (middle column, top) of the measurement arrangement. The sensor surface is shown schematically (left and right column): (1) Unmodified sensor, (2) after PAH adsorption, (3) after ssDNA immobilization, (4) after cDNA hybridization; + and – symbols indicate the respective surface charge. The graph (middle column, bottom) represents the expected (ConCap) sensor signal for the surface states (1-4).

Table 7.1: Names, lengths, and sequences of the used single-stranded DNA oligonucleotides.

Name	Length	Sequence
probe ssDNA	52-mer	5′-TGGAT-CGCTG-TGTAA-GGACA-CGTCGGCGTG-GTCGT-CTGCT-GGGTT-GATCT-GG-3′
target cDNA	72-mer	5′-ACCTC-CGTAA-CCGTC-ATTGT-CCAGATCAAC-CCAGC-AGACG-ACCAC-GCCGACGTGT-CCTTA-CACAG-CGATC-CA-3′
reverse primer	20-mer	5′-TGGAT-CGCTG-TGTAA-GGACA-3′
forward primer	20-mer	5′-ACCTC-CGTAA-CCGTC-ATTGT-3′

7.2.3 EIS-sensor exposure to test solutions and electrochemical measurements

The PAH/ssDNA-modified sensors used in this work were exposed to three different test solutions: *artificial PCR solution*, *PCR-components solution*, and *real PCR solution*. The compositions are presented in **Table 7.2**. The *artificial PCR solution* represents a solution containing components after a typical PCR-amplification process, including high concentration of complementary target cDNA. This solution was used for evaluation of hybridization experiments, determination of the sensitivity, and the lower detection limit with the PAH/ssDNA-modified EIS sensors. The *PCR-components solution* contains all required constituents for PCR amplification but without primer, deoxynucleotide triphosphates (dNTPs), and DNA. It was used to determine the background signal. The *real PCR solution* was prepared by diluting the respective components (**Table 7.2**) in DI water and performing a PCR (initial denaturation at 94 °C for 2 min; 40 cycles: 94 °C for 15 s, 56 °C for 30 s, and 68 °C for 45 s; final elongation at 68 °C for 5 min). The template DNA was extracted and isolated from human saliva sample, which has been spiked with *Mycobacterium avium paratuberculosis*. This solution was used to study the capability of detection of amplified DNA fragments (amplicons) with the PAH/ssDNA sensors.

Table 7.2: Composition of test solutions.[1]

Name	Components
artificial PCR solution	▪ 1× OneTaq standard reaction buffer (New England Biolabs GmbH, Frankfurt am Main, Germany); composition: 20 mM Tris(tris(hydroxymethyl)-aminomethane))-HCl, 22 mM KCl, 22 mM NH_4Cl, 1.8 mM $MgCl_2$, 0.06% IGEPAL CA-630 (polyethylene glycoloctylphenol ether), 0.05% Tween 20 (polyoxyethylene (20) sorbitan monolaurate) ▪ 10.42 mkat (0.625 U) Taq polymerase (New England Biolabs GmbH, Frankfurt am Main, Germany) ▪ 0.04% bovine serum albumin (BSA, Sigma-Aldrich, Taufkirchen, Germany) ▪ 600 nM target cDNA
PCR-components solution	▪ 1× OneTaq standard reaction buffer ▪ 10.42 mkat Taq polymerase ▪ 0.04% BSA
real PCR solution (composition before amplification)	▪ 1× OneTaq standard reaction buffer ▪ 10.42 mkat Taq polymerase ▪ 0.04% BSA ▪ 300 nM reverse primer DNA ▪ 300 nM forward primer DNA ▪ 200 µM dNTPs solution (equimolar mix of deoxyadenosine-, deoxycytidine-, deoxyguanosine-, and deoxythymidine-triphosphate, each 50 µM) ▪ 20% extracted and isolated template DNA from human saliva sample, which was spiked with *Mycobacterium avium paratuberculosis*

[1] DI water was used as solvent

100 µL of the respective test solution was pipetted onto the sensors surfaces and incubated for 40 min. Afterward, the surfaces were rinsed three times with measurement solution.

The EIS-sensor chips were electrochemically characterized after each modification or incubation step. For characterization, the chamber has been filled with 1 mL of measurement solution in which a double-junction Ag/AgCl reference electrode (filled with 3 M KCl, Metrohm, Filderstadt, Germany) is immersed. The reference electrode and the rear-side contact of the EIS chip are connected to a Zennium electrochemical workstation (Zahner Elektrik, Kronach, Germany). The electrochemical characterization includes the recording of leakage current (by applied voltage from −3 to +3 V, sweeping rate of 100 mV/s), C–V characteristics (−3 to +3 V, steps of 100 mV), and measurements in ConCap mode, where the capacitance of the sensor system is kept constant by applying a feedback sign-inverted voltage. C–V- and ConCap measurements were performed with a superimposed 120 Hz voltage with 20 mV (peak-to-peak) amplitude. All electrochemical characterization experiments have been done in a Faradaic cage at room temperature. Details for operation of the ConCap-measuring mode are described elsewhere [43, 44]. The mounted sensor chip with measurement chamber as well as the exemplarily expected ConCap-sensor signal before and after each modification step are shown in **Figure 7.1** (middle column).

The pH values of measurement solutions inside the measurement chamber have been additionally controlled with a MPC227 pH Meter (Mettler-Toledo, Gießen, Germany) before and after each electrochemical experiment.

7.2.4 Fluorescence staining

The SG-working solution has been prepared by 1:1000 dilution of SG-stock solution (obtained from Sigma-Aldrich, Taufkirchen, Germany) with DI water. The fluorescence staining was carried out by pipetting 100 µL of SG-working solution onto the EIS-sensor surface. After 40 min of incubation time, the unbound SG molecules were removed by rinsing the sensor surface with measurement solution three times and dried with nitrogen gas. The fluorescence images of the dried surfaces have been taken with an Axio Imager A1m fluorescence microscope (Zeiss, Jena, Germany).

7.3 RESULTS AND DISCUSSION

7.3.1 Electrical detection of DNA immobilization and hybridization with capacitive EIS sensors

The leakage current of all used sensor chips was measured to verify the SiO_2 quality. Sensors with a leakage current of more than 20 nA were sorted out and not used for further experiments.

As an example, **Figure 7.2** shows results of a C–V- (a) and a ConCap (b) measurement of an unmodified sensor chip, after PAH adsorption, after immobilization with probe ssDNA, and after incubation in *artificial PCR solution*. Each C–V curve shows a

characteristic sigmoidal-like shape with an accumulation (less than −1 V), depletion (between −1 V and ~0.5 V), and inversion (more than ~0.5 V) region. By comparing the respective C–V curves, within the depletion region, a shift along the voltage axis of −121 mV after the modification with PAH is noticeable. PAH is known as a weak polyelectrolyte with an isoelectric point between pH 10 and pH 11 [45, 46]. The pH of the measurement solution was 7.0; therefore, the PAH molecules are positively charged, which allows the electrostatic adsorption of PAH to the negatively charged SiO_2 surface. The PAH adsorption leads to a change of the surface potential that results in a shift of the C–V curve in the direction of more negative potential.

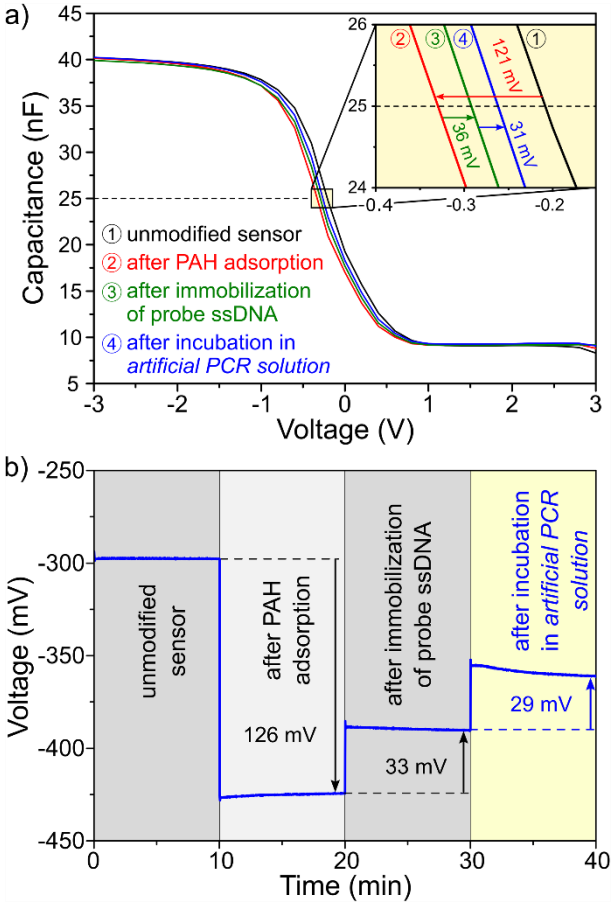

Figure 7.2: C–V- (a) and ConCap (b) response of an EIS sensor, recorded before and after adsorption of PAH, after probe ssDNA immobilization, and after incubation in *artificial PCR solution*. The dashed line in (a) indicates the chosen working point at 25 nF for ConCap measurements in (b). Distinct signal shifts after each modification step can be seen.

The recorded signal shift is in good correlation with previous studies on PAH modification of field-effect devices with a SiO_2 surface [7, 29, 47, 48]. A shift of the C–V curve of +36 mV could be identified after the exposure of the sensor to probe ssDNA solution. This shift is also caused by a surface-potential change; it is induced by immobilization of negatively charged probe ssDNA molecules onto the PAH-modified

SiO_2 surface. The following shift of +31 mV was observed after incubation in *artificial PCR solution*, containing 600 nM of target cDNA. The target cDNA molecules hybridize with the probe ssDNA during the incubation and lead to a further increase of negative charge at the surface, which results in the observed C–V-curve shift.

Besides C–V measurements, investigations by means of ConCap-signal recording have also been performed during the experiment. The working point for ConCap measurements has been chosen from the depletion region of the recorded C–V curve and was set to 25 nF. The ConCap-recording time after each modification step was 10 min. Similar to the signal shifts of C–V curves, three potential changes were observed during the ConCap experiment: The signal drops by −126 mV after adsorption of PAH and increases by +33 mV after immobilization of probe ssDNA and again by +29 mV after incubation in *artificial PCR solution*. Averaged values of five sensors were −99 mV ± 17 mV, +38 mV ± 7 mV, and +32 mV ± 8 mV for PAH adsorption, probe ssDNA immobilization, and cDNA hybridization, respectively. These voltage changes are in good correlation to the recorded shifts of C–V measurements within the depletion region and serve also as an evidence for surface-potential changes induced by adsorption of PAH and ssDNA as well as hybridization of target cDNA molecules.

In additional experiments, the sensitivity and lower detection limit of the PAH/ssDNA-modified EIS chips for cDNA have been studied. In order to evaluate these parameters, a series of *artificial PCR solutions* with different target cDNA concentrations (from 1 nM to 5 µM) was exposed to the sensor chips. The solutions have been applied to the PAH/ssDNA-modified EIS chips for 40 min in order of increasing concentrations, each step followed by surface washing with measurement solution and ConCap-signal recording. This procedure has been repeated for each concentration. **Figure 7.3a** shows the ConCap signal of an EIS-sensor chip after surface-modification steps with PAH and probe ssDNA and after incubation in *artificial PCR solutions* containing different concentrations of a 72-mer target cDNA. A clear dependence between the signal amplitude and the cDNA concentration has been observed. The signal change was 12 mV for a target cDNA concentration of 1 nM and increases up to 39 mV after incubation of *artificial PCR solution* with 5 µM cDNA. Plotting the amplitude values versus the respective cDNA concentrations results in a calibration curve (**Figure 7.3b**) from which the sensitivity was estimated to be ∼7.2 mV/decade. The curve depicts a logarithmic behavior of the sensor signal as a function of the target cDNA concentration. The averaged background signal for three EIS sensors in *PCR-components solution* was 3 mV ± 1.4 mV. The lower detection limit was evaluated according to Shrivastava and Gupta [49] by the intersection between the calibration curve and the mean background signal plus 3-fold background standard deviation. The estimated lower detection limit was ∼0.3 nM. In comparison to other works with planar FET and EIS sensors, the obtained values for sensitivity and lower detection limit are similar for this concentration range [50].

The amplification of one single-template DNA molecule, which could be extracted, for instance, from a human sputum sample, requires a minimum of 34 amplification cycles to generate a concentration of >0.3 nM target cDNA in a sample volume of 50 µL (50 µL is enough to cover the whole sensor surface during incubation in target solution). Therefore, the developed sensing device might be able to detect amplified oligonucleotides from one single-template DNA under ideal conditions with a standard PCR technique.

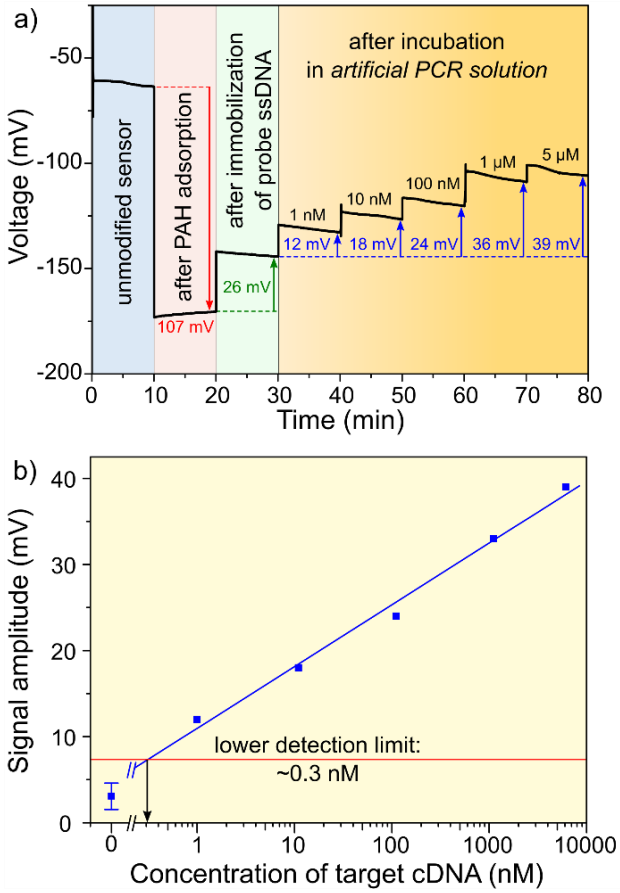

Figure 7.3: ConCap response of an EIS sensor exposed to *artificial PCR solution* with different concentrations from 1 nM to 5 µM (a). Calibration curve with lower detection-limit (b).

7.3.2 Influence of PCR components on the sensor signal

In order to evaluate a possible interaction of PCR components with the PAH/ssDNA-modified EIS-sensor surface and, therefore, an influence onto the sensor signal, an additional experiment has been performed in which a PAH/ssDNA-modified EIS chip has been exposed to *PCR-components solution*. **Figure 7.4** overviews a recorded ConCap signal of this experiment. The signal changes after PAH adsorption and probe ssDNA immobilization were −103 and +37 mV, while only a small signal change of +5 mV was recorded after the incubation of the *PCR-components solution*. Since the *PCR-components solution* contains no target cDNA molecules, no hybridization can occur at the chip surface. The small signal change might be induced because of minor interaction of the PCR components with the modified sensor surface. In comparison to the results obtained with *artificial PCR solution* (containing target cDNA molecules), which is shown in **Figure 7.2**, a six times lower signal was measured in this experiment.

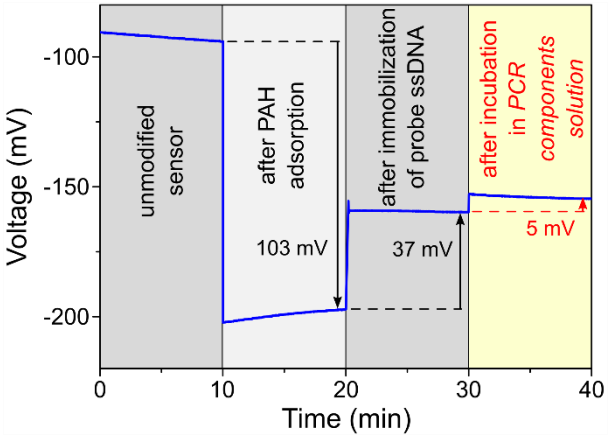

Figure 7.4: ConCap response of an EIS sensor, recorded before and after adsorption of PAH, after probe ssDNA immobilization, and after incubation in *PCR-components solution*.

7.3.3 Detection of amplified target DNA in *real PCR solution*

In order to test the developed sensor device under more realistic conditions, the PAH/ssDNA-modified sensors were incubated in *real PCR solutions*, containing amplified DNA fragments with a sequence of *Mycobacterium tuberculosis* genome. The World Health Organization announced that in 2016 about 10.4 million people fell ill with tuberculosis disease. Due to the high mortality rate, tuberculosis is the ninth leading cause of death worldwide and the leading cause from a single-infectious agent, ranking above HIV/AIDS [51]. The detection of tuberculosis mycobacteria in human individuals is of great interest for the respective treatment.

The amplicons have a complementary sequence to the immobilized oligonucleotides, which allows hybridization of the molecules. **Figure 7.5** shows the recorded ConCap response of a sensor which was exposed to *real PCR solution* with amplified target DNA (40 cycles). Before electrochemical measurements, the tube that contains 50 µL of *real PCR solution* was heated up to 95 °C for 2 min in order to denature the amplicons followed by a rapid cooling step, where the tube was placed immediately into an ice bath for approximately 20 s until the solution temperature reached room temperature. This so-called rapid cooling procedure has been carried out in order to keep the amplicons in single-stranded form. After the incubation time of 40 min and three washing steps, the ConCap signal was determined in measurement solution.

A ConCap signal increase of +41 mV was recorded after the incubation in *real PCR solution*. These experiments demonstrate the ability of label-free detection of the hybridization of PCR-amplified DNA with PAH/ssDNA-modified EIS sensors.

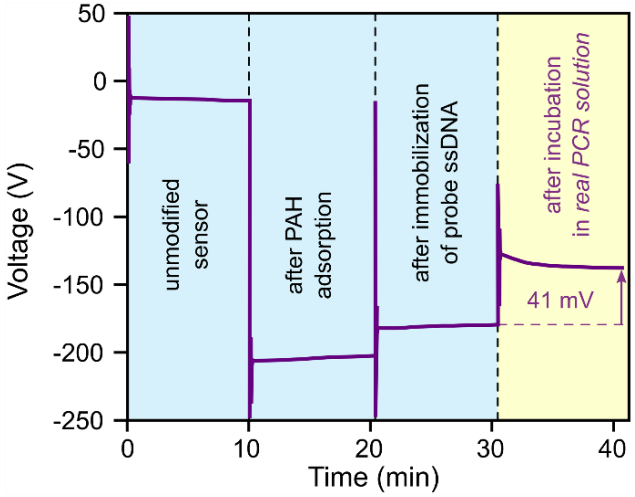

Figure 7.5: ConCap response of a PAH- and ssDNA-modified EIS sensor after incubation in *real PCR solution* containing DNA, which has been extracted from tuberculosis-spiked sputum samples and amplified by 40 cycles.

7.3.4 Fluorescence measurements of EIS-sensor surfaces

In order to verify the results of electrochemical experiments, investigations by means of fluorescence microscopy have been performed. The used fluorescence dye was SG, which is well-known to increase its fluorescence intensity dramatically by binding with dsDNA [52–55]. For fluorescence experiments, surfaces of EIS-sensor chips, which were incubated in different test solutions, were exposed to SG-working solution for staining. The recorded fluorescence images of the dry sensor surfaces are presented in **Figure 7.6**. The first image (a) serves as a control, it was taken from a PAH/ssDNA-modified sensor without incubation in the test solution. Almost no fluorescence signal was observed. In contrast, a strong and bright fluorescence image was recorded of a PAH/ssDNA-modified surface, which has been exposed to *artificial PCR solution* (**Figure 7.6b**).

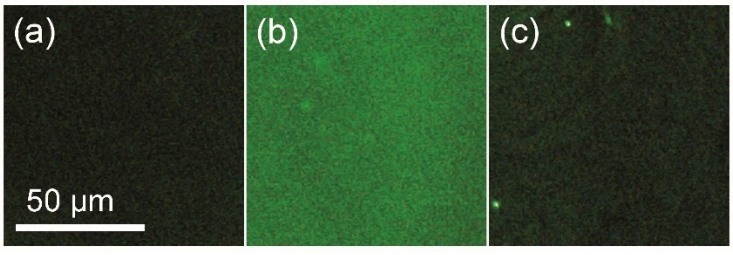

Figure 7.6: Fluorescence images of three PAH/ssDNA-EIS chip surfaces: (a) After immobilization of ssDNA, (b) after incubation in *artificial PCR solution*, and (c) after incubation in *PCR-components solution*.

The high fluorescence signal indicates that dsDNA molecules are present on the chip surface. The dsDNA molecules are formed by hybridization of target cDNA molecules of *artificial PCR solution* with the immobilized ssDNA molecules. Another fluorescence

image has been taken of a PAH/ssDNA-modified sensor, which has been incubated in *PCR-components solution* (**Figure 7.6c**). A very weak fluorescence signal was observed that is comparable to the signal in **Figure 7.6a**. Since the *PCR-components solution* contains no cDNA, only ssDNA is present on the sensor surface. Thus, the observations made by fluorescence measurements support the results of electrochemical experiments.

7.4 CONCLUSIONS

The label-free detection of target oligonucleotides in different test solutions, *artificial PCR solution* and *real PCR solution*, has been realized by the use of field-effect-based EIS sensors. In order to evaluate the influence of PCR components onto the sensor signal, additional experiments with *PCR-components solution* have been carried out. The charge-sensitive EIS sensors have been modified with a layer of positively charged PAH- and probe ssDNA molecules prior to the incubation in test solutions. Electrochemical investigations by means of C–V- and ConCap measurements were used to monitor the signal changes after each modification step. The electrochemical results show clear signal changes and a shift of +32 ± 8 mV after incubation in *artificial PCR solution* containing 600 nM of target cDNA, while only a small signal shift of 5 mV was measured after incubation in *PCR-components solution* without target cDNA. The experiments demonstrate the possibility of the detection of target cDNA in PCR solution. The sensitivity as well as the lower detection limit were determined to be ∼7.2 mV/decade and ∼0.3 nM, respectively. Investigations by means of fluorescence staining with the dye SG prove the on-chip hybridization after exposing the sensor surface to test solution containing target cDNA and verify the electrochemical results.

The final tests for detecting a hybridization event of genomic tuberculosis target DNA were carried out by incubation of PAH/ssDNA-modified sensors in *real PCR solution*. The template DNA of this solution was extracted from *Mycobacterium tuberculosis*-spiked human sputum and amplified by PCR. A sensor signal of 41 mV demonstrates the successful detection of the genomic DNA extracted from human sputum samples, which has been spiked with tuberculosis bacteria.

The developed capacitive EIS chip can serve as a fast, digital sensing device for providing a logical yes/no answer to a successful/unsuccessful PCR process. Further experiments will focus on testing samples obtained from infected individuals; moreover, the influences of DNA length and sequence as well as investigation of reusability of the sensors will be studied.

ACKNOWLEDGEMENTS

The authors thank T. Weinand and C. Metzger-Boddien (gerbion GmbH & Co. KG, Kornwestheim, Germany) for providing *real PCR solutions* and C.S. Wu for valuable discussion and technical support. The authors gratefully acknowledge the financial support from the German Federal Ministry of Education and Research (BMBF, DiaCharge project 031A192D).

REFERENCES

[1] P. Bergveld: *Development of an ion sensitive solid state device for neurophysiological measurements*, IEEE Trans. Biomed. Eng. 17 (1970) 70–71.

[2] J.C. Owicki, L.J. Bousse, D.G. Hafeman, G.L. Kirk, J.D. Olson, H.G. Wada, J.W. Parce: *The light-addressable potentiometric sensor: Principles and biological applications*, Annu. Rev. Biophys. Biomol. Struct. 23 (1994) 87–113.

[3] T. Yoshinobu, K. Miyamoto, T. Wagner, M.J. Schöning: *Recent developments of chemical imaging sensor systems based on the principle of the light-addressable potentiometric sensor*, Sens. Actuators B 207 (2015) 926–932.

[4] T. Yoshinobu, K. Miyamoto, C.F. Werner, A. Poghossian, T. Wagner, M.J. Schöning: *Light-addressable potentiometric sensors for quantitative spatial imaging of chemical species*, Annu. Rev. Anal. Chem. 10 (2017) 225–246.

[5] T. Bronder, C.S. Wu, A. Poghossian, C.F. Werner, M. Keusgen, M.J. Schöning: *Label-free detection of DNA hybridization with light-addressable potentiometric sensors: Comparison of various DNA-immobilization strategies*, Procedia Eng. 87 (2014) 755–758.

[6] A. Seki, S.I. Ikeda, I. Kubo, I. Karube: *Biosensors based on light-addressable potentiometric sensors for urea, penicillin and glucose*, Anal. Chim. Acta 373 (1998) 9–13.

[7] J. Wang, Y. Zhou, M. Watkinson, J. Gautrot, S. Krause: *High-sensitivity light-addressable potentiometric sensors using silicon on sapphire functionalized with self-assembled organic monolayers*, Sens. Actuators B 209 (2015) 230–236.

[8] Z. Li, Y. Chen, X. Li, T.I. Kamins, K. Nauka, R.S. Williams: *Sequence-specific label-free DNA sensors based on silicon nanowires*, Nano Lett. 4 (2004) 245–247.

[9] P. Namdari, H. Daraee, A. Eatemadi: *Recent advances in silicon nanowire biosensors: Synthesis methods, properties, and applications*, Nanoscale Res. Lett. 11 (2016) 406–422.

[10] F. Patolsky, G. Zheng, C.M. Lieber: *Nanowire-based biosensors*, Anal. Chem. 78 (2006) 4260–4269.

[11] G.J. Zhang, Y. Ning: *Silicon nanowire biosensor and its applications in disease diagnostics: A review*, Anal. Chim. Acta 749 (2012) 1–15.

[12] Y. Zhang, R. Chen, L. Xu, Y. Ning, S. Xie, G.J. Zhang: *Silicon nanowire biosensor for highly sensitive and multiplexed detection of oral squamous cell carcinoma biomarkers in saliva*, Anal. Sci. 31 (2015) 73–78.

[13] Y.G. Vlasov, Y.A. Tarantov, P.V. Bobrov: *Analytical characteristics and sensitivity mechanisms of electrolyte-insulator-semiconductor system-based chemical sensors – a critical review*, Anal. Bioanal. Chem. 376 (2003) 788–796.

[14] M.J. Schöning, A. Poghossian: *Bio FEDs (field-effect devices): State-of-the-art and new directions*, Electroanal. 18 (2006) 1893–1900.

[15] M. Beyer, C. Menzel, R. Quack, T. Scheper, K. Schügerl, W. Treichel, H. Voigt, M. Ullrich, R. Ferretti: *Development and application of a new enzyme sensor type based on the EIS-capacitance structure for bioprocess control*, Biosens. Bioelectron. 9 (1994) 17–21.

[16] J. García-Cantón, A. Merlos, A. Baldi: *A wireless LC chemical sensor based on a high quality factor EIS capacitor*, Sens. Actuators B 126 (2007) 648–654.

[17] C. Menzel, T. Lerch, T. Scheper, K. Schügerl: *Development of biosensors based on an electrolyte isolator semiconductor (EIS) -capacitor structure and their application for process monitoring. Part I. Development of the biosensors and their characterization*, Anal. Chim. Acta 317 (1995) 259–264.

[18] T.S. Bronder, A. Poghossian, M. Keusgen, M.J. Schöning: *Label-free detection of double-stranded DNA molecules with polyelectrolyte-modified capacitive field-effect sensors*, Tech. Mess. 84 (2017) 628–634.

[19] T.M. Pan, C.Y. Chen, T.Y. Wu, S.T. Pang: *Impact of postdeposition annealing on the sensing and impedance characteristics of TbY_xO_y electrolyte–insulator–semiconductor pH sensors*, RSC Adv. 6 (2016) 76673–76678.

[20] M.J. Schöning, A. Kurowski, M. Thust, P. Kordos, J.W. Schultze, H. Lüth: *Capacitive microsensors for biochemical sensing based on porous silicon technology*, Sens. Actuators B 64 (2000) 59–64.

[21] C.H. Kao, H. Chen, M.L. Lee, C.C. Liu, H.Y. Ueng, Y.C. Chu, Y.J. Chen, K.M. Chang: *Multianalyte biosensor based on pH-sensitive ZnO electrolyte–insulator–semiconductor structures*, Appl. Phys. 115 (2014) 184701-1–6.

[22] J.Y. Oh, H.J. Jang, W.J. Cho, M.S. Islam: *Highly sensitive electrolyte-insulator-semiconductor pH sensors enabled by silicon nanowires with Al_2O_3/SiO_2 sensing membrane*, Sens. Actuators B 171–172 (2012) 238–243.

[23] T.M. Pan, M.D. Huang, W.Y. Lin, M.H. Wu: *A urea biosensor based on pH-sensitive Sm_2TiO_5 electrolyte–insulator–semiconductor*, Anal. Chim. Acta 669 (2010) 68–74.

[24] J.R. Siqueira, M.H. Abouzar, A. Poghossian, V. Zucolotto, O.N. Oliveira, M.J. Schöning: *Penicillin biosensor based on a capacitive field-effect structure functionalized with a dendrimer/carbon nanotube multilayer*, Biosens. Bioelectron. 25 (2009) 497–501.

[25] M.J. Schöning: *"Playing around" with field-effect sensors on the basis of EIS structures, LAPS and ISFETs*, Sensors 5 (2005) 126–138.

[26] T.M. Pan, J.C. Lin, M.H. Wu, C.S. Lai: *Structural properties and sensing performance of high-k Nd_2TiO_5 thin layer-based electrolyte–insulator–semiconductor for pH detection and urea biosensing*, Biosens. Bioelectron. 24 (2009) 2864–2870.

[27] R. Chand, D. Han, Y. Kim: *Rapid detection of protein kinase on capacitive sensing platforms*, IEEE T. Nanobiosci. 15 (2016) 843–848.

[28] M.H. Abouzar, A. Poghossian, A.G. Cherstvy, A.M. Pedraza, S. Ingebrandt, M.J. Schöning: *Label-free electrical detection of DNA by means of field-effect nanoplate capacitors: Experiments and modeling*, Phys. Status Solidi A 209 (2012) 925–934.

[29] A. Poghossian, M.H. Abouzar, M. Sakkari, T. Kassab, Y. Han, S. Ingebrandt, A. Offenhäusser, M.J. Schöning: *Field-effect sensors for monitoring the layer-by-layer adsorption of charged macromolecules*, Sens. Actuators B 118 (2006) 163–170.

[30] J.C. Liao, M. Mastali, V. Gau, M.A. Suchard, A.K. Møller, D.A. Bruckner, J.T. Babbitt, Y. Li, J. Gornbein, E.M. Landaw, E.R.B. McCabe, B.M. Churchill, D.A. Haake: *Use of electrochemical DNA biosensors for rapid molecular identification of uropathogens in clinical urine specimens*, J. Clin. Microbiol. 44 (2006) 561–570.

[31] W. Ittarat, S. Chomean, C. Sanchomphu, N. Wangmaung, C. Promptmas, W. Ngrenngarmlert: *Biosensor as a molecular malaria differential diagnosis*, Clin. Chim. Acta 419 (2013) 47–51.

[32] J. Gray, L.J. Coupland: *The increasing application of multiplex nucleic acid detection tests to the diagnosis of syndromic infections*, Epidemiol. Infect. 142 (2013) 1–11.

[33] R. Sosnowski, M.J. Heller, E. Tu, A.H. Forster, R. Radtkey: *Active microelectronic array system for DNA hybridization, genotyping and pharmacogenomic applications*, Psychiatr. Genet. 12 (2002) 181–192.

[34] R.L. Edelstein, C.R. Tamanaha, P.E. Sheehan, M.M. Miller, D.R. Baselt, L.J. Whitman, R.J. Colton: *The BARC biosensor applied to the detection of biological warfare agents*, Biosens. Bioelectron. 14 (2000) 805–813.

[35] D.L. Morris: *DNA-bound metal ions: Recent developments*, Biomol. Concepts 5 (2014) 397–407.

[36] M.R. Green, J. Sambrook: *Precipitation of DNA with ethanol*, Cold Spring Harb. Protoc. 2016 (2016) 1116–1120.

[37] T.S. Bronder, A. Poghossian, S. Scheja, C. Wu, M. Keusgen, D. Mewes, M.J. Schöning: *DNA immobilization and hybridization detection by the intrinsic molecular charge using capacitive field-effect sensors modified with a charged weak polyelectrolyte layer*, ACS Appl. Mater. Interfaces 7 (2015) 20068–20075.

[38] C.S.J. Hou, N. Milovic, M. Godin, P.R. Russo, R. Chakrabarti, S.R. Manalis: *Label-free microelectronic PCR quantification*, Anal. Chem. 78 (2006) 2526–2531.

[39] C.S.J. Hou, M. Godin, K. Payer, R. Chakrabarti, S.R. Manalis: *Integrated microelectronic device for label-free nucleic acid amplification and detection*, Lab Chip 7 (2007) 347–354.

[40] T.S. Bronder, A. Poghossian, S. Scheja, C.S. Wu, M. Keusgen, M.J. Schöning: *Electrostatic detection of unlabelled single- and double-stranded DNA using capacitive field-effect devices functionalized with a positively charged polyelectrolyte layer*, Procedia Eng. 120 (2015) 544–547.

[41] J. Fritz, E.B. Cooper, S. Gaudet, P.K. Sorger, S.R. Manalis: *Electronic detection of DNA by its intrinsic molecular charge*, Proc. Natl. Acad. Sci. U.S.A. 99 (2002) 14142–14126.

[42] M.H. Abouzar, A. Poghossian, J.R. Siqueira, O.N. Oliveira, W. Moritz, M.J. Schöning: *Capacitive electrolyte–insulator–semiconductor structures functionalised with a polyelectrolyte/enzyme multilayer: New strategy for enhanced field-effect biosensing*, Phys. Status Solidi A 207 (2010) 884–890.

[43] A. Poghossian, M. Weil, A.G. Cherstvy, M.J. Schöning: *Electrical monitoring of polyelectrolyte multilayer formation by means of capacitive field-effect devices*, Anal. Bioanal. Chem. 405 (2013) 6425–6436.

[44] J. Arreola, M. Keusgen, M.J. Schöning: *Effect of O_2 plasma on properties of electrolyte-insulator-semiconductor structures*, Phys. Status Solidi A 214 (2017) 1700025.

[45] M. Morga, Z. Adamczyk: *Monolayers of cationic polyelectrolytes on mica – electrokinetic studies*, J. Colloid Interface Sci. 407 (2013) 196–204.

[46] B. Jachimska, T. Jasiński, P. Warszyński, Z. Adamczyk: *Conformations of poly(allylamine hydrochloride) in electrolyte solutions: Experimental measurements and theoretical modeling*, Colloids Surf. A 355 (2010) 7–15.

[47] M.J. Schöning, M.H. Abouzar, A. Poghossian: *pH and ion sensitivity of a field-effect EIS (electrolyte-insulator-semiconductor) sensor covered with polyelectrolyte multilayers*, J. Solid State Electrochem. 13 (2009) 115–122.

[48] C. Wu, A. Poghossian, T.S. Bronder, M.J. Schöning: *Sensing of double-stranded DNA molecules by their intrinsic molecular charge using the light-addressable potentiometric sensor*, Sens. Actuators B 229 (2016) 506–512.

[49] A. Shrivastava, V.B. Gupta: *Methods for the determination of limit of detection and limit of quantitation of the analytical methods*, Chronicles Young Sci. 2 (2011) 21–25.

[50] C. Kataoka-Hamai, Y. Miyahara: *Label-free detection of DNA by field-effect devices*, IEEE Sens. J. 11 (2011) 3153–3160.

[51] World Health Organization: *Global Tuberculosis Report 2017*, WHO: Geneva (2017).

[52] G. Cosa, K.S. Focsaneanu, J.R.N. McLean, J.P. McNamee, J.C. Scaiano: *Photophysical properties of fluorescent DNA-dyes bound to single- and double-stranded DNA in aqueous buffered solution*, Photochem. Photobiol. 73 (2001) 585–599.

[53] H. Zipper, C. Buta, K. Lämmle, H. Brunner, J. Bernhagen, F. Vitzthum: *Mechanisms underlying the impact of humic acids on DNA quantification by SYBR Green I and consequences for the analysis of soils and aquatic sediments*, Nucleic Acids Res. 31 (2003) e39-1–16.

[54] H. Zipper, H. Brunner, J. Bernhagen, F. Vitzthum: *Investigations on DNA intercalation and surface binding by SYBR Green I, its structure determination and methodological implications*, Nucleic Acids Res. 32 (2004) e103-1–10.

[55] A.I. Dragan, R. Pavlovic, J.B. McGivney, J.R. Casas-Finet, E.S. Bishop, R.J. Strouse, M.A. Schenerman, C.D. Geddes: *SYBR Green I: Fluorescence properties and interaction with DNA*, J. Fluoresc. 22 (2012) 1189–1199.

8 Concluding remarks and perspectives

This work describes the development of a label-free DNA-detection principle which relies on electrochemical measurements with capacitive field-effect sensor chips. In the five presented publications (**Chapter 3** to **Chapter 7**), EIS (and LAPS) sensors were surface-modified using PAH polyelectrolyte so that DNA can adsorptively bind onto the treated surfaces. The technique allows the electrochemical detection of DNA based on sensing of a surface-potential change caused by the presence of the intrinsic negative charges of the bound DNA. Immobilization of ssDNA or dsDNA is possible to detect as well as hybridization between target DNA and previously immobilized probe DNA. The following part describes the main conclusions of each publication and put them into context. Moreover, possible fields of application for the obtained results and developed protocols are pointed out. Advantages and drawbacks of the investigated method are compared with currently using DNA-detection techniques. Finally, potential perspectives, ideas and future visions on what is possible with the developed device and the gained achievements are discussed.

8.1 CONCLUDING REMARKS

The two general aims of the experiments, presented in **Chapter 3**, were: First, to develop a surface-modification protocol for EIS sensors in order to establish a fundamental method for successful DNA immobilization, and second, to validate the chosen read-out and DNA detection principle to verify the successful immobilization. An important factor was, that the protocol fulfills the requirements on a quick, easy and cheap realization of DNA detection. In these initial experiments, the focus relies on dsDNA immobilization.

Prior of choosing a proper modification protocol, a suitable detection platform was selected concerning similar requirements: Easy and cheap to fabricate, simple and convenient to readout. Moreover, the platform should inhere sensing parameters, like high sensitivity, sufficient detection limit and be able for reuse. Besides other types of field-effect sensors, EIS sensors are the most advantageous representatives of this sensor category because of their beneficial attributes concerning fabrication effort and costs. EIS sensors can be manufactured in large quantity from whole wafers and represent the simplest type of field-effect devices; lithography steps for structuring the metal layer including photoresist coating, etching (except of the rear-side oxide), lift-off processes, etc. are not necessary for fabrication. The EIS sensors in this work consist of a silicon substrate, which has been only modified with a thin layer of SiO_2 by a dry oxidation process and a rear-side metal contact for connectivity. The use of additional oxidation layers, like Ta_2O_5 or Al_2O_3, was avoided to maintain the fabrication procedure as easy and as fast as possible.

In order to operate the EIS sensing-setup, a high-Ohmic impedance analyzer, a reference electrode, respective connection cables, the EIS chip itself and a suitable (measurement) chamber is required. The measurement principle of the EIS setup allows the calculation of the sensor capacitance from the obtained impedance values. The change of the sensor

capacitance can serve as an indicator for surface-potential changes. Such changes occur, when DNA has been bound to the surface.

In **Chapter 3**, C–V- and ConCap curves before and after surface modification with PAH and immobilization with dsDNA are shown and investigated. PAH was selected as polyelectrolyte for surface modification because of its excellent physical (high charge density, (chemical) stability, long shelf-life (e.g., for storage), etc.) and moderate harmful properties [1]. The experimental data prove the successful PAH modification and the DNA-immobilization process. In order to verify the electrochemical results and exclude errors in the measurement, fluorescence experiments have been carried out, too. For this purpose, SG as a fluorescence dye was chosen to detect the dsDNA molecules. SG binds to dsDNA mainly in an intercalative manner [2]. Although, SG is not specific to the dsDNA sequence, its enormous brightness intensity increases (factor >1000) upon binding to dsDNA and makes it to a favorable indicator.

The results of electrochemical (and fluorescence) experiments could clearly demonstrate that the developed protocol is suitable for the binding of double-stranded DNA onto oxide surfaces of EIS-sensor chips. In addition, measuring of the C–V- and ConCap signal with EIS-sensor chips represents a valid method for indicating the dsDNA-binding event.

The detection of adsorbed dsDNA onto a layer of PAH has also been tested using LAPS chips, which are structurally (nearly) identical to EIS sensors. The results of these experiments are presented in **Chapter 4**. Both, EIS- and LAPS chips, are also based on the same physical signal-generation principle: A capacitance change, which is induced by a surface-potential change inside the semiconductor, can be electronically read out. Therefore, both methods are well comparable.

Firstly, the LAPS chips were characterized in terms of leakage-current measurements. This has been done in order to validate the oxide quality and to ensure comparable signals to the previously performed measurements with EIS chips. The oxide layer of SiO_2 was 60 nm in thickness and therefore similar to the layer thickness used for EIS sensors previously (it was 50 nm). The measured leakage currents of the LAPS chips were comparable to the values measured for EIS sensors (a few nA). The used protocol including PAH adsorption and surface modification with DNA has been slightly adjusted. The change was an extension of the DNA sequences from previously 20 bp to 52 bp and 72 bp for probe ssDNA and target cDNA, respectively. This change has been done because of the following reason: Detectable DNA material is usually amplified by a PCR reaction; this requires a sequence, which contains a part for binding to the primer sequence (short sequence of 20 bp). Therefore, the amplified sequence must be longer than 20 bp. A length of 72 bp for target DNA ensures enough “genetic code” (32 bp) for specific binding of primers to both ends (each primer has 20 bp) and remains also enough for specific hybridization. Much shorter sequence parts than 32 bp could not guarantee a cross-sensitivity and specifity with other DNA material.

Recorded I–V curves show a sigmoidal-like shaped signal, which is in good accordance to the results obtained from EIS sensors. A clear potential shift after PAH binding as well as after dsDNA immobilization could be successfully detected. The binding of both, PAH and DNA, has been checked by means of AFM measurements as a reference method. The

surface roughness of the scanned chips has been increased after PAH- and DNA binding, which serves as indication for verification of the electrochemical results. In order to get a better insight into the sensitivity, a concentration range starting from 0.1 nM to 5 µM target cDNA has been recorded with the LAPS. A linear dependence of the LAPS signal from target cDNA concentration could be observed, moreover, a lower detection limit down to be about 0.1 nM dsDNA was determined. The detection limit is of huge relevance for the future application of the used method. Since the acquired (genomic) target DNA must be amplified by means of PCR, the number of amplification cycles are i) in direct correlation with the required preparation time and ii) somehow limited, thus the amount of output material is limited, too. The lower the detection limit of the used method, the less amplification cycles are required to generate enough material for detection. With a lower detection limit of 0.1 nM, a PCR reaction can be shortened to get a faster preparation time and even for low DNA-starting concentrations, enough material is generated for detection. As an example, a single DNA strand needs to be amplified only by 31 cycles to achieve a concentration >0.1 nM (precise: 0.14 nM, extraction volume of 25 µL).

For all experiments in **Chapter 4**, a multi-spot LAPS (with 16 spots)-sensing platform was chosen. The major feature of LAPS is the ability to perform surface potential-change measurements in a spatially resolved way. This feature – especially in combination with DNA measurements – leads to particular advantages:

- A spatially resolved read out of a multi-spot LAPS allows a measurement of multiple analyte solutions nearly at the same time. For this, the sensor surface needs to be separated into single chambers (e.g., by microfluidics) in which the different analyte solutions are introduced in. Although the total measurement time is not reduced, because it is mainly defined by the modification and read-out protocol, however, the total number of analyzed test solutions can be increased according to the number of chambers used per chip. A multi-spot LAPS can read out the individual spots with a high frequency, thus, all spots are detected (nearly) simultaneously. A simultaneous measurement of 16 spots (or more) is possible with one single LAPS chip.

- The sensor surface of the LAPS chip can be modified spot-by-spot (e.g., realized by micro-spotting) with different kinds of DNA molecules, so that a single target DNA from a solution can interact and be tested with a variety of different probe DNA molecules. This procedure is limited by the size of the spot, which is determined, on the one hand, by the size of the illuminated area of the light source, and on the other hand, by the area of immobilized DNA.
  The type of immobilized probe DNA can be very diverse: Probe DNA molecules with same base-pair length and difference sequence or same sequence and different length can be immobilized in order to investigate the selectivity or the hybridization efficiency of this method. No additional microfluidic system is required here.

All in all, the results of the performed experiments with LAPS, which were modified with the previously developed PAH/DNA-binding protocol, showed that LAPS might be a

promising platform for the DNA detection with the used method. Nonetheless, working with LAPS chips requires a more complex measurement setup due to the light sources (LEDs) and additional (electronic) components such as the LED driver and a special controller for the FFT, when compared to EIS sensors.

In the previous chapters, experiments were carried out in which only the immobilization of dsDNA molecules onto a PAH-modified sensor surface was detected but not the hybridization event itself. Although the detection of DNA immobilization on PAH-modified EIS chips can reveal the general presence of DNA in an analyte solution and can be useful as an indicator for the successfulness of a PCR reaction, this process might be too unspecific: No information about the DNA sequence is gained by this procedure. Therefore, distinguishing the origin of the detected DNA by simple immobilization, whether the DNA is, e.g., from human or a bacterium is not possible.

One way (and most probably the simplest and easiest way) of getting information about the DNA sequence is the monitoring of an (on-chip)-hybridization reaction. This was accomplished in **Chapter 5** by using EIS chips that were modified with a LbL-adsorbed PAH/ssDNA bilayer and afterwards incubated in cDNA target-solution for detection of the hybridization event. The hybridization detection gives information about the complementarity between the immobilized (known) sequence and the (unknown) sequence to be detected. These information serves as an evidence for the origin of the target cDNA and could therefore later used to indicate, e.g., a potential infection of an organism.

The results from the performed C–V- and ConCap measurements show a signal shift after applying the cDNA to the chip surface after probe ssDNA immobilization. This shift underlines that a hybridization event occurred after the immobilization step. Prior to the hybridization step, the utilized protocol was also supplemented with a blocking step with BSA. To get a better comparability between the DNA-detection results with EIS sensors showed in **Chapter 3**, the DNA sequences were reduced from the previously chosen 52-mer and 72-mer to 20-mer for both probe ssDNA and target cDNA, again. TE buffer was chosen as buffer solution, which is known for its stabilizing and DNase-inhibiting properties. The blocking step with BSA should guarantee that target cDNA molecules effectively hybridize because of preventing of non-specific binding to minor ssDNA-uncovered regions on the PAH layer. An unspecific binding would result in a surface-potential increase towards the same direction (towards negative potential) as for a hybridization reaction. This signal could be misunderstood/interpreted as false hybridization.

Besides the monitoring of the hybridization reaction, the specifity of the sensor was investigated. For this, the sensor surface was exposed to ncDNA solution prior to the hybridization step. The measured signals recorded after cDNA hybridization and after ncDNA incubation differ by a factor >10. This difference proves the good specificity of the developed EIS biosensor.

A high measured signal of 43 mV for the hybridization event was able to be detected because of the geometric positioning of the DNA onto the EIS sensor-surface: The developed protocol of PAH/DNA adsorption let the DNA molecules (probe ssDNA and target cDNA) bind in a flat-oriented manner. In comparison to many covalent-binding strategies for DNA – at which mostly one end of the strand is connected with the surface

[3] (so-called terminated DNA bond), adsorptively immobilized DNA is bound along the DNA backbone. As a result, the negative charges of the DNA strands are located close to the sensor surface and contribute more to the surface-potential change – and thus to the sensor signal. More details and considerations about the orientation of immobilized DNA are presented in **Chapter 1.2.2**.

In order to validate the electrochemical observations, reference experiments using fluorescence microscopy were carried out. High fluorescence signals were measured after DNA immobilization and DNA hybridization, respectively. In contrast, no fluorescence signal was measured after the incubation step with ncDNA. The achieved results confirm the ability of the EIS chip to be used as a label-free DNA immobilization and hybridization sensor.

Since many biochips are designed as so-called disposables for single-use purpose, a possibility of reuse could optimize and increase the efficiency of those chips. For that reason, a surface-regeneration procedure was developed. A popular strategy for this is to remove the (previously) adsorbed layers (here: PAH and DNA) and re-modify the surface again. This approach often comes along with additional time-consuming and complicated removal processes and usually requires toxic and harmful chemicals, like strong acid solutions. Such solutions also may not only affect the attached PAH/DNA layer but also the underlying oxide surface, which could lead to a decreased reproducibility of the biosensor. Therefore, an alternative way of regeneration was selected: A simple (additional) re-modification of the already modified sensor surface without any removal step. This strategy in combination with DNA detection is described in detail in **Chapter 6**.

The sequence length of the used DNA material was again increased from the previous 20-mer (probe ssDNA and target cDNA) to 52-mer (for probe ssDNA) and 72-mer (for target cDNA), because of the following reason: In the previous experiments (described in **Chapter 5**), the first on-chip hybridization was desired to realize. After reaching this milestone, the sequences as well as the concentration and composition of the solvents were adjusted in order to simulate more realistic conditions. For the reusing cycle, the sensors were repeatedly modified with the three reasonable combinations for DNA detection: 1. PAH/ssDNA, 2. PAH/dsDNA and 3. PAH/ssDNA-cDNA. For characterization, C–V- and ConCap measurements, which have been well established during previous experiments, were used for signal monitoring.

The repeating procedure was carried out up to five times. For each modification step, a signal change was detectable. These experiments demonstrate that a successful reuse of the chips by the described procedure is possible: With increasing number of reusing cycles, the signal changes steadily decrease and might reach a limit – more cycles than five would have been most probably unable to be detected by using the chosen conditions (especially, ionic strength of the solution) because of getting too small signal changes. Different conditions (ionic strength of the solution, thickness of the oxide layer, lower (background) noise, charge and size of the adsorbed molecules, and other parameters which might influence the signal amplitude), which lead to a higher sensitivity, could allow more than five reusing cycles with reliable/detectable signal changes.

Besides the reusing experiments, the impact of the Debye-screening effect onto the signal amplitude was also investigated, since the charge screening can have a major

influence onto the sensitivity of EIS- and other field-effect devices. Each modification step was monitored individually by using measurement solutions with different ionic strength. A clear dependence between an increased signal amplitude and the used solution with (decreased) ionic strength was obtained. These results might help for further investigations and optimization of the used protocol, e.g., for applying more reusing cycles.

The successful modifications of the surfaces were, again, verified by means of fluorescence microscopy using individual fluorescence dyes for PAH- and DNA detection: FITC, FAM and SG. All in all, the reuse of EIS-sensor chips for multiple DNA detection-experiments were successfully carried out.

The main goal of this thesis was to develop a field-effect chip-based DNA sensing-method which is suitable for label-free detection of tuberculosis DNA from a sample solution (ideally from human origin). For this purpose, a protocol for sensor fabrication (and modification) was investigated and established. Furthermore, a suitable measurement procedure for the label-free DNA detection was selected and examined. Both, the protocol for sensor fabrication and measurement were described in previous chapters. In the final step, the DNA detection using a real (infected) tuberculosis sample has been investigated to validate the readiness of the developed DNA biosensor for a point-of-care application. This detection approach is described in **Chapter 7**.

Getting a real sputum sample with tuberculosis bacteria is difficult in Germany and Europe due to the availability but also because of restrictions and legal regulations [4]. Therefore, we tested sample solutions, which are as identical as possible to real samples. Overall, three different test solutions were required for performing the desired experiments:

- Artificial PCR solution, which contains – unless otherwise stated – high concentration (5 µM) of target cDNA and all components that would be present after a successful PCR reaction. This solution mimics a positive sample with defined target cDNA concentration. It was used to evaluate the developed protocol on hybridization detection and parameters such as sensitivity and lower detection limit.
- A PCR-components solution was used as a control sample to simulate negative tests. It contains no target DNA strands but all other PCR components to mimic a not-successful PCR reaction.
- Real PCR solution as a PCR product that contains target DNA, which was amplified from a template DNA strand. This template DNA was extracted from a tuberculosis-spiked human sputum sample. This solution represents a positive test solution after probe preparation.

With these three test solutions, nearly full-realistic measurement conditions can be simulated.

From the obtained C–V- and ConCap curves, a significant signal change for DNA hybridization of 29 mV was detectable using artificial PCR solution. In contrast to that, only a small signal change of 5 mV was measured after incubating the sensor to PCR-components solution. These experiments demonstrate a good selectivity and specifity for the developed protocol to detect DNA from PCR solutions. The results are also in good

agreement to the previously recorded DNA-detection experiments using laboratory solutions, which are described in **Chapter 5**. Moreover, artificial PCR solutions containing different amounts of target cDNA (from 1 nM to 5 µM) were analyzed in order to determine the sensitivity and lower detection limit. These parameters were estimated to be approximately 7.2 mV/decade and 0.3 nM, respectively. Finally, real PCR solutions were analyzed by means of ConCap measurements. A clear signal change after exposing the chip to the real PCR solution indicates a successful hybridization. The developed method is therefore suitable for detection of extracted and amplified DNA from sputum-spiked human saliva samples.

The experimental data from this work clearly demonstrate that the goal of realizing a sensor platform for the label-free detection of "real" tuberculosis DNA was successfully accomplished. Several tests and optimization steps that are described in **Chapter 3** to **Chapter 7** have been necessary to reach this goal.

8.2 FUTURE PERSPECTIVES AND OUTLOOK

The developed DNA-detection protocol can serve as a basis for further sensing platforms. The following part describes possible future developments and takes also the respective challenges into consideration. Moreover, potential fields of application and possibilities are discussed.

Target-oriented adaptations on the developed EIS modification- and DNA-detection protocols can be done to design alternative conditions for experimental determination of additional parameters and information, such as, the possibility to detect i) DNA from other baterica, ii) longer or shorter DNA sequences, and iii) genomic material from difference sources.

Here, possible modifications are suggested and briefly discussed:

- Other DNA sequences (from different species/organism) could be investigated. The developed protocol is not limited by the chosen sequence (in this thesis, we used sequence from *Mycobacteria tuberculosis* because of the clinical relevance). The detection of DNA sequences from, e.g., viruses or *Mycobacterium leprae* could be also tested.
- The length of probe- and/or target DNA can be varied. The longer the probe ssDNA, the more variations on binding onto the PAH is expected due to the ssDNA flexibility. Upon hybridization, the formed dsDNA strand becomes more rigid, which might reduce the hybridization efficiency, but would be interesting to be investigated.
- More detectable reuse steps could be tried to be achieved by, e.g., changing the composition of the measurement solutions (e.g., the ionic strength).
- Instead of using DNA sequences, also RNA sequences can be used (or PNA for immobilization). RNA is present in a variety of different microorganisms or viruses, which can cause infectious diseases in the human body (e.g., Ebola disease). A detection of those RNA-containing organisms could also be of clinical relevance. However, RNase enzymes are much more present in the environment compared to DNase. Therefore, in order to prevent a degradation of the

immobilized genomic material (in this example, RNA), the biochips and all associated material (solutions, swaps, pipettes, etc.) must be handled very carefully and the sterile conditions must be completely maintained. Otherwise, the RNase enzymes might catalyze the degradation of the immobilized RNA, so that a detection becomes impossible. Thus, realizing a detection platform based on RNA could be quite difficult.

- The most common variation of DNA is the SNP. If such SNPs occur at coded regions of the genome, they can result in a genetically caused disease such as beta thalassemia [5, 6] or Crohn's disease [7]. Detecting of SNPs could help to get a better insight into the mechanisms of DNA variation (and also mutation). Preliminary experiments for the detection of DNA molecules containing SNP variations have been already studied during this thesis (see **Chapter 8.3.1**).
- In principle, a distinction between ssDNA- and dsDNA adsorption onto the modified EIS sensors should be possible to be detected, because the amount of charges per dsDNA molecule is doubled in comparison to ssDNA. However, this consideration assumes that the amount of ssDNA molecules and dsDNA molecules adsorbed to the surface is the same or similar. The discrimination between both DNA-strand types can be useful for verification of the successfulness of a PCR reaction. First experiments were performed during this thesis and published already [8]. It is worth to note that for further investigations, the used DNA sequence should be carefully chosen to prevent mass- and molar concentration differences between ssDNA- and dsDNA molecules. The following calculation describes an example of mixing two solutions (same volume) of ssDNA and cDNA with resulting differences in molar- and mass concentration after hybridization:
  5 µM cDNA (1 µg/L) + 5 µM ssDNA (1 µg/L) => 2.5 µM dsDNA (1 µg/L).
  The problem here is, that the molar concentration has changed (from 5 µM to 2.5 µM) but the mass concentration remains constant (1 µg/L). Therefore, poly-sequences (e.g., a sequence of 20-mer A and 20-mer T) are recommended to prevent this problem. Such sequences tend to self-hybridize and can be used as defined dsDNA material:
  5 µM poly-A-poly-T sequence (1 µg/L) = 5 µM dsDNA (1 µg/L).

Besides the variation of specific parameters and conditions, the implementation of other technologies can be used to gain new insights and improve the existing biosensor system:

- By combining the developed method for PAH surface-modification with an adequate DNA-spotting technique, whole (probe) DNA arrays can be realized. For an easy readout, LAPS technology is recommended for this approach because of the spatial-resolved addressing of LAPS. High amounts of simultaneous DNA tests can be performed. The number of tests is mainly limited by geometric parameters such as the spotting diameter, the minimum-illuminated area and the chip size. DNA arrays can also be very useful for detection of mutations [9, 10] due to the high number of simultaneous tests and they can be used to realize electrochemical Boolean logic systems [11].

- The developed EIS sensors can be implemented into microfluidic systems to further automize the modification, the rinsing steps and the recording. Parameters such as flow, volume, mixing and even temperature of the applied solutions can be more precisely regulated with a microfluidic system in comparison to conventional pipetting. The implementation into a microfluidic system also allows an on-chip PCR reaction. Pre-experiments for investigation of the sensing behavior in a microfluidic setup were performed during this thesis (see **Chapter 8.3.2**).
  The reliability of DNA detection with EIS sensors can be further increased by combining different transducer principles for the detection of the same parameter/event. An approach is described as follows: Coating an EIS- or EOS chip with a metal layer on top of the oxide layer results in an EMOS (electrolyte-metal-oxide-insulator) structure. Adding a counter electrode to the arrangement of the EMOS sensor and a reference electrode allows to measure – besides the sensor capacitance – two more sensing parameters, namely the impedance and the redox current. A detailed description and preliminary experiments related to this topic are presented in the supporting information in **Chapter 8.3.3**.

The developed technology has the potential to be used in a very broad field of applications; here, only a few are pointed out:

- The sensing protocol and setup arrangement for detection of a tuberculosis infection, developed in this thesis, can be further transferred to realize a complete mobile point-of-care diagnostic system. Probe preparation, signal processing, display unit and some minor data-processing electronics need to be implemented. Such a system could be used for field-tests in countries with high incidence of tuberculosis; it can be used for fast detection of tuberculosis-infected individuals.
- The by far most important and revolutionary (DNA modification) technologies of the 21st century is/will be genetic-editing methods, e.g., with the CRISPR/Cas system (CRISPR: clustered-regulatory-interspaced-short-palindromic-repeats, Cas: CRISPR-associated proteins). Although this technique works very precise, a certain amount of errors appears during the gene-editing event resulting in a certain amount of incorrect-modified tissue. The developed DNA-detection method with PAH/EIS sensors could be used to detect, e.g., the respective sequence after the editing process, which can be extracted from a small sample of edited tissue. By analyzing the sample, an indication about the successfulness of the gene-editing event can be provided.
- In order to prevent a global spreading of harmful and high-infectious diseases, the developed method for DNA detection might be also used for a permanent monitoring of travelers at traffic-agglomeration spots such as airports or railway stations. As an example, in 2013/2014, a new outbreak of the Ebola-virus disease occurs in western Africa and resulted into an epidemic with 11,316 reported death cases [12]. The enormous spreading might have been prevented if infected persons were early and reliably identified and separated. This plan was actually focused by many African governments, such as Kenya, but their detection strategy was reduced to a simple measurement of the body temperature of travelers at airports.

From personal experience/observations, the testing was performed only by measuring the body temperature of all travelers with a basic thermometer at Mombasa airport in December 2014 in order to determine a fever, which affects nearly all Ebola-infected individuals. However, no other reliable tests were applied and false negative results could lead to a further spreading of the disease. The use of an adequate, cheap and trustful diagnostic method would be highly recommended and might have been very helpful. Although recent findings showed that Altona Diagnostics (Hamburg, Germany) developed a RT-PCR-based kit for Ebola detection in May 2020 [13], another suggested method for such testing could be based on the DNA-detection procedure, which was developed in this thesis: Individuals could be tested by providing a saliva sample, e.g., when they check-in or deposit their luggage at the airport. A biosensor (with immobilized DNA-sequences from the respective microorganism (e.g., Ebola)) will then be exposed to the sample and identify the presence of the microorganism's DNA. By using isothermal amplification, enough DNA material can be created within 5-15 min and decrease the overall detection time significantly. Other methods, like serological (antibody) tests and virus-isolation techniques via cell culturing [14], can also be used for Ebola detection, but have significant drawbacks such as lower accuracy or long preparation time.

8.3 SUPPORTING INFORMATION

8.3.1 SNP detection

An EIS sensor chip was modified with PAH and 5 µM 52-mer probe ssDNA according to the protocol used in **Chapter 6**. Afterwards, a series of solutions containing 5 µM of 72-mer target DNA molecules was applied (each for 40 min) to the sensor surface. The target DNAs have different numbers of SNP in their sequences (**Table 8.1**). The ConCap response was recorded after each modification step. All other solutions were used as described in **Chapter 6.2**.

Table 8.1: List of sequences of 72-mer target cDNA with target SNP-DNA. Identical parts were marked as E (25-mer) and F (20-mer) for better visualization, where E is ACCTC-CGTAA-CCGTC-ATTGT-CCAGA and F is TGTCC-TTACA-CAGCG-ATCCA. The different sequence parts are written bold and underlined for comparison.

Name	Sequence
20 SNP	E-TCAA**GGGTCGTCTGCTGGTGCGGC**ACG-F
10 SNP	E-TCAACCCAGCAG**TGCTGGTGCG**CGACG-F
5 SNP	E-TCAACCCAGCAGAC**CTGGT**CGCCGACG-F
3 SNP	E-TCAACCCAGCAGACG**TGG**ACGCCGACG-F
2 SNP	E-TCAACCCAGCAGACGA**GG**ACGCCGACG-F
1 SNP	E-TCAACCCAGCAGACGAC**G**ACGCCGACG-F
cDNA	E-TCAACCCAGCAGACGACCACGCCGACG-F

Figure 8.1 shows an exemplary ConCap curve of a PAH/ssDNA-modified EIS sensor, which was exposed to target cDNA molecules with various numbers of SNPs from 20 SNPs to 0 SNP (0 SNP = cDNA).

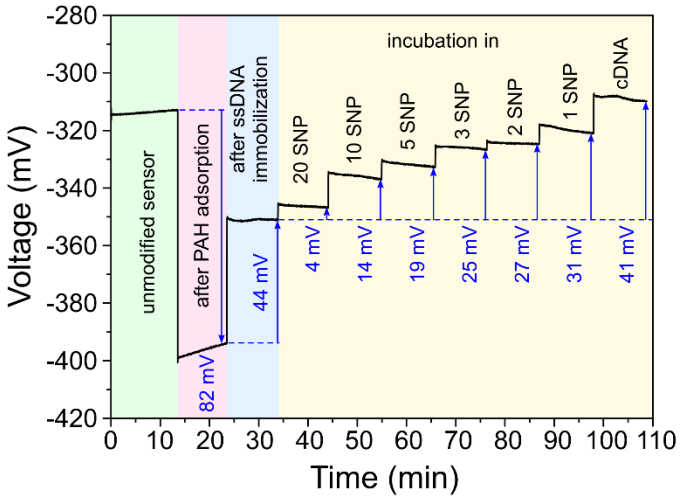

Figure 8.1: ConCap curve of a PAH/DNA-modified EIS sensor, which was exposed to different target cDNA solutions containing different amounts of SNP (from 20 to cDNA (cDNA = 0 SNP)).

The modification with PAH and ssDNA was performed according to the protocol described in **Chapter 7**. The measured signal amplitudes correlate inversely with the number of SNPs indicating a change in hybridization efficiency. The more SNPs are present in a sequence the higher similarity to a full-mismatch DNA exists. Therefore, the affinity for hybridization is higher for lower SNP numbers. A rough estimation is given by the rule that a 1% mismatch results in a 1 °C decrease of T_m [15]. Since T_m is an important factor for the resulting hybridization efficiency, the observed signal changes can be explained by this hypothesis. Similar additional experiments have shown same signal trends after incubation in SNP solutions. The shown graph has been the first results and needs to be extensively evaluated by further experiments.

8.3.2 Microfluidic implementation

As a first test for microfluidic implementation, buffer solution was pumped via a microfluidic "plug" (the technical drawing of it is shown in **Figure 8.2**) to the sensor surface during the measurement. Even for low flow rates of approx. 600 µL/min high signal fluctuation of approx. ±10 mV in ConCap mode were observed (data not shown). But in stationary conditions (deactivated pump) a stable signal was measurable.

In a different experiment, heated buffer solution was used for measurements. Here, moderate signal fluctuations but very long drift periods were detected (**Figure 8.3**).

Although all three modification steps of PAH adsorption, DNA immobilization and hybridization could also be monitored at a working temperature of 63 °C, the implementation of these techniques requires more optimization, e.g., the temperature

dependence of the EIS should be taken also into account. The temperature of 63 °C was chosen for possible application of an on-chip PCR.

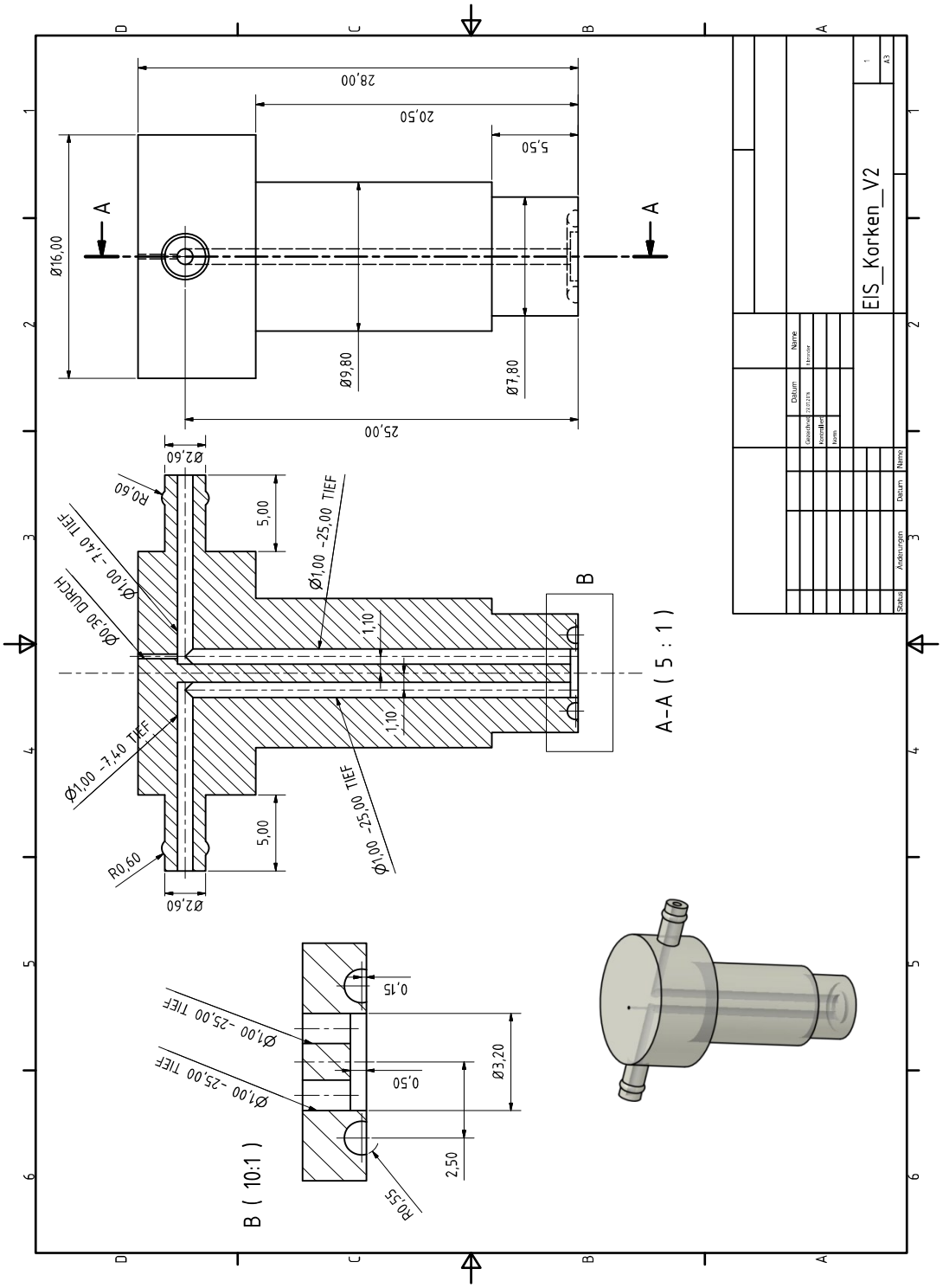

Figure 8.2: Technical drawing of the microfluidic plug for EIS-measurement chambers. The hole on top of the plug is for the Ag/AgCl reference-electrode wire. Solution inlet and outlet can be connected with standard microfluidic tubes.

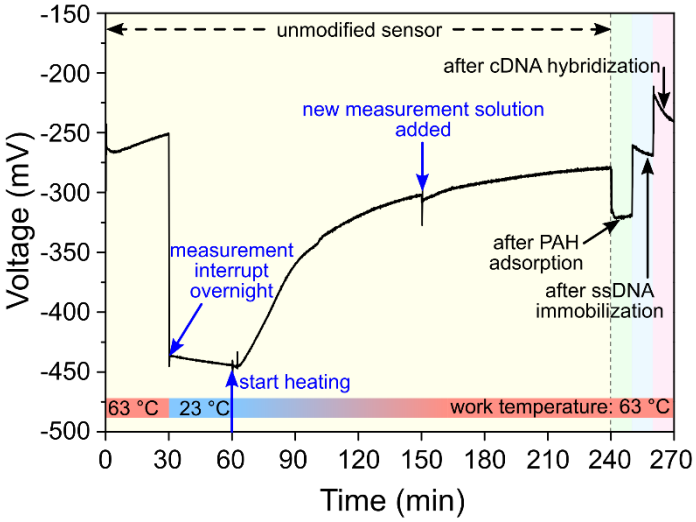

Figure 8.3: Influence of increased buffer-solution temperature on the ConCap signal for the unmodified chip, after PAH adsorption, after ssDNA immobilization and after cDNA hybridization. A long signal-stabilizing phase of 1.5 h to 3 h was monitored. The temperature value was measured directly inside the measurement chamber using a previously calibrated Pt1000 resistor.

8.3.3 Combined (EMOS) sensor[1]

Monitoring of more than one single transducer principle (e.g., combined field-effect and impedimetric (charge transfer resistance) measurement) during an experiment might further increase the reliability of the detection process. The following part describes DNA-detection experiments with EMOS-sensor chips, which were characterized in three different measurement modes: field-effect (capacitance) mode, impedance mode and cyclic-voltammetry mode to acquire different sensing parameters. All three characterizations were performed after each sensor-modification step including DNA immobilization and hybridization. The used chips had an EMOS structure with 200 nm Au/20 nm Cr/60 nm Ta_2O_5/30 nm SiO_2/p-Si/300 nm Al and were connected into a three-electrode arrangement (see **Figure 8.4**).

The different sensing modes require individual measurement solutions: We used 0.33 mM PBS for measuring the sensor capacitance while 1 mM $K_3[Fe(CN)_6]$ diluted in 0.1 M KH_2PO_4 buffer was utilized for impedance- and cyclic-voltammetry measurements. The immobilization- and hybridization methods differ from the previously presented PAH/DNA-modification protocol for SiO_2 surfaces. The immobilization was carried out by 1 h incubation of 5 µM thiol-modified probe ssDNA (72-mer) in 1 M KH_2PO_4 on the sensor surface. A hybridization was realized for 1 h by incubation of 5 µM target cDNA (52-mer) in 1x PBS, 0.5 M NaCl. The DNA sequences were the same as described in **Chapter 7**; only on the probe DNA was a thiol-group added at the 5'-end.

[1] Parts of this work has been already presented during the Engineering of Functional Interfaces (EnFI) conference 2018 in Meinsberg, Germany.

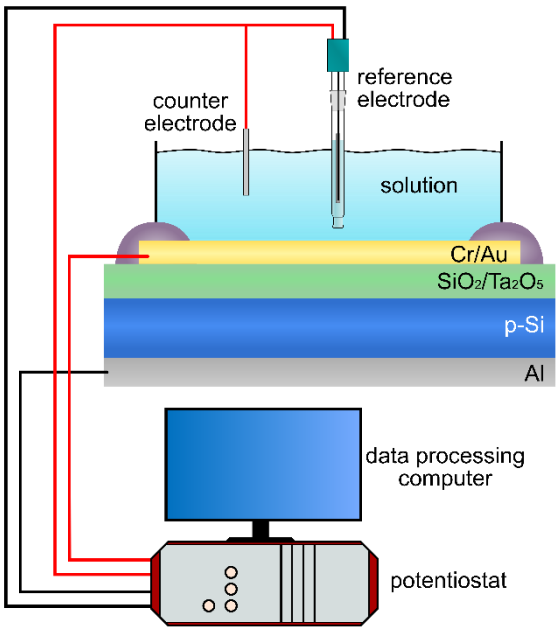

Figure 8.4: Schematic of sensor setup including a counter electrode (Pt), a reference electrode (Ag/AgCl) and an EMOS chip. The colored lines represent the respective connection arrangement: Black for capacitance measurement, red for impedance- and redox-current measurements.

In field-effect mode, C–V measurements were performed in which a clear signal shift after the immobilization and hybridization towards more positive voltage direction was observable (**Figure 8.5a**). This shift describes a change in surface potential same as for EIS sensors. Due to the immobilization- and hybridization reaction, in both cases, negatively charged DNA molecules are transferred to the surface resulting in a surface-potential change. Here, the immobilized DNA is not bound to the surface via adsorptive forces but interact with a strong covalent/ionic bond between the thiol group and the Au layer [16].

The signal change after hybridization is much smaller than for immobilization. This can be explained by a model of the geometric orientation of the DNA after immobilization and after hybridization: Immobilized ssDNA lays flat onto the sensor, upon hybridization, the unbound ends of the formed rigid dsDNA molecules lift up away from the sensor surface. The most part of the DNA is then out of the Debye-screening length in the solution, resulting in a reduced affection of the intrinsic negative charge onto the sensor potential.

The cyclic-voltammetry analyses (see **Figure 8.5b**) show a high redox current for the unmodified gold sensor surface at the typical reduction- and oxidation voltages of approximately +150 mV and +300 mV [17, 18], respectively, for $K_3[Fe(CN)_6]$ versus Au. The redox agent $K_3[Fe(CN)_6]$ can freely react at the metal surface and transfer electrons from or to the sensor-chip surface, therefore a high current value was measured. The current drops severely after the immobilization step, because the bounded DNA molecules lay flat on the metal layer and block the free regions of the metal surface. Due to the immobilized DNA molecules, the redox agent's surface reaction is decreased because of the reduced electrode area resulting in a low electrical current. After the hybridization reaction, again a

significant increase of the current was measurable. According to the already described DNA surface-binding model, the DNA molecules tilt up upon hybridization and uncover the metal surface. More redox-agent molecules can now react at the sensor surface resulting in an increased current.

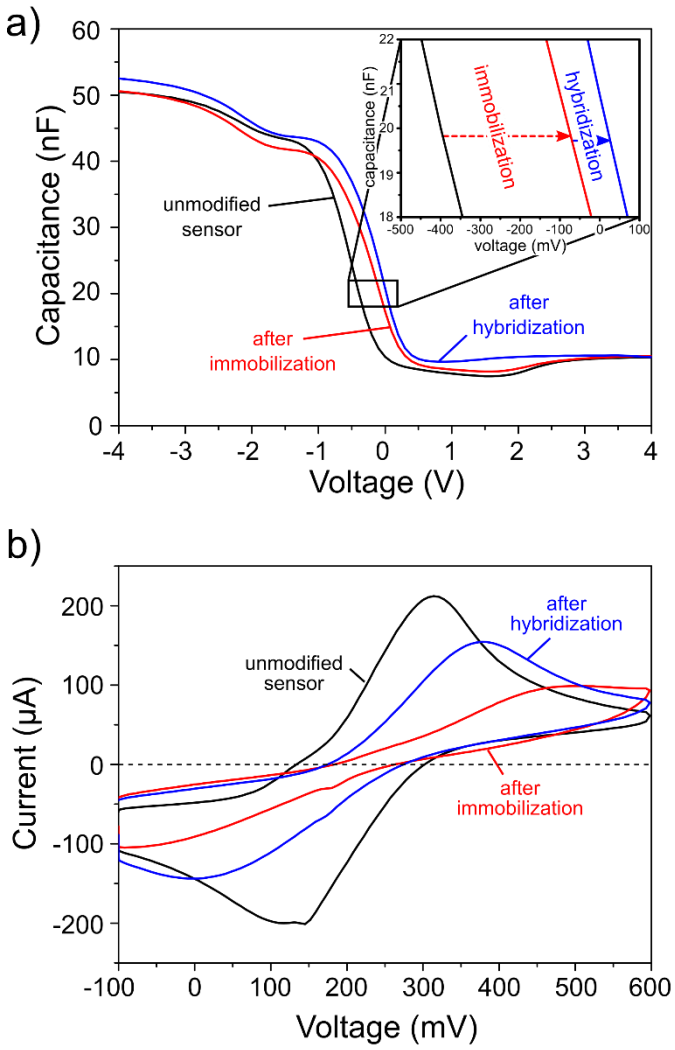

Figure 8.5: a) Recorded C–V (here: capacitance-voltage) curves for the unmodified EMOS sensor, after DNA immobilization and after hybridization. b) The same sensor has been characterized by means of a cyclic-voltammogram before and after immobilization and hybridization.

In addition to the capacitance- and cyclic-voltammetry measurements, characterizations in impedance mode were also carried out (data not shown). Here, an +50% increase of the charge-transfer resistance measured for the unmodified chip was observed after immobilization. The impedance trend is expected to behave reciprocally to the recorded current of the cyclic-voltammetry measurements. After hybridization, a signal decrease of –42% was measured. The results confirm the obtained results from the other measurement modes. All experiments for EMOS sensors are coincident and explainable by the assumed

binding theory. Similar experiments according to impedance analyzes for DNA detection (without field-effect sensors) have already been performed by another group; the interested reader is referred to the respective literature [19–21].

The results shown here are the first experiments of a combined EMOS sensor approach for detection of DNA. It was shown that a (nearly) simultaneous measurement of three sensing parameters is possible with such device, which might lead to an increased reliability. The results point out the great potential of this combined sensor system.

REFERENCES

[1] Product description sheet: Renvela® (sevelamer carbonate), Sanofi, http://products.sanofi.us/renvela/renvela.pdf, downloaded from internet: 09. February 2019.

[2] A.I. Dragan, R. Pavlovic, J.B. McGivney, J.R. Casas-Finet, E. S. Bishop, R.J. Strouse, M.A. Schenerman, C.D. Geddes: *SYBR Green I: Fluorescence properties and interaction with DNA*, J. Fluoresc. 22 (2012) 1189–1199.

[3] S. Wenmackers, V. Vermeeren, M. vandeVen, M. Ameloot, N. Bijnens, K. Haenen, L. Michiels, P. Wagner: *Diamond-based DNA sensors: Surface functionalization and read-out strategies*, Phys. Status Solidi A 206 (2009) 391–408.

[4] World Health Organization: ANNEX III Regional and global profiles, *Global Tuberculosis Report 2018*; WHO: Geneva (2018).

[5] C. Ding, R.W. Chiu, T.K. Lau, T.N. Leung, L.C. Chan, A.Y. Chan, P. Charoenkwan, I.S. Ng, H.Y. Law, E.S. Ma, X. Xu, C. Wanapirak, T. Sanguansermsri, C. Lia, M.A. Ai, D.H. Chui, C.R. Cantor, M.Y. Lo: *MS analysis of single-nucleotide differences in circulating nucleic acids: Application to noninvasive prenatal diagnosis*, Proc. Natl. Acad. Sci. U.S.A. 101 (2004) 10762–10767.

[6] Y.M. Lo: *Recent developments in fetal nucleic acids in maternal plasma: Implications to noninvasive prenatal fetal blood group genotyping*, Transfus. Clin. Biol. 13 (2006) 50–52.

[7] S. Schmechel, A. Konrad, J. Diegelmann, J. Glas, M. Wetzke, E. Paschos, P. Lohse, B. Göke, S. Brand: *Linking genetic susceptibility to Crohn's disease with Th17 cell function: IL-22 serum levels are increased in Crohn's disease and correlate with disease activity and IL23R genotype status*, Inflamm. Bowel Dis. 14 (2008) 204–212.

[8] T.S. Bronder, A. Poghossian, S. Scheja, C.S. Wu, M. Keusgen, M.J. Schöning: *Electrostatic detection of unlabelled single- and double-stranded DNA using capacitive field-effect devices functionalized with a positively charged polyelectrolyte layer*, Procedia Eng. 120 (2015) 544–547.

[9] R.J. Lipshutz, D. Morris, M. Chee, E. Hubbell, M.J. Kozal, N. Shah, N. Shen, R. Yang, S.P.A. Fodor: *Using oligonucleotide probe arrays to access genetic diversity*, Biotechniques 19 (1995) 442–447.

[10] J. Cheng, P. Fortina, S. Surrey, L.J. Kricka, P. Wilding: *Microchip-based devices for molecular diagnosis of genetic diseases*, Molecular Diagnosis 1 (1996) 183–200.

[11] A. Poghossian, K. Malzahn, M.H. Abouzar, P. Mehndiratta, E. Katz, M.J. Schöning: *Integration of biomolecular logic gates with field-effect transducers*, Electrochim. Acta 56 (2011) 9661–9665.

[12] World Health Organization: *Ebola Situation Report 2016*; WHO: Geneva (2016).

[13] Data sheet: *RealStar ebolavirus RT-PCR Kit 1.0*, https://altona-diagnostics.com/files/public/Content%20Homepage/-%2002%20RealStar/EUA-USA/RealStar%20Ebolavirus%20RT-PCR%20Kit%201.0_WEB_EUA_EN-Rev05.pdf, information downloaded from internet: 27. June 2020.

[14] https://www.rki.de/SharedDocs/FAQ/Ebola/Ebola.html, information downloaded from internet: 27. June 2020.

[15] R.C. King: *Handbook of Genetics, Volume 5: Molecular Genetics*, Plenum Press, New York, USA (1976).

[16] E. Pensa, E. Cortes, G. Corthey, P. Carro, C. Vericat, M.H. Fonticelli, G. Benitez, A.A. Rubert, R.C. Salvarezza: *The chemistry of the sulfur–gold interface: In search of a unified model*, Acc. Chem. Res. 45 (2012) 1183–1192.

[17] S. Bollo, C. Yanez, J. Sturm, L. Nunez-Vergara, J.A. Squella: *Cyclic voltammetric and scanning electrochemical microscopic study of thiolated β-cyclodextrin adsorbed on a gold electrode*, Langmuir 19 (2003) 3365–3370.

[18] M.M. Radhi, E.A.J. Al-Mulla, W.T. Tan: *Electrochemical characterization of the redox couple of Fe(III)/Fe(II) mediated by grafted polymer electrode*, Res. Chem. Intermed. 40 (2014) 179–192.

[19] J. Kafka, O. Pänke, B. Abendroth, F. Lisdat: *A label-free DNA sensor based on impedance spectroscopy*, Electrochim. Acta 53 (2008) 7467–7474.

[20] F. Lisdat, D. Schäfer: *The use of electrochemical impedance spectroscopy for biosensing*, Anal. Bioanal. Chem. 391 (2008) 1555–1567.

[21] M. Riedel, J. Kartchemnik, M.J. Schöning, F. Lisdat: *Impedimetric DNA detection – steps forward to sensorial application*, Anal. Chem. 86 (2014) 7867–7874.

9 Zusammenfassung

Der Nachweis von Krankheitserregern aus Probenmaterial von infizierten Patienten stellt die Grundlage dar, auf der eine aussagekräftige medizinische Diagnose gestellt werden kann. Krankheitserreger können sehr zuverlässig und eindeutig anhand ihres genomischen Materials (DNA) identifiziert werden. Es haben sich eine Vielzahl von verschiedenen DNA-Nachweisverfahren, mit individuellen Vor- und Nachteilen, etabliert. Möchte man solche Methoden für bestimmte Anwendungen, wie z.B. für die Vor-Ort-Analytik, einsetzen bzw. implementieren, so ergeben sich eine Reihe von Anforderungen: Eine Messung muss sehr schnell, günstig, einfach und zuverlässig ablaufen. Es hat sich gezeigt, dass vor allem markierungsfreie Nachweisprinzipien, die auf Basis der Feldeffekt-Ladungsdetektion beruhen, den zuvor genannten Anforderungen gerecht werden.

Diese Arbeit beschreibt deshalb die Entwicklung eines neuartigen Messverfahrens zur Detektion von DNA (mit Sequenzen von *Mycobacterium tuberculosis*) mit Hilfe von Feldeffekt-Sensoren. Als Sensor wurde der Elektrolyt-Isolator-Halbleiter- (EIS)-Chip ausgewählt, da dieser den einfachsten Aufbau von allen Feldeffekt-Sensoren hat und kostengünstig herzustellen ist. EIS-Sensoren sind kapazitive Strukturen, die mit Hilfe eines Impedanz-Analysators messtechnisch auszulesen sind. Dabei wird ein Messwert erfasst, der in direktem Zusammenhang mit dem Oberflächenpotential des Sensors steht. Bringt man nun die DNA, die in Lösung negativ geladen ist, nah an die Sensoroberfläche, so bewirkt dies über eine Veränderung der Ladungssituation an der Chipoberfläche eine Oberflächenpotentialänderung. Mit Hilfe der EIS-Sensoren kann diese Potentialänderung ausgelesen werden:

Die Nachweismethode beruht grundsätzlich auf dem Erkennen eines Hybridisierungsereignisses an der Sensoroberfläche, bei der zunächst „Fänger"-Einzelstrang-DNA (engl.: probe ssDNA) mit bekannter und zur nachweisenden DNA komplementären Sequenz an die Sensoroberfläche immobilisiert wird. Sobald nun „Ziel"-Einzelstrang-DNA (engl.: target ssDNA) an die Oberfläche gelangt, kann es zur Hybridisierung kommen, sofern die Sequenzen komplementär sind, wodurch eine Signalverschiebung gemessen werden kann. Im Falle von nicht-komplementärer target-DNA bleibt die Hybridisierung aus und das Signal konstant.

Die Immobilisierung der Fänger-ssDNA wurde mit Hilfe einer Oberflächenmodifikation mittels positiv geladenem Polyelektrolyt (Poly(Allylamin-Hydrochlorid), PAH) durchgeführt. Im Vergleich zu anderen Immobilisierungsstrategien, die in der Literatur beschrieben sind, bindet die Fänger-ssDNA bei der gewählten Art rein adsorptiv und selbstständig an der Sensoroberfläche, wodurch sich die Vorbereitung stark vereinfacht sowie schnell und günstig vollzogen werden kann.

Der Hauptteil dieser Dissertation beginnt mit der Sensorauslegung (EIS-Sensor mit SiO_2 als Oberflächenoxid), der Beschreibung der Oberflächenmodifikation mittels PAH, dem Nachweis der Anbindung von zunächst Doppelstrang-DNA und der Evaluierung der Messdatenerfassung mittels kapazitiver Messungen. Aufgrund der adsorptiven Anbindung liegen die DNA-Stränge flach auf der Sensoroberfläche; damit befindet sich die negative

Ladung der DNA nah an der Oberfläche, wodurch ein hohes Messsignal erfasst werden kann.

Das entwickelte Verfahren wurde außerdem auf lichtadressierbare potentiometrische Sensoren (LAPS) übertragen. LAPS-Chips haben eine große strukturelle Ähnlichkeit zu EIS-Sensoren und den Vorteil, dass sie Änderungen des Oberflächenpotentials örtlich aufgelöst detektieren können. Daraus ergibt sich beispielsweise die Möglichkeit zur Array-Anordnung, um mehrere DNA-Experimente simultan auf einem Chip durchführen zu können. Allerdings ist der Messaufbau komplizierter, was für einen späteren, autarken Praxiseinsatz als nachteilig bewertet werden muss.

Im nächsten Schritt wurde auf Basis des entwickelten Verfahrens eine Messung der DNA-Hybridisierung auf der Sensoroberfläche realisiert; dazu wurden PAH/ssDNA-modifizierte EIS-Chips mit cDNA-Lösungen in Kontakt gebracht. Messbare Oberflächenpotentialänderungen konnten zeigen, dass die Hybridisierung erfolgreich war. Im direkten Vergleich mit Messwerten, bei denen nicht-komplementäre ncDNA auf den modifizierten Sensor gegeben wurde, wurden ca. 11-fach höhere Signalunterschiede gemessen.

Das entwickelte Verfahren erlaubt wiederholende Modifizierungen der Oberfläche, selbst wenn ein Sensor bereits für eine Messung eingesetzt wurde. Diese Wiederverwendbarkeit der Sensoren wurde untersucht, indem bis zu fünf wiederholende Oberflächenmodifizierungs- und DNA-Anbindungsexperimente mit nur einem Chip sequentiell durchgeführt wurden. Dabei konnte zwar eine stetige Abnahme des Sensorsignals nach jeder zusätzlichen Schicht (PAH oder DNA) beobachtet werden; diese Beobachtung hängt allerdings mit dem Debye-Abschirmungseffekt von Ladungen in Lösungen zusammen. Weitere Untersuchungen haben den Einfluss der Ionenstärke auf die Höhe des Messsignals für alle Modifizierungsschritte bestätigt.

Abschließend wurde der entwickelte Biosensor verwendet, um PCR-amplifizierte cDNA nachzuweisen. Eine Detektion der Ziel-cDNA ist trotz der in Lösung befindlichen (Stör)substanzen, die für den PCR-Prozess notwendig sind (Enzyme, etc.), gelungen. Messungen, in denen Konzentrationsreihen von cDNA eingesetzt wurden, dienten zur Bestimmung der unteren Nachweisgrenze (0.3 nM) und der Sensitivität (7.2 mV/Dekade). Es wurde außerdem extrahierte und amplifizierte Ziel-DNA aus *Mycobacterium tuberculosis*-gespikten humanen Speichelproben mit dem Verfahren untersucht. Dabei konnte eine eindeutige Unterscheidung zwischen Positiv- und Negativ-Material, mit Hilfe der PAH/ssDNA-modifizierten EIS-Sensorchips, erkannt werden.

Alle entwickelten Prozessschritte wurden mit Hilfe von Fluoreszenzmessungen als Referenzmethode validiert, indem das Vorhandensein der DNA auf der Sensoroberfläche optisch nachgewiesen wurde. Mit dem in dieser Arbeit entwickelten kapazitiven Feldeffekt-Biosensor ist eine schnelle, einfache und kostengünstige Messung einer DNA-Hybridisierungsreaktion möglich. Der Nachweis von amplifizierter genomischer DNA, aus realen *Mycobacterium tuberculosis*-gespikten Speichelproben, untermauert das Potential dieser Technologie als Sensoransatz für die medizinische Erregererkennung.

List of publications

PUBLICATIONS IN PEER-REVIEWED JOURNALS

1. H. Iken, **T. Bronder**, A. Goretzki, J. Kriesel, K. Ahlborn, F. Gerlach, W. Vonau, W. Zander, J. Schubert, M.J. Schöning: *Development of a combined pH- and redox-sensitive bi-electrode glass thin-film sensor*, Phys. Status Solidi A 216 (2019) 1900114.
2. **T.S. Bronder**, A. Poghossian, M.P. Jessing, M. Keusgen, M.J. Schöning: *Surface regeneration and reusability of label-free DNA biosensors based on weak polyelectrolyte-modified capacitive field-effect structures*, Biosens. Bioelectron. 126 (2019) 510–517.
3. A. Poghossian, M. Jablonski, C. Koch, **T.S. Bronder**, D. Rolka, C. Wege, M.J. Schöning: *Field-effect biosensor using virus particles as scaffolds for enzyme immobilization*, Biosens. Bioelectronics 110 (2018) 168–174.
4. **T.S. Bronder**, M.P. Jessing, M. Keusgen, M.J. Schöning: *Detection of PCR amplified tuberculosis DNA fragments with polyelectrolyte-modified field-effect sensors*, Anal. Chem. 90 (2018) 7747–7753.
5. **T.S. Bronder**, A. Poghossian, M. Keusgen, M.J. Schöning: *Label-free detection of double-stranded DNA molecules with polyelectrolyte-modified capacitive field-effect sensors*, Tech. Mess. 84 (2017) 628–634.
6. C. Wu, A. Poghossian, **T.S. Bronder**, M.J. Schöning: *Sensing of double-stranded DNA molecules by their intrinsic molecular charge using the light-addressable potentiometric sensor*, Sens. Actuators B 229 (2016) 506–512.
7. **T.S. Bronder**, A. Poghossian, S. Scheja, C. Wu, M. Keusgen, D. Mewes, M.J. Schöning: *DNA immobilization and hybridization detection by the intrinsic molecular charge using capacitive field-effect sensors modified with a charged weak polyelectrolyte layer*, ACS Appl. Mater. Interfaces 7 (2015) 20068–20075.
8. C. Wu, **T. Bronder**, A. Poghossian, C.F. Werner, M.J. Schöning: *Label-free detection of DNA using a light-addressable potentiometric sensor modified with a positively charged polyelectrolyte layer*, Nanoscale 7 (2015) 6143–6150.
9. C. Wu, **T. Bronder**, A. Poghossian, C.F. Werner, M. Bäcker, M.J. Schöning: *Label-free electrical detection of DNA with a multi-spot LAPS: First step towards light-addressable DNA chips*, Phys. Status Solidi A 211 (2014) 1423–1428.

PROCEEDINGS

1. F. Gerlach, K. Ahlborn, H. Iken, **T. Bronder**, M.J. Schöning, W. Vonau: *Funktionelle Glasmembranen für elektrochemische Sensoren in Dünnfilmtechnik*, Proceedings of the 13th Dresdner Sensor-Symposium (2017) 236–241.
2. M.J. Schöning, **T.S. Bronder**, C. Wu, S. Scheja, M. Jessing, C. Metzger-Boddien, M. Keusgen, A. Poghossian: *Label-free DNA detection with capacitive field-effect devices – challenges and opportunities*, Proc. MDPI 1 (2017) 719.
3. M. Jablonski, C. Koch, **T.S. Bronder**, A. Poghossian, C. Wege, M.J. Schöning: *Field-effect biosensors modified with tobacco mosaic virus nanotubes as enzyme nanocarrier*, Proc. MDPI 1 (2017) 505.
4. A. Poghossian, **T.S. Bronder**, S. Scheja, C. Wu, T. Weinand, C. Metzger-Boddien, M. Keusgen, M.J. Schöning: *Label-free electrostatic detection of DNA amplification by PCR using capacitive field-effect devices*, Procedia Eng. 168 (2016) 514–517.
5. A. Poghossian, **T. Bronder**, C.S. Wu, M.J. Schöning: *Label-free sensing of biomolecules by their intrinsic molecular charge using field-effect devices*, Proc. 10th Int. Conf. Semiconductor Micro- and Nanoelectronics, Yerevan, Armenia (11.–13. Sep. 2015) 61–63.
6. **T.S. Bronder**, A. Poghossian, S. Scheja, C.S. Wu, M. Keusgen, M.J. Schöning: *Electrostatic detection of unlabelled single- and double-stranded DNA using capacitive field-effect devices functionalized with a positively charged polyelectrolyte layer*, Procedia Eng. 120 (2015) 544–547.
7. **T. Bronder**, C.S. Wu, A. Poghossian, C.F. Werner, M. Keusgen, M.J. Schöning: *Label-free detection of DNA hybridization with light-addressable potentiometric sensors: Comparison of various DNA-immobilization strategies*, Procedia Eng. 87 (2014) 755–758.
8. C. Wu, **T. Bronder**, A. Poghossian, C.F. Werner, M.J. Schöning: *DNA-hybridization detection using light-addressable potentiometric sensor modified with gold layer*, Sensoren und Messsysteme 2014 VDE Verlag GmbH (2014), 1–4.
9. C. Wu, A. Poghossian, C.F. Werner, **T. Bronder**, M. Bäcker, P. Wang, M.J. Schöning: *An application of a scanning light-addressable potentiometric sensor for label-free DNA detection*, Proceedings of the 11th Dresdner Sensor-Symposium (2013) 164–168.

ORAL AND POSTER PRESENTATIONS

1. D. Özsoylu. **T.S. Bronder**, S. Dantism, H. Iken, Th. Schnitzler, S. Kizildag, M.J. Schöning, T. Wagner: *Cryopreservation of cells on electrolyte insulator semiconductor (EIS)-based sensor*s, 11th Engineering of Functional Interfaces (EnFI 2018), Lutherstadt Wittenberg, Germany (01.–03. Jul. 2018).
2. **T.S. Bronder**, S. Güney, A. Poghossian, M. Keusgen, M.J. Schöning: *Concept of a combined field-effect/redox-current EMOS sensing platform for detection of DNA*, 11th Engineering of Functional Interfaces (EnFI 2018), Lutherstadt Wittenberg, Germany (01.–03. Jul. 2018).
3. H. Iken, **T. Bronder**, K. Ahlborn, F. Gerlach, W. Vonau, W. Zander, J. Schubert, M.J. Schöning: *Development of a combined pH- and redox-sensitive bi-electrode glass thin-film sensor*, 17th International Meeting on Chemical Sensors (IMCS 2018), Wien, Austria (15.–19. Jun. 2018).
4. F. Gerlach, K. Ahlborn, H. Iken, **T. Bronder**, M.J. Schöning, W. Vonau: *Funktionelle Glasmembranen für elektrochemische Sensoren in Dünnfilmtechnik*, 13th Dresdner Sensor-Symposium 2017 (DSS 2017), Dresden, Germany (04.–06. Dec. 2017).
5. M.J. Schöning, **T.S. Bronder**, C. Wu, S. Scheja, M. Jessing, C. Metzger-Boddien, M. Keusgen, A. Poghossian: *Label-free DNA detection with capacitive field-effect devices – challenges and opportunities*, 5th International Symposium on Sensor Science (I3S 2017), Barcelona, Spain (27.–29. Sep. 2017).
6. M. Jablonski, C. Koch, **T. Bronder**, A. Poghossian, C. Wege, M. Schöning: *Field-effect biosensors modified with tobacco mosaic virus nanotubes as enzyme nanocarrier*, 31th Eurosensors Conference, Paris, France (03.–06. Sep. 2017).
7. **T.S. Bronder**, A. Poghossian, T. Weinand, C. Metzger-Boddien, M. Keusgen, M.J. Schöning: *Sensing of PCR-amplified tuberculosis DNA with polyelectrolyte-modified field-effect capacitive sensors*, 10th Engineering of Functional Interfaces (EnFI 2017), Marburg, Germany (28.–29. Aug. 2017).
8. **T.S. Bronder**, H. Iken, A. Goretzki, J. Kriesel, K. Ahlborn, F. Gerlach, W. Vonau, M.J. Schöning: *Fabrication of thin-film solid-state pH sensors by means of pulsed laser deposition (PLD)*, 10th Engineering of Functional Interfaces (EnFI 2017), Marburg, Germany (28.–29. Aug. 2017).
9. M. Jablonski, A. Poghossian, C. Koch, **T.S. Bronder**, C. Wege, M.J. Schöning: *Capacitive field-effect biosensors using tobacco mosaic virus nanotubes as enzyme nanocarrier*, 10th Engineering of Functional Interfaces (EnFI 2017), Marburg, Germany (28.–29. Aug. 2017).
10. N. Samiseresht, F. Brings, **T. Bronder**, M.J. Schöning, A. Offenhäusser, D. Mayer: *Aptamer-based field-effect biosensor for malaria detection on heterofunctional supports*, 10th Engineering of Functional Interfaces (EnFI 2017), Marburg, Germany (28.–29. Aug. 2017).
11. **T.S. Bronder**, A. Poghossian, M.P. Jessing, S. Scheja, M. Keusgen, M.J. Schöning: *Detection of tuberculosis DNA by means of polyelectrolyte-modified field-effect based capacitive semiconductor sensors*, 1st European & 10th German BioSensor Symposium, Potsdam, Germany (20.–23. Mar. 2017).

12. **T.S. Bronder**, M.P. Jessing, S. Scheja, A. Poghossian, M. Keusgen, M.J. Schöning: *Electrical detection of tuberculosis DNA by means of polyelectrolyte modified field-effect based semiconductor sensors*, 150th ICB Seminar, Warsaw, Poland, (12.–14. Oct. 2016).
13. **T.S. Bronder**, S. Scheja, A. Poghossian, M. Keusgen, M.J. Schöning: *Label-free detection of on-chip and in-solution hybridization of DNA by means of a capacitive field-effect sensor*, 7th Kurt-Schwabe-Symposium, Mittweida, Germany (04.–07. Sep. 2016).
14. A. Poghossian, **T.S. Bronder**, S. Scheja, C. Wu, M. Keusgen, M.J. Schöning: *Label-free electrostatic detection of DNA amplification by PCR using capacitive field-effect devices*, 30th Eurosensors Conference, Budapest, Hungary (04.–07. Sep. 2016).
15. **T.S. Bronder**, M. Jessing, A. Poghossian, M. Keusgen, M.J. Schöning: *On-chip and in-solution DNA-hybridization detection by capacitive field-effect devices modified with weak polyelectrolyte layer*, 16th International Meeting on Chemical Sensors (IMCS 2016), Jeju, Jeju Island, Korea (10.–13. Jul. 2016).
16. **T.S. Bronder**, A. Poghossian, M. Keusgen, M.J. Schöning: *Real-time monitoring of surface potential changes of semiconductor field-effect sensors during polyelectrolyte and DNA adsorption*, 9th Engineering of Functional Interfaces (EnFI 2016), Wildau, Germany (03.–05. Jul. 2016).
17. **T. Bronder**, A. Poghossian, S. Scheja, C. Wu, M. Keusgen, M.J. Schöning: *Electrostatic detection of unlabelled single- and double-stranded DNA using capacitive field-effect devices functionalized with a positively charged polyelectrolyte layer*, 29th Eurosensors Conference, Freiburg, Germany (06.–09. Sep. 2015).
18. A. Poghossian, **T. Bronder**, S. Scheja, C. Wu, M.J. Schöning: *Label-free detection of DNA molecules by their intrinsic molecular charge using field-effect sensors modified with a positively charged weak-polyelectrolyte layer*, 4th Intenational Symposium on Sensor Science (I3S 2015), Basel, Switzerland (13.–15. Jul. 2015).
19. **T.S. Bronder**, S. Scheja, C.S. Wu, A. Poghossian, M. Keusgen, M.J. Schöning: *Electrical detection of unlabeled DNA with polyelectrolyte-modified EIS sensors: Comparison between ssDNA and dsDNA adsorption*, 8th Engineering of Functional Interfaces (EnFI 2015), Hannover, Germany (06.–07. Jul. 2015).
20. **T. Bronder**, C.S. Wu, A. Poghossian, M. Keusgen, M.J. Schöning: *Markierungsfreie Detektion von DNA-Hybridisierung mittels LAPS (Licht-adressierbare potentiometrische Sensoren): Ein Vergleich von verschiedenen DNA-Immobilisierungsstrategien*, 9th German BioSensor Symposium, München, Germany (11.–13. Mar. 2015).
21. **T. Bronder**, C.S. Wu, C.F. Werner, A. Poghossian, M.J. Schöning: *Chip-based, label-free detection of single-stranded DNA with field-effect light-addressable potentiometric sensors (LAPS),* 17th ITG/GMA Fachtagung Sensoren und Messsysteme, Nürnberg, Germany (03.–05. Jun. 2014).

22. **T. Bronder**, C. Wu, A. Poghossian, M. Bäcker, D. Mewes, M.J. Schöning: *Label-free electrical detection of DNA immobilization and hybridization with a capacitive field-effect biosensor modified with a positively charged polyelectrolyte layer*, 15th International Meeting on Chemical Sensors (IMCS 2015), Buenos Aires, Argentina (16.–19. Mar. 2014).
23. **T. Bronder**, C.S. Wu, A. Poghossian, C.F. Werner, M. Keusgen, M.J. Schöning: *Label-free detection of DNA hybridization with light-addressable potentiometric sensors: Comparison of various DNA-immobilization strategies*, 28th Eurosensors Conference, Brescia, Italy (07.–10. Sep. 2014).
24. **T. Bronder**, C.S. Wu, A. Poghossian, C.F. Werner, M.J. Schöning: *Label-free detection of DNA using light-addressable potentiometric sensor modified with a positively charged polyelectrolyte layer*, 7th Engineering of Functional Interfaces (EnFI 2014), Jülich, Germany (03.–05. Jul. 2014).
25. C.S. Wu, A. Poghossian, C.F. Werner, **T. Bronder**, M. Bäcker, P. Wang, M.J. Schöning: *An application of a scanning light-addressable potentiometric sensor for label-free DNA detection*, 11th Dresdner Sensor-Symposium (DSS 2013), Dresden, Germany (09.–11. Dec. 2013).
26. C.S. Wu, A. Poghossian, C.F. Werner, M. Bäcker, **T. Bronder**, H. Iken, P. Wang, M.J. Schöning: *Label-free detection of DNA immobilization and hybridization with a scanning light-addressable potentiometric sensor*, 6th Engineering of Functional Interfaces (EnFI 2013), Hasselt, Belgium (08.–09. Jul. 2013).

Acknowledgement

I would like to start my Acknowledgement-Chapter with my thanks to **Prof. Dr.-Ing. Michael J. Schöning**. Thank you for giving me the opportunity to write my thesis at the Institute of Nano- and Biotechnologies (INB) at FH Aachen, Campus Jülich, Germany. Thank you for the permanent effort for finding possible ways of funding, which made the time as PhD student much simpler and calmer. Thank you for giving me many opportunities of conference participation at great locations, like Argentina, South Korea, Poland and Italy, at which I could improve my presentation skills, got a lot of experience and also had a very nice time. I really acknowledge your support for many of my ideas and suggested experiments as well as your effort for making it possible to perform complex experiments together with specialized cooperation partners (Forschungszentrum Jülich, Fraunhofer IAF Freiburg, Joint Lab Bioelectronics Berlin/Frankfurt-Oder). Also thank you for the proofreading of countless papers, abstracts, reports and this thesis. Thank you for giving good advices for presentations before (and sometimes even during conferences).

Prof. Dr. rer. nat. Arshak Poghossian, thank you for the broad technical supervision, for plenty, very professional discussions about diverse scientific topics and for proofreading of countless papers, abstracts, reports and this thesis. Also thank you for your good advices and always constructive criticism of my presentations. I really acknowledge that you always had an "open ear" for questions. Thanks for providing a huge variety of tips and important information during my time as PhD student – I really learned a lot. I highly honor your great scientific knowledge.

Prof. Dr. rer. nat. Michael Keusgen, many thanks for the external support from University of Marburg. Thank you for the good advises for the thesis preparation and for the inspiring considerations about several scientific topics during our meetings. Special thanks for your support and uncomplicated handling of collaboration between FH and University which allows us/me to get a doctoral degree in this constellation. Thanks also for proofreading of my thesis.

Special thanks for the fantastic time to **Melanie Jablonski**. You were a great office mate and I appreciate our very inspiring conversations about all kind of topics. I highly honor you for your fair, honest and trustful character. Special thanks also to my friend **Carl Frederik Werner**, you helped me so many times and I also honor you as a very fair and honest person.

Many thanks to all other colleagues and other PhD students who made the time very pleasant and funny. Especially **Julio Arreola**, for the countless conversations about social topics, **Shahriar Dantism** for conversations about culture, religion and friendship, **Benno Schneider**, **Lars Breuer** and **Johanna Pilas** for realization of really great "off-topic" evenings. I would also like to thank **Prof. Dr. rer. nat. Torsten Wagner** a for answering all my questions; you helped me many times see the things from a different point of view.

Many thanks to **David Rolka** for really great talks and for your permanent helpfulness. I will never forget that you brought my forgotten passport to my home so that I could travel to Argentina. Many thanks to **Dua Özsoylu** for really friendly and pleasant conversations, I wish you all the best for the future here in Germany. Thanks to **Dr. rer. nat. Elke Börmann-El-Kholy** for your engagement to support the students and organizing tasks, plans, schedules, summer- and Christmas parties and many more. Thanks to **Rene Welden** for the nice time and the technical conversations.

Great thanks to all my students: Your ambition and effort in conducting countless experiments build the fundament for our scientific research and achieved goals. **Eva Dollhäubl** and **Tessa Schleypen**, thank you for your endurance during the experimentation, I (must) also learned a lot about leading, controlling and managing. **Alexander Goretzki**, **Laura Wenzel**, **Blaise Nwotchouang** and **Jana Kriesel**, you have always refreshed the daily routine in the lab and created a good and funny atmosphere.

Best thanks to **Sabrina Scheja** for the excellent teamwork, your diligence and your positive attitude. Thank you so much for having a really great time with unforgettable memories, e.g., during our time in New York City. Also best thanks to **Max Jessing** for the very professional teamwork and collaboration, thank you for our great discussions, I am really looking forward to work with you in the future.

Thank you to all my students, I learned so much from you guys and girls, I wish you all the best!

Thanks to my other office mates **Kristina Schönenborn**, **Alexander Bartz**, **Tobias Kerschgens**, **Farnoosh Vahidpour** for creating a very nice and comfortable working environment.

I thank the BMBF (Project DiaCharge, 031A192D) and the FH Aachen Promotionskolleg for the financial support of this work. Thanks to the project partners Dr. Christoph Metzger-Boddien (gerbion Gmbh & Co. KG) and Dr. Heinz Busch (NTTF Coatings GmbH) for technical support and fruitful discussions.

I would like to express my final thanks to my family and friends. Many thanks to my brother **Viktor Bronder**, my parents **Gisela** and **Roman Bronder** and my grandparents **Angelika** und **Stefan Frukacz** für Eure großartige und unermüdliche Unterstützung in allen Lebenslagen. Many thanks to my former girlfriend **Jing Zhao** who mentally supported and encouraged me and gave me strength when things didn't go well. Lastly, my thanks also go to my friends from Mönchengladbach (**Tanja Nießen, Christina Marticke**, **Hermann & Stefanie Stefes**, **Patrick Pauen**) and Jülich (**Philipp Rateike, Berit Rothkranz** and **Sina Eidt**) for all the support and strength you gave to me!

Curriculum vitae

The curriculum vitae is not part of the online version.

The curriculum vitae is not part of the online version.